EPIGENOMES OF ZEBRAFISH MATURE SPERM AND EARLY EMBRYOS

by

Shan-Fu Wu

A dissertation submitted to the faculty of
The University of Utah
in partial fulfillment of the requirements for the degree of

Doctor of Philosophy

Department of Oncological Sciences

The University of Utah

December 2013

The University of Utah Graduate School

STATEMENT OF DISSERTATION APPROVAL

The dissertation of **Shan-Fu Wu**

has been approved by the following supervisory committee members:

Bradley R. Cairns	, Chair	**June 25, 2013** Date Approved
David A. Jones	, Member	**June 25, 2013** Date Approved
Dean Tantin	, Member	**June 25, 2013** Date Approved
Richard I. Dorsky	, Member	**June 25, 2013** Date Approved
J. Kimble Frazer	, Member	Date Approved

and by **Bradley R. Cairns**, Chair/Dean of

the Department/College/School of **Oncological Sciences**

and by David B. Kieda, Dean of The Graduate School.

ABSTRACT

One central question in development is how totipotency and pluripotency are established. In mature human sperm, genes of importance for embryo development (i.e. transcription factors) lack DNA methylation and bear nucleosomes with distinctive histone modifications, suggesting the specialized packaging of these developmental genes in the germline. Here, we explored the tractable zebrafish model and found conceptual conservation as well as several new features. Biochemical and mass spectrometric approaches reveal the zebrafish sperm genome packaged in nucleosomes and histone variants (and not protamine), and we find linker histones high and H4K16ac absent—key factors which may contribute to genome condensation. We examined several activating (H3K4me2/3, H3K14ac, H2AFV) and repressing (H3K27me3, H3K36me3, H3K9me3, hypoacetylation) modifications/compositions genome-wide, and find developmental genes packaged in large blocks of chromatin with coincident activating and repressing marks and DNA hypomethylation, revealing complex "multivalent" chromatin. Notably, genes that acquire DNA methylation in the soma (muscle) are enriched in transcription factors for alternative cell fates. Remarkably, we find H3K36me3 located in "silent" developmental gene promoters, and not present at the 3' ends of coding regions of genes heavily transcribed during sperm maturation, suggesting different rules for H3K36me3 in

the germline and soma. We also reveal the chromatin patterns of transposons, rDNA, and tRNAs. Finally, high levels of H3K4me3 and H3K14ac in sperm are correlated with genes activated in embryos prior to the mid-blastula transition (MBT), whereas multivalent genes are correlated with activation at or after MBT. Taken together, gene sets with particular functions in the embryo are packaged by distinctive types of complex and often atypical chromatin in sperm.

Bivalent marks, as the chromatin signature of pluripotency, are not persistent and diluted during early synchronous cell division, making them arguable to be heritable epigenetic marks. Studies in early embryos indicate DNA methylation status is the fundamental to confer totipotency and pluripotency. The anticorrelation between DNA methylation profiles and H2A.Z occupancy is conserved from plants to vertebrates. Here, we examined H2afva occupancy in early embryos in zebrafish by ChIP-seq. We found both H2afva level and enrichment remain consistent from sperm to embryos. H2afva is enriched in proximal promoter region in the first nucleosome. Consistent with previous studies, H2afva occupancy is anticorrelated to DNA methylation both in the promoters and outside of promoters. These data suggest H2afva is potentially a heritable epigenetic mark and sets up DNA methylation profiles of totipotency and pluripotency.

To Mom.

TABLE OF CONTENTS

LIST OF FIGURES

LIST OF TABLES

ACKNOWLEDGEMENTS

As an international student coming all the way from Taiwan, I am very thankful for everything around me. Studying in the U.S. was one of my dreams, and pursuing a Ph.D degree was another one. I still cannot believe how lucky I am to have two dreams come true. To complete this dissertation, I first would like to thank my mentor Brad Cairns for his great ideas, enthusiasm, kindness, and support. I am so glad I chose a good mentor and worked on great projects. I thank my dissertation committee members Rich Dorsky, Dean Tantin, Dave Jones, and Kimble Frazer for their helpful comments. They were incredible when discussing my projects. Rich was my first employer and I enjoyed working in his lab. I really thank Rich for offering me that opportunity.

I thank the members in Cairns lab for discussion and help, especially Tim Parnell for helping me with many things. Our core facility is always helpful, David Nix and Brett Milash in Bioinformatics, Microarray facility, Mutation facility, and CZAR to keep my fish. To keep me at a good academic record, I thank Jessica Askin and Dee DalPonte for their help. I would like to thank the Molecular Biology program for all the support back to my first year.

I deeply thank my family and parents-in-law in Taiwan for their support and encouragement. We do not usually say this, but I love you all very much. Your support is what keeps me pursuing my dreams. I also want to thank my wife Pin-An Chen and my

son Yen-Cheng Wu. I am so fortunate to have both of you. Either it is a good day or a bad day, as long as we are sitting together and enjoying a meal, ha, it would be a perfect day. I love you two and let's enjoy our life everyday.

CHAPTER 1

INTRODUCTION

Epigenetic status refers to any heritable functionally relevant modifications to the genome other than changes in the DNA sequence. Both genetic and epigenetic features play important roles in the regulation of gene expression and cell identity. Developmental processes are often accompanied with dynamic changes of epigenetic modifications. One central question I am interested in is how pluripotency and totipotency are established through epigenomic features in stem cells and germline, respectively. To confer pluripotency and totipotency to embryonic stem cells (ES cells) and germline, respectively, the epigenetic status (including heritable DNA methylation and chromatin modifications) is required to be reprogrammed. Yet, little is known about the dynamic changes of epigenetic status in gametes and early embryos. This dissertation aims to understand how the epigenetic pattern helps guide development by characterizing mature sperm and early embryos in zebrafish. Zebrafish have been widely appreciated as a powerful animal model—for their feasibility for genetic manipulation, rapid maturation, and transparent and staged embryos—all of which are crucial for this study.

The Role of Epigenetics in Transcription and Genome Regulation

The Role of DNA Methylation in Gene Silencing

DNA methylation primarily occurs on cytosine position 5 in the context of CpG dinucleotide in higher eukaryotes (Bird 1996). CpG dinucleotide is under-represented in the vertebrate genome due to the high rate of deamination of methylated cytosine into thymidine (Bird et al. 1995). CpG-rich regions referred to as CpG islands (CGIs) often occur in the promoter regions of housekeeping genes and genes with tissue-specific

expression patterns. Intriguingly, most CGIs are unmethylated and regulation of gene expression is achieved by coordinating transcription factors and underlying chromatin status (Jones 2012).

DNA methylation is catalyzed by the DNA methyltransferase (DNMT) family. In early development, *de novo* methylation is established by DNMT3A and DNMT3B (Law and Jacobsen 2010). The established pattern is then faithfully maintained by DNMT1 through cell divisions. DNA methylation has long been considered as a fixed and stable mark, but more and more studies have shown DNA methylation is dynamic and reversible (Bhutani et al. 2011). For example, global decreases of DNA methylation soon after fertilization were reported in mouse and zebrafish embryos (Heby 1995; Mhanni and McGowan 2004). Moreover, dynamic DNA methylation is observed during cell lineage specification, and methylation on retina-specific genes in early embryos could be erased later to guide retina specification (Borgel et al. 2010).

DNA demethylation can be achieved by passive and active mechanisms. Passive dilution of DNA methylation occurs during DNA replication and cell division. A potential model for active DNA demethylation is proposed by Jones and Cairns labs (Rai et al. 2008). AID/Apobec2 acts as a deaminase which converts methylated cytosine to thymine. MBD4 then catalyzes glycosylation to remove thymine in the T:G mismatch and also plays a role in targeting AID/Apobec2. The resulting abasic site is repaired by base excision repair (BER) machinery to insert an unmethylated deoxycytidine monophosphate. The demethylation process is promoted by Gadd45α upon DNA damage signal (Barreto et al. 2007). Recently, hydroxymethylation of cytosine position 5 (5hmC) catalyzed by TET enzymes has been reported in mammalian tissues and can be detected

highly in brain and ES cells (Tahiliani et al. 2009; Ficz et al. 2011; Pastor et al. 2011). 5hmC is proposed as an intermediate for both passive and active mechanisms of DNA demethylation: (1) 5hmC impairs DNMT and maintenance of DNA methylation during cell divisions, and (2) Active replacement of methylated cytosine is via DNA repair (Bhutani et al. 2011).

DNA methylation is proposed to be involved in long-term gene silencing in somatic cells (such as transposons), and monoallelic X chromosome inactivation and genomic imprinting in animals and plants (Heard et al. 2001; Martienssen et al. 2004). The typical silencing mechanisms by DNA methylation involve (1) Direct inhibition of binding of transcription factors or transcriptional machinery and (2) Methyl-CpG binding domain (MBD) proteins recognize DNA methylation and then recruit co-repressors such as histone deacetylase (HDAC) (Lande-Diner and Cedar 2005). Research in recent years, however, has advanced our understanding of DNA methylation involved in genome regulation through chromatin organization (more details in the following with related aspects) (Reddington et al. 2013).

Permissive Chromatin Modifications for Transcriptional Competence

The basic unit of chromatin is the nucleosome, which consists of two copies of each core histone (H2A, H2B, H3, and H4), and the histone octamer is wrapped with 147 bp of DNA. Linker DNA and linker histones (such as H1 or H5) in higher eukaryotes reside in regions of highly packaged chromosomes (Kornberg 1974). The length of linker DNA varies among species and cell types, ranging from 10 bp to 50 bp. Linker histones

bind nucleosomes in a 1:1 ratio to form chromatosomes to prevent DNA unwrapping, and this leads to increased average nucleosome repeat length (Huynh et al. 2005; Robinson et al. 2006; Zhou et al. 2007).

For transcription factors and transcriptional machinery to access DNA, chromatin structure needs to be reorganized, and multiple mechanisms have been proposed: histone modifications, histone variant incorporation, chromatin remodeling, and nucleosome ejection (this dissertation will focus on the first two) (Li et al. 2007; Clapier and Cairns 2009). Posttranslational modifications on histones are involved in regulation of transcription, DNA repair, DNA replication, and chromatin condensation (Kouzarides 2007). Chromatin features and their associated transcriptional activity are summarized in Table 1.1. "Histone code" was proposed based on association between gene activity and various modifications at different histone positions.

Methylation of H3K4 (H3K4me) is catalyzed by proteins containing SET domain such as Set1 in yeast and Trithorax group (TrxG) and mixed lineage leukemia proteins (MLL) in metazoans (Ruthenburg et al. 2007). Deletion of the yeast H3K4 methyltransferase, *SET1* gene, abolishes di- and tri-methylation on H3K4 (Santos-Rosa et al. 2002). H3K4me is associated with transcriptional activation and competence. H3K4me1 is enriched in enhancer regions, and both H3K4me2 and H3K4me3 are enriched in proximal promoter regions in eukaryotes (Santos-Rosa et al. 2002; Cuthbert et al. 2004; Barski et al. 2007; Heintzman et al. 2007). Interestingly, H3K4me3 is bound by the PHD finger of TAF3 in TFIID, and stimulates preinitiation complex (PIC) formation to enhance transcription (Vermeulen et al. 2007; Lauberth et al. 2013). In the promoters of chicken β-globin genes, the level of H3K4me2 can be detected either when

β-globin genes are active or inactive, suggesting that methylation on H3K4 maintains the locus in a poised state (Schneider et al. 2004). The poised state implies a transcriptional competent state that prepares a gene to switch from inactive status to active status.

In yeast, Set1 is recruited by initiation form of RNA polymerase II (Pol II) (phosphorylation at Serine 5 of CTD) but not by elongation form (phosphorylation at Serine 2 of CTD) (Ng et al. 2003). Targeting of MLL in mammals, however, is largely unknown. CGIs have been suggested to recruit MLL complex via its subunit, Cfp1 (Lee and Skalnik 2005; Thomson et al. 2010; Schuettengruber et al. 2011). Cfp1 binds unmethylated CG dinucleotides, and loss of Cfp1 in ES or mammalian cells leads to loss of H3K4me3 at active genes (Voo et al. 2000; Lee and Skalnik 2002; Thomson et al. 2010; Clouaire et al. 2012). Interestingly, methylation on H3K4 is often enriched at promoter regions where CGI resides (Weber et al. 2007). Genomic analyses revealed H3K4me enriched regions are exclusive of DNA methylation. In germ cells, DNMT3L, the regulator of *de novo* DNA methylation, binds unmethylated histone H3 but not H3 with methylated K4, suggesting a potential mechanism on how H3K4me3 antagonizes DNA methylation (Ooi et al. 2007).

In the aspect of transcription, histone acetylation is strongly associated with active transcription (Shahbazian and Grunstein 2007). Acetylation on histones disrupts electrostatic interaction between histones and DNA, thus loosening the chromatin structure. Acetylation also serves as a binding platform for factors that promote transcription. For example, acetylation on H3K14 is recognized by Rsc4 and recruits the rest of chromatin remodeler components to promote transcription (Agalioti et al. 2002; Kasten et al. 2004). Acetylation on H3K9 blocks methylation mark on this residue and

correlates with gene activation. Acetylation on H4K16 prevents spreading of heterochromatin and the nucleosome remodeler ISWI which orders nucleosomes arrangement (Johnson et al. 1992; Thompson et al. 1994; Clapier et al. 2001; Corona et al. 2002).

Repressive Chromatin Modifications for Gene Silencing

During development, H3K9me3 and H3K27me3 are associated with transcriptional repression (Barski et al. 2007). H3K9 is methylated by another SET domain containing family, called Su(var)3-9 family. The chromodomain of HP1 recognizes methylation on H3K9 and this combination contributes to formation of heterochromatin (Shilatifard 2006). DNA methylation coordinates with H3K9me or H3K27me3 for heterochromatin establishment or X-inactivation in mammalian female, respectively. The cooperation among DNA methylation and histone marks is supported by physical interactions between DNMT1 and SUV39H1 (Fuks et al. 2003). This connection mechanistically links epigenetic repression systems between DNA methylation and histone methylation.

Methylation on H3K27 is catalyzed by Polycomb repressor complex 2 (PRC2) that belongs to Polycomb group (PcG) proteins. Ezh2 in PRC2 contains a SET domain and is responsible for H3K27 methylation (Cao et al. 2002; Muller et al. 2002). H3K27me3 is recognized by PRC1 complex to maintain the inactive state of genes during development (Schwartz and Pirrotta 2007). However, how H3K27me3 or PRC1 contributes to gene silencing remains unknown. Targeting of PcG is of high interest but still unclear in mammals. In *Drosophila*, PcG proteins are recruited by Polycomb

response elements (PREs), which are found in many developmentally regulated genes (Simon et al. 1993). So far, only two respective PREs in mammals have been identified to confer PcG repression (Sing et al. 2009; Woo et al. 2010). By surveying bacterial genomic fragments, GC-rich elements lack of activating transcription factor motif is able to recruit PRC2, suggesting CGI has the potential to recruit PRC2 (Mendenhall et al. 2010). Although PREs in flies do not show GC-rich feature, PREs and CGIs still share some similarities: (1) Associate with developmental genes, (2) Organized with unstable nucleosomes, and (3) Bound by paused RNA Pol II (Sharif et al. 2013). In addition to DNA elements, other factors such as noncoding RNAs are possibly involved in recruitment of PcG (Schuettengruber et al. 2007; Tsai et al. 2010).

Poised Chromatin Modifications for Transcriptional Competence

In ES cells, H3K27me3 coincides with H3K4me3 in the highly conserved noncoding regions, which encompass many developmentally important regulators (Bernstein et al. 2006). The combination of active and silent modifications is termed "bivalent domain," and this feature actually keeps genes expression at very low levels or none. Bivalent domain is proposed to poise developmental genes for activation or repression during lineage specification and is considered as the chromatin signature of pluripotency in ES cells (Mikkelsen et al. 2007; Li et al. 2012a). Additional features have been unveiled along with bivalent domains to insure their robustness in poising genes. For example, dimethylation on H3K4 is enriched with bivalent domains as another permissive mark (Meissner et al. 2008). H3K9me3 catalyzed by SetDB1 is also enriched with bivalent domain and contributes to repression of developmental genes—even though

this is the only report so far that shows this feature (Bilodeau et al. 2009). Notably, the underlying DNA is GC-rich and unmethylated (Meissner et al. 2008). Paused RNA Pol II is associated with developmental regulators in ES cells and no transcript has been detected (Guenther et al. 2007; Marks et al. 2012). Repressive genes associated with RNA Pol II have the potential to respond to developmental cues synchronously and promptly (Levine 2011). Histone variants such as H2AZ are also involved in poising genes for expression (see below for details).

The epigenome refers to epigenetic attributes in a genome-wide scale. Epigenetic attributes include DNA methylation, histone modifications, and histone variants, which together define chromatin structure, gene activity, and cellular identity. The epigenetic status in stem cells and differentiated cells has been widely studied, yet little is known about the timing of establishing the epigenetic feature during life cycle. This dissertation aims to understand the epigenetic setup in male gametes and if any specific epigenetic pattern is established in sperm.

Potential Epigenetic Contribution to Pluripotency and Totipotency

Pluripotency Is Set Up by a Network of Pluripotency Factors and Chromatin Regulators

Pluripotent ES cells are able to generate all cell types during development. Studies have shown the importance of a network of pluripotency factors for maintaining ES cell pluripotency and self-renewal. These pluripotency factors include Oct4, Nanog, Sox2, and Tcf3 (Masui et al. 2007; Tam et al. 2008; Ng and Surani 2011). ES cells are

specified by Oct4 at inner cell mass (ICM) of blastocysts (Nichols et al. 1998). Nanog is then expressed to maintain ES cell fate and self-renewal (Chambers et al. 2003). Ectopic expression of Oct4, Sox3, Klf4, and c-Myc is able to reprogram any tissue toward the formation of induced pluripotent cells (iPSCs) in mouse and human (Takahashi and Yamanaka 2006; Takahashi et al. 2007; Hanna et al. 2010). Fully reprogrammed iPSCs like ES cells can contribute to all germ layers and embryonic germ cells that can form complete and fertile mice by tetraploid complementation (Zhao et al. 2009; Hanna et al. 2010).

To keep developmental regulators inactive while maintaining self-renewal genes active in ES cells, pluripotency factors function in a regulatory circuitry and cooperate with chromatin regulatory proteins. Knock out of Ezh2, H3K27 methyltransferase, in mice leads to early embryonic lethality and failure in establishing ES cell lines (O'Carroll et al. 2001). Genome-wide studies show Polycomb complexes occupy and repress developmental regulators in ES cells, and these developmental regulators are enriched with H3K27me3 (Bernstein et al. 2006; Boyer et al. 2006; Lee et al. 2006). Remarkably, these developmental regulators occupied by PRC2 in ES cells are also occupied by Oct4, Sox2, and Nanog. The TrxG protein WDR5 is required for self-renewal in ES cells (Ang et al. 2011). WDR5 physically interacts with Oct4 and strongly colocalizes with Oct4 in the genome, including genes involved in self-renewal. WDR5 and TrxG complex maintain high levels of H3K4me3 and transcriptional activity of these self-renewal genes in ES cells. Moreover, studies have shown chromatin remodelers play an essential role in regulating ES cell pluripotency and self-renewal (Koh et al. 2010). Chd1, a chromatin remodeler associated with active transcription, is required to maintain open chromatin

status and pluripotency in ES cells (Gaspar-Maia et al. 2009). ES cell BAF complex, a chromatin remodeler of the SWI/SNF family, interacts with the pluripotency factors and maintains ES cell pluripotency (Ho et al. 2009a; Ho et al. 2009b; Ho et al. 2011). Taken together, pluripotency is set up by cooperation between pluripotency factors and chromatin regulatory factors.

Potential Epigenetic Contribution to Totipotency/Pluripotency in Primordial Germ Cells and Mature Sperm

Establishment of epigenetic features for totipotency in primordial germ cells (PGCs) undergoes global chromatin reprogramming (Cantone and Fisher 2013). In mice PGCs, a genome-wide DNA demethylation is observed between E11.5 and E12.5, when PGCs enter the gonads (Hajkova et al. 2002; Popp et al. 2010). This removes the DNA methylation pattern that controls somatic gene expression and imprinted genes. The demethylation process depends in part on the cytidine deaminase AID and base excision repair (BER) pathway (Rai et al. 2008; Hajkova et al. 2010). The erasure of DNA methylation accompanies extensive erasure of H3K27me3, H3K9me3, and H3K9Ac, and exchange of histone variants (Hajkova et al. 2008). At E12.5, H3K27me3 and H3K9me3 are regained in PGC. Due to a limited number of PGCs, it remains unknown at what loci reprogramming occurs in a genome-wide scale.

The promoter DNA methylation pattern of embryonic germ (EG) cells (cultured PGCs) and sperm resembles ES cells with a significant R-value (Farthing et al. 2008). Given the pluripotency for both ES and EG cells, the DNA methylation pattern in both cell types only differs in a small number of promoters. The similarity of methylation

pattern between sperm and ES and EG cells suggests that overall promoter methylation patterns in sperm are maintained at a status inherited from PGCs and probably passed to ES cells.

In mammals and some fishes, sperm chromatin is packaged with protamines that are small cationic proteins into a highly condensed and compact structure. This tightly packaged genome correlates with transcriptional silence in sperm (Kierszenbaum and Tres 1975). It has long been thought that epigenetic contribution of sperm chromatin to embryo development is very limited. A landmark paper, however, shows the human sperm genome is not completely exchanged to protamine and there is ~4% genome retained with nucleosomes (Hammoud et al. 2009). Interestingly, the remaining nucleosomes occupy genes involved in transcription, signaling, and developmental processes. Further examination of epigenetic features shows enrichment of both H3K4me3 and H3K27me3, consisting of bivalent domains, in the promoter regions of developmental regulators. These bivalent genes in human sperm have a significant overlap with that in ES cells. H3K4me3 alone is highly enriched at genes related to spermatogenesis, nuclear architecture, and RNA metabolism, representing a memory from prior process and a potential poising for future program. Similarly, ES cells show the epigenetic demarcation—bivalent marks for developmental regulators that are silent and active marks for active genes involved in self-renewal. Notably, the underlying DNA of the bivalent domain in human sperm is lack of methylation as in ES cells. The bivalent chromatin signature is also observed in mouse sperm, suggesting a conserved packaging strategy in mammalian sperm (Brykczynska et al. 2010). Taken together, important genes

such as developmental regulators in mature sperm are packaged with poised chromatin as in ES cells and both sperm and ES cell genomes are programmed by epigenetic features.

Potential Epigenetic Contribution to Pluripotency in Early Embryos

Bivalent domain, the chromatin signature of pluripotency, has been established in mature sperm. The next open question is if the signature is inherited or reestablished in early embryos. In addition to epigenetic contribution to pluripotency, other factors such as histone variants, transcription, and noncoding RNA have the potential as well but remain largely unknown (here the focus is on chromatin attributes and see below for DNA methylation and H2AZ). The zygotic genome is activated between 2- to 8- cell stage in mammals, but at 1000-cell stage (midblastula transition, MBT) in zebrafish. Before zygotic genome activation (ZGA), embryos undergo synchronous cell divisions and the genome is inactive. At this period of time, embryonic cells (blastomeres) are pluripotent and basically identical (Schier and Talbot 2005). Therefore, the possibility to collect enough cells makes zebrafish an ideal model system to address if chromatin signature is inherited in early embryos.

Studies from Vastenhouw et al. (2010) show chromatin attributes (H3K4me3, H3K27me3, and H3K36me3) are not detected by immunoblotting until MBT and chromatin signature is reestablished when the zygotic genome activates in zebrafish (Vastenhouw et al. 2010). After ZGA, more than 80% of genes are marked by H3K4me3, and developmental regulators are enriched with bivalent domain. These data suggest chromatin signature is not inherited but reestablished in early embryos. In contrast,

studies from Wu et al. (2011) and Lindeman et al. (2011) suggest an inheritance model and show a similar chromatin signature to sperm before MBT (Lindeman et al. 2011; Wu et al. 2011). They are able to detect the bulk level of H3K4me3 by immunoblotting and immunostaining before MBT. Bivalent marks are enriched in the promoters of developmental regulators before ZGA—though at a lower level compared to post ZGA. Notably, pre-MBT embryos share a significant portion of bivalent genes with sperm, and most of these genes are expressed at MBT or after MBT, suggesting the developmental program is prepatterned by epigenetic features prior to ZGA.

Dynamic DNA methylation accompanies and potentially guides developmental processes. To confer pluripotency in the embryo, methylation on paternal genome is erased globally by active demethylation before first cell division in the zygote, whereas the maternal genome is demethylated by passive dilution over cleavage divisions (Mayer et al. 2000; Oswald et al. 2000; Howell et al. 2001). A comprehensive study in zebrafish examines DNA methylation from gametes to early embryos and suggests DNA methylation underlies embryo totipotency and pluripotency (Potok et al. 2013). Zebrafish appear to achieve a totipotent chromatin state when the zygotic genome activates and this involves: (1) paternal genome competency since the paternal genome is already set up as that at zygotic genome activation (ZGA), (2) maternal genome DNA demethylation/reprogramming to a state corresponding to the paternal genome, and (3) imposition of DNA methylation on genes needed later in development. Notably, programming of DNA methylation to reach ZGA follows the “CG-rule”—DNA with low CG content acquires methylation whereas high CG content resists methylation.

Dynamic DNA methylation profiles in zebrafish suggest embryos achieve totipotent state at MBT. It is still unclear how and when pluripotency/totipotency is established. Gametes represent a unique stage during development—they are terminally differentiated but become a totipotent zygote once fertilized. The question is if pluripotency/totipotency is already embedded in gametes and if this is set up through bivalent chromatin. This dissertation studies the epigenomes in male gametes and early embryos in zebrafish and aims to understand how the epigenome helps set up pluripotency/totipotency.

H2A.Z

H2A.Z, H2A Histone Variant

Replacement of canonical histones by histone variants is important in regulation of gene activity and DNA-related cellular processes (Zlatanova and Thakar 2008; Marques et al. 2010). Canonical histones are synthesized in a replication-dependent manner in S phase, whereas histone variants are synthesized and incorporated into chromatin throughout the cell cycle (Ahmad and Henikoff 2002; Krogan et al. 2003; Kobor et al. 2004). H2A.Z is one of the H2A variants, which also include H2A.X, H2A-Bbd, and macroH2A (Talbert and Henikoff 2010). H2A.Z is evolutionarily conserved from protozoan (*Plasmodium falciparum*), budding yeast (*Saccharomyces cerevisiae*), to humans with 90% sequence conservation (Iouzalen et al. 1996). Budding yeast has a single copy of the H2A.Z gene (HTZ1), whereas mammals have two H2A.Z genes (H2afv and H2afz), whose protein products differ by three residues, and they are possibly not redundant (Faast et al. 2001; Eirin-Lopez et al. 2009). Here, H2A.Z will be referred to

as the general name of the variant in different species. Zebrafish have two H2A.Z genes, h2afva and h2afvb. The H2afva protein sequence is 100% identical to mammalian H2A.Z, and h2afvb has an extra 21 residues in the N-terminus and 2 different residues in the rest of the 128 residues; little is known about h2afvb. H2A.Z shares 60% of sequence identity to H2A, suggesting the uniqueness and importance of H2A.Z (Jackson and Gorovsky 2000). In budding yeast, H2A.Z is not essential but is involved in many biological processes, including transcriptional activation and repression, chromosome stability, and DNA repair (Santisteban et al. 2000; Meneghini et al. 2003; Krogan et al. 2004; Mizuguchi et al. 2004; Zhang et al. 2005). In mammalian cells, H2A.Z is important for transcriptional regulation, chromosome segregation, centromeric functions, and cancer metastasis (Rangasamy et al. 2003; Rangasamy et al. 2004; Gevry et al. 2007; Gevry et al. 2009). Moreover, deletion of H2A.Z leads to lethality in many organisms, such as *Tetrahymena thermophile*, *Drosophila melanogaster*, *Xenopus leavis*, and *Mus musculus* (van Daal and Elgin 1992; Iouzalen et al. 1996; Liu et al. 1996; Clarkson et al. 1999; Faast et al. 2001; Ridgway et al. 2004).

Exchange of H2A-H2B dimers to H2A.Z-H2B dimers depends on the ATP-dependent Swr1 complex in yeast, named after the SWR1 catalytic subunit (Krogan et al. 2003; Kobor et al. 2004; Mizuguchi et al. 2004). Orthologs of Swr1 complex in vertebrates are SRCAP and P400 complexes, and there is no functional overlap between these two for incorporation of H2A.Z (Wu et al. 2005; Cai et al. 2006). Transcription factors associated with SRCAP or P400 could possibly play a role in targeting H2A.Z deposition, but the details remain to be elucidated.

H2A.Z, Transcription, and Associated Nucleosomes

In *Tetrahymena*, H2A.Z is only found in the transcriptionally active macronucleus, an initial suggestion that H2A.Z is involved in active regulation of transcription (Allis et al. 1980). H2A.Z is localized to the nucleosomes flanking the nucleosome-deficient region (NDR) at the transcription start site, where H2A.Z efficiently recruits RNA Pol II in both yeast and human cells (Adam et al. 2001; Zlatanova and Thakar 2008; Hardy et al. 2009). Loss of H2A.Z in *Arabidopsis thaliana* leads to reduced expression of the flowering gene and premature flowering (Deal et al. 2007). Moreover, H2A.Z in *Caenorhabditis elegans* is required to activate a subset of foregut genes for normal foregut development (Updike and Mango 2006). However, the role of H2A.Z in transcription is contradictory. In human cells and *Drosophila*, the level of H2A.Z in promoter regions is positively correlated with gene activity, whereas in yeast cells, it is inversely correlated (Guillemette et al. 2005; Li et al. 2005; Zhang et al. 2005; Barski et al. 2007; Mavrich et al. 2008). Interestingly, in response to changes in growth conditions, H2A.Z in yeast cells is required to promote full gene activation and shows redistribution from activated promoters to repressed/basal promoters (Li et al. 2005; Zhang et al. 2005). Biochemical studies further show H2A.Z-associated nucleosomes are more susceptible to loss, suggesting H2A.Z poises repressed/basal promoters for activation through loss of histones—see below for the poising role of H2A.Z in ES cells (Placek et al. 2005; Zhang et al. 2005). Posttranslational modifications of H2A.Z could partially explain the conflicting role of H2A.Z in transcription. Acetylation in the N-terminus of H2A.Z is associated with active transcription in yeast and mammalian cells, whereas monoubiquitylation in the C-terminus of H2A.Z is found on the inactive X

chromosome of female mammals (Millar et al. 2006; Sarcinella et al. 2007; Talbert and Henikoff 2010; Ku et al. 2012; Valdes-Mora et al. 2012).

In mammalian cells, H2A.Z often coincides with the H3 variant, H3.3, in NDR of active promoters, enhancers, and insulator regions (Jin et al. 2009). The H3.3/H2A.Z double variants-containing nucleosomes are very unstable and are proposed to be involved in maintaining accessible chromatin structures (Jin and Felsenfeld 2007).

The Role of H2A.Z in Pluripotency

Loss of H2A.Z in mice leads to embryonic lethality by the gastrulation stage (Faast et al. 2001). The mutant embryo develops normal ICM and trophectoderm but fails to further differentiate beyond blastocyst stage, suggesting H2A.Z is indispensable for efficient differentiation of stem cells (Banaszynski et al. 2010). Genomic localization of H2A.Z in ES cells coincides with Suz12, a core subunit of the PRC2 complex, in the promoters of developmental regulators, and the co-occupancy is interdependent (Creyghton et al. 2008). Consistent with mouse models, the H2A.Z-depleted ES cells fail to differentiate upon induction.

Analyses of nucleosome dynamics during ES cell differentiation show both nucleosome depletion and *de novo* occupation occur, typically in the promoters and exons of genes (Li et al. 2012b). Interestingly, H2A.Z is localized to nucleosome depletion regions in undifferentiated ES cells (Li et al. 2012b; Hu et al. 2013). H2A.Z-associated nucleosomes are enriched with H3K4me3 in promoters and enhancers. Furthermore, H2A.Z-associated nucleosomes encompass binding sites for the endoderm "pioneer" transcription factor FoxA2. Both H2A.Z and FoxA2 are required for nucleosome depletion and efficient ES cell differentiation. Knockdown of H2A.Z impairs

Oct4, MLL, and PRC2 complexes for efficient binding to target genes. Taken together, these data suggest H2A.Z maintains chromatin accessibility in ES cells and poises genes for activation during differentiation.

H2A.Z and DNA Methylation

H2A.Z incorporation and DNA methylation are reported as antagonistic in both animals and plants (Zilberman et al. 2008; Conerly et al. 2010; Zemach et al. 2010). DNA methylation is often observed on cytosine in the context of CpG dinucleotide. CpG-rich regions, CGIs, mostly occur in the promoter regions but lack methylation irrespective of the transcription status. H2A.Z in *Arabidopsis* is found specifically at the 5' promoter regions of genes where CGIs reside, and DNA are unmethylated (Zilberman et al. 2008). Another profound example is the pericentromere regions, which contain many transposons and heavily methylated DNA, but very low levels of H2A.Z. Loss of MET1 DNA methyltransferase in *Arabidopsis* causes both losses and gains of DNA methylation and leads to opposite changes in H2A.Z deposition. Conversely, loss of PIE1, homolog of SWR1, leads to loss of H2A.Z deposition, especially at intragenic regions, and corresponding gain of DNA methylation. During B-cell lymphomagenesis, H2A.Z is progressively lost and this is generally correlated to a gain of DNA methylation (Conerly et al. 2010). Differential comparison on H2A.Z occupancy and DNA methylation between cell states shows that gain of H2A.Z occupancy at the gene body corresponds to a loss of DNA methylation in the transition from transformed cells to tumors. When 5-azacytidine, a cytosine analogue that inhibits DNMTs, is applied to mammalian culture cells, regional loss of DNA methylation corresponds to gain of

H2A.Z despite CG density (Yang et al. 2012). Moreover, mutual exclusion between H2A.Z and DNA methylation is observed in the entire gene region in puffer fish (Zemach et al. 2010). These data suggest the conserved anticorrelation relationship between H2A.Z occupancy and DNA methylation and a potential mechanism for the targeting of DNA methylation.

Dissertation Overview

We have characterized the epigenetic status in mature sperm and the genomic localization of H2afva in early embryos by using zebrafish as a model system.

Zebrafish use nucleosomes rather than protamine to package the sperm genome. Despite this difference, our studies reveal remarkable conservation between mammals and zebrafish in the use of distinctive chromatin states to package embryonic developmental regulators in sperm, including the use of coincident permissive and repressive modifications and DNA demethylation. In addition, we greatly extended the analysis of chromatin composition to several other histone modifications and a histone variant, showing contiguous block of "multivalent" programmatic chromatin build over the promoters (or full genes) for developmental regulators, suggesting a complex and robust packaging network. Furthermore, we find features in this germline chromatin not observed in ES cells or in the soma, including the presence of H3K36me3 in these large blocks at developmental regulators.

The genomic localization of H2afva is investigated by ChIP-seq in early embryos, before, during, and after zygotic genome activation. H2afva is enriched in the promoters of genes, including both early and late expressed genes in early embryos. This promoter-

enriched pattern in zebrafish is consistent with other vertebrates. Notably, H2afva profile in early embryos is very similar to that in sperm and potentially inherited from sperm. DNA methylation pattern is proposed to underlie embryo totipotency and pluripotency. Interestingly, we observed a strong anticorrelation between H2afva occupancy and DNA methylation in sperm and early embryos. These data suggest H2afva could potentially be a heritable epigenetic marker and sets up DNA methylation profiles of totipotency and pluripotency in early embryos.

References

Adam M, Robert F, Larochelle M, Gaudreau L. 2001. H2A.Z is required for global chromatin integrity and for recruitment of RNA polymerase II under specific conditions. *Mol Cell Biol* **21**(18): 6270–6279.

Agalioti T, Chen G, Thanos D. 2002. Deciphering the transcriptional histone acetylation code for a human gene. *Cell* **111**(3): 381–392.

Ahmad K, Henikoff S. 2002. Histone H3 variants specify modes of chromatin assembly. *Proc Natl Acad Sci* **99 Suppl 4**: 16477–16484.

Allis CD, Glover CV, Bowen JK, Gorovsky MA. 1980. Histone variants specific to the transcriptionally active, amitotically dividing macronucleus of the unicellular eucaryote, Tetrahymena thermophila. *Cell* **20**(3): 609–617.

Ang YS, Tsai SY, Lee DF, Monk J, Su J, Ratnakumar K, Ding J, Ge Y, Darr H, Chang B et al. 2011. Wdr5 mediates self-renewal and reprogramming via the embryonic stem cell core transcriptional network. *Cell* **145**(2): 183–197.

Banaszynski LA, Allis CD, Lewis PW. 2010. Histone variants in metazoan development. *Dev Cell* **19**(5): 662–674.

Barreto G, Schafer A, Marhold J, Stach D, Swaminathan SK, Handa V, Doderlein G, Maltry N, Wu W, Lyko F et al. 2007. Gadd45a promotes epigenetic gene activation by repair-mediated DNA demethylation. *Nature* **445**(7128): 671–675.

Barski A, Cuddapah S, Cui K, Roh TY, Schones DE, Wang Z, Wei G, Chepelev I, Zhao K. 2007. High-resolution profiling of histone methylations in the human genome. *Cell* **129**(4): 823–837.

Bernstein BE, Mikkelsen TS, Xie X, Kamal M, Huebert DJ, Cuff J, Fry B, Meissner A, Wernig M, Plath K et al. 2006. A bivalent chromatin structure marks key developmental genes in embryonic stem cells. *Cell* **125**(2): 315–326.

Bhutani N, Burns DM, Blau HM. 2011. DNA demethylation dynamics. *Cell* **146**(6): 866–872.

Bilodeau S, Kagey MH, Frampton GM, Rahl PB, Young RA. 2009. SetDB1 contributes to repression of genes encoding developmental regulators and maintenance of ES cell state. *Genes Dev* **23**(21): 2484–2489.

Bird A, Tate P, Nan X, Campoy J, Meehan R, Cross S, Tweedie S, Charlton J, Macleod D. 1995. Studies of DNA methylation in animals. *J Cell Sci Suppl* **19**: 37–39.

Bird AP. 1996. The relationship of DNA methylation to cancer. *Cancer Surv* **28**: 87–101.

Borgel J, Guibert S, Li Y, Chiba H, Schubeler D, Sasaki H, Forne T, Weber M. 2010. Targets and dynamics of promoter DNA methylation during early mouse development. *Nat Genet* **42**(12): 1093–1100.

Boyer LA, Plath K, Zeitlinger J, Brambrink T, Medeiros LA, Lee TI, Levine SS, Wernig M, Tajonar A, Ray MK et al. 2006. Polycomb complexes repress developmental regulators in murine embryonic stem cells. *Nature* **441**(7091): 349–353.

Brykczynska U, Hisano M, Erkek S, Ramos L, Oakeley EJ, Roloff TC, Beisel C, Schubeler D, Stadler MB, Peters AH. 2010. Repressive and active histone methylation mark distinct promoters in human and mouse spermatozoa. *Nat Struct Mol Biol* **17**(6): 679–687.

Cai Y, Jin J, Gottschalk AJ, Yao T, Conaway JW, Conaway RC. 2006. Purification and assay of the human INO80 and SRCAP chromatin remodeling complexes. *Methods* **40**(4): 312–317.

Cantone I, Fisher AG. 2013. Epigenetic programming and reprogramming during development. *Nat Struct Mol Biol* **20**(3): 282–289.

Cao R, Wang L, Wang H, Xia L, Erdjument-Bromage H, Tempst P, Jones RS, Zhang Y. 2002. Role of histone H3 lysine 27 methylation in Polycomb-group silencing. *Science* **298**(5595): 1039–1043.

Chambers I, Colby D, Robertson M, Nichols J, Lee S, Tweedie S, Smith A. 2003. Functional expression cloning of Nanog, a pluripotency sustaining factor in embryonic stem cells. *Cell* **113**(5): 643–655.

Clapier CR, Cairns BR. 2009. The biology of chromatin remodeling complexes. *Annu Rev Biochem* **78**: 273–304.

Clapier CR, Langst G, Corona DF, Becker PB, Nightingale KP. 2001. Critical role for the histone H4 N terminus in nucleosome remodeling by ISWI. *Mol Cell Biol* **21**(3): 875–883.

Clarkson MJ, Wells JR, Gibson F, Saint R, Tremethick DJ. 1999. Regions of variant histone His2AvD required for Drosophila development. *Nature* **399**(6737): 694–697.

Clouaire T, Webb S, Skene P, Illingworth R, Kerr A, Andrews R, Lee JH, Skalnik D, Bird A. 2012. Cfp1 integrates both CpG content and gene activity for accurate H3K4me3 deposition in embryonic stem cells. *Genes Dev* **26**(15): 1714–1728.

Conerly ML, Teves SS, Diolaiti D, Ulrich M, Eisenman RN, Henikoff S. 2010. Changes in H2A.Z occupancy and DNA methylation during B-cell lymphomagenesis. *Genome Res* **20**(10): 1383–1390.

Corona DF, Clapier CR, Becker PB, Tamkun JW. 2002. Modulation of ISWI function by site-specific histone acetylation. *EMBO Rep* **3**(3): 242–247.

Creyghton MP, Markoulaki S, Levine SS, Hanna J, Lodato MA, Sha K, Young RA, Jaenisch R, Boyer LA. 2008. H2AZ is enriched at Polycomb complex target genes in ES cells and is necessary for lineage commitment. *Cell* **135**(4): 649–661.

Cuthbert GL, Daujat S, Snowden AW, Erdjument-Bromage H, Hagiwara T, Yamada M, Schneider R, Gregory PD, Tempst P, Bannister AJ et al. 2004. Histone deimination antagonizes arginine methylation. *Cell* **118**(5): 545–553.

Deal RB, Topp CN, McKinney EC, Meagher RB. 2007. Repression of flowering in Arabidopsis requires activation of FLOWERING LOCUS C expression by the histone variant H2A.Z. *Plant Cell* **19**(1): 74–83.

Eirin-Lopez JM, Gonzalez-Romero R, Dryhurst D, Ishibashi T, Ausio J. 2009. The evolutionary differentiation of two histone H2A.Z variants in chordates (H2A.Z-1 and H2A.Z-2) is mediated by a stepwise mutation process that affects three amino acid residues. *BMC Evol Biol* **9**: 31.

Faast R, Thonglairoam V, Schulz TC, Beall J, Wells JR, Taylor H, Matthaei K, Rathjen PD, Tremethick DJ, Lyons I. 2001. Histone variant H2A.Z is required for early mammalian development. *Curr Biol* **11**(15): 1183–1187.

Farthing CR, Ficz G, Ng RK, Chan CF, Andrews S, Dean W, Hemberger M, Reik W. 2008. Global mapping of DNA methylation in mouse promoters reveals epigenetic reprogramming of pluripotency genes. *PLoS Genet* **4**(6): e1000116.

Ficz G, Branco MR, Seisenberger S, Santos F, Krueger F, Hore TA, Marques CJ, Andrews S, Reik W. 2011. Dynamic regulation of 5-hydroxymethylcytosine in mouse ES cells and during differentiation. *Nature* **473**(7347): 398–402.

Fuks F, Hurd PJ, Deplus R, Kouzarides T. 2003. The DNA methyltransferases associate with HP1 and the SUV39H1 histone methyltransferase. *Nucleic Acids Res* **31**(9): 2305–2312.

Gaspar-Maia A, Alajem A, Polesso F, Sridharan R, Mason MJ, Heidersbach A, Ramalho-Santos J, McManus MT, Plath K, Meshorer E et al. 2009. Chd1 regulates open chromatin and pluripotency of embryonic stem cells. *Nature* **460**(7257): 863–868.

Gevry N, Chan HM, Laflamme L, Livingston DM, Gaudreau L. 2007. p21 transcription is regulated by differential localization of histone H2A.Z. *Genes Dev* **21**(15): 1869–1881.

Gevry N, Hardy S, Jacques PE, Laflamme L, Svotelis A, Robert F, Gaudreau L. 2009. Histone H2A.Z is essential for estrogen receptor signaling. *Genes Dev* **23**(13): 1522–1533.

Guenther MG, Levine SS, Boyer LA, Jaenisch R, Young RA. 2007. A chromatin landmark and transcription initiation at most promoters in human cells. *Cell* **130**(1): 77–88.

Guillemette B, Bataille AR, Gevry N, Adam M, Blanchette M, Robert F, Gaudreau L. 2005. Variant histone H2A.Z is globally localized to the promoters of inactive yeast genes and regulates nucleosome positioning. *PLoS Biol* **3**(12): e384.

Hajkova P, Ancelin K, Waldmann T, Lacoste N, Lange UC, Cesari F, Lee C, Almouzni G, Schneider R, Surani MA. 2008. Chromatin dynamics during epigenetic reprogramming in the mouse germ line. *Nature* **452**(7189): 877–881.

Hajkova P, Erhardt S, Lane N, Haaf T, El-Maarri O, Reik W, Walter J, Surani MA. 2002. Epigenetic reprogramming in mouse primordial germ cells. *Mech Dev* **117**(1–2): 15–23.

Hajkova P, Jeffries SJ, Lee C, Miller N, Jackson SP, Surani MA. 2010. Genome-wide reprogramming in the mouse germ line entails the base excision repair pathway. *Science* **329**(5987): 78–82.

Hammoud SS, Nix DA, Zhang H, Purwar J, Carrell DT, Cairns BR. 2009. Distinctive chromatin in human sperm packages genes for embryo development. *Nature* **460**(7254): 473–478.

Hanna JH, Saha K, Jaenisch R. 2010. Pluripotency and cellular reprogramming: facts, hypotheses, unresolved issues. *Cell* **143**(4): 508–525.

Hardy S, Jacques PE, Gevry N, Forest A, Fortin ME, Laflamme L, Gaudreau L, Robert F. 2009. The euchromatic and heterochromatic landscapes are shaped by antagonizing effects of transcription on H2A.Z deposition. *PLoS Genet* **5**(10): e1000687.

Heard E, Rougeulle C, Arnaud D, Avner P, Allis CD, Spector DL. 2001. Methylation of histone H3 at Lys-9 is an early mark on the X chromosome during X inactivation. *Cell* **107**(6): 727–738.

Heby O. 1995. DNA methylation and polyamines in embryonic development and cancer. *Int J Dev Biol* **39**(5): 737–757.

Heintzman ND, Stuart RK, Hon G, Fu Y, Ching CW, Hawkins RD, Barrera LO, Van Calcar S, Qu C, Ching KA et al. 2007. Distinct and predictive chromatin signatures of transcriptional promoters and enhancers in the human genome. *Nat Genet* **39**(3): 311–318.

Ho L, Jothi R, Ronan JL, Cui K, Zhao K, Crabtree GR. 2009a. An embryonic stem cell chromatin remodeling complex, esBAF, is an essential component of the core pluripotency transcriptional network. *Proc Natl Acad Sci* **106**(13): 5187–5191.

Ho L, Miller EL, Ronan JL, Ho WQ, Jothi R, Crabtree GR. 2011. esBAF facilitates pluripotency by conditioning the genome for LIF/STAT3 signalling and by regulating Polycomb function. *Nat Cell Biol* **13**(8): 903–913.

Ho L, Ronan JL, Wu J, Staahl BT, Chen L, Kuo A, Lessard J, Nesvizhskii AI, Ranish J, Crabtree GR. 2009b. An embryonic stem cell chromatin remodeling complex, esBAF, is essential for embryonic stem cell self-renewal and pluripotency. *Proc Natl Acad Sci* **106**(13): 5181–5186.

Howell CY, Bestor TH, Ding F, Latham KE, Mertineit C, Trasler JM, Chaillet JR. 2001. Genomic imprinting disrupted by a maternal effect mutation in the Dnmt1 gene. *Cell* **104**(6): 829–838.

Hu G, Cui K, Northrup D, Liu C, Wang C, Tang Q, Ge K, Levens D, Crane-Robinson C, Zhao K. 2013. H2A.Z facilitates access of active and repressive complexes to chromatin in embryonic stem cell self-renewal and differentiation. *Cell Stem Cell* **12**(2): 180–192.

Huynh VA, Robinson PJ, Rhodes D. 2005. A method for the in vitro reconstitution of a defined "30 nm" chromatin fibre containing stoichiometric amounts of the linker histone. *J Mol Biol* **345**(5): 957–968.

Iouzalen N, Moreau J, Mechali M. 1996. H2A.ZI, a new variant histone expressed during Xenopus early development exhibits several distinct features from the core histone H2A. *Nucleic Acids Res* **24**(20): 3947–3952.

Jackson JD, Gorovsky MA. 2000. Histone H2A.Z has a conserved function that is distinct from that of the major H2A sequence variants. *Nucleic Acids Res* **28**(19): 3811–3816.

Jin C, Felsenfeld G. 2007. Nucleosome stability mediated by histone variants H3.3 and H2A.Z. *Genes Dev* **21**(12): 1519–1529.

Jin C, Zang C, Wei G, Cui K, Peng W, Zhao K, Felsenfeld G. 2009. H3.3/H2A.Z double variant-containing nucleosomes mark 'nucleosome-free regions' of active promoters and other regulatory regions. *Nat Genet* **41**(8): 941–945.

Johnson LM, Fisher-Adams G, Grunstein M. 1992. Identification of a non-basic domain in the histone H4 N-terminus required for repression of the yeast silent mating loci. *EMBO J* **11**(6): 2201–2209.

Jones PA. 2012. Functions of DNA methylation: islands, start sites, gene bodies and beyond. *Nat Rev Genet* **13**(7): 484–492.

Kasten M, Szerlong H, Erdjument-Bromage H, Tempst P, Werner M, Cairns BR. 2004. Tandem bromodomains in the chromatin remodeler RSC recognize acetylated histone H3 Lys14. *EMBO J* **23**(6): 1348–1359.

Kierszenbaum AL, Tres LL. 1975. Structural and transcriptional features of the mouse spermatid genome. *J Cell Biol* **65**(2): 258–270.

Kobor MS, Venkatasubrahmanyam S, Meneghini MD, Gin JW, Jennings JL, Link AJ, Madhani HD, Rine J. 2004. A protein complex containing the conserved Swi2/Snf2-Related ATPase Swr1p deposits histone variant H2A.Z into euchromatin. *PLoS Biol* **2**(5): E131.

Koh FM, Sachs M, Guzman-Ayala M, Ramalho-Santos M. 2010. Parallel gateways to pluripotency: open chromatin in stem cells and development. *Curr Opin Genet Dev* **20**(5): 492–499.

Kornberg RD. 1974. Chromatin structure: a repeating unit of histones and DNA. *Science* **184**(4139): 868–871.

Kouzarides T. 2007. Chromatin modifications and their function. *Cell* **128**(4): 693–705.

Krogan NJ, Baetz K, Keogh MC, Datta N, Sawa C, Kwok TC, Thompson NJ, Davey MG, Pootoolal J, Hughes TR et al. 2004. Regulation of chromosome stability by the histone H2A variant Htz1, the Swr1 chromatin remodeling complex, and the histone acetyltransferase NuA4. *Proc Natl Acad Sci* **101**(37): 13513–13518.

Krogan NJ, Keogh MC, Datta N, Sawa C, Ryan OW, Ding H, Haw RA, Pootoolal J, Tong A, Canadien V et al. 2003. A Snf2 family ATPase complex required for recruitment of the histone H2A variant Htz1. *Mol Cell* **12**(6): 1565–1576.

Ku M, Jaffe JD, Koche RP, Rheinbay E, Endoh M, Koseki H, Carr SA, Bernstein BE. 2012. H2A.Z landscapes and dual modifications in pluripotent and multipotent stem cells underlie complex genome regulatory functions. *Genome Biol* **13**(10): R85.

Lande-Diner L, Cedar H. 2005. Silence of the genes—mechanisms of long-term repression. *Nat Rev Genet* **6**(8): 648–654.

Lauberth SM, Nakayama T, Wu X, Ferris AL, Tang Z, Hughes SH, Roeder RG. 2013. H3K4me3 interactions with TAF3 regulate preinitiation complex assembly and selective gene activation. *Cell* **152**(5): 1021–1036.

Law JA, Jacobsen SE. 2010. Establishing, maintaining and modifying DNA methylation patterns in plants and animals. *Nat Rev Genet* **11**(3): 204–220.

Lee JH, Skalnik DG. 2002. CpG-binding protein is a nuclear matrix- and euchromatin-associated protein localized to nuclear speckles containing human trithorax. Identification of nuclear matrix targeting signals. *J Biol Chem* **277**(44): 42259–42267.

Lee JH, Skalnik DG. 2005. CpG-binding protein (CXXC finger protein 1) is a component of the mammalian Set1 histone H3-Lys4 methyltransferase complex, the analogue of the yeast Set1/COMPASS complex. *J Biol Chem* **280**(50): 41725–41731.

Lee TI, Jenner RG, Boyer LA, Guenther MG, Levine SS, Kumar RM, Chevalier B, Johnstone SE, Cole MF, Isono K et al. 2006. Control of developmental regulators by Polycomb in human embryonic stem cells. *Cell* **125**(2): 301–313.

Levine M. 2011. Paused RNA polymerase II as a developmental checkpoint. *Cell* **145**(4): 502–511.

Li B, Carey M, Workman JL. 2007. The role of chromatin during transcription. *Cell* **128**(4): 707–719.

Li B, Pattenden SG, Lee D, Gutierrez J, Chen J, Seidel C, Gerton J, Workman JL. 2005. Preferential occupancy of histone variant H2AZ at inactive promoters influences local histone modifications and chromatin remodeling. *Proc Natl Acad Sci* **102**(51): 18385–18390.

Li M, Liu GH, Izpisua Belmonte JC. 2012a. Navigating the epigenetic landscape of pluripotent stem cells. *Nat Rev Mol Cell Biol* **13**(8): 524–535.

Li Z, Gadue P, Chen K, Jiao Y, Tuteja G, Schug J, Li W, Kaestner KH. 2012b. Foxa2 and H2A.Z mediate nucleosome depletion during embryonic stem cell differentiation. *Cell* **151**(7): 1608–1616.

Lindeman LC, Andersen IS, Reiner AH, Li N, Aanes H, Ostrup O, Winata C, Mathavan S, Muller F, Alestrom P et al. 2011. Prepatterning of developmental gene expression by modified histones before zygotic genome activation. *Dev Cell* **21**(6): 993–1004.

Liu X, Li B, GorovskyMa. 1996. Essential and nonessential histone H2A variants in Tetrahymena thermophila. *Mol Cell Biol* **16**(8): 4305–4311.

Marks H, Kalkan T, Menafra R, Denissov S, Jones K, Hofemeister H, Nichols J, Kranz A, Stewart AF, Smith A et al. 2012. The transcriptional and epigenomic foundations of ground state pluripotency. *Cell* **149**(3): 590–604.

Marques M, Laflamme L, Gervais AL, Gaudreau L. 2010. Reconciling the positive and negative roles of histone H2A.Z in gene transcription. *Epigenetics* **5**(4): 267–272.

Martienssen RA, Rabinowicz PD, O'Shaughnessy A, McCombie WR. 2004. Sequencing the maize genome. *Curr Opin Plant Biol* **7**(2): 102–107.

Masui S, Nakatake Y, Toyooka Y, Shimosato D, Yagi R, Takahashi K, Okochi H, Okuda A, Matoba R, Sharov AA et al. 2007. Pluripotency governed by Sox2 via regulation of Oct3/4 expression in mouse embryonic stem cells. *Nat Cell Biol* **9**(6): 625–635.

Mavrich TN, Jiang C, Ioshikhes IP, Li X, Venters BJ, Zanton SJ, Tomsho LP, Qi J, Glaser RL, Schuster SC et al. 2008. Nucleosome organization in the Drosophila genome. *Nature* **453**(7193): 358–362.

Mayer W, Niveleau A, Walter J, Fundele R, Haaf T. 2000. Demethylation of the zygotic paternal genome. *Nature* **403**(6769): 501–502.

Meissner A, Mikkelsen TS, Gu H, Wernig M, Hanna J, Sivachenko A, Zhang X, Bernstein BE, Nusbaum C, Jaffe DB et al. 2008. Genome-scale DNA methylation maps of pluripotent and differentiated cells. *Nature* **454**(7205): 766–770.

Mendenhall EM, Koche RP, Truong T, Zhou VW, Issac B, Chi AS, Ku M, Bernstein BE. 2010. GC-rich sequence elements recruit PRC2 in mammalian ES cells. *PLoS Genet* **6**(12): e1001244.

Meneghini MD, Wu M, Madhani HD. 2003. Conserved histone variant H2A.Z protects euchromatin from the ectopic spread of silent heterochromatin. *Cell* **112**(5): 725–736.

Mhanni AA, McGowan RA. 2004. Global changes in genomic methylation levels during early development of the zebrafish embryo. *Dev Genes Evol* **214**(8): 412–417.

Mikkelsen TS, Ku M, Jaffe DB, Issac B, Lieberman E, Giannoukos G, Alvarez P, Brockman W, Kim TK, Koche RP et al. 2007. Genome-wide maps of chromatin state in pluripotent and lineage-committed cells. *Nature* **448**(7153): 553–560.

Millar CB, Xu F, Zhang K, Grunstein M. 2006. Acetylation of H2AZ Lys 14 is associated with genome-wide gene activity in yeast. *Genes Dev* **20**(6): 711–722.

Mizuguchi G, Shen X, Landry J, Wu WH, Sen S, Wu C. 2004. ATP-driven exchange of histone H2AZ variant catalyzed by SWR1 chromatin remodeling complex. *Science* **303**(5656): 343–348.

Muller J, Hart CM, Francis NJ, Vargas ML, Sengupta A, Wild B, Miller EL, O'Connor MB, Kingston RE, Simon JA. 2002. Histone methyltransferase activity of a Drosophila Polycomb group repressor complex. *Cell* **111**(2): 197–208.

Ng HH, Robert F, Young RA, Struhl K. 2003. Targeted recruitment of Set1 histone methylase by elongating Pol II provides a localized mark and memory of recent transcriptional activity. *Mol Cell* **11**(3): 709–719.

Ng HH, Surani MA. 2011. The transcriptional and signalling networks of pluripotency. *Nat Cell Biol* **13**(5): 490–496.

Nichols J, Zevnik B, Anastassiadis K, Niwa H, Klewe-Nebenius D, Chambers I, Scholer H, Smith A. 1998. Formation of pluripotent stem cells in the mammalian embryo depends on the POU transcription factor Oct4. *Cell* **95**(3): 379–391.

O'Carroll D, Erhardt S, Pagani M, Barton SC, Surani MA, Jenuwein T. 2001. The Polycomb-group gene Ezh2 is required for early mouse development. *Mol Cell Biol* **21**(13): 4330–4336.

Ooi SK, Qiu C, Bernstein E, Li K, Jia D, Yang Z, Erdjument-Bromage H, Tempst P, Lin SP, Allis CD et al. 2007. DNMT3L connects unmethylated lysine 4 of histone H3 to de novo methylation of DNA. *Nature* **448**(7154): 714–717.

Oswald J, Engemann S, Lane N, Mayer W, Olek A, Fundele R, Dean W, Reik W, Walter J. 2000. Active demethylation of the paternal genome in the mouse zygote. *Curr Biol* **10**(8): 475–478.

Pastor WA, Pape UJ, Huang Y, Henderson HR, Lister R, Ko M, McLoughlin EM, Brudno Y, Mahapatra S, Kapranov P et al. 2011. Genome-wide mapping of 5-hydroxymethylcytosine in embryonic stem cells. *Nature* **473**(7347): 394–397.

Placek BJ, Harrison LN, Villers BM, Gloss LM. 2005. The H2A.Z/H2B dimer is unstable compared to the dimer containing the major H2A isoform. *Protein Sci* **14**(2): 514–522.

Popp C, Dean W, Feng S, Cokus SJ, Andrews S, Pellegrini M, Jacobsen SE, Reik W. 2010. Genome-wide erasure of DNA methylation in mouse primordial germ cells is affected by AID deficiency. *Nature* **463**(7284): 1101–1105.

Potok ME, Nix DA, Parnell TJ, Cairns BR. 2013. Reprogramming the maternal zebrafish genome after fertilization to match the paternal methylation pattern. *Cell* **153**(4): 759–772.

Rai K, Huggins IJ, James SR, Karpf AR, Jones DA, Cairns BR. 2008. DNA demethylation in zebrafish involves the coupling of a deaminase, a glycosylase, and gadd45. *Cell* **135**(7): 1201–1212.

Rangasamy D, Berven L, Ridgway P, Tremethick DJ. 2003. Pericentric heterochromatin becomes enriched with H2A.Z during early mammalian development. *EMBO J* **22**(7): 1599–1607.

Rangasamy D, Greaves I, Tremethick DJ. 2004. RNA interference demonstrates a novel role for H2A.Z in chromosome segregation. *Nat Struct Mol Biol* **11**(7): 650–655.

Reddington JP, Pennings S, Meehan RR. 2013. Non-canonical functions of the DNA methylome in gene regulation. *Biochem J* **451**(1): 13–23.

Ridgway P, Brown KD, Rangasamy D, Svensson U, Tremethick DJ. 2004. Unique residues on the H2A.Z containing nucleosome surface are important for Xenopus laevis development. *J Biol Chem* **279**(42): 43815–43820.

Robinson PJ, Fairall L, Huynh VA, Rhodes D. 2006. EM measurements define the dimensions of the "30-nm" chromatin fiber: evidence for a compact, interdigitated structure. *Proc Natl Acad Sci* **103**(17): 6506–6511.

Ruthenburg AJ, Allis CD, Wysocka J. 2007. Methylation of lysine 4 on histone H3: intricacy of writing and reading a single epigenetic mark. *Mol Cell* **25**(1): 15–30.

Santisteban MS, Kalashnikova T, Smith MM. 2000. Histone H2A.Z regulates transcription and is partially redundant with nucleosome remodeling complexes. *Cell* **103**(3): 411–422.

Santos-Rosa H, Schneider R, Bannister AJ, Sherriff J, Bernstein BE, Emre NC, Schreiber SL, Mellor J, Kouzarides T. 2002. Active genes are tri-methylated at K4 of histone H3. *Nature* **419**(6905): 407–411.

Sarcinella E, Zuzarte PC, Lau PN, Draker R, Cheung P. 2007. Monoubiquitylation of H2A.Z distinguishes its association with euchromatin or facultative heterochromatin. *Mol Cell Biol* **27**(18): 6457–6468.

Schier AF, Talbot WS. 2005. Molecular genetics of axis formation in zebrafish. *Annu Rev Genet* **39**: 561–613.

Schneider R, Bannister AJ, Myers FA, Thorne AW, Crane-Robinson C, Kouzarides T. 2004. Histone H3 lysine 4 methylation patterns in higher eukaryotic genes. *Nat Cell Biol* **6**(1): 73–77.

Schuettengruber B, Chourrout D, Vervoort M, Leblanc B, Cavalli G. 2007. Genome regulation by Polycomb and trithorax proteins. *Cell* **128**(4): 735–745.

Schuettengruber B, Martinez AM, Iovino N, Cavalli G. 2011. Trithorax group proteins: switching genes on and keeping them active. *Nat Rev Mol Cell Biol* **12**(12): 799–814.

Schwartz YB, Pirrotta V. 2007. Polycomb silencing mechanisms and the management of genomic programmes. *Nat Rev Genet* **8**(1): 9–22.

Shahbazian MD, Grunstein M. 2007. Functions of site-specific histone acetylation and deacetylation. *Annu Rev Biochem* **76**: 75–100.

Sharif J, Endo TA, Ito S, Ohara O, Koseki H. 2013. Embracing change to remain the same: conservation of Polycomb functions despite divergence of binding motifs among species. *Curr Opin Cell Biol* **25**(3): 305–313.

Shilatifard A. 2006. Chromatin modifications by methylation and ubiquitination: implications in the regulation of gene expression. *Annu Rev Biochem* **75**: 243–269.

Simon J, Chiang A, Bender W, Shimell MJ, O'Connor M. 1993. Elements of the Drosophila bithorax complex that mediate repression by Polycomb group products. *Dev Biol* **158**(1): 131–144.

Sing A, Pannell D, Karaiskakis A, Sturgeon K, Djabali M, Ellis J, Lipshitz HD, Cordes SP. 2009. A vertebrate Polycomb response element governs segmentation of the posterior hindbrain. *Cell* **138**(5): 885–897.

Tahiliani M, Koh KP, Shen Y, Pastor WA, Bandukwala H, Brudno Y, Agarwal S, Iyer LM, Liu DR, Aravind L et al. 2009. Conversion of 5-methylcytosine to 5-hydroxymethylcytosine in mammalian DNA by MLL partner TET1. *Science* **324**(5929): 930–935.

Takahashi K, Tanabe K, Ohnuki M, Narita M, Ichisaka T, Tomoda K, Yamanaka S. 2007. Induction of pluripotent stem cells from adult human fibroblasts by defined factors. *Cell* **131**(5): 861–872.

Takahashi K, Yamanaka S. 2006. Induction of pluripotent stem cells from mouse embryonic and adult fibroblast cultures by defined factors. *Cell* **126**(4): 663–676.

Talbert PB, Henikoff S. 2010. Histone variants—ancient wrap artists of the epigenome. *Nat Rev Mol Cell Biol* **11**(4): 264–275.

Tam WL, Lim CY, Han J, Zhang J, Ang YS, Ng HH, Yang H, Lim B. 2008. T-cell factor 3 regulates embryonic stem cell pluripotency and self-renewal by the transcriptional control of multiple lineage pathways. *Stem Cells* **26**(8): 2019–2031.

Thompson JS, Ling X, Grunstein M. 1994. Histone H3 amino terminus is required for telomeric and silent mating locus repression in yeast. *Nature* **369**(6477): 245–247.

Thomson JP, Skene PJ, Selfridge J, Clouaire T, Guy J, Webb S, Kerr AR, Deaton A, Andrews R, James KD et al. 2010. CpG islands influence chromatin structure via the CpG-binding protein Cfp1. *Nature* **464**(7291): 1082–1086.

Tsai MC, Manor O, Wan Y, Mosammaparast N, Wang JK, Lan F, Shi Y, Segal E, Chang HY. 2010. Long noncoding RNA as modular scaffold of histone modification complexes. *Science* **329**(5992): 689–693.

Updike DL, Mango SE. 2006. Temporal regulation of foregut development by HTZ-1/H2A.Z and PHA-4/FoxA. *PLoS Genet* **2**(9): e161.

Valdes-Mora F, Song JZ, Statham AL, Strbenac D, Robinson MD, Nair SS, Patterson KI, Tremethick DJ, Stirzaker C, Clark SJ. 2012. Acetylation of H2A.Z is a key epigenetic modification associated with gene deregulation and epigenetic remodeling in cancer. *Genome Res* **22**(2): 307–321.

van Daal A, Elgin SC. 1992. A histone variant, H2AvD, is essential in Drosophila melanogaster. *Mol Biol Cell* **3**(6): 593–602.

Vastenhouw NL, Zhang Y, Woods IG, Imam F, Regev A, Liu XS, Rinn J, Schier AF. 2010. Chromatin signature of embryonic pluripotency is established during genome activation. *Nature* **464**(7290): 922–926.

Vermeulen M, Mulder KW, Denissov S, Pijnappel WW, van Schaik FM, Varier RA, Baltissen MP, Stunnenberg HG, Mann M, Timmers HT. 2007. Selective anchoring of TFIID to nucleosomes by trimethylation of histone H3 lysine 4. *Cell* **131**(1): 58–69.

Voo KS, Carlone DL, Jacobsen BM, Flodin A, Skalnik DG. 2000. Cloning of a mammalian transcriptional activator that binds unmethylated CpG motifs and shares a CXXC domain with DNA methyltransferase, human trithorax, and methyl-CpG binding domain protein 1. *Mol Cell Biol* **20**(6): 2108–2121.

Weber M, Hellmann I, Stadler MB, Ramos L, Paabo S, Rebhan M, Schubeler D. 2007. Distribution, silencing potential and evolutionary impact of promoter DNA methylation in the human genome. *Nat Genet* **39**(4): 457–466.

Woo CJ, Kharchenko PV, Daheron L, Park PJ, Kingston RE. 2010. A region of the human HOXD cluster that confers Polycomb-group responsiveness. *Cell* **140**(1): 99–110.

Wu SF, Zhang H, Cairns BR. 2011. Genes for embryo development are packaged in blocks of multivalent chromatin in zebrafish sperm. *Genome Res* **21**(4): 578–589.

Wu WH, Alami S, Luk E, Wu CH, Sen S, Mizuguchi G, Wei D, Wu C. 2005. Swc2 is a widely conserved H2AZ-binding module essential for ATP-dependent histone exchange. *Nat Struct Mol Biol*: 1064–1071.

Yang X, Noushmehr H, Han H, Andreu-Vieyra C, Liang G, Jones PA. 2012. Gene reactivation by 5-aza-2'-deoxycytidine-induced demethylation requires SRCAP-mediated H2A.Z insertion to establish nucleosome depleted regions. *PLoS Genet* **8**(3): e1002604.

Zemach A, McDaniel IE, Silva P, Zilberman D. 2010. Genome-wide evolutionary analysis of eukaryotic DNA methylation. *Science* **328**(5980): 916–919.

Zhang H, Roberts DN, Cairns BR. 2005. Genome-wide dynamics of Htz1, a histone H2A variant that poises repressed/basal promoters for activation through histone loss. *Cell* **123**(2): 219–231.

Zhao XY, Li W, Lv Z, Liu L, Tong M, Hai T, Hao J, Guo CL, Ma QW, Wang L et al. 2009. iPS cells produce viable mice through tetraploid complementation. *Nature* **461**(7260): 86–90.

Zhou J, Fan JY, Rangasamy D, Tremethick DJ. 2007. The nucleosome surface regulates chromatin compaction and couples it with transcriptional repression. *Nat Struct Mol Biol* **14**(11): 1070–1076.

Zilberman D, Coleman-Derr D, Ballinger T, Henikoff S. 2008. Histone H2A.Z and DNA methylation are mutually antagonistic chromatin marks. *Nature* **456**(7218): 125–129.

Zlatanova J, Thakar A. 2008. H2A.Z: view from the top. *Structure* **16**(2): 166–179.

Table 1.1 Summary of chromatin features and their associated transcriptional activity.

Chromatin feature	Associated transcriptional activity
DNA methylation	Repressed
H3K4me3	Active
H3K4me2	Active
H3K14ac	Active
H3K9ac	Active
H3K27me3	Repressed
H3K9me3	Repressed
H2AZ	Repressed/Poised
H3K4me3/H3K27me3	Repressed/Poised

CHAPTER 2

GENES FOR EMBRYO DEVELOPMENT ARE PACKAGED IN BLOCKS OF MULTIVALENT CHROMATIN IN ZEBRAFISH SPERM

Wu, et al., 2011. Originally published in Genome Research. VOL. 21(4): 578-89

Research

Genes for embryo development are packaged in blocks of multivalent chromatin in zebrafish sperm

Shan-Fu Wu, Haiying Zhang, and Bradley R. Cairns[1]

Howard Hughes Medical Institute, Department of Oncological Sciences, Huntsman Cancer Institute, University of Utah School of Medicine, Salt Lake City, Utah 84112, USA

In mature human sperm, genes of importance for embryo development (i.e., transcription factors) lack DNA methylation and bear nucleosomes with distinctive histone modifications, suggesting the specialized packaging of these developmental genes in the germline. Here, we explored the tractable zebrafish model and found conceptual conservation as well as several new features. Biochemical and mass spectrometric approaches reveal the zebrafish sperm genome packaged in nucleosomes and histone variants (and not protamine), and we find linker histones high and H4K16ac absent, key factors that may contribute to genome condensation. We examined several activating (H3K4me2/3, H3K14ac, H2AFV) and repressing (H3K27me3, H3K36me3, H3K9me3, hypoacetylation) modifications/compositions genome-wide and find developmental genes packaged in large blocks of chromatin with coincident activating and repressing marks and DNA hypomethylation, revealing complex "multivalent" chromatin. Notably, genes that acquire DNA methylation in the soma (muscle) are enriched in transcription factors for alternative cell fates. Remarkably, whereas H3K36me3 is located in the 3′ coding region of heavily transcribed genes in somatic cells, H3K36me3 is present in the promoters of "silent" developmental regulators in sperm, suggesting different rules for H3K36me3 in the germline and soma. We also reveal the chromatin patterns of transposons, rDNA, and tDNAs. Finally, high levels of H3K4me3 and H3K14ac in sperm are correlated with genes activated in embryos prior to the mid-blastula transition (MBT), whereas multivalent genes are correlated with activation at or after MBT. Taken together, gene sets with particular functions in the embryo are packaged by distinctive types of complex and often atypical chromatin in sperm.

[Supplemental material is available for this article. The microarray data from this study have been submitted to the NCBI Gene Expression Omnibus (http://www.ncbi.nlm.nih.gov/geo/) under accession no. GSE26609.]

A central question in early development is how totipotency and pluripotency are established in germline and embryonic stem (ES) cells, respectively. Studies in ES cells cultured in vitro have provided many interesting concepts for pluripotency, such as the use of special transcription factor combinations (POU5F1 [also known as OCT4], SOX2, others) that operate as a network to promote pluripotency and self renewal, and the presence of specialized chromatin at developmental regulators in ES cells to ensure their silencing and poising until later in development (Rao and Orkin 2006; Wang et al. 2006; Jaenisch and Young 2008; Kim et al. 2008). Due to technical limitations, little is known about the mechanisms underlying the totipotency of vertebrate eggs (Seydoux and Braun 2006), but multiple contributing mechanisms can be envisioned, including maternal RNAs (coding and noncoding) that promote totipotency, the loading and function of key transcription factor proteins (including pluripotency/self-renewal factors), and chromatin structures that enable (or prevent) the expression of particular embryonic developmental regulators.

Until recently, options (beyond DNA methylation) for the sperm genome to provide epigenetic contribution to totipotency appeared limited (Seydoux and Braun 2006), as spermatogenesis involves the replacement of the vast majority of the histone-based chromatin by protamine (Ward and Coffey 1991; Wykes and Krawetz 2003), which is not known to propagate information via modifications. One view is that the male genome need not carry any gene packaging information (beyond methylated imprinted genes), as it can simply be "reprogrammed" and repackaged by the egg following fertilization to achieve totipotency. One clear event in mice and humans involves active DNA demethylation of the paternal genome upon fertilization, prior to the fusion of the two nuclei and the onset of replication (Mayer et al. 2000; Oswald et al. 2000; Hajkova et al. 2008, 2010; Abdalla et al. 2009; Okada et al. 2010). Although this clearly occurs, we currently lack an understanding of which genes in the genome are susceptible or resistant to DNA demethylation, beyond the resistant imprinted genes. Indeed, a full understanding of the methylation state of the gametes before and after fertilization will be an important step forward.

Another view is that specialized gene packaging may indeed occur in sperm. Recently, a small percentage of the human and mouse genomes have been shown to remain enriched with modified nucleosomes in mature sperm (Arpanahi et al. 2009; Hammoud et al. 2009; Brykczynska et al. 2010). These studies revealed the packaging of the genes encoding most key embryonic developmental and morphogenesis regulators by nucleosomes with histone modifications that correlate both with activation and silencing. The observed silencing mark was trimethylation of lysine 27 on histone H3 (H3K27me3), a modification catalyzed by the PRC2 (Polycomb Repressive Complex 2) (Cao et al. 2002; Czermin et al. 2002; Kuzmichev et al. 2002; Muller et al. 2002). Resident activating marks included di- and trimethylation of lysine 4 on histone H3 (H3K4me2/3), a modification catalyzed in the soma by MLL, Set1, and Set7/9 histone methyltransferases (Byrd and Shearn 2003; Dou et al. 2005; Wysocka et al. 2005). The coincidence of these two marks is termed bivalency and has been

[1]**Corresponding author.**
E-mail brad.cairns@hci.utah.edu.
Article published online before print. Article, supplemental material, and publication date are at http://www.genome.org/cgi/doi/10.1101/gr.113167.110. Freely available online through the *Genome Research* Open Access option.

21:578–589 © 2011 by Cold Spring Harbor Laboratory Press; ISSN 1088-9051/11; www.genome.org

described previously at the promoters of developmental regulators in ES cells (Bernstein et al. 2006). These antagonistic marks are believed to help poise these genes in a repressed state. Furthermore, developmental regulators in human sperm are profoundly DNA demethylated (Down et al. 2008; Farthing et al. 2008; Hammoud et al. 2009), a result that makes the genome-wide demethylation of the paternal genome all the more curious, if needed (in part) for totipotency. Finally, genes that are involved in spermatogenesis and metabolic processes are solely coated with the active mark H3K4me3 in both human and mouse sperm (Hammoud et al. 2009; Brykczynska et al. 2010). Thus, human and mouse sperm display two very distinct chromatin patterns for two different classes of genes: active genes (in sperm) and embryonic transcription factors.

These studies prompt several key questions. First, why place embryonic developmental regulators in bivalent chromatin in mature sperm cells? One possibility is to poise these genes for expression in the embryo. Another possibility is to protect them from DNA methylation through the use of "activating" chromatin, while simultaneously placing repressive chromatin on them to prevent their expression in the germline (Bernstein et al. 2006; Okitsu and Hsieh 2007; Ooi et al. 2007; Ciccone et al. 2009). Another key question is the complexity of the packaging and marking of developmental genes. Also, one might expect this packaging/marking system, if indeed instructive, to require additional modifications or histone variants to maintain robustness in the embryo. Furthermore, is this system for gene packaging in sperm identical to the system already established in ES cells, or are there unique aspects to packaging developmental regulators in the germline? Finally, it is of high interest to understand how this packaging is established and maintained in the germline and whether a similar system exists in the egg.

To begin to investigate these questions, we turned to the zebrafish animal model, due to the ease of obtaining both sperm and eggs and to the possibilities for future genetic manipulation. One apparent difference between humans and zebrafish is the use (revealed below) of nucleosomes rather than protamine to package the sperm genome. In spite of this difference, our studies reveal remarkable conservation between humans and zebrafish in the use of distinctive chromatin states to package embryonic developmental regulators in sperm, including the use of coincident activating and silencing modifications, and DNA demethylation. In addition, we greatly extended the analysis of chromatin composition to several other histone modifications and a histone variant, showing contiguous blocks of "multivalent" programmatic chromatin built over the promoters (or full genes) for developmental regulators, suggesting a complex and robust packaging network. Furthermore, we find features in this germline chromatin not observed in ES cells or in the soma, including the presence of H3K36me3 in these large blocks at developmental regulators.

Results

Biochemical composition of the zebrafish sperm genome

We began by characterizing the proteins that package the genome of mature zebrafish sperm. Sperm cells were collected from sexually mature males, which exhibited a sperm head morphology more rounded than those derived from mammals, suggesting an alternative compaction strategy (Fig. 1A). Chromatin preparations from sperm and a zebrafish fibroblast cell line were analyzed by SDS-PAGE, revealing prominent bands migrating at the exact size and distribution of histones. Mass spectrometric analysis revealed

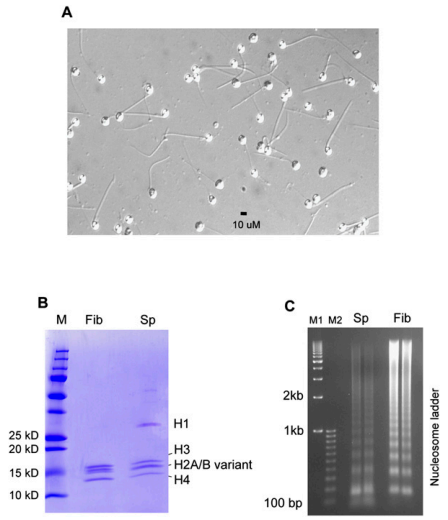

Figure 1. Sperm morphology and biochemical composition of zebrafish sperm chromatin. (*A*) Zebrafish sperm have a round head morphology (~10-μM diameter). (*B*) Whole-cell extracts were prepared from sperm and fibroblasts (ZF4) by lysing cells in 2× SDS-PAGE sample buffer. SDS-PAGE analysis of the cell extracts reveals a shared canonical histone pattern, with sperm displaying a higher level of linker histones. Histone components in sperm were verified by mass spectrometry (Supplemental Table 1). (*C*) Internucleosomal distances are longer in zebrafish sperm. Nucleosomes in sperm and fibroblasts (ZF4) were released by MNase digestion, and the DNA was analyzed by agarose gel electrophoresis and staining with EtBr (duplicate loading for each sample). Sperm displayed a longer average internucleosomal distance, 50 bp, than did the fibroblast, 40 bp. M indicates protein marker; Sp, sperm; Fib, fibroblast; and M1 and M2, DNA markers start from 1 kb with 1-kb increments and from 100 bp in 100-bp increments, respectively.

the presence of the canonical histones H2A, H2B, H3, and H4, as well as certain canonical histone variants (H2AFX, and H2AFV), and linker H1 histones and variants (related to human HISTH1C, -D, and -E; and H1FX; H1F0) (Fig. 1B; Supplemental Table 1), known to package the somatic genome. Here, we note that Western analysis reveals the clear presence of H1 linker histone in ZF4 fibroblasts, but at levels that are about 25% of those in sperm, normalized for ploidy (Supplemental Fig. 1A,B). Somewhat surprisingly, protamine, transition proteins, and testis-specific histone variants—proteins that constitute the vast majority of proteins in mammalian sperm—were not identified in zebrafish sperm, either through acid-urea gel analysis (data not shown) or mass spectrometry. Furthermore, the current zebrafish genome (Zv8) lacks the structural genes encoding orthologs of mammalian testis-specific histones, transition proteins, or protamine; though we note the presence of a gene distantly-related to protamine (zgc:114104, 492 amino acids), of unknown function and not detected in our sperm chromatin preparations. Consistent with the lack of protamine, the round head morphology of mature zebrafish sperm is similar to the "round spermatid" stage of human sperm development, the stage preceding protamine replacement of histones. Taken together, the mature zebrafish sperm genome is packaged by histones but contains a higher relative level of linker histone than does a somatic cell (Fig. 1B).

Sperm genome packaging and condensation

As zebrafish sperm lack protamine, one interesting question is how the genome is condensed to a moderately-high level in zebrafish sperm. As previewed above, sperm chromatin has abundant linker histone H1 variants, appearing nearly stoichiometric with histone octamers (Fig. 1B). Linker histones promote higher-order chromatin compaction, bind nucleosomes in a 1:1 ratio to form "chromatosomes," and increase the average nucleosome repeat length (Huynh et al. 2005; Robinson et al. 2006; Zhou et al. 2007). To determine repeat length, nucleosomes from sperm or fibroblast cells were released by limited micrococcal nuclease (MNase) digestion (Fig. 1C), revealing a longer average internucleosomal distance in sperm (50 bp) than fibroblasts (40 bp), consistent with global H1 packaging in sperm (Godde and Ura 2009). Our interpretation is that zebrafish sperm, in comparison to fibroblasts, have a higher proportion of their genome in chromatosomes as opposed to nucleosomes.

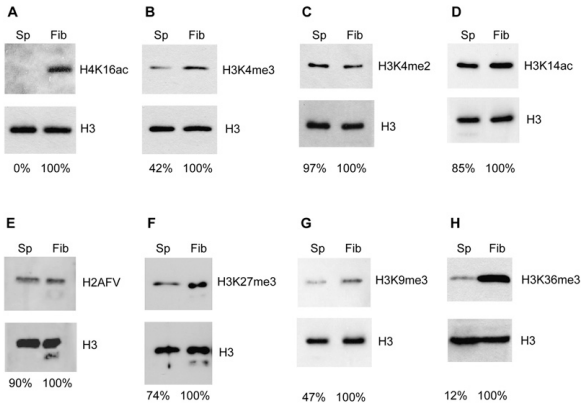

Figure 2. Bulk levels of histone modifications and histone variants in sperm. Immunoblotting was applied to quantify the level of modifications in sperm by comparing to ZF4 fibroblast cells and normalizing with H3 levels. (*A*) H4K16ac is not detected in sperm. (*B–H*) The levels of active and repressive marks and a histone variant (H2AFV/H2A.Z) in sperm compared with ZF4 fibroblast cells.

A second mode of promoting compaction was suggested through our analysis of histone modifications. The histone modification most closely associated with regulating compaction is the acetylation of lysine 16 on histone H4 (H4K16ac), which alone deters the transition of 10-nm nucleosome arrays to more compact 30-nm fibers (Shogren-Knaak et al. 2006; Zhou et al. 2007; Robinson et al. 2008; Kan et al. 2009). Furthermore, H4K16ac uniquely antagonizes the chromatin remodeling ATPases (ISWI- and CHD-family) responsible for organizing nucleosomes in ordered arrays of consistent spacing (Clapier et al. 2001; Corona et al. 2002). Remarkably, immunoblot analyses demonstrate that H4K16ac is virtually absent in zebrafish sperm chromatin (Fig. 2A; Supplemental Fig. 1C), a result of distinction given the relative abundance of other histone modifications in zebrafish sperm (detailed below). We note that H4R3me2 is robustly detected (Supplemental Fig. 1D), ensuring that the H4 tail is present and intact in zebrafish sperm chromatin. Furthermore, we detect in the zebrafish male gonad (data not shown) robust expression of the two zebrafish orthologs of the human ISWI family members SMARCA1 and SMARCA5. These results raise the possibility that zebrafish sperm promotes genome condensation by utilizing linker histones and the lack of H4K16ac, which coordinate with assembly remodelers to promote compaction in somatic cells.

Active and repressive histone modifications in zebrafish sperm chromatin

Histone modifications in sperm chromatin were assessed by comparison to levels in fibroblasts by immunoblotting (normalized to histone H3 levels) (Supplemental Fig. 1B). We find the common "repressive/silencing" modifications (those correlated with gene silencing) such as H3K9me3 and H3K27me3 present and at levels comparable to or slightly lower than that of fibroblasts (Fig. 2F,G). We note that mature sperm of humans and mice are transcriptionally inactive and lack RNA polymerase (Pol) II (Miteva et al. 1995; Naz 1998; Grootegoed et al. 2000; data not shown). In keeping, we find RNA Pol II barely detectable in zebrafish sperm (<0.5% the level in fibroblasts). Nevertheless, sperm chromatin retains "active/positive" histone modifications (those correlated with gene activity/competency) at levels within twofold of fibroblasts, including H3K4me3, H3K4me2, and H3K14ac (Fig. 2B–D)—though as discussed above, H4K16ac is absent. Furthermore, levels of the histone variant H2AFV (ortholog of H2A.Z in mammals), which has been linked with gene poising and chromatin boundaries (Meneghini et al. 2003; Zhang et al. 2005), are comparable in sperm and fibroblasts (Fig. 2E). Thus, sperm chromatin resembles somatic chromatin in bulk levels of the many active and repressive histone modifications tested, as well as a key histone variant.

Approaches for localizing histone modifications and DNA methylation

Chromatin immunoprecipitation (ChIP) and methylated DNA immunoprecipitation (MeDIP) were performed in mature sperm to localize histone modifications and DNA methylation, respectively. From native sperm chromatin, nucleosomes were released by MNase digestion to mainly di- and mononucleosomes and utilized for ChIP, involving multiple modification-specific antibodies (Supplemental Fig. 2). For MeDIP, sperm DNA was purified and sheared into fragments (~400 bp) and then immunoprecipitated with anti-5-methylcytosine antibodies (Weber et al. 2007). Following amplification and labeling (see Methods), the ChIP eluate and input were then hybridized to customized zebrafish promoter arrays that tiled (at 250-bp resolution) 12 kb of the promoter region of about 13,000 genes, as well as many other chromosomal elements and loci (miRNAs, repetitive sequences, tRNAs, etc.) to provide a genome-wide perspective of chromatin packaging. Enriched loci were determined and ranked, and enriched gene promoters were subjected to Gene Ontology (GO) term analyses, summarized in Table 1 (for full lists, see Supplemental Materials; for GO analyses, see Methods).

Table 1. Summary of enriched gene categories for particular chromatin marks and a histone variant

H3K27me3	Brain development Neuron fate specification Ear morphogenesis Endocrine system development Regulation of transcription
H2AFV	Endocrine system development Hindbrain development Embryonic morphogenesis Regulation of cellular protein metabolic process Regulation of transcription
H3K4me2[a]	Chromosome organization Cell division Cellular metabolic process Chromatin assembly Nucleosome assembly
H3K4me3[a]	Cell cycle Microtubule based process Cellular protein catabolic process M phase Flagellum organization
H3K14ac[a]	Microtubule based process Intracellular transport Protein modification process M phase Protein metabolic process
H3K36me3	Regulation of transcription RNA biosynthetic process Central nervous system development Regulation of metabolic process Developmental process
DNA hypomethylated genes in sperm	Central nervous system development Regulation of transcription Regulation of biosynthetic process Developmental process Organ development

Top five nonredundant gene categories were retrieved from GO analyses. FDR < 0.001; enrichment fold over random > 2.0 unless otherwise specified.
[a]FDR between 0.0001 and 0.2.

Multivalent and regional chromatin packages developmental loci

One clear and striking feature of our chromatin maps is regional blocks of coincident "multivalent" chromatin at developmental transcription factors utilized in embryonic development. First, blocks of H3K27me3 are strikingly enriched at developmental loci, a feature most clearly evident at *hox* loci (but not at flanking genes) and also evident at stand-alone transcription factors, with varying degrees of spreading (Fig. 3A–C; Table 1; Supplemental Table 2). Remarkably, of the 250 loci most enriched with H3K27me3, 90% are the promoters of embryonic transcription factors, including the vast majority of homeobox, T-box, GATA, and ETS family members (Fig. 3A,B; Supplemental Table 3). In addition, the promoters of many embryonic signaling molecules also displayed H3K27me3 enrichment, including *shha*, *fgf8a*, *wnt1*, and *wnt10b* genes (Fig. 3C). Indeed, GO analysis of the top 800 enriched loci generates almost exclusively developmental gene classes with high significance (Supplemental Table 2).

Interestingly, we observe general coincidence of H3K27me3 with the histone variant H2AFV (the zebrafish ortholog of mammalian H2A.Z) at developmental loci (Fig. 3A–C; top 250 genes, Supplemental Table 4); intersecting of the respective top 800 genes displays a 40% overlap (correlation *P*-value < 0.001). GO term analysis showed H2AFV is highly enriched at the promoters of genes involved in transcription and developmental processes (Table 1; Supplemental Table 5), in keeping with previous observations in stem cells (Creyghton et al. 2008).

Notably, H3K4me2 and H3K4me3 are moderately enriched at developmental loci bearing H3K27me3 (Supplemental Table 3). H3K4me2/3 levels at developmental loci are higher than at average promoters (2.3- or 2.0-fold higher for H3K4me3 and H3K4me2, respectively) and coincident with H3K27me3 (Fig. 3A–C). This aligns with the observations in human sperm and ES cells of the presence of "bivalent domains"—coincident H3K4me3 and H3K27me3—on the orthologous developmental regulators (Bernstein et al. 2006; Mikkelsen et al. 2007). To address whether H3K27me3 and H3K4me3 are present on the same nucleosome and at high density, we performed a sequential ChIP experiment using mononucleosomes from sperm. However, this procedure failed to provide enrichment (data not shown), suggesting that most nucleosomes do not contain both marks, a result supported by experiments described later suggesting that H3K4me3 is only at moderate density at developmental genes, while H3K27me3 is at high density. Curiously, certain gene clusters are enriched in H3K4me3 while also deficient in H3K4me2 (i.e., *hoxb* and *hoxd* clusters, but not *hoxa*) (Fig. 3A; Supplemental Fig. 3A,B), suggesting precise and regional H3K4me states at certain loci. Finally, developmental loci lack significant H3K14ac enrichment, a mark correlated with transcription in somatic cells (Supplemental Table 3), and also generally lack significant enrichment of the repressive mark H3K9me3 (data not shown), a mark present at other types of repressed loci, described later.

Taken together, the vast majority of developmental transcription factors, as well as considerable number of key signaling proteins, is bound by coincident blocks of H3K27me3, H3K4me2/3, and H2AFV but lacks significant H3K14ac enrichment. These blocks can extend for tens of kilobases at clustered gene loci, whereas at stand-alone transcription factors genes, the blocks are typically 2–5 kb (with variation), extending from the TSS into the proximal promoter and sometimes encompassing the entire gene.

Pronounced DNA hypomethylation at developmental loci

Although the bulk zebrafish sperm genome is hypermethylated (Mhanni and McGowan 2004), GO analysis reveals three categories of DNA hypomethylated promoters (false discovery rate [FDR] < 0.1%): developmental regulators, transcription factors, and metabolism/biosynthesis (Table 1; Fig. 3A–C; Supplemental Table 6). Indeed, the top 250 hypomethylated genes are dominated by embryonic transcription factors (Supplemental Table 7). One example is the *hoxa* locus, where hypomethylation covers almost the entire locus (Fig. 3A). This observation extends beyond the clustered developmental transcription factors to many stand-alone developmental regulators (Fig. 3B). DNA hypomethylation at developmental loci in sperm was further confirmed by bisulfite sequencing (Supplemental Fig. 4), which revealed a nearly quantitative absence of methylation. To identify loci that acquire methylation in development, we compared DNA methylation profiles in sperm to a differentiated cell type, adult zebrafish muscle. These examinations revealed extensive methylation of developmental transcription factor promoters not expressed in muscle cells (almost all *hox* genes), but the lack of methylation at the *mef2* and *hoxa13* promoters, which are expressed in muscle (Fig. 3; data not shown).

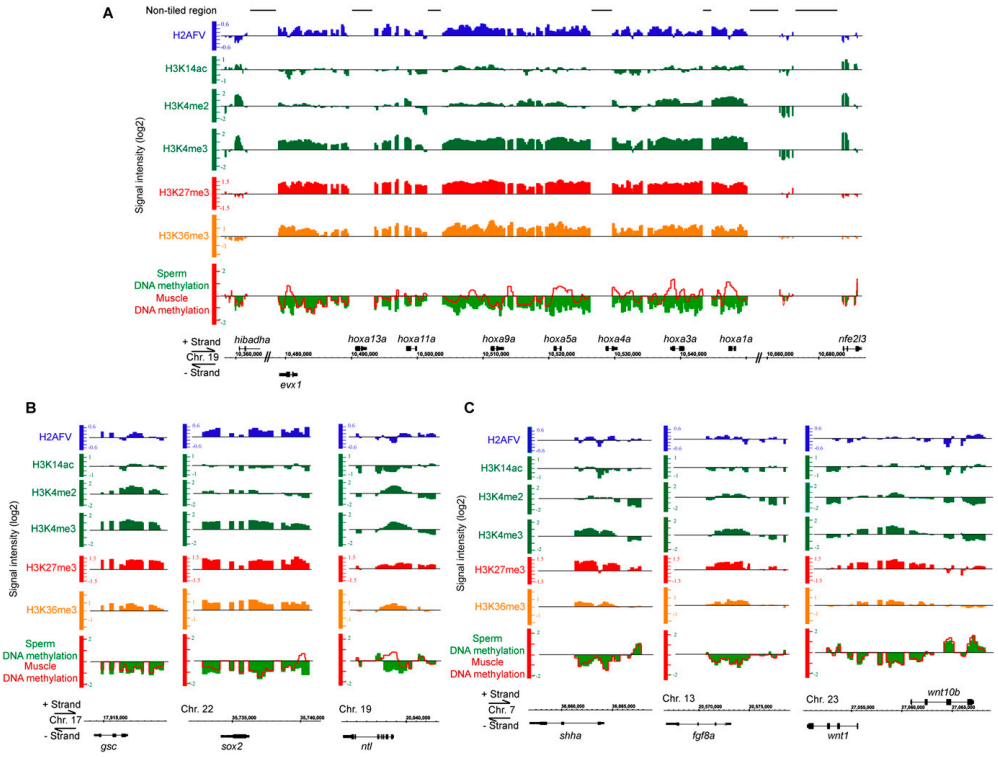

Figure 3. Developmental loci contain multivalent and regional chromatin features. ChIP-chip and MeDIP-chip profiles of developmental loci, with fold enrichment over input in $\log_2$ scale (*y*-axis). (*A*) *hoxa* cluster. Lines *above* the tracks indicate nontiled regions on the array. (*B*) Stand-alone transcription factors: *gsc*, *sox2*, and *ntl*. (C) Signaling factors: *shha*, *fgf8a*, *wnt1*, and *wnt10b*. Distance between minor scales is 500 bp. Chr indicates chromosome.

Indeed, 35% of the top 250 genes that acquire DNA methylation in their proximal promoter region in muscle cells are developmental regulators such as transcription factors (Supplemental Table 8). In contrast, along the majority of the genome, DNA methylation profiles are virtually superimposable in sperm and muscle (Supplemental Fig. 3C). The acquisition of methylation at developmental promoters in muscle was further confirmed by bisulfite sequencing (Supplemental Fig. 4). Together, these results suggest that development in zebrafish is accompanied by the methylation of developmental loci for alternative transcription programs.

We find multivalent chromatin and DNA hypomethylation residing at the promoters of the vast majority of developmental transcription factors and a large number of signaling factors in zebrafish sperm. Exceptions to this include the promoters for the transcription factors *atoh7*, *atoh2a*, *pou1f1*, *foxn1*, *tal2*, and *gata1a*, among others (data not shown). Notably, these genes are not generally expressed during early patterning or organ specification but rather are expressed during or after segmentation—with many of these types of factors being expressed during the later stages of eye, thymus, blood, or neuronal development. Thus, the multivalent chromatin may be more important for helping to regulate gene expression in early embryos than during terminal differentiation. Furthermore, the promoters of a subset of signaling factors such as *wnt5b*, *fgf10*, *egf*, and *bmp7* are also not marked with H3K27me3 (or H3K4me2/3) and are DNA methylated (data not shown). However, we have not identified a clear biological or temporal attribute of this group of signaling factors that might underlie their alternative marking, but these loci are of interest to examine for DNA demethylation in embryos.

Loci bearing high levels of multiple active marks in zebrafish sperm

We find the general coincidence of the three active marks tested (H3K4me3, H3K4me2, and H3K14ac), as pairwise intersection analyses of their respective top 250 enriched genes show significant overlap (~25%–35%; $P < 0.001$) (Supplemental Tables 9–11). GO analysis reveals H3K4me3 and H3K14ac significantly (FDR <10%) enriched at the promoters of housekeeping genes and genes for sperm-specific processes, including flagella/microtubules, catabolic processes, regulation of M-phase, DNA repair, and nucleotide metabolism (Table 1; Supplemental Tables 12, 13). Intuitively,

their presence at genes for sperm-related functions likely represents retention of chromatin modifications from spermatogenesis. Thus, to provide proper context, developmental loci show only low-moderate enrichment with H3K4me2/3 (2.0- to 2.5-fold) in comparison to the gene categories for sperm-specific processes (H3K4me2/3, 4.0- to 5.0-fold; H3K14ac, 2.3-fold). Finally, we observed one large and curious region on chromosome 19 with a continuous block of very high H3K14ac extending through genes and intergenics, including the genes *daxx* and *sdha* and certain protease subunits (data not shown).

Atypical placement of H3K36me3 in zebrafish sperm

Methylation on H3K36 is catalyzed by Set2-family methyltransferases, and deposition is generally coupled with RNA Pol II elongation (Krogan et al. 2003; Carrozza et al. 2005; Joshi and Struhl 2005; Keogh et al. 2005), leading to H3K36me3 placement along gene bodies. In yeast, H3K36me3 recruits the Rpd3S complex bearing histone deacetylase (HDAC) activity to prevent spurious transcription in the coding region.

Remarkably, we do not observe H3K36me3 on the coding regions of genes known to be expressed during spermatogenesis and genes displaying robust levels of H3K4me3 and H3K14ac at their TSS, known marks of transcriptional activity (Fig. 4A). Rather, we find H3K36me3 at two types of loci. The type with the highest levels of H3K36me3 is found at certain repetitive genes (*U6* genes) and elements (Fig. 4B). The second enriched type has clear H3K36me3 in regional blocks and is coincident with developmental loci (Fig. 3A-C). This is most strikingly observed at the clustered *hox* gene loci and also at divergent developmental genes, which display clear enrichment of H3K36me3 in the intergenic, such as the divergent *wnt1-wnt10* genes (Fig. 3C). We found 137 unique genes overlapping or adjacent to high levels of H3K36me3 (more than 2.7-fold enriched) (Supplemental Table 14), and of these, over 37% are categorized into transcription and developmental processes (FDR < 0.001) (Supplemental Table 15). Intersection analyses show that H3K36me3 in gene promoters is strongly correlated with H3K27me3, H2AFV, or H3K4me3 (each correlation $P < 0.001$) (Supplemental Fig. 5), but not with H3K14ac—properties evident at developmental genes (Fig. 3). Here, sequential ChIP was performed to test H3K36me3 and H3K27me3 coincidence, and co-enrichment was observed at the promoter region of several developmental regulators tested (Supplemental Fig. 6). These correlation data and localization of H3K36me3 indicate a potential repressive role for H3K36me3 in zebrafish sperm. Importantly, genes with H3K36me3 lack significant H3K14ac in zebrafish sperm, consistent with observations in somatic cells (Figs. 3A–C, 5C; Carrozza et al. 2005; Bell et al. 2007). This raises the possibility that in spite of its atypical placement, H3K36me3 in the germline might still recruit HDACs to help silence loci. Notably, the atypical placement of H3K36me3 is not restricted to clustered genes, as stand-alone developmental transcription and signaling factors contain blocks of H3K36me3 in their promoter region, coincident with H3K27me3, H3K4me2/3, and H2AFV (Fig. 3B,C).

The presence of H3K36me3 enrichment at intergenics and gene promoters/5′ ends has not been reported previously in vertebrates. This anomaly is not simply species specificity, as zebrafish late embryos display typical H3K36me3 profiles involving enrichment at 3′ ends of transcribed genes (Vastenhouw et al. 2010), a result confirmed here (Supplemental Fig. 7A). One question is which methyltransferase is responsible for the placement of atypical H3K36me3. Previous work in mice and humans has revealed additional H3K36 methyltransferases, including *nsd1* and *nsd2* (Wang et al. 2007). We find the orthologs *nsd1a*, *nsd1b*, and *nsd2* expressed in zebrafish testis (data not shown), revealing candidates for future investigation.

As H3K36me3 distribution was atypical, we therefore examined H3K36me2 at selected genes. We examined two genes expressed in spermatogenesis (*bactin2*, *ddx5*) by ChIP-qPCR and found H3K36me2 higher in their coding regions than their 5′ ends (Supplemental Fig. 7B). Furthermore, the levels of H3K36me2 in coding regions of expressed genes were much higher than were levels detected at two developmental genes (*gsc*, *klf4*) that are not expressed in spermatogenesis (Supplemental Fig. 7B). Therefore, the distribution of H3K36me2 in sperm appears similar in concept to somatic cells, whereas the distribution of H3K36me3 is atypical; though for H3K36me2, we have only examined a few genes and have not extended this examination genome-wide.

Chromatin features of repeat regions and noncoding RNAs

Our arrays included various regions of the genome, enabling an analysis of chromatin profiles in repetitive regions, *5S/5.8S* rDNA repeats, tRNAs, and tRNA clusters. We emphasize that the majority of the regions discussed in this section are nonunique and that chromatin maps derived from array formats represent a class average of the element described. First, we find that type 1 transposons (LINE) are typically DNA methylated and deficient in the activating marks tested but are (somewhat surprisingly) not enriched in any of the repressive marks tested (including H3K9me3), nor are they deficient in H3K14ac (Supplemental Fig. 8A). Type 2 transposons (SINE) displayed a similar pattern, though with only moderate levels of DNA methylation (Supplemental Fig. 8B). We note that our examination of data sets from human T cells (Barski et al. 2007) likewise does not generally reveal H3K9me3 at LINE or SINE elements (data not shown). In counter-distinction, we find the repeated genes encoding the noncoding RNAs *U1* and *U6* highly DNA-methylated and associated with particular silencing marks (high H3K36me3 and moderate H3K9me3), while highly deficient in activating marks (H3K4me2/3, H3K14ac, or H2AFV) and lacking H3K27me3 (Fig. 4B). A similar pattern is noted for the zebrafish *5S* and *5.8S* rRNA repeats, although *5.8S* rDNA repeats display much higher levels of H3K9me3 than do the *5S* repeats and lack H2AFV deficiency (Supplemental Fig. 8C,D). In contrast, our examination of data sets from human T cells (Barski et al. 2007) reveals a general lack of H3K9me3 at the *U1/U6* and *5S/5.8S* loci, suggesting some differences in the packaging of repetitive loci in zebrafish and humans. The tRNA clusters all showed profiles similar to that of the *U1/U6* repeats, while most stand-alone tRNAs were found in regions of active chromatin—bearing moderate to high levels of H3K14ac and H3K4me2/3 while lacking H3K27me3, H3K9me3, or H3K36me3 (Supplemental Fig. 8E,F). This partitioning of tRNAs into very different chromatin environments (active or repressive) is reminiscent of recent studies in human cells, where those tRNAs in active chromatin environments were occupied by the RNA Pol III machinery and those unoccupied by Pol III were in repressive chromatin (Oler et al. 2010).

Transcripts retained in mature sperm and their chromatin profiles

Mature sperm of vertebrates are transcriptionally inert (Miteva et al. 1995; Naz 1998; Grootegoed et al. 2000). Consistent with this

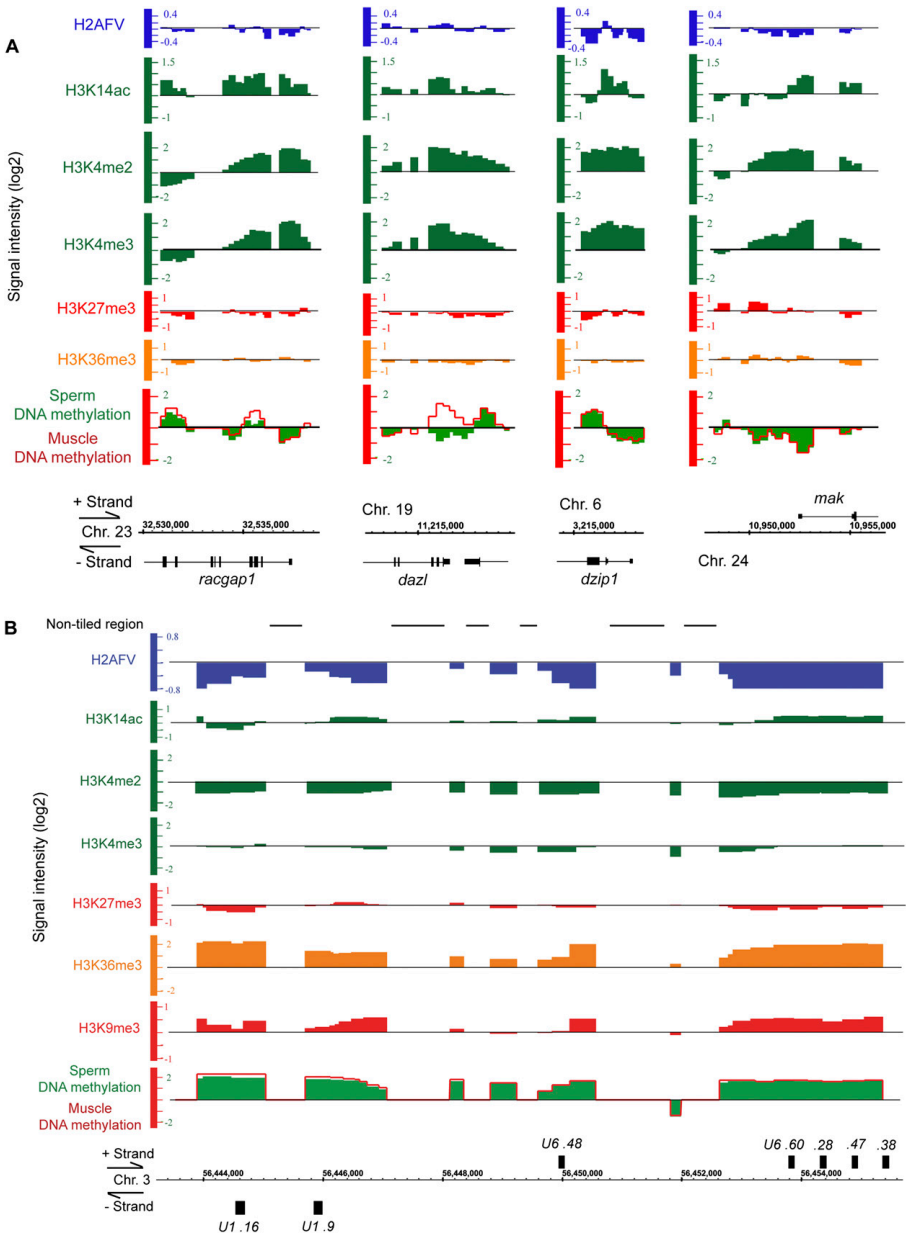

Figure 4. Chromatin features of genes expressed during spermatogenesis and of repetitive regions reveal atypical use of H3K36me3. (*A*) Genes involved in spermatogenesis show strong enrichment of active marks, but not H3K36me3 or other repressive marks. (*B*) *U1* and *U6* repetitive genes are enriched with H3K36me3, DNA methylation, and the repressive mark, H3K9me3.

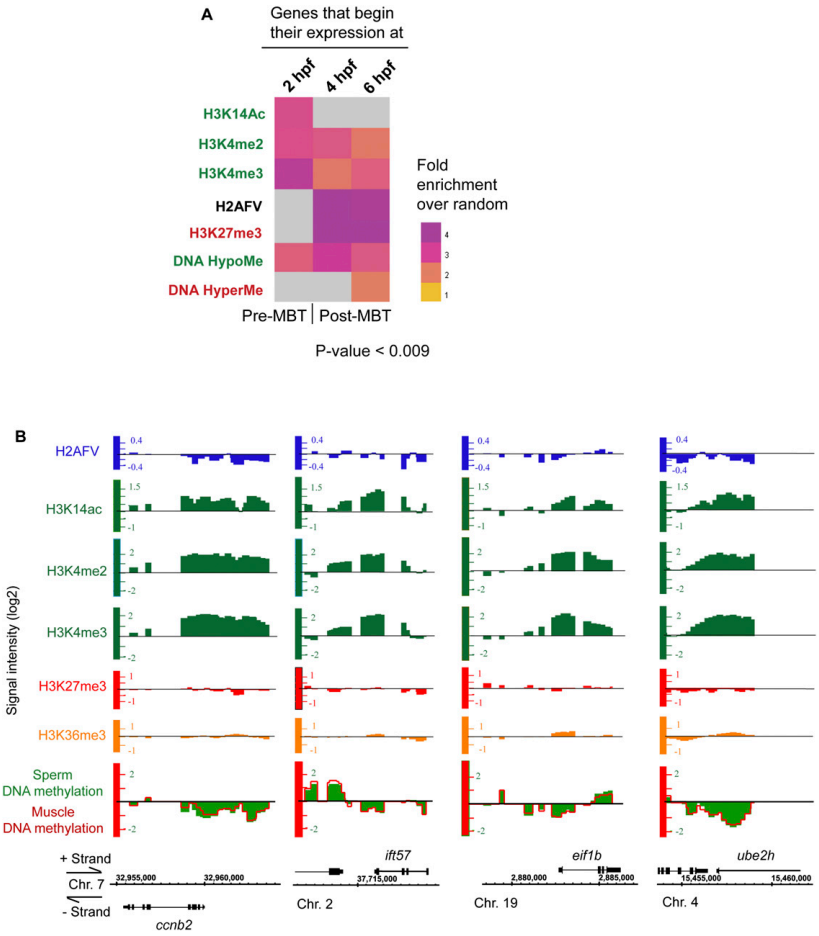

Figure 5. Certain chromatin modification patterns in sperm correlate with the timing of embryonic gene expression. (*A*) Heat map showing the correlations between genes that initiate expression at particular times during early development (2-hpf, 4-hpf, and 6-hpf columns from Mathavan et al. 2005) and particular histone modifications (or H2AFV enrichment) present at those genes in sperm (rows). Here, the color gradient shows the level of fold enrichment (over random) of a pairwise intersection between the list of expressed genes (Supplemental Table 18), and the list of genes with the respective histone modification/composition. A lack of significant intersection is depicted with a gray box. Genes expressed early/before MBT tend to have the highest levels of active histone modifications (acetylation and H3K4me2/3) in sperm, and those expressed after MBT tend to have repressive modifications (H3K27me3) in sperm. (*B*) Genes expressed before/early in MBT (3 hpf in zebrafish) are those that drive the cell cycle and promote metabolism, and are enriched with high levels of active histone modifications.

observation, RNA Pol II protein levels in mature sperm are barely detectable (<0.5% compared with fibroblasts) (data not shown). In spite of this, we reasoned that an examination of transcript profiles of mature sperm might reflect, in part, the recent transcriptional program of spermatocytes and spermatogenesis and might also correlate with regions of active chromatin retained following the cessation of transcription. To this end, we performed expression profiling by microarray, and enriched RNAs (more than 5.8-fold over background) were retrieved, yielding 1731 genes, which revealed largely genes predicted to be highly expressed (encoding ribosomal proteins, actin, tubulin, etc.) (Supplemental Table 16). As expected, transcripts in mature sperm were well correlated with active chromatin marks (H3K4me2/3 or H3K14ac) and DNA hypomethylation (all $P < 0.01$), but not with the repressive mark H3K27me3 or the poising mark H2AFV (Fig. 4A; Supplemental Table 17).

Sperm chromatin features and timing of gene expression in embryos

Previous work suggests that a small number of loci might be transcribed before or during an early phase of the mid-blastula transition (MBT), the time when general zygotic transcription initiates in the embryo (Mathavan et al. 2005). These genes include factors that promote the cell cycle and those that assist with RNA translation and metabolism, whose increased levels might help prepare cells for handling the RNAs generated during zygotic transcription. One possibility is that genes that are transcribed prior to (or early in) the MBT in zebrafish (3 h post-fertilization [hpf]) might have been marked in the sperm with particular chromatin modifications or histone variants that might help facilitate their early activation in the embryo. Although certain marks/proteins are likely lost at fertilization (see Discussion), some might be retained and instructive. Here, we reasoned that if marking in the sperm does occur, then genes that contain high levels of active marks in mature sperm might be correlated with the genes activated prior to general zygotic transcription. We find that genes bearing active histone marks (H3K4me2/3 or H3K14ac) in sperm are indeed correlated with an early zygotic expression profile (genes that others defined as initiating their expression at 2 hpf) (Fig. 5A; Mathavan et al. 2005). We note that genes that drive the cell cycle and promote metabolism in very early embryos bear very high levels of active histone marks in sperm (Table 1; Fig. 5B). In contrast, genes in sperm bearing high levels of the repressive mark H3K27me3 and also the histone variant H2AFV are better correlated with a post-MBT expression profile, when developmental regulators begin to be expressed (Fig. 5A; exemplified in Fig. 3A–C). Genes that lack DNA methylation in sperm are correlated with embryonic transcription, both pre- and post-MBT, but better with post-MBT. In conclusion, although a causal relationship has not been established, we do observe correlations between chromatin modification patterns in sperm and gene expression timing in embryos.

Discussion

Zebrafish sperm utilize nucleosomes and linker histones for packaging

Our goals are to understand chromatin-transcription relationships and their contributions to totipotency in germ cells and early embryos, and here we explore the zebrafish model. We find that zebrafish packages its sperm genome in nucleosomes rather than protamine, which is widely utilized in mammals. Curiously, sperm genome packaging systems utilized in teleost fish vary widely; some utilize only histone, while others use protamine or protamine-like proteins (Shimizu et al. 2000). At present, it is not clear why certain fish utilize particular packaging strategies, as they cannot be partitioned on simple attributes such as salt versus fresh water. However, our analysis of histone modification states and packaging composition suggest an intuitive strategy for the compaction of the histone genome involving the coordinated use of nucleosomes lacking H4K16ac, various linker histones, and possibly ISWI-type remodelers—based on extensive work on this process in somatic cells. We note that the packaging of the sperm genome by nucleosomes prevents its effectiveness as a model for understanding the histone–protamine transition. However, as discussed below, zebrafish appear very similar to humans in their packaging of genes important for embryonic development, suggesting they may serve as an important model for developmental gene packaging and marking.

Features of gene packaging in germ cells and ES cells

Key issues in germ cells include understanding the mechanisms for totipotency and the relative contributions of the egg and sperm genomes to this process. Here, chromatin structure could play an important role, given its known roles in gene regulation and gene poising. Currently, little is known in vertebrate eggs regarding the chromatin structure that packages the key embryonic self-renewal and developmental transcription factors. However, previous work in mature human and mouse sperm has revealed that genes of importance for embryo development (i.e., transcription factors) lack DNA methylation and bear nucleosomes with distinctive histone modifications, suggesting the specialized packaging and/or poising of developmental genes in the germline (Weber et al. 2007; Down et al. 2008; Farthing et al. 2008; Arpanahi et al. 2009; Hammoud et al. 2009; Brykczynska et al. 2010). This packaging is similar in some respects to their packaging in ES cells, as they share H3K4me3/H3K27me3 "bivalency," DNA hypomethylation near the TSS, and the presence of H2AFV (Bernstein et al. 2006; Creyghton et al. 2008; Fouse et al. 2008). These similarities strongly suggest some degree of overlap in the chromatin mechanisms that contribute to the pluripotency of ES cells and totipotency in germ cells. This also raises the interesting possibility that the chromatin signatures of totipotency arose initially in the germline—and were then largely maintained (or re-established) to achieve pluripotency in somatic cells.

Furthermore, our studies extend on those before to reveal considerable additional complexity in gene packaging in sperm, as well as features thus far unique to germ cells. First, our examination of multiple modifications argues for complex "multivalent" chromatin involving multiple positive and negative marks. Likewise, we speculate that additional histone modifications and packaging proteins might be present at developmental genes in ES cells and contribute to the robustness of their transcription states.

Also, whereas developmental genes in human or mouse ES cells display bivalency in a relatively narrow range near the TSS of genes (Bernstein et al. 2006; Mikkelsen et al. 2007; Hammoud et al. 2009; Brykczynska et al. 2010), *hox* loci in zebrafish sperm display a contiguous block of modifications that typically (though not uniformly) extend throughout the locus. For stand-alone transcription factors in sperm, blocks of multivalent chromatin are also present and typically extend over many kilobases. The size and typical uniformity of these chromatin blocks strongly suggests a program for their establishment in the germline. Although the mechanistic basis for this program (including the targeting, establishment, and maintenance) has not been determined, we speculate that the self-renewal factors may have roles in targeting chromatin, based on a precedent in ES cells for the targeting and establishment of bivalent chromatin (Boyer et al. 2005, 2006a,b; Orkin 2005; Welstead et al. 2008). Another outstanding question is how these regions are bounded, as the boundaries for this chromatin are often quite sharp, raising the possibility of a boundary factor such as CTCF. Further work in this area will involve an examination of the packaging of these genes in spermatogonial stem cells.

H3K36me3 at developmental genes and relationships to transcription

Remarkably, we find H3K36me3 located in developmental gene promoters in sperm and not present at the 3′ ends of coding regions of genes, even when examining genes heavily transcribed in spermatogenesis and spermiogenesis. Our results raise multiple

possibilities, which are not mutually exclusive. One possibility is that the rules for H3K36me3 deposition are the same in the germline and soma—with H3K36me laid down during Pol II elongation (Krogan et al. 2003; Keogh et al. 2005)—but that histone demethylases remove the mark from highly transcribed genes before sperm cell maturation. Another possibility is that the Set2d histone H3K36 methyltransferase, or a Set2 paralog such as *nsd1/2*, does not methylate highly transcribed genes but instead methylates genes inside the chromatin domains of developmental genes (such as *hox* clusters) in a manner independent of transcription. Finally, one attractive but speculative model is that the promoters of developmental loci (and perhaps more extensive regions at clustered *hox* loci) are briefly and promiscuously transcribed in the germline, leading to blocks of overlapping H3K4me2/3, H3K27me3, and H3K36me3 patterns. By this model, the observed chromatin patterns are dependent on initial promiscuous transcription (generating H3K4me3 in initiation regions and H3K36me in elongation regions), followed by the silencing of the gene by the attraction of PRC2/H3K27 by the nascent RNAs produced (Zhao et al. 2008; Lee 2009; Tsai et al. 2010) and deacetylation through resident H3K36me3 and its recruitment of HDACs (Carrozza et al. 2005; Joshi and Struhl 2005; Keogh et al. 2005).

The purpose of zebrafish sperm chromatin

Loci of developmental importance in the embryo bear complex multivalent chromatin in sperm and resemble several ways the chromatin present at these loci during MBT, when developmental loci must be repressed but able to be activated (Hammoud et al. 2009; Lindeman et al. 2010; Vastenhouw et al. 2010). Indeed, work from several laboratories now suggests that totipotent/pluripotent states of the germline and embryos share at developmental promoters unmethylated and complex "multivalent" chromatin (Hammoud et al. 2009; Lindeman et al. 2010; Vastenhouw et al. 2010). A clear question is whether this complex multivalent chromatin built in the sperm is needed solely for the proper gene regulation in the germline, or whether this multivalent chromatin (or any portion) is maintained and instructive in the embryo. One clear role for complex multivalent chromatin in the germline is to repress the many fate-determining developmental embryonic transcription factors. However, this does not explain the presence at these genes of positive marks such as H3K4me2/3 and H2AFV, which one would expect to be absent if the sole purpose is repression. Alternatively, we speculate that the negative marks are indeed present to repress these genes in the germline but that the positive marks are present to prevent DNA methylation of these loci, as even modest DNA methylation might bias these genes for repression in the embryo. This notion is in keeping with previous results that both H3K4me3 and H2A.Z/H2AFV are strongly anti-correlated with DNA methylation (Okitsu and Hsieh 2007; Weber et al. 2007; Zilberman et al. 2008).

The next issue is whether the epigenetic marks other than DNA methylation (histone modifications and variants) are maintained in the embryo and are instructive. We observe correlations of chromatin marking in sperm with expression in the embryo, which might suggest the use of a chromatin memory to instruct expression timing. However, for two reasons, these data must be interpreted with caution. First, the genes with high H3K4me3 and H3K14ac in sperm that are transcribed prior to MBT are strongly transcribed in virtually every somatic cell type, so early expression might be a result of their exceptionally strong promoters, not prior marking in the sperm. Second, recent experiments in zebrafish have demonstrated that the bulk levels of H3K4me3 and H3K27me3 are greatly diminished between fertilization and MBT, and these reductions also occur at developmental genes (Vastenhouw et al. 2010). Furthermore, these marks are then visible again after MBT, thus re-establishing this signature of pluripotency after zygotic transcription. As they are diminished prior to MBT, these two marks cannot solely be instructive for regulating the timing of gene activation.

However, our description of multivalent chromatin raises the possibility that one or more of the alternative marks, histone variants, or possibly noncoding RNAs may still be maintained and utilized to affect gene expression, though this remains to be tested. However, we note that if a mark/protein does persist, it must have a mechanism for self-renewal as new histones deposited during each cell division must be newly marked. An alternative view proposed previously (Vastenhouw et al. 2010) is of a naïve chromatin genome prior to MBT—with developmental loci completely unmarked prior to MBT and with chromatin modifiers (like H3K4 MTases) targeted to these loci at or just prior to MBT. A blending of these mechanisms is also possible, with the use of transcription factors to gain access to the open chromatin soon after fertilization, which then help facilitate the reestablishment of those chromatin marks and RNA Pol II recruitment at MBT. Future experiments will help distinguish between these and other models.

Methods

Zebrafish stocks and cells

The wild-type zebrafish line (Tübingen) and ZF4 cells (zebrafish fibroblast cells) were maintained as described previously (Rai et al. 2007). Sperm cells were collected from sexually mature zebrafish males by standard procedures (Westerfield 2000).

Western blotting and antibodies

The sperm or fibroblasts were counted using a hemacytometer, washed with PBS, and then lysed in 2× sample buffer. Western blotting was done according to standard procedures. Antibodies were as follows: H3K4me3 (Abcam ab8580 and Active Motif 39159), H3K4me2 (Abcam ab7766), H3K14Ac (Upstate 07-353), H2AZ (Abcam ab4174), H3K27me3 (Upstate 07-449), H3K9me3 (Active Motif 39161), H3K36me3 (Abcam ab9050), H3K36me2 (Abcam ab9049), H4K16Ac (Abcam ab1762), H4tetraAc (Upstate 06-866), and H3 (Abcam ab1791).

MeDIP, ChIP, and sequential ChIP

The procedures of MeDIP and ChIP were described previously (Hammoud et al. 2009). Briefly, for MeDIP, 4 μg of sheared genomic DNA (~400 bp) from mature sperm cells or dissected muscle tissues was incubated with Dynabeads (Invitrogen) conjugated with antibody against 5-methylcytidine (Eurogentec BI-MECY-1000). For ChIP, 10^7 of sperm cells was treated with 0.05% lysophosphatidylcholine (Sigma L1381) in PBS on ice for 10 min. Fifteen units of MNase (USB 70196Y) was then applied to release oligonucleosomes for 5 min at 37°C. Two micrograms of specific antibody conjugated to Dynabeads was incubated with the oligonucleosomes. The pulled-down fragments and input from MeDIP and ChIP were amplified by whole-genome amplification kit (Sigma WGA2), labeled with cy3 or cy5, and then hybridized to customized Agilent 244k-feature slides. Two biological replicas were used for each ChIP and labeled with dye swap.

For sequential ChIP, 2×10^7 of sperm cells was crosslinked and lysed in sperm cell lysis buffer (50 mM Tris at pH 8.0, 10 mM EDTA, 1 mM EGTA, 150 mM NaCl, 1% SDS, 3 mM DTT). The lysate was diluted with IP dilution buffer (16.7 mM Tris at pH 8.0, 167 mM NaCl, 1.2 mM EDTA, 1.1% Triton X-100, 0.01% SDS) and sheared by sonication to obtain fragments of mononucleosome size. Antibody was applied to first IP as above. After washing out the nonspecific binding, chromatin-associated beads were incubated in elution buffer (30 mM DTT, 0.1% SDS, 500 mM NaCl) for 15 min at 37°C. The eluate was diluted 30-fold with IP dilution buffer for the second IP and then treated as in standard IP procedures (Bernstein et al. 2006).

Customized zebrafish promoter microarray

The customized zebrafish promoter microarray, Z-array+, was adapted from the Whitehead zebrafish promoter chipsets (Wardle et al. 2006), by adding hundreds of additional genes and genetic elements. Z-array+ constitutes of a pair of 244,000 feature arrays with 60-mer oligos tiled an average 250 bp in the extended promoter region (−9 to +3 kb) of approximately 13,000 mRNA genes, miRNAs, tRNAs, rRNAs, repeat elements, CpG islands, and two centromeric heterochromatin regions.

RNA extraction and expression microarray

As in standard procedures (Westerfield 2000), mature sperm cells were screened under a microscope. RNA from 6×10^7 of mature sperm cells was extracted with a Qiagen RNA isolation kit. The zebrafish gene expression microarray (Agilent) includes 43,803 probes covering approximately 21,500 genes.

Data availability

The data have been deposited in the Gene Expression Omnibus (GEO) under accession number GSE26609. The processed data are available for programmatic access using the GenoPub DAS/2 data distribution server (description, http://bioserver.hci.utah.edu/BioInfo/index.php/Software:DAS2; GenoPub web app, http://bioserver.hci.utah.edu:8080/DAS2DB/genopub (type "guest" for both the user name and password); and the DAS/2 Data Access URL, http://bioserver.hci.utah.edu:8080/DAS2DB/genome). DAS/2 compliant genome browsers such as IGB (http://www.bioviz.org/igb/) can be used to view the data sets, found under *Danio rerio*→D_rerio_Jul_2007→Wu_2011.

Acknowledgments

We thank G. Bell (Whitehead Institute) for the design of a majority of the microarray probes, D. Nix for computational analysis and discussion, B. Dalley for microarray expertise, T. Parnell for technical advice, B. Demarest for imaging help, I. Jafri for initial validation of MeDIP, V. Khoddami for bisulfite sequencing, J. Hansen for H3K36me3 qPCR, and S. Hammoud for comments. Financial support was provided by NIH 5R01HD058506 and the Howard Hughes Medical Institute. We are grateful for grant CA24014 to the Huntsman Cancer Institute for support of core facilities. B.R.C. is an investigator with HHMI.

Note added in proof

Two studies have recently shown the deposition of H3K36me in a transcription-independent manner in the germline of *C. elegans* (Furuhashi et al. 2010; Rechtsteiner et al. 2010).

References

Abdalla H, Yoshizawa Y, Hochi S. 2009. Active demethylation of paternal genome in mammalian zygotes. *J Reprod Dev* **55:** 356–360.

Arpanahi A, Brinkworth M, Iles D, Krawetz SA, Paradowska A, Platts AE, Saida M, Steger K, Tedder P, Miller D. 2009. Endonuclease-sensitive regions of human spermatozoal chromatin are highly enriched in promoter and CTCF binding sequences. *Genome Res* **19:** 1338–1349.

Barski A, Cuddapah S, Cui K, Roh TY, Schones DE, Wang Z, Wei G, Chepelev I, Zhao K. 2007. High-resolution profiling of histone methylations in the human genome. *Cell* **129:** 823–837.

Bell O, Wirbelauer C, Hild M, Scharf AN, Schwaiger M, MacAlpine DM, Zilbermann F, van Leeuwen F, Bell SP, Imhof A, et al. 2007. Localized H3K36 methylation states define histone H4K16 acetylation during transcriptional elongation in *Drosophila*. *EMBO J* **26:** 4974–4984.

Bernstein BE, Mikkelsen TS, Xie X, Kamal M, Huebert DJ, Cuff J, Fry B, Meissner A, Wernig M, Plath K, et al. 2006. A bivalent chromatin structure marks key developmental genes in embryonic stem cells. *Cell* **125:** 315–326.

Boyer LA, Lee TI, Cole MF, Johnstone SE, Levine SS, Zucker JP, Guenther MG, Kumar RM, Murray HL, Jenner RG, et al. 2005. Core transcriptional regulatory circuitry in human embryonic stem cells. *Cell* **122:** 947–956.

Boyer LA, Mathur D, Jaenisch R. 2006a. Molecular control of pluripotency. *Curr Opin Genet Dev* **16:** 455–462.

Boyer LA, Plath K, Zeitlinger J, Brambrink T, Medeiros LA, Lee TI, Levine SS, Wernig M, Tajonar A, Ray MK, et al. 2006b. Polycomb complexes repress developmental regulators in murine embryonic stem cells. *Nature* **441:** 349–353.

Brykczynska U, Hisano M, Erkek S, Ramos L, Oakeley EJ, Roloff TC, Beisel C, Schubeler D, Stadler MB, Peters AH. 2010. Repressive and active histone methylation mark distinct promoters in human and mouse spermatozoa. *Nat Struct Mol Biol* **17:** 679–687.

Byrd KN, Shearn A. 2003. ASH1, a *Drosophila* trithorax group protein, is required for methylation of lysine 4 residues on histone H3. *Proc Natl Acad Sci* **100:** 11535–11540.

Cao R, Wang L, Wang H, Xia L, Erdjument-Bromage H, Tempst P, Jones RS, Zhang Y. 2002. Role of histone H3 lysine 27 methylation in Polycomb-group silencing. *Science* **298:** 1039–1043.

Carrozza MJ, Li B, Florens L, Suganuma T, Swanson SK, Lee KK, Shia WJ, Anderson S, Yates J, Washburn MP, et al. 2005. Histone H3 methylation by Set2 directs deacetylation of coding regions by Rpd3S to suppress spurious intragenic transcription. *Cell* **123:** 581–592.

Ciccone DN, Su H, Hevi S, Gay F, Lei H, Bajko J, Xu G, Li E, Chen T. 2009. KDM1B is a histone H3K4 demethylase required to establish maternal genomic imprints. *Nature* **461:** 415–418.

Clapier CR, Langst G, Corona DF, Becker PB, Nightingale KP. 2001. Critical role for the histone H4 N terminus in nucleosome remodeling by ISWI. *Mol Cell Biol* **21:** 875–883.

Corona DF, Clapier CR, Becker PB, Tamkun JW. 2002. Modulation of ISWI function by site-specific histone acetylation. *EMBO Rep* **3:** 242–247.

Creyghton MP, Markoulaki S, Levine SS, Hanna J, Lodato MA, Sha K, Young RA, Jaenisch R, Boyer LA. 2008. H2AZ is enriched at polycomb complex target genes in ES cells and is necessary for lineage commitment. *Cell* **135:** 649–661.

Czermin B, Melfi R, McCabe D, Seitz V, Imhof A, Pirrotta V. 2002. Drosophila enhancer of Zeste/ESC complexes have a histone H3 methyltransferase activity that marks chromosomal Polycomb sites. *Cell* **111:** 185–196.

Dou Y, Milne TA, Tackett AJ, Smith ER, Fukuda A, Wysocka J, Allis CD, Chait BT, Hess JL, Roeder RG. 2005. Physical association and coordinate function of the H3 K4 methyltransferase MLL1 and the H4 K16 acetyltransferase MOF. *Cell* **121:** 873–885.

Down TA, Rakyan VK, Turner DJ, Flicek P, Li H, Kulesha E, Graf S, Johnson N, Herrero J, Tomazou EM, et al. 2008. A Bayesian deconvolution strategy for immunoprecipitation-based DNA methylome analysis. *Nat Biotechnol* **26:** 779–785.

Farthing CR, Ficz G, Ng RK, Chan CF, Andrews S, Dean W, Hemberger M, Reik W. 2008. Global mapping of DNA methylation in mouse promoters reveals epigenetic reprogramming of pluripotency genes. *PLoS Genet* **4:** e1000116. doi: 10.1371/journal.pgen.1000116.

Fouse SD, Shen Y, Pellegrini M, Cole S, Meissner A, Van Neste L, Jaenisch R, Fan G. 2008. Promoter CpG methylation contributes to ES cell gene regulation in parallel with Oct4/Nanog, PcG complex, and histone H3 K4/K27 trimethylation. *Cell Stem Cell* **2:** 160–169.

Furuhashi H, Takasaki T, Rechtsteiner A, Li T, Kimura H, Checchi PM, Strome S, Kelly WG. 2010. Trans-generational epigenetic regulation of *C. elegans* primordial germ cells. *Epigenetics Chromatin* **3:** 15. doi: 10.1186/1756-8935-3-15.

Godde JS, Ura K. 2009. Dynamic alterations of linker histone variants during development. *Int J Dev Biol* **53:** 215–224.

Grootegoed JA, Siep M, Baarends WM. 2000. Molecular and cellular mechanisms in spermatogenesis. *Best Pract Res Clin Endocrinol Metab* **14:** 331–343.
Hajkova P, Ancelin K, Waldmann T, Lacoste N, Lange UC, Cesari F, Lee C, Almouzni G, Schneider R, Surani MA. 2008. Chromatin dynamics during epigenetic reprogramming in the mouse germ line. *Nature* **452:** 877–881.
Hajkova P, Jeffries SJ, Lee C, Miller N, Jackson SP, Surani MA. 2010. Genome-wide reprogramming in the mouse germ line entails the base excision repair pathway. *Science* **329:** 78–82.
Hammoud SS, Nix DA, Zhang H, Purwar J, Carrell DT, Cairns BR. 2009. Distinctive chromatin in human sperm packages genes for embryo development. *Nature* **460:** 473–478.
Huynh VA, Robinson PJ, Rhodes D. 2005. A method for the in vitro reconstitution of a defined "30 nm" chromatin fibre containing stoichiometric amounts of the linker histone. *J Mol Biol* **345:** 957–968.
Jaenisch R, Young R. 2008. Stem cells, the molecular circuitry of pluripotency and nuclear reprogramming. *Cell* **132:** 567–582.
Joshi AA, Struhl K. 2005. Eaf3 chromodomain interaction with methylated H3-K36 links histone deacetylation to Pol II elongation. *Mol Cell* **20:** 971–978.
Kan PY, Caterino TL, Hayes JJ. 2009. The H4 tail domain participates in intra- and internucleosome interactions with protein and DNA during folding and oligomerization of nucleosome arrays. *Mol Cell Biol* **29:** 538–546.
Keogh MC, Kurdistani SK, Morris SA, Ahn SH, Podolny V, Collins SR, Schuldiner M, Chin K, Punna T, Thompson NJ, et al. 2005. Cotranscriptional set2 methylation of histone H3 lysine 36 recruits a repressive Rpd3 complex. *Cell* **123:** 593–605.
Kim J, Chu J, Shen X, Wang J, Orkin SH. 2008. An extended transcriptional network for pluripotency of embryonic stem cells. *Cell* **132:** 1049–1061.
Krogan NJ, Kim M, Tong A, Golshani A, Cagney G, Canadien V, Richards DP, Beattie BK, Emili A, Boone C, et al. 2003. Methylation of histone H3 by Set2 in *Saccharomyces cerevisiae* is linked to transcriptional elongation by RNA polymerase II. *Mol Cell Biol* **23:** 4207–4218.
Kuzmichev A, Nishioka K, Erdjument-Bromage H, Tempst P, Reinberg D. 2002. Histone methyltransferase activity associated with a human multiprotein complex containing the Enhancer of Zeste protein. *Genes Dev* **16:** 2893–2905.
Lee JT. 2009. Lessons from X-chromosome inactivation: long ncRNA as guides and tethers to the epigenome. *Genes Dev* **23:** 1831–1842.
Lindeman LC, Winata CL, Aanes H, Mathavan S, Alestrom P, Collas P. 2010. Chromatin states of developmentally-regulated genes revealed by DNA and histone methylation patterns in zebrafish embryos. *Int J Dev Biol* **54:** 803–813.
Mathavan S, Lee SG, Mak A, Miller LD, Murthy KR, Govindarajan KR, Tong Y, Wu YL, Lam SH, Yang H, et al. 2005. Transcriptome analysis of zebrafish embryogenesis using microarrays. *PLoS Genet* **1:** 260–276.
Mayer W, Niveleau A, Walter J, Fundele R, Haaf T. 2000. Demethylation of the zygotic paternal genome. *Nature* **403:** 501–502.
Meneghini MD, Wu M, Madhani HD. 2003. Conserved histone variant H2A.Z protects euchromatin from the ectopic spread of silent heterochromatin. *Cell* **112:** 725–736.
Mhanni AA, McGowan RA. 2004. Global changes in genomic methylation levels during early development of the zebrafish embryo. *Dev Genes Evol* **214:** 412–417.
Mikkelsen TS, Ku M, Jaffe DB, Issac B, Lieberman E, Giannoukos G, Alvarez P, Brockman W, Kim TK, Koche RP, et al. 2007. Genome-wide maps of chromatin state in pluripotent and lineage-committed cells. *Nature* **448:** 553–560.
Miteva K, Valkov N, Goncharova-Peinoval J, Kovachev K, Zlatarev S, Pironcheva G, Russev G. 1995. Electron microscopic data for the presence of post-meiotic gene expression in isolated ram sperm chromatin. *Cytobios* **83:** 85–90.
Muller J, Hart CM, Francis NJ, Vargas ML, Sengupta A, Wild B, Miller EL, O'Connor MB, Kingston RE, Simon JA. 2002. Histone methyltransferase activity of a *Drosophila* Polycomb group repressor complex. *Cell* **111:** 197–208.
Naz RK. 1998. Effect of actinomycin D and cycloheximide on human sperm function. *Arch Androl* **41:** 135–142.
Okada Y, Yamagata K, Hong K, Wakayama T, Zhang Y. 2010. A role for the elongator complex in zygotic paternal genome demethylation. *Nature* **463:** 554–558.
Okitsu CY, Hsieh CL. 2007. DNA methylation dictates histone H3K4 methylation. *Mol Cell Biol* **27:** 2746–2757.
Oler AJ, Alla RK, Roberts DN, Wong A, Hollenhorst PC, Chandler KJ, Cassiday PA, Nelson CA, Hagedorn CH, Graves BJ, et al. 2010. Human RNA polymerase III transcriptomes and relationships to Pol II promoter chromatin and enhancer-binding factors. *Nat Struct Mol Biol* **17:** 620–628.
Ooi SK, Qiu C, Bernstein E, Li K, Jia D, Yang Z, Erdjument-Bromage H, Tempst P, Lin SP, Allis CD, et al. 2007. DNMT3L connects unmethylated lysine 4 of histone H3 to de novo methylation of DNA. *Nature* **448:** 714–717.
Orkin SH. 2005. Chipping away at the embryonic stem cell network. *Cell* **122:** 828–830.
Oswald J, Engemann S, Lane N, Mayer W, Olek A, Fundele R, Dean W, Reik W, Walter J. 2000. Active demethylation of the paternal genome in the mouse zygote. *Curr Biol* **10:** 475–478.
Rai K, Chidester S, Zavala CV, Manos EJ, James SR, Karpf AR, Jones DA, Cairns BR. 2007. Dnmt2 functions in the cytoplasm to promote liver, brain, and retina development in zebrafish. *Genes Dev* **21:** 261–266.
Rao S, Orkin SH. 2006. Unraveling the transcriptional network controlling ES cell pluripotency. *Genome Biol* **7:** 230. doi: 10.1186/gb-2006-7-8-230.
Rechtsteiner A, Ercan S, Takasaki T, Phippen TM, Egelhofer TA, Wang W, Kimura H, Lieb JD, Strome S. 2010. The histone H3K36 methyltransferase MES-4 acts epigenetically to transmit the memory of germline gene expression to progeny. *PLoS Genet* **6:** e1001091. doi: 10.1371/journal.pgen.1001091.
Robinson PJ, Fairall L, Huynh VA, Rhodes D. 2006. EM measurements define the dimensions of the "30-nm" chromatin fiber: evidence for a compact, interdigitated structure. *Proc Natl Acad Sci* **103:** 6506–6511.
Robinson PJ, An W, Routh A, Martino F, Chapman L, Roeder RG, Rhodes D. 2008. 30 nm chromatin fibre decompaction requires both H4-K16 acetylation and linker histone eviction. *J Mol Biol* **381:** 816–825.
Seydoux G, Braun RE. 2006. Pathway to totipotency: lessons from germ cells. *Cell* **127:** 891–904.
Shimizu Y, Mita K, Tamura M, Onitake K, Yamashita M. 2000. Requirement of protamine for maintaining nuclear condensation of medaka (*Oryzias latipes*) spermatozoa shed into water but not for promoting nuclear condensation during spermatogenesis. *Int J Dev Biol* **44:** 195–199.
Shogren-Knaak M, Ishii H, Sun JM, Pazin MJ, Davie JR, Peterson CL. 2006. Histone H4-K16 acetylation controls chromatin structure and protein interactions. *Science* **311:** 844–847.
Tsai MC, Manor O, Wan Y, Mosammaparast N, Wang JK, Lan F, Shi Y, Segal E, Chang HY. 2010. Long noncoding RNA as modular scaffold of histone modification complexes. *Science* **329:** 689–693.
Vastenhouw NL, Zhang Y, Woods IG, Imam F, Regev A, Liu XS, Rinn J, Schier AF. 2010. Chromatin signature of embryonic pluripotency is established during genome activation. *Nature* **464:** 922–926.
Wang J, Rao S, Chu J, Shen X, Levasseur DN, Theunissen TW, Orkin SH. 2006. A protein interaction network for pluripotency of embryonic stem cells. *Nature* **444:** 364–368.
Wang GG, Cai L, Pasillas MP, Kamps MP. 2007. NUP98-NSD1 links H3K36 methylation to Hox-A gene activation and leukaemogenesis. *Nat Cell Biol* **9:** 804–812.
Ward WS, Coffey DS. 1991. DNA packaging and organization in mammalian spermatozoa: comparison with somatic cells. *Biol Reprod* **44:** 569–574.
Wardle FC, Odom DT, Bell GW, Yuan B, Danford TW, Wiellette EL, Herbolsheimer E, Sive HL, Young RA, Smith JC. 2006. Zebrafish promoter microarrays identify actively transcribed embryonic genes. *Genome Biol* **7:** R71.
Weber M, Hellmann I, Stadler MB, Ramos L, Paabo S, Rebhan M, Schubeler D. 2007. Distribution, silencing potential and evolutionary impact of promoter DNA methylation in the human genome. *Nat Genet* **39:** 457–466.
Welstead GG, Schorderet P, Boyer LA. 2008. The reprogramming language of pluripotency. *Curr Opin Genet Dev* **18:** 123–129.
Westerfield M. 2000. *The zebrafish book. A guide for the laboratory use of zebrafish (*Danio rerio*)*, 4th ed. University of Oregon Press, Eugene, Oregon.
Wykes SM, Krawetz SA. 2003. The structural organization of sperm chromatin. *J Biol Chem* **278:** 29471–29477.
Wysocka J, Swigut T, Milne TA, Dou Y, Zhang X, Burlingame AL, Roeder RG, Brivanlou AH, Allis CD. 2005. WDR5 associates with histone H3 methylated at K4 and is essential for H3 K4 methylation and vertebrate development. *Cell* **121:** 859–872.
Zhang H, Roberts DN, Cairns BR. 2005. Genome-wide dynamics of Htz1, a histone H2A variant that poises repressed/basal promoters for activation through histone loss. *Cell* **123:** 219–231.
Zhao J, Sun BK, Erwin JA, Song JJ, Lee JT. 2008. Polycomb proteins targeted by a short repeat RNA to the mouse X chromosome. *Science* **322:** 750–756.
Zhou J, Fan JY, Rangasamy D, Tremethick DJ. 2007. The nucleosome surface regulates chromatin compaction and couples it with transcriptional repression. *Nat Struct Mol Biol* **14:** 1070–1076.
Zilberman D, Coleman-Derr D, Ballinger T, Henikoff S. 2008. Histone H2A.Z and DNA methylation are mutually antagonistic chromatin marks. *Nature* **456:** 125–129.

Received July 25, 2010; accepted in revised form January 6, 2011.

Supplemental Figure 1

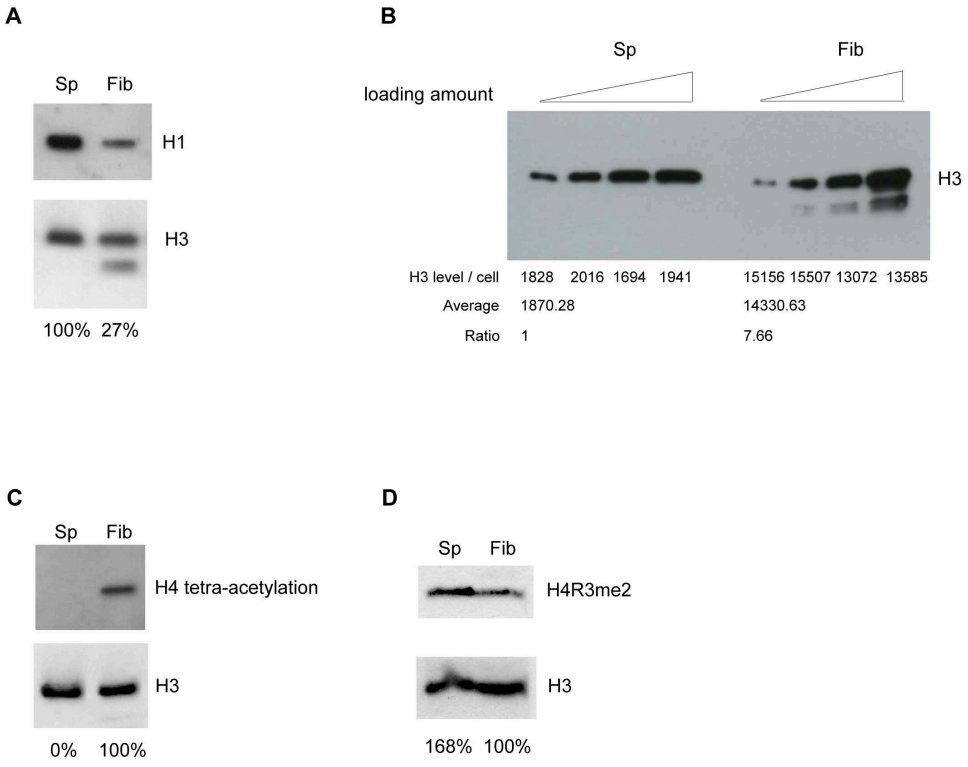

Supplemental Figure 2

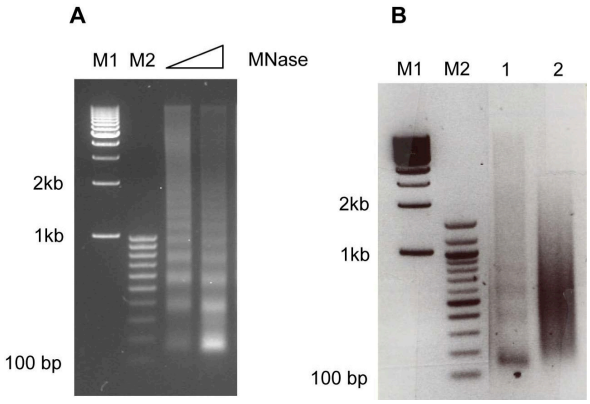

Supplemental Figure 3

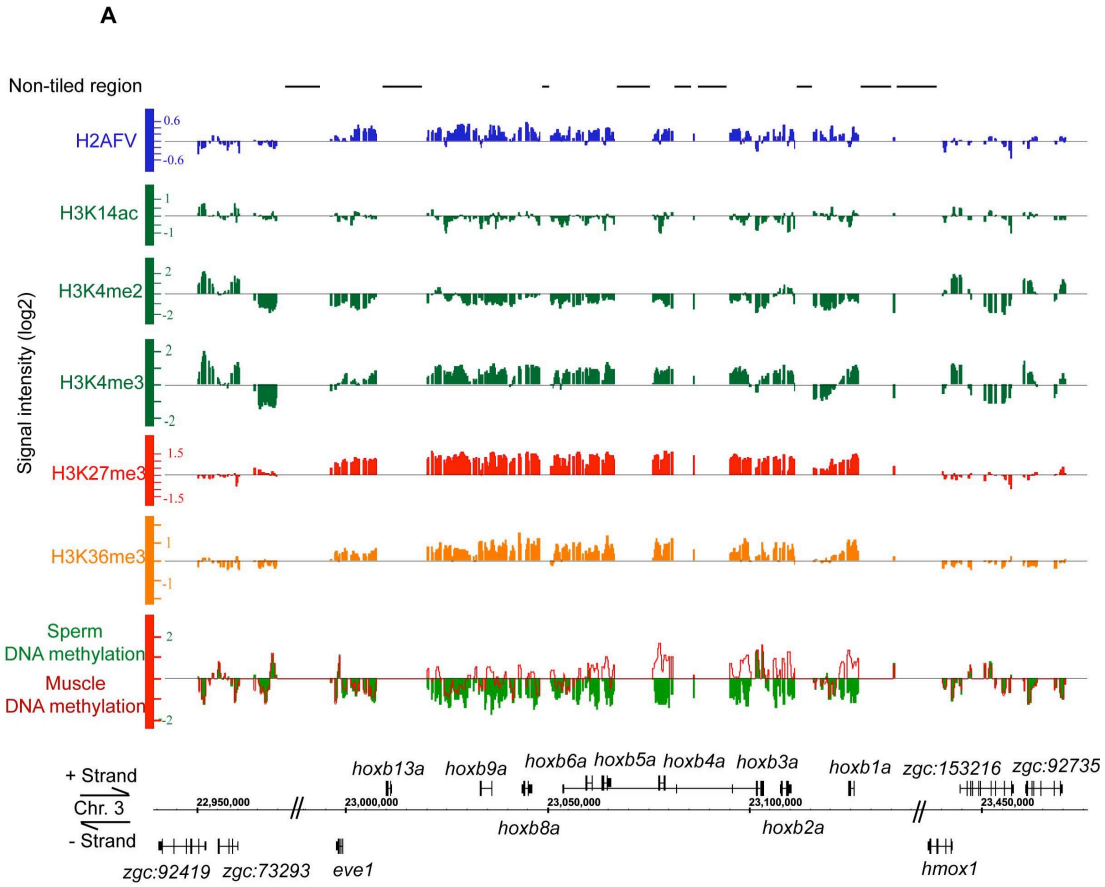

Supplemental Figure 3

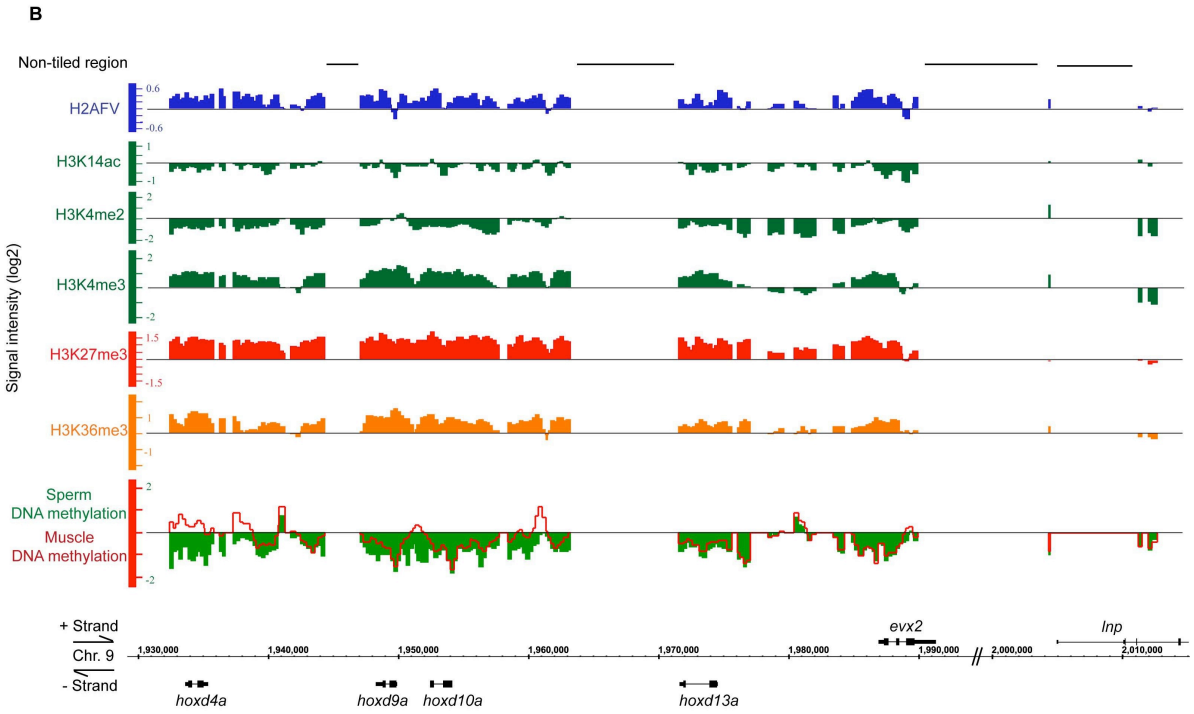

Supplemental Figure 3

C

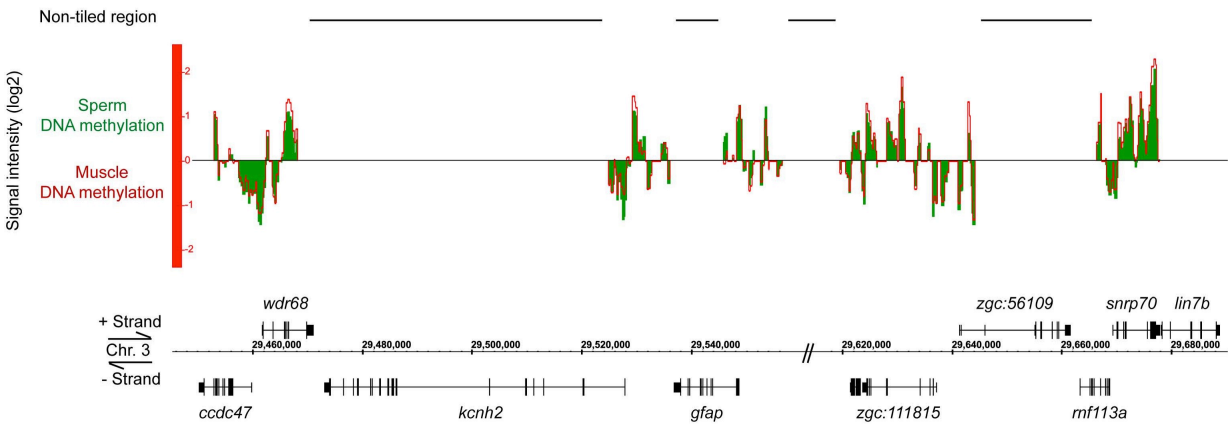

Supplemental Figure 4

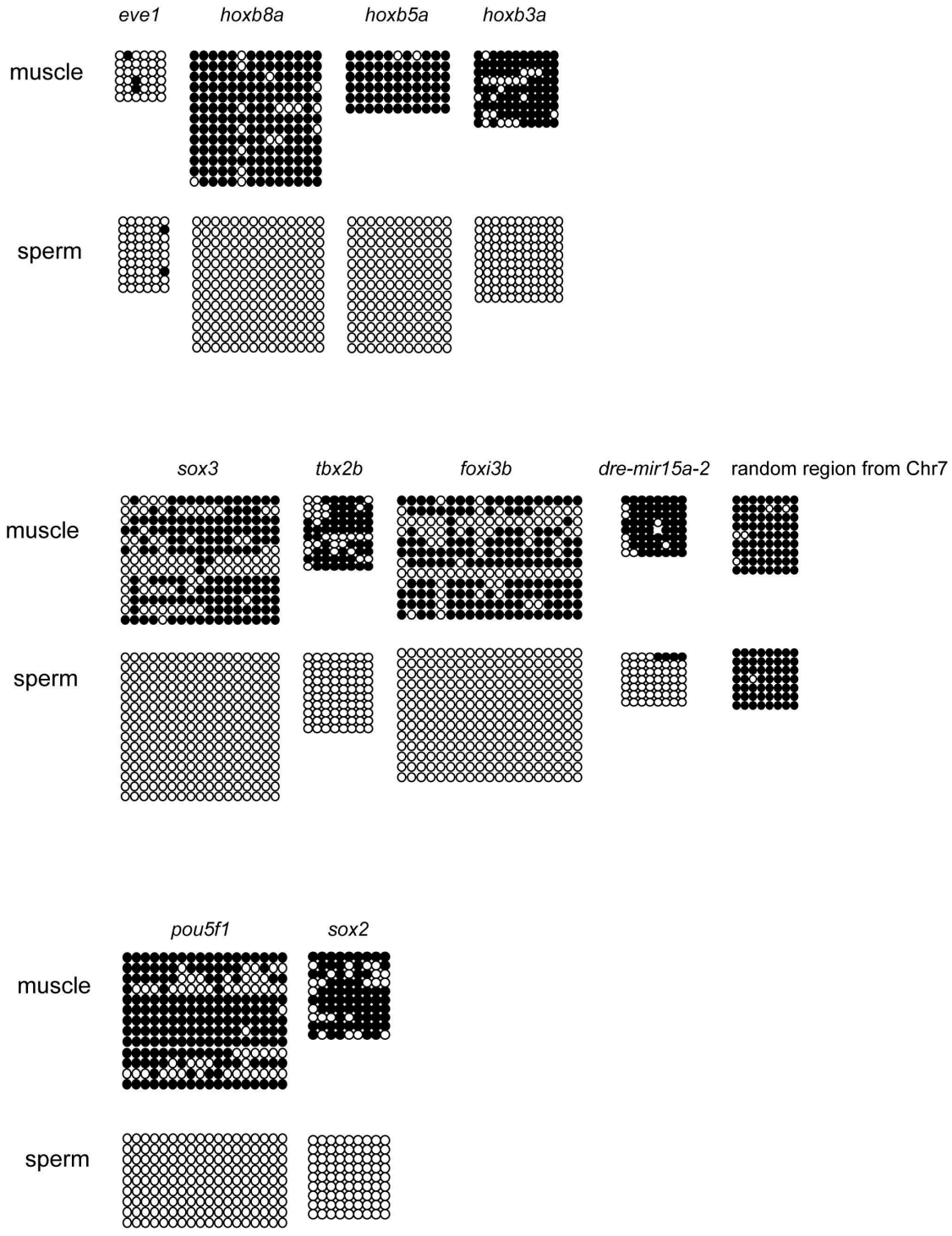

Supplemental Figure 5

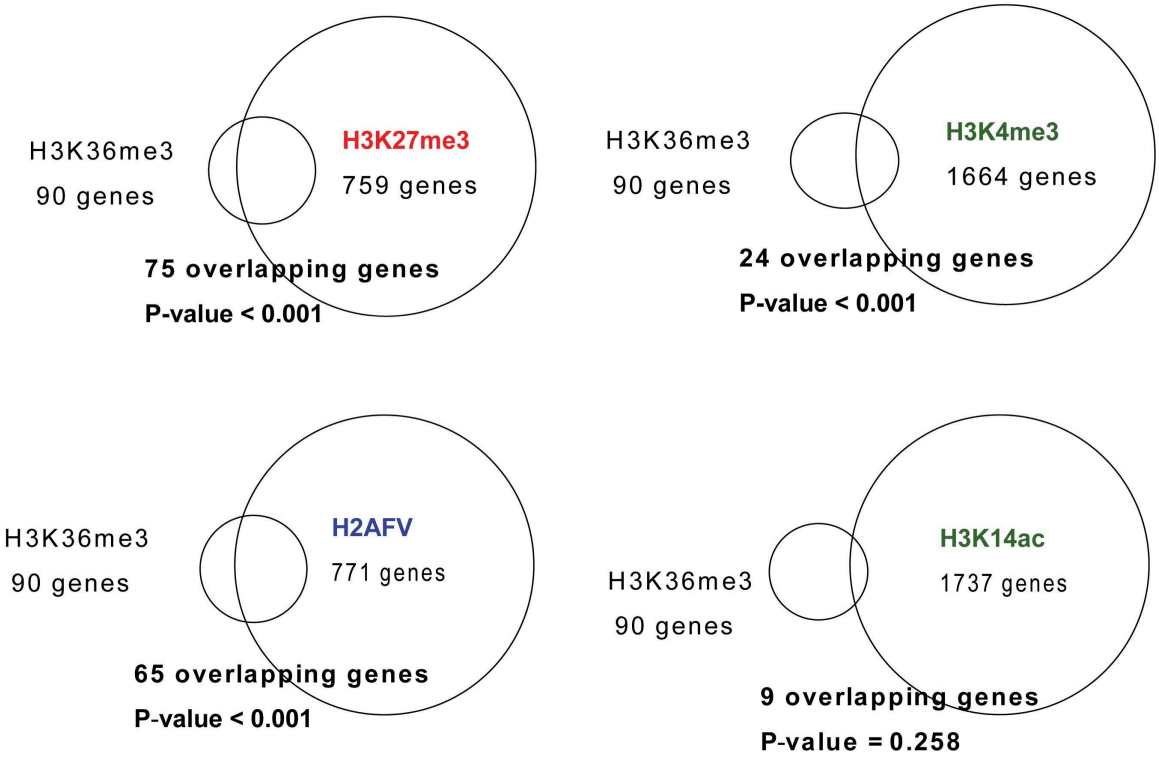

Supplemental Figure 6

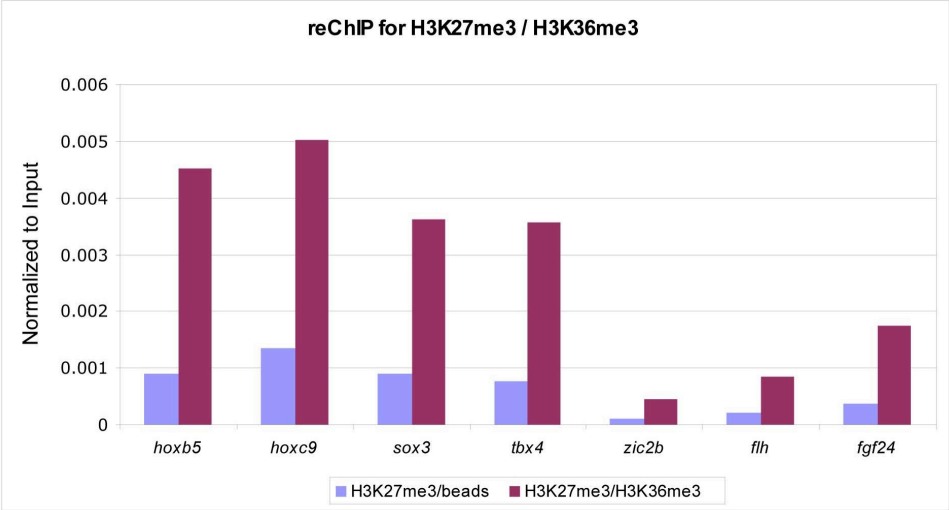

Supplemental Figure 7

A

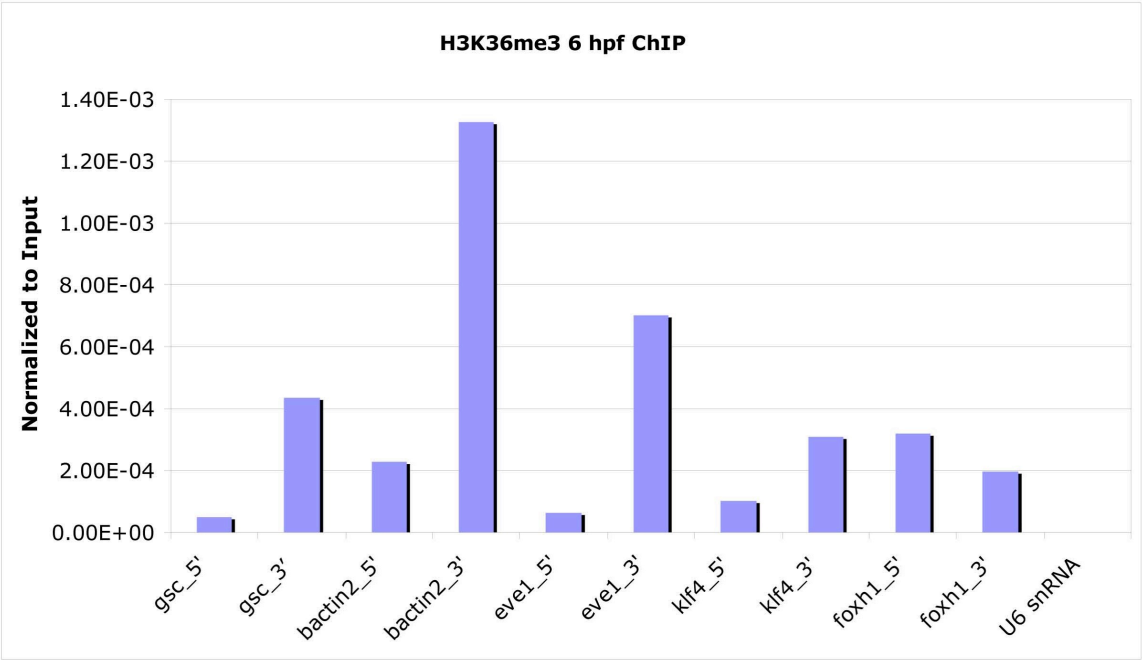

B

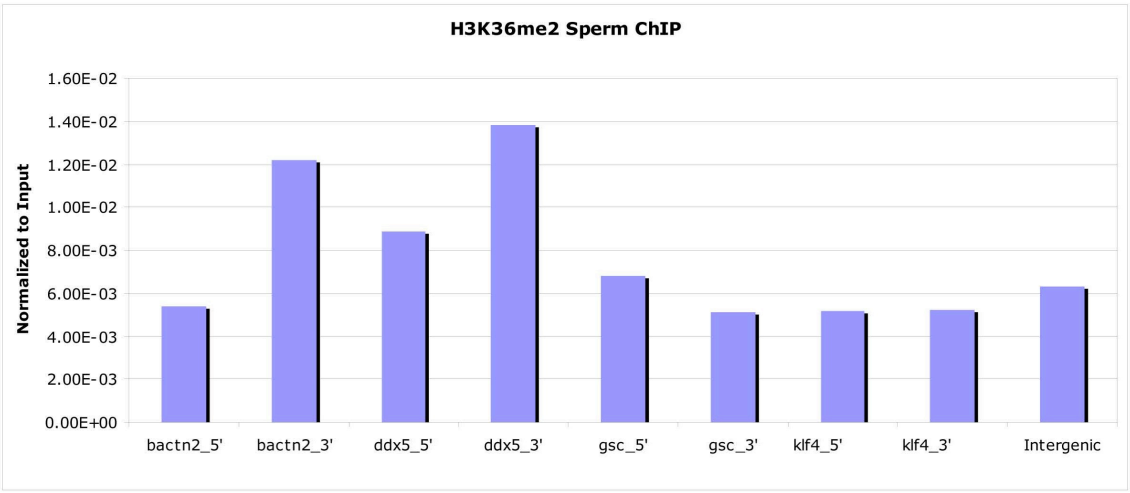

Supplemental Figure 8

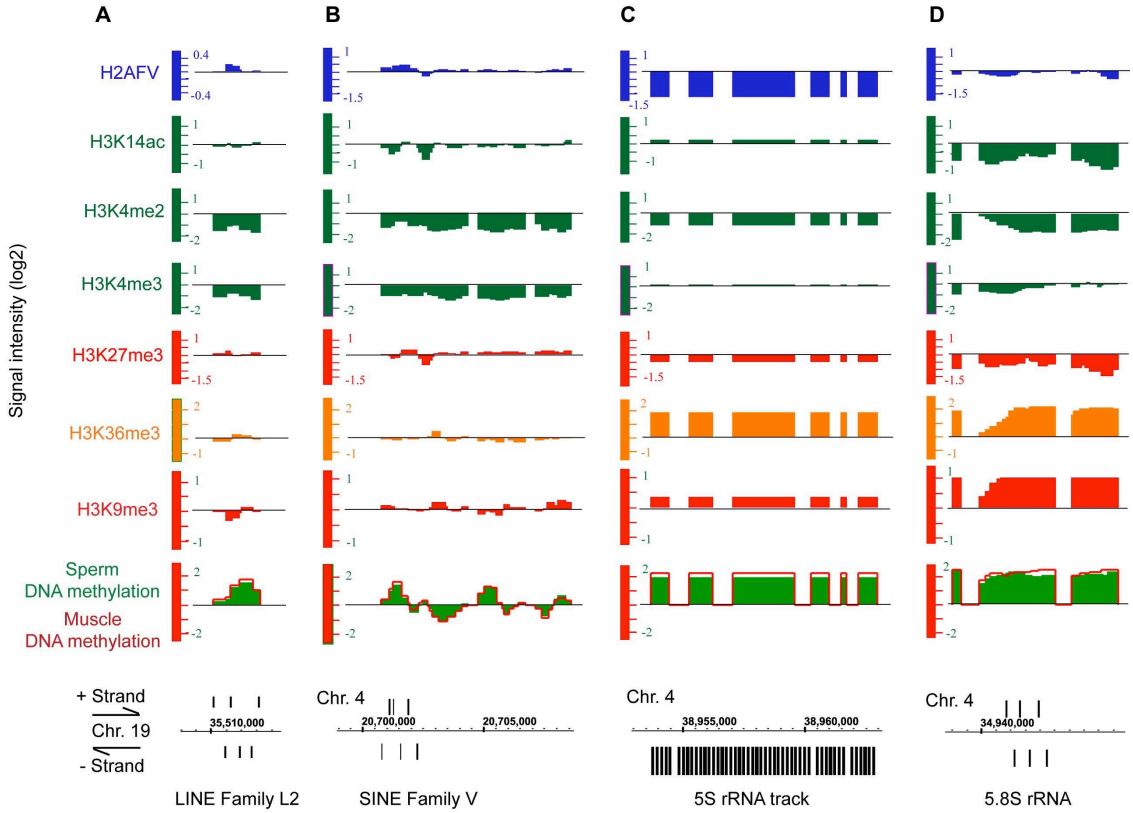

Supplemental Figure 8

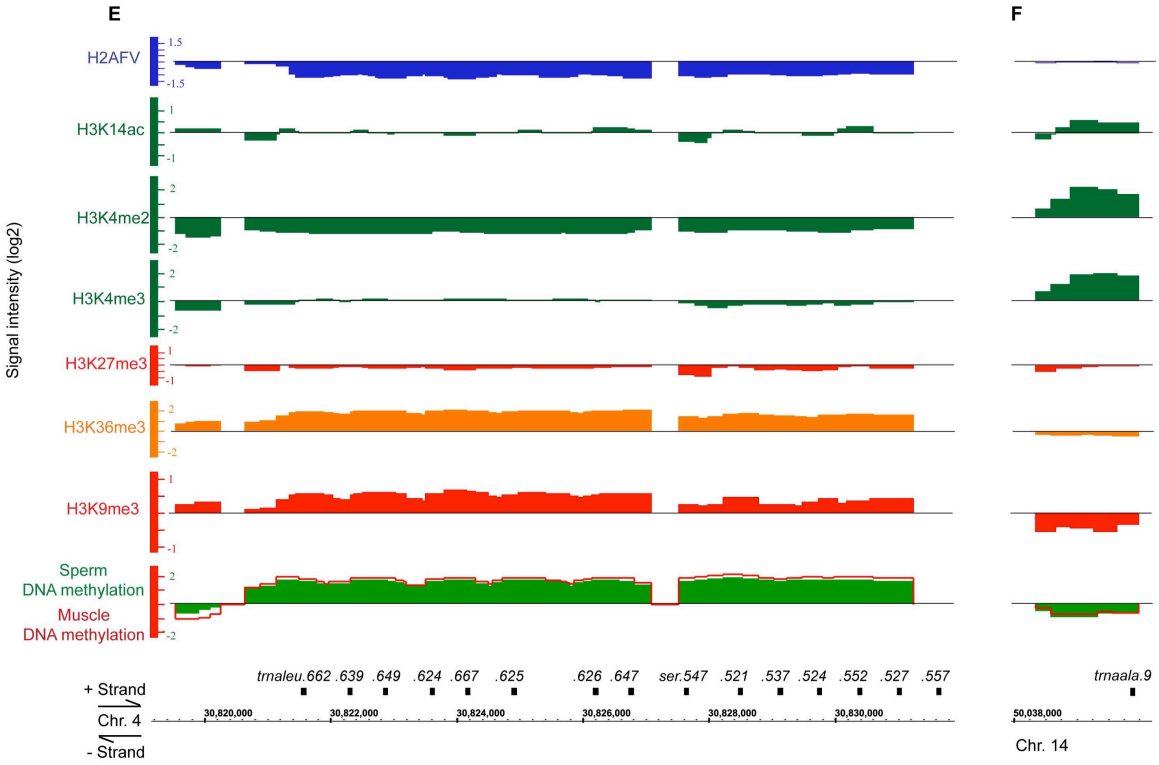

Supplemental Table 1. List of histones in zebrafish sperm identified from mass spectrometry.

	Histone	Number of peptides identified	Accession number and description
Band 1	H1	18	Q6DH38, human orthologue, HIST1H1C
	H1	6	human orthologue, HIST1H1D
	H1FX	2	Q802U8, H1 member X (H1 variant)
Band 2	H1	6	human orthologue, HIST1H1E
	H1F0	5	H1F0 (H1 family member 0)
Band 3	H2B	10	H2B 1/2, H2B1_BRARE, ENSDARP00000055902
	H2AFX	12	H2AFX, H2A member X (H2A variant)
	H2AFV	4	H2AFV, H2A member V (H2A variant), orthologue HTZ1
Band 4	H4	26	zgc:165555, H4 (Histone cluster 1, H4-like, HIST1H4F)

Supplemental Table 2. H3K27me3 GO

HYPERLINKED GO CATEGORY	TOTAL GENES	CHANGED	ENRICHMENT	FALSE DISCOVERY RATE
GO:0021575_hindbrain_morphogenesis	6	6	13.253566	0
GO:0030878_thyroid_gland_development	9	8	11.780947	0
GO:0021546_rhombomere_development	6	5	11.044638	0
GO:0048663_neuron_fate_commitment	11	8	9.638957	0
GO:0048732_gland_development	21	15	9.466833	0
GO:0048665_neuron_fate_specification	7	5	9.466833	0
GO:0048709_oligodendrocyte_differentiation	7	5	9.466833	0
GO:0043049_otic_placode_formation	15	10	8.835711	0
GO:0035270_endocrine_system_development	31	20	8.550688	0
GO:0030901_midbrain_development	14	9	8.520149	0
GO:0015669_gas_transport	17	10	7.796215	0
GO:0015671_oxygen_transport	17	10	7.796215	0
GO:0030916_otic_vesicle_formation	17	10	7.796215	0
GO:0042063_gliogenesis	17	10	7.796215	0
GO:0042127_regulation_of_cell_proliferation	12	7	7.731247	0
GO:0042472_inner_ear_morphogenesis	28	16	7.573466	0
GO:0010001_glial_cell_differentiation	16	9	7.455131	0
GO:0045165_cell_fate_commitment	47	26	7.33176	0
GO:0030902_hindbrain_development	38	21	7.324339	0
GO:0042471_ear_morphogenesis	29	16	7.312312	0
GO:0007420_brain_development	100	55	7.289461	0
GO:0021532_neural_tube_patterning	20	11	7.289461	0
GO:0021903_rostrocaudal_neural_tube_patterning	20	11	7.289461	0
GO:0001708_cell_fate_specification	30	16	7.068568	0
GO:0030917_midbrain-hindbrain_boundary_development	15	8	7.068568	0
GO:0007422_peripheral_nervous_system_development	17	9	7.016594	0
GO:0007417_central_nervous_system_development	137	71	6.868636	0
GO:0021510_spinal_cord_development	14	7	6.626783	0
GO:0021515_cell_differentiation_in_spinal_cord	14	7	6.626783	0
GO:0030900_forebrain_development	27	13	6.381346	0
GO:0021915_neural_tube_development	25	11	5.831569	0
GO:0009952_anterior_posterior_pattern_formation	83	35	5.588853	0
GO:0033339_pectoral_fin_development	19	8	5.580449	0
GO:0048646_anatomical_structure_formation	82	34	5.495381	0
GO:0007399_nervous_system_development	236	96	5.391281	0
GO:0048839_inner_ear_development	45	18	5.301426	0
GO:0048598_embryonic_morphogenesis	83	33	5.26949	0
GO:0043583_ear_development	46	18	5.186178	0
GO:0030903_notochord_development	23	9	5.186178	0
GO:0003002_regionalization	128	50	5.177174	0
GO:0035050_embryonic_heart_tube_development	34	13	5.06754	0
GO:0051216_cartilage_development	37	14	5.014863	0
GO:0001704_formation_of_primary_germ_layer	24	9	4.970087	0
GO:0006355_regulation_of_transcription__DNA-dependen	747	272	4.82593	0
GO:0051252_regulation_of_RNA_metabolic_process	748	272	4.819478	0
GO:0008283_cell_proliferation	25	9	4.771284	0
GO:0045595_regulation_of_cell_differentiation	28	10	4.733416	0
GO:0006351_transcription__DNA-dependent	766	273	4.723529	0
GO:0032774_RNA_biosynthetic_process	769	273	4.705102	0
GO:0009953_dorsal_ventral_pattern_formation	48	17	4.693971	0
GO:0045449_regulation_of_transcription	833	290	4.614087	0
GO:0035295_tube_development	46	16	4.609936	0
GO:0007389_pattern_specification_process	170	59	4.599767	0
GO:0019219_regulation_of_nucleobase__nucleoside__nu	837	290	4.592036	0
GO:0006353_transcription_termination	310	106	4.531864	0
GO:0031554_regulation_of_transcription_termination	310	106	4.531864	0
GO:0031555_transcriptional_attenuation	310	106	4.531864	0
GO:0031564_transcription_antitermination	310	106	4.531864	0
GO:0043244_regulation_of_protein_complex_disassembly	310	106	4.531864	0
GO:0016055_Wnt_receptor_signaling_pathway	41	14	4.525608	0
GO:0022411_cellular_component_disassembly	312	106	4.502814	0
GO:0032984_macromolecular_complex_disassembly	312	106	4.502814	0
GO:0043241_protein_complex_disassembly	312	106	4.502814	0
GO:0043624_cellular_protein_complex_disassembly	312	106	4.502814	0
GO:0010468_regulation_of_gene_expression	857	291	4.500336	0
GO:0001501_skeletal_development	56	19	4.496746	0
GO:0006350_transcription	859	291	4.489858	0
GO:0031323_regulation_of_cellular_metabolic_process	865	291	4.458714	0
GO:0007507_heart_development	81	27	4.417855	0
GO:0009880_embryonic_pattern_specification	33	11	4.417855	0
GO:0007498_mesoderm_development	37	12	4.298454	0
GO:0032268_regulation_of_cellular_protein_metabolic_pr	331	107	4.284385	0
GO:0007423_sensory_organ_development	130	42	4.281921	0
GO:0019222_regulation_of_metabolic_process	908	291	4.247563	0
GO:0009887_organ_morphogenesis	172	55	4.238059	0
GO:0007156_homophilic_cell_adhesion	44	14	4.217044	0
GO:0022008_neurogenesis	104	33	4.205458	0
GO:0048592_eye_morphogenesis	38	12	4.185337	0
GO:0043010_camera-type_eye_development	61	19	4.12816	0
GO:0001654_eye_development	87	27	4.113176	0

GO:0009790_embryonic_development	255	79	4.106007	0
GO:0009792_embryonic_development_ending_in_birth_or	84	26	4.102294	0
GO:0043009_chordate_embryonic_development	84	26	4.102294	0
GO:0051128_regulation_of_cellular_component_organizat	349	108	4.10139	0
GO:0048513_organ_development	482	149	4.097057	0
GO:0035282_segmentation	55	17	4.096557	0
GO:0048731_system_development	571	175	4.061951	0
GO:0016070_RNA_metabolic_process	905	276	4.041971	0
GO:0030182_neuron_differentiation	82	25	4.040721	0
GO:0009888_tissue_development	110	33	3.97607	0
GO:0048699_generation_of_neurons	98	29	3.921974	0
GO:0001756_somitogenesis	51	15	3.898108	0
GO:0002520_immune_system_development	51	15	3.898108	0
GO:0048534_hemopoietic_or_lymphoid_organ_developme	51	15	3.898108	0
GO:0030097_hemopoiesis	48	14	3.865623	0
GO:0009799_determination_of_symmetry	55	16	3.855583	0
GO:0009855_determination_of_bilateral_symmetry	55	16	3.855583	0
GO:0048856_anatomical_structure_development	627	182	3.847128	0
GO:0007368_determination_of_left_right_symmetry	45	13	3.828808	0
GO:0051246_regulation_of_protein_metabolic_process	373	107	3.801961	0
GO:0007275_multicellular_organismal_development	725	207	3.784122	0
GO:0048568_embryonic_organ_development	53	15	3.751009	0
GO:0051093_negative_regulation_of_developmental_proc	53	15	3.751009	0
GO:0050794_regulation_of_cellular_process	1269	346	3.613659	0
GO:0048514_blood_vessel_morphogenesis	49	13	3.516252	0
GO:0050789_regulation_of_biological_process	1345	352	3.468591	0
GO:0009653_anatomical_structure_morphogenesis	347	90	3.437524	0
GO:0010467_gene_expression	1143	296	3.432245	0
GO:0032501_multicellular_organismal_process	844	217	3.407611	0
GO:0016337_cell-cell_adhesion	55	14	3.373635	0
GO:0006139_nucleobase__nucleoside__nucleotide_and_	1221	302	3.278114	0
GO:0032502_developmental_process	869	214	3.263824	0
GO:0001568_blood_vessel_development	65	16	3.262416	0
GO:0001944_vasculature_development	66	16	3.212986	0
GO:0065007_biological_regulation	1594	377	3.134626	0
GO:0030154_cell_differentiation	394	83	2.791995	0
GO:0048869_cellular_developmental_process	394	83	2.791995	0
GO:0048522_positive_regulation_of_cellular_process	100	20	2.650713	0
GO:0050793_regulation_of_developmental_process	141	27	2.537917	0
GO:0048519_negative_regulation_of_biological_process	299	57	2.526599	0
GO:0048523_negative_regulation_of_cellular_process	289	55	2.522305	0
GO:0009968_negative_regulation_of_signal_transduction	204	38	2.468801	0
GO:0043283_biopolymer_metabolic_process	1699	307	2.394847	0
GO:0006816_calcium_ion_transport	176	31	2.334435	0
GO:0048468_cell_development	277	47	2.2488	0
GO:0009966_regulation_of_signal_transduction	277	44	2.10526	0
GO:0016043_cellular_component_organization_and_biog	876	132	1.997113	0
GO:0015674_di-__tri-valent_inorganic_cation_transport	313	47	1.990152	0
GO:0043170_macromolecule_metabolic_process	2338	331	1.87636	0
GO:0007166_cell_surface_receptor_linked_signal_transdu	427	58	1.80025	0
GO:0044237_cellular_metabolic_process	2799	372	1.76146	0
GO:0044238_primary_metabolic_process	2744	363	1.753296	0
GO:0008152_metabolic_process	3336	387	1.537509	0
GO:0030001_metal_ion_transport	940	105	1.480451	0
GO:0009987_cellular_process	4369	488	1.480371	0
GO:0044267_cellular_protein_metabolic_process	1486	152	1.355681	0
GO:0019538_protein_metabolic_process	1572	159	1.340532	0
GO:0044260_cellular_macromolecule_metabolic_process	1504	152	1.339456	0
GO:0006811_ion_transport	1076	114	1.404188	0.000071
GO:0006812_cation_transport	982	106	1.430629	0.000072
GO:0033333_fin_development	40	11	3.644731	0.000139
GO:0048736_appendage_development	40	11	3.644731	0.000139
GO:0021536_diencephalon_development	12	6	6.626783	0.000141
GO:0003007_heart_morphogenesis	27	9	4.417855	0.000142
GO:0035108_limb_morphogenesis	18	7	5.154164	0.000323
GO:0035136_forelimb_morphogenesis	18	7	5.154164	0.000323
GO:0035138_pectoral_fin_morphogenesis	18	7	5.154164	0.000323
GO:0060173_limb_development	18	7	5.154164	0.000323
GO:0030326_embryonic_limb_morphogenesis	13	6	6.11703	0.000331
GO:0035113_embryonic_appendage_morphogenesis	13	6	6.11703	0.000331
GO:0035115_embryonic_forelimb_morphogenesis	13	6	6.11703	0.000331
GO:0035118_embryonic_pectoral_fin_morphogenesis	13	6	6.11703	0.000331
GO:0048518_positive_regulation_of_biological_process	110	20	2.409739	0.00034
GO:0007369_gastrulation	70	15	2.84005	0.000342
GO:0016331_morphogenesis_of_embryonic_epithelium	23	8	4.609936	0.000345
GO:0033334_fin_morphogenesis	36	10	3.681546	0.000382
GO:0035107_appendage_morphogenesis	36	10	3.681546	0.000382
GO:0050767_regulation_of_neurogenesis	30	9	3.97607	0.000506
GO:0007223_Wnt_receptor_signaling_pathway__calcium_	19	7	4.882893	0.000688
GO:0009967_positive_regulation_of_signal_transduction	19	7	4.882893	0.000688
GO:0031016_pancreas_development	25	8	4.241141	0.000807
GO:0021983_pituitary_gland_development	6	4	8.835711	0.000859

GO:0021984_adenohypophysis_development	6	4	8.835711	0.000859
GO:0001840_neural_plate_development	20	7	4.638748	0.001037
GO:0007418_ventral_midline_development	10	5	6.626783	0.001176
GO:0031076_embryonic_camera-type_eye_development	10	5	6.626783	0.001176
GO:0050768_negative_regulation_of_neurogenesis	10	5	6.626783	0.001176
GO:0051090_regulation_of_transcription_factor_activity	10	5	6.626783	0.001176
GO:0051098_regulation_of_binding	10	5	6.626783	0.001176
GO:0051101_regulation_of_DNA_binding	10	5	6.626783	0.001176
GO:0009798_axis_specification	15	6	5.301426	0.001453
GO:0048565_gut_development	15	6	5.301426	0.001453
GO:0007155_cell_adhesion	114	19	2.208928	0.002265
GO:0022610_biological_adhesion	114	19	2.208928	0.002265
GO:0001525_angiogenesis	28	8	3.786733	0.002291
GO:0002009_morphogenesis_of_an_epithelium	56	12	2.84005	0.002303
GO:0040007_growth	64	13	2.692131	0.002308
GO:0007492_endoderm_development	11	5	6.024348	0.002316
GO:0021522_spinal_cord_motor_neuron_differentiation	11	5	6.024348	0.002316
GO:0030334_regulation_of_cell_migration	11	5	6.024348	0.002316
GO:0048546_digestive_tract_morphogenesis	11	5	6.024348	0.002316
GO:0051270_regulation_of_cell_motility	11	5	6.024348	0.002316
GO:0009791_post-embryonic_development	7	4	7.573466	0.002781
GO:0009948_anterior_posterior_axis_specification	7	4	7.573466	0.002781
GO:0045743_positive_regulation_of_fibroblast_growth_fac	7	4	7.573466	0.002781
GO:0048483_autonomic_nervous_system_development	7	4	7.573466	0.002781
GO:0048484_enteric_nervous_system_development	7	4	7.573466	0.002781
GO:0016477_cell_migration	99	17	2.275865	0.003016
GO:0007167_enzyme_linked_receptor_protein_signaling_	82	15	2.424433	0.003032
GO:0021517_ventral_spinal_cord_development	12	5	5.522319	0.00342
GO:0042461_photoreceptor_cell_development	12	5	5.522319	0.00342
GO:0042462_eye_photoreceptor_cell_development	12	5	5.522319	0.00342
GO:0045596_negative_regulation_of_cell_differentiation	12	5	5.522319	0.00342
GO:0042692_muscle_cell_differentiation	30	8	3.534284	0.003557
GO:0048593_camera-type_eye_morphogenesis	18	6	4.417855	0.003744
GO:0007267_cell-cell_signaling	31	8	3.420275	0.003929
GO:0001706_endoderm_formation	8	4	6.626783	0.0045
GO:0043388_positive_regulation_of_DNA_binding	8	4	6.626783	0.0045
GO:0051091_positive_regulation_of_transcription_factor_a	8	4	6.626783	0.0045
GO:0051099_positive_regulation_of_binding	8	4	6.626783	0.0045
GO:0001570_vasculogenesis	13	5	5.097525	0.004726
GO:0001707_mesoderm_formation	19	6	4.185337	0.005396
GO:0048666_neuron_development	55	11	2.650713	0.00601
GO:0051146_striated_muscle_cell_differentiation	26	7	3.568268	0.006127
GO:0000904_cellular_morphogenesis_during_differentiatic	56	11	2.603379	0.006488
GO:0006928_cell_motility	108	17	2.086209	0.006555
GO:0051674_localization_of_cell	108	17	2.086209	0.006555
GO:0001754_eye_photoreceptor_cell_differentiation	14	5	4.733416	0.006618
GO:0046530_photoreceptor_cell_differentiation	14	5	4.733416	0.006618
GO:0021508_floor_plate_formation	9	4	5.890474	0.006651
GO:0021990_neural_plate_formation	9	4	5.890474	0.006651
GO:0030111_regulation_of_Wnt_receptor_signaling_pathv	9	4	5.890474	0.006651
GO:0007517_muscle_development	49	10	2.704809	0.006995
GO:0014706_striated_muscle_development	42	9	2.84005	0.008318
GO:0001710_mesodermal_cell_fate_commitment	5	3	7.952139	0.010274
GO:0021953_central_nervous_system_neuron_differentiat	5	3	7.952139	0.010274
GO:0032835_glomerulus_development	5	3	7.952139	0.010274
GO:0045446_endothelial_cell_differentiation	5	3	7.952139	0.010274
GO:0048333_mesodermal_cell_differentiation	5	3	7.952139	0.010274
GO:0008543_fibroblast_growth_factor_receptor_signaling_	15	5	4.417855	0.0105
GO:0007169_transmembrane_receptor_protein_tyrosine_l	51	10	2.598738	0.010995
GO:0031018_endocrine_pancreas_development	10	4	5.301426	0.011956
GO:0048547_gut_morphogenesis	10	4	5.301426	0.011956
GO:0048880_sensory_system_development	10	4	5.301426	0.011956
GO:0048925_lateral_line_system_development	10	4	5.301426	0.011956
GO:0006783_heme_biosynthetic_process	79	13	2.180967	0.013805
GO:0019748_secondary_metabolic_process	88	14	2.108522	0.013833
GO:0048332_mesoderm_morphogenesis	23	6	3.457452	0.014474
GO:0001889_liver_development	11	4	4.819478	0.015647
GO:0040036_regulation_of_fibroblast_growth_factor_rece	11	4	4.819478	0.015647
GO:0042659_regulation_of_cell_fate_specification	11	4	4.819478	0.015647
GO:0050769_positive_regulation_of_neurogenesis	11	4	4.819478	0.015647
GO:0048262_determination_of_dorsoventral_asymmetry	17	5	3.898108	0.01618
GO:0042168_heme_metabolic_process	81	13	2.127115	0.018099
GO:0001709_cell_fate_determination	6	3	6.626783	0.018133
GO:0008285_negative_regulation_of_cell_proliferation	6	3	6.626783	0.018133
GO:0022037_metencephalon_development	6	3	6.626783	0.018133
GO:0045597_positive_regulation_of_cell_differentiation	6	3	6.626783	0.018133
GO:0046849_bone_remodeling	6	3	6.626783	0.018133
GO:0048771_tissue_remodeling	6	3	6.626783	0.018133
GO:0048882_lateral_line_development	6	3	6.626783	0.018133
GO:0048884_neuromast_development	6	3	6.626783	0.018133
GO:0046148_pigment_biosynthetic_process	82	13	2.101175	0.018939
GO:0000902_cell_morphogenesis	91	14	2.03901	0.019016

GO:0032989_cellular_structure_morphogenesis	91	14	2.03901	0.019016
GO:0006779_porphyrin_biosynthetic_process	83	13	2.07586	0.01939
GO:0007219_Notch_signaling_pathway	18	5	3.681546	0.020405
GO:0002376_immune_system_process	121	17	1.862071	0.020444
GO:0008038_neuron_recognition	12	4	4.417855	0.021486
GO:0006778_porphyrin_metabolic_process	85	13	2.027016	0.022709
GO:0042440_pigment_metabolic_process	85	13	2.027016	0.022709
GO:0006766_vitamin_metabolic_process	19	5	3.48778	0.023651
GO:0007154_cell_communication	1120	104	1.230688	0.025402
GO:0009996_negative_regulation_of_cell_fate_specificatic	7	3	5.6801	0.025462
GO:0010453_regulation_of_cell_fate_commitment	7	3	5.6801	0.025462
GO:0010454_negative_regulation_of_cell_fate_commitme	7	3	5.6801	0.025462
GO:0021782_glial_cell_development	7	3	5.6801	0.025462
GO:0035121_tail_morphogenesis	7	3	5.6801	0.025462
GO:0042391_regulation_of_membrane_potential	7	3	5.6801	0.025462
GO:0042664_negative_regulation_of_endodermal_cell_fat	7	3	5.6801	0.025462
GO:0048752_semicircular_canal_morphogenesis	7	3	5.6801	0.025462
GO:0006873_cellular_ion_homeostasis	156	20	1.699175	0.028023
GO:0008037_cell_recognition	13	4	4.07802	0.028092
GO:0033014_tetrapyrrole_biosynthetic_process	88	13	1.957913	0.029167
GO:0055082_cellular_chemical_homeostasis	158	20	1.677667	0.030302
GO:0050801_ion_homeostasis	159	20	1.667115	0.030639
GO:0048729_tissue_morphogenesis	28	6	2.84005	0.031236
GO:0033013_tetrapyrrole_metabolic_process	90	13	1.914404	0.031791
GO:0031017_exocrine_pancreas_development	14	4	3.786733	0.032841
GO:0035272_exocrine_system_development	14	4	3.786733	0.032841
GO:0060042_retina_morphogenesis_in_camera-type_eye	14	4	3.786733	0.032841
GO:0035162_embryonic_hemopoiesis	21	5	3.155611	0.03326
GO:0040008_regulation_of_growth	21	5	3.155611	0.03326
GO:0048878_chemical_homeostasis	161	20	1.646406	0.035782
GO:0031214_biomineral_formation	8	3	4.970087	0.035876
GO:0007165_signal_transduction	1056	97	1.21742	0.037464
GO:0016481_negative_regulation_of_transcription	22	5	3.012174	0.039025
GO:0000041_transition_metal_ion_transport	666	64	1.273616	0.045252
GO:0001714_endodermal_cell_fate_specification	9	3	4.417855	0.049464
GO:0042663_regulation_of_endodermal_cell_fate_specific	9	3	4.417855	0.049464
GO:0055001_muscle_cell_development	23	5	2.88121	0.050993
GO:0055002_striated_muscle_cell_development	23	5	2.88121	0.050993
GO:0014032_neural_crest_cell_development	24	5	2.76116	0.057193
GO:0045934_negative_regulation_of_nucleobase__nuclec	24	5	2.76116	0.057193
GO:0051239_regulation_of_multicellular_organismal_proc	24	5	2.76116	0.057193
GO:0003008_system_process	108	14	1.718055	0.057622
GO:0007601_visual_perception	41	7	2.262804	0.057639
GO:0050953_sensory_perception_of_light_stimulus	41	7	2.262804	0.057639
GO:0001763_morphogenesis_of_a_branching_structure	10	3	3.97607	0.062966
GO:0048705_skeletal_morphogenesis	10	3	3.97607	0.062966
GO:0030099_myeloid_cell_differentiation	17	4	3.118486	0.064983
GO:0048469_cell_maturation	25	5	2.650713	0.066633
GO:0048741_skeletal_muscle_fiber_development	25	5	2.650713	0.066633
GO:0048747_muscle_fiber_development	25	5	2.650713	0.066633
GO:0006826_iron_ion_transport	132	16	1.606493	0.069424
GO:0046483_heterocycle_metabolic_process	112	14	1.656696	0.070878
GO:0045445_myoblast_differentiation	18	4	2.945237	0.073244
GO:0048627_myoblast_development	18	4	2.945237	0.073244
GO:0048628_myoblast_maturation	18	4	2.945237	0.073244
GO:0001711_endodermal_cell_fate_commitment	11	3	3.614609	0.078567
GO:0065008_regulation_of_biological_quality	289	30	1.375803	0.078709
GO:0042074_cell_migration_involved_in_gastrulation	44	7	2.108522	0.078904
GO:0014031_mesenchymal_cell_development	27	5	2.454364	0.080621
GO:0014033_neural_crest_cell_differentiation	27	5	2.454364	0.080621
GO:0021700_developmental_maturation	27	5	2.454364	0.080621
GO:0060041_retina_development_in_camera-type_eye	27	5	2.454364	0.080621
GO:0051179_localization	1764	150	1.127004	0.089172
GO:0001503_ossification	5	2	5.301426	0.089231
GO:0001569_patterning_of_blood_vessels	5	2	5.301426	0.089231
GO:0003006_reproductive_developmental_process	5	2	5.301426	0.089231
GO:0006970_response_to_osmotic_stress	5	2	5.301426	0.089231
GO:0007194_negative_regulation_of_adenylate_cyclase_a	5	2	5.301426	0.089231
GO:0007548_sex_differentiation	5	2	5.301426	0.089231
GO:0009651_response_to_salt_stress	5	2	5.301426	0.089231
GO:0021548_pons_development	5	2	5.301426	0.089231
GO:0030178_negative_regulation_of_Wnt_receptor_signa	5	2	5.301426	0.089231
GO:0030325_adrenal_gland_development	5	2	5.301426	0.089231
GO:0030855_epithelial_cell_differentiation	5	2	5.301426	0.089231
GO:0030947_regulation_of_vascular_endothelial_growth_	5	2	5.301426	0.089231
GO:0031280_negative_regulation_of_cyclase_activity	5	2	5.301426	0.089231
GO:0045786_negative_regulation_of_cell_cycle	5	2	5.301426	0.089231
GO:0045926_negative_regulation_of_growth	5	2	5.301426	0.089231
GO:0048263_determination_of_dorsal_identity	5	2	5.301426	0.089231
GO:0048754_branching_morphogenesis_of_a_tube	5	2	5.301426	0.089231
GO:0050935_iridophore_differentiation	5	2	5.301426	0.089231
GO:0051350_negative_regulation_of_lyase_activity	5	2	5.301426	0.089231

GO:0001666_response_to_hypoxia	19	4	2.790224	0.092416
GO:0065009_regulation_of_molecular_function	75	10	1.767142	0.094573
GO:0006879_cellular_iron_ion_homeostasis	138	16	1.536645	0.094879
GO:0055072_iron_ion_homeostasis	138	16	1.536645	0.094879
GO:0008361_regulation_of_cell_size	28	5	2.366708	0.095723
GO:0016049_cell_growth	28	5	2.366708	0.095723
GO:0035239_tube_morphogenesis	12	3	3.313391	0.098358
GO:0048264_determination_of_ventral_identity	12	3	3.313391	0.098358
GO:0048840_otolith_development	12	3	3.313391	0.098358
GO:0045935_positive_regulation_of_nucleobase__nucleos	37	6	2.149227	0.099377
GO:0045941_positive_regulation_of_transcription	37	6	2.149227	0.099377
GO:0019226_transmission_of_nerve_impulse	20	4	2.650713	0.102722
GO:0050877_neurological_system_process	77	10	1.721242	0.10469
GO:0031175_neurite_development	48	7	1.932812	0.110735
GO:0001655_urogenital_system_development	21	4	2.524489	0.113275
GO:0001822_kidney_development	21	4	2.524489	0.113275
GO:0006767_water-soluble_vitamin_metabolic_process	13	3	3.058515	0.117081
GO:0030510_regulation_of_BMP_signaling_pathway	13	3	3.058515	0.117081
GO:0045892_negative_regulation_of_transcription__DNA-	13	3	3.058515	0.117081
GO:0051253_negative_regulation_of_RNA_metabolic_pro	13	3	3.058515	0.117081
GO:0001508_regulation_of_action_potential	6	2	4.417855	0.127618
GO:0006721_terpenoid_metabolic_process	6	2	4.417855	0.127618
GO:0006775_fat-soluble_vitamin_metabolic_process	6	2	4.417855	0.127618
GO:0006776_vitamin_A_metabolic_process	6	2	4.417855	0.127618
GO:0007272_ensheathment_of_neurons	6	2	4.417855	0.127618
GO:0008366_axon_ensheathment	6	2	4.417855	0.127618
GO:0019228_regulation_of_action_potential_in_neuron	6	2	4.417855	0.127618
GO:0022414_reproductive_process	6	2	4.417855	0.127618
GO:0031279_regulation_of_cyclase_activity	6	2	4.417855	0.127618
GO:0042552_myelination	6	2	4.417855	0.127618
GO:0045761_regulation_of_adenylate_cyclase_activity	6	2	4.417855	0.127618
GO:0048702_embryonic_neurocranium_morphogenesis	6	2	4.417855	0.127618
GO:0048881_mechanosensory_lateral_line_system_devel	6	2	4.417855	0.127618
GO:0048915_posterior_lateral_line_system_development	6	2	4.417855	0.127618
GO:0051339_regulation_of_lyase_activity	6	2	4.417855	0.127618
GO:0007519_skeletal_muscle_development	30	5	2.208928	0.132802
GO:0031324_negative_regulation_of_cellular_metabolic_p	30	5	2.208928	0.132802
GO:0048762_mesenchymal_cell_differentiation	30	5	2.208928	0.132802
GO:0051188_cofactor_biosynthetic_process	122	14	1.520901	0.134603
GO:0042592_homeostatic_process	223	23	1.36696	0.134973
GO:0009893_positive_regulation_of_metabolic_process	40	6	1.988035	0.135163
GO:0031325_positive_regulation_of_cellular_metabolic_pr	40	6	1.988035	0.135163
GO:0009892_negative_regulation_of_metabolic_process	31	5	2.137672	0.139539
GO:0030003_cellular_cation_homeostasis	146	16	1.452446	0.139838
GO:0030005_cellular_di-__tri-valent_inorganic_cation_hor	146	16	1.452446	0.139838
GO:0051186_cofactor_metabolic_process	147	16	1.442565	0.145764
GO:0055066_di-__tri-valent_inorganic_cation_homeostasi	147	16	1.442565	0.145764
GO:0001757_somite_specification	7	2	3.786733	0.162249
GO:0007379_segment_specification	7	2	3.786733	0.162249
GO:0035051_cardiac_cell_differentiation	7	2	3.786733	0.162249
GO:0042364_water-soluble_vitamin_biosynthetic_process	7	2	3.786733	0.162249
GO:0048010_vascular_endothelial_growth_factor_recepto	7	2	3.786733	0.162249
GO:0006829_zinc_ion_transport	526	48	1.209451	0.163615
GO:0055080_cation_homeostasis	149	16	1.423202	0.165553
GO:0007218_neuropeptide_signaling_pathway	15	3	2.650713	0.169974
GO:0030218_erythrocyte_differentiation	15	3	2.650713	0.169974
GO:0030239_myofibril_assembly	15	3	2.650713	0.169974
GO:0034101_erythrocyte_homeostasis	15	3	2.650713	0.169974
GO:0048872_homeostasis_of_number_of_cells	15	3	2.650713	0.169974
GO:0051726_regulation_of_cell_cycle	15	3	2.650713	0.169974
GO:0051094_positive_regulation_of_developmental_proce	43	6	1.849335	0.172661
GO:0007411_axon_guidance	24	4	2.208928	0.174175
GO:0007409_axonogenesis	44	6	1.807304	0.178226
GO:0045893_positive_regulation_of_transcription__DNA-c	16	3	2.485044	0.182941
GO:0051254_positive_regulation_of_RNA_metabolic_proc	16	3	2.485044	0.182941
GO:0001839_neural_plate_morphogenesis	8	2	3.313391	0.19199
GO:0006633_fatty_acid_biosynthetic_process	8	2	3.313391	0.19199
GO:0006769_nicotinamide_metabolic_process	8	2	3.313391	0.19199
GO:0007187_G-protein_signaling__coupled_to_cyclic_nuc	8	2	3.313391	0.19199
GO:0007188_G-protein_signaling__coupled_to_cAMP_nu	8	2	3.313391	0.19199
GO:0009110_vitamin_biosynthetic_process	8	2	3.313391	0.19199
GO:0019362_pyridine_nucleotide_metabolic_process	8	2	3.313391	0.19199
GO:0019933_cAMP-mediated_signaling	8	2	3.313391	0.19199
GO:0019935_cyclic-nucleotide-mediated_signaling	8	2	3.313391	0.19199
GO:0030514_negative_regulation_of_BMP_signaling_path	8	2	3.313391	0.19199
GO:0042398_amino_acid_derivative_biosynthetic_process	8	2	3.313391	0.19199
GO:0048667_neuron_morphogenesis_during_differentiatic	45	6	1.767142	0.193614
GO:0048812_neurite_morphogenesis	45	6	1.767142	0.193614
GO:0003013_circulatory_system_process	26	4	2.03901	0.19697
GO:0008015_blood_circulation	26	4	2.03901	0.19697

Supplemetal Table 3. H3K27me3 top 250 genes scores and other marks.
Enrichment of modifications are scored in proximal promoter region (-2 ~ +1 kb of TSS).

	K27me3 -2+1	fold	H2AFV -2+1	fold	K4me3 -2+1	fold	K4me2 -2+1	fold	K14ac -2+1	fold
foxb1.2	1.824	3.54	0.4587	1.37	1.1699	2.25	2.1309	4.38	0.3367	1.26
dlx1a	1.8205	3.53	0.6521	1.57	1.6015	3.03	2.025	4.07	0.402	1.32
hoxa11a	1.7721	3.42	0.5176	1.43	1.8448	3.59	2.1114	4.32	0.3162	1.25
fli1b	1.7643	3.40	0.5282	1.44	1.5839	3.00	1.9529	3.87	0.5663	1.48
six2.1	1.7513	3.37	0.4871	1.40	1.6492	3.14	1.9268	3.80	0.6302	1.55
hoxc6a	1.7384	3.34	0.5132	1.43	1.4666	2.76	1.6821	3.21	0.3417	1.27
pax7	1.7248	3.31	0.5495	1.46	1.291	2.45	2.2619	4.80	0.2929	1.23
hoxa5a	1.7112	3.27	0.6255	1.54	1.6236	3.08	1.3117	2.48	0.2415	1.18
zic2a	1.7028	3.26	0.3771	1.30	1.3841	2.61	2.0741	4.21	0.4168	1.33
hoxd9a	1.701	3.25	0.5277	1.44	1.4831	2.80	1.7966	3.47	-0.0103	0.99
nkx2.9	1.6955	3.24	0.3211	1.25	1.1547	2.23	1.7986	3.48	0.1713	1.13
meis1	1.691	3.23	0.4309	1.35	1.6445	3.13	1.8639	3.64	0.5624	1.48
hoxa9a	1.6797	3.20	0.6559	1.58	1.6262	3.09	1.8388	3.58	0.5059	1.42
tfap2a	1.6777	3.20	0.4558	1.37	1.3402	2.53	1.5551	2.94	0.6934	1.62
hoxc12b	1.6774	3.20	0.59	1.51	1.6164	3.07	1.6378	3.11	0.4544	1.37
hoxd10a	1.6623	3.17	0.4599	1.38	1.2551	2.39	1.9172	3.78	0.0443	1.03
arx	1.6622	3.16	0.4758	1.39	1.4652	2.76	1.6412	3.12	0.558	1.47
zgc:114196	1.6501	3.14	0.533	1.45	1.4797	2.79	1.4827	2.79	0.3706	1.29
pax9	1.6493	3.14	0.2802	1.21	1.6	3.03	1.3559	2.56	0.3653	1.29
hoxb6a	1.6481	3.13	0.3174	1.25	0.9786	1.97	1.7742	3.42	0.0803	1.06
zgc:85811	1.6469	3.13	-0.5558	0.68	-1.9882	0.25	1.8179	3.53	0.5822	1.50
gad1	1.6345	3.10	0.4365	1.35	0.7745	1.71	1.7582	3.38	0.4875	1.40
hoxc8a	1.6235	3.08	0.4177	1.34	1.6202	3.07	1.7223	3.30	0.2757	1.21
zgc:154123 (zic4)	1.6182	3.07	0.5013	1.42	1.0991	2.14	1.7561	3.38	0.2719	1.21
foxc1b	1.6036	3.04	0.5472	1.46	1.3836	2.61	1.515	2.86	0.5625	1.48
evx2	1.6034	3.04	0.5796	1.49	1.1237	2.18	1.9135	3.77	0.1612	1.12
zic1	1.6033	3.04	0.3893	1.31	0.8695	1.83	1.9135	3.77	0.1833	1.14
six3a	1.6022	3.04	0.7201	1.65	1.7537	3.37	1.7701	3.41	0.5892	1.50
hoxc9a	1.5967	3.02	0.4231	1.34	1.4873	2.80	1.4838	2.80	0.2344	1.18
otx1	1.5949	3.02	0.5903	1.51	1.6573	3.15	1.6448	3.13	0.4973	1.41
ptf1a	1.5862	3.00	0.4763	1.39	1.2229	2.33	1.6448	3.13	0.3047	1.24
irx1a	1.5843	3.00	0.5812	1.50	0.6262	1.54	0.6427	1.56	0.0834	1.06
gsx2	1.5825	2.99	0.3712	1.29	1.0529	2.07	0.8543	1.81	-0.032	0.98
tfap2b	1.5775	2.98	0.5338	1.45	1.3748	2.59	0.6585	1.58	0.6125	1.53
commd3	1.5727	2.97	0.5868	1.50	1.6806	3.21	1.8207	3.53	0.7452	1.68
hoxc6b	1.5701	2.97	0.5765	1.49	1.7141	3.28	1.1413	2.21	0.5719	1.49
tbx1	1.5689	2.97	0.434	1.35	1.6579	3.16	1.4458	2.72	0.5986	1.51
pitx2a	1.562	2.95	0.6609	1.58	1.4642	2.76	1.6443	3.13	0.3211	1.25
hoxc5a	1.5593	2.95	0.4037	1.32	1.6057	3.04	0.7114	1.64	0.5655	1.48
hoxc13a	1.5542	2.94	0.5765	1.49	1.2305	2.35	1.4571	2.75	0.3203	1.25
evx1	1.5536	2.94	0.5218	1.44	1.3127	2.48	1.7666	3.40	0.0768	1.05
foxd1	1.552	2.93	0.651	1.57	1.5263	2.88	0.8421	1.79	0.155	1.11
coe2	1.5514	2.93	0.62	1.54	1.5609	2.95	1.3191	2.50	0.3779	1.30
dmrta2	1.5483	2.92	0.3236	1.25	1.3275	2.51	1.1206	2.17	0.2489	1.19
zgc:113499 (eng1b)	1.5473	2.92	0.3709	1.29	2.0144	4.04	1.6388	3.11	0.7664	1.70
tbx2b	1.5458	2.92	0.3099	1.24	1.4706	2.77	1.0524	2.07	0.1632	1.12
hoxb5a	1.5406	2.91	0.3821	1.30	1.1337	2.19	1.0226	2.03	0.0489	1.03
zic5	1.5401	2.91	0.4292	1.35	1.0799	2.11	1.5081	2.84	0.3581	1.28
hoxd4a	1.5399	2.91	0.5993	1.51	1.0537	2.08	1.6174	3.07	-0.0424	0.97
dlx3b	1.5381	2.90	0.5853	1.50	1.3068	2.47	1.4099	2.66	0.2307	1.17
hlx1	1.5317	2.89	0.415	1.33	1.0649	2.09	1.7724	3.42	-0.0283	0.98
zgc:112001	1.5302	2.89	0.697	1.62	0.6259	1.54	1.2767	2.42	0.5897	1.50
foxd3	1.5244	2.88	0.4813	1.40	1.617	3.07	1.6376	3.11	0.3255	1.25
her3	1.5236	2.88	0.6674	1.59	1.1447	2.21	1.3799	2.60	0.3473	1.27
vox	1.523	2.87	0.4939	1.41	1.8005	3.48	0.6196	1.54	0.4165	1.33
pax6a	1.5161	2.86	0.4201	1.34	1.114	2.16	0.522	1.44	0.4386	1.36
dlx6a	1.5154	2.86	0.3652	1.29	1.5084	2.84	1.5405	2.91	0.3339	1.26
tbx5	1.5144	2.86	0.3507	1.28	1.4126	2.66	1.4967	2.82	0.2203	1.16
hoxb8a	1.5144	2.86	0.5717	1.49	1.1146	2.17	1.2644	2.40	0.1919	1.14
gata3	1.5099	2.85	0.2313	1.17	1.032	2.04	0.157	1.11	0.1794	1.13
barhl2	1.5031	2.83	0.7296	1.66	1.4	2.64	1.0976	2.14	0.4231	1.34
nkx2.1b	1.5016	2.83	0.5319	1.45	1.057	2.08	1.287	2.44	0.2144	1.16
fgf3	1.4994	2.83	0.3976	1.32	1.1998	2.30	1.9648	3.90	0.0769	1.05
tbx2a	1.4967	2.82	0.4341	1.35	1.633	3.10	1.9648	3.90	0.3402	1.27
zgc:101606	1.4937	2.82	0.2094	1.16	0.9089	1.88	1.3508	2.55	-0.0263	0.98
msxe	1.4925	2.81	0.5525	1.47	1.1886	2.28	1.0514	2.07	0.1838	1.14
zgc:162280 (ccnd2)	1.4876	2.80	0.5365	1.45	1.6436	3.12	1.2884	2.44	0.2263	1.17
sox1a	1.4844	2.80	0.3945	1.31	1.1921	2.28	1.4409	2.71	0.0507	1.04
flh	1.484	2.80	0.489	1.40	1.1769	2.26	1.0867	2.12	0.4583	1.37
si:ch211-103o12.1	1.4795	2.79	0.5777	1.49	1.1625	2.24	1.5154	2.86	0.1404	1.10
tlx3b	1.479	2.79	0.6751	1.60	1.0683	2.10	1.837	3.57	0.0681	1.05
sp8l	1.478	2.79	0.4518	1.37	1.2486	2.38	1.5979	3.03	0.2482	1.19
nkx2.1a	1.4758	2.78	0.4227	1.34	1.0325	2.05	1.6083	3.05	0.0629	1.04
otpb	1.4753	2.78	0.4343	1.35	1.4349	2.70	1.3304	2.51	0.3533	1.28
otx2	1.4698	2.77	0.4219	1.34	1.5156	2.86	0.992	1.99	0.4173	1.34
hoxb3a	1.4643	2.76	0.3449	1.27	0.8607	1.82	1.5183	2.86	-0.02	0.99

pcdh2ab12	1.4642	2.76	0.5148	1.43	0.9024	1.87	0.8321	1.78	0.0046	1.00
irx3a	1.4596	2.75	0.4635	1.38	1.0532	2.08	1.385	2.61	0.0555	1.04
foxi2	1.4588	2.75	0.2765	1.21	1.1104	2.16	1.2655	2.40	0.2257	1.17
emx1	1.4582	2.75	0.5518	1.47	1.0519	2.07	0.6762	1.60	0.0596	1.04
hoxa2b	1.4572	2.75	0.6904	1.61	1.3955	2.63	1.0458	2.06	0.4565	1.37
pcdh2ab10	1.4552	2.74	0.4285	1.35	0.9024	1.87	1.1751	2.26	-0.0701	0.95
pcdh2ab11	1.4552	2.74	0.4285	1.35	0.9024	1.87	1.1954	2.29	-0.0701	0.95
si:rp71-45k5.2	1.4549	2.74	0.5009	1.42	1.2421	2.37	1.0101	2.01	0.5292	1.44
neurog3	1.4526	2.74	0.44	1.36	0.9315	1.91	1.4919	2.81	0.5721	1.49
sp9	1.4524	2.74	0.4251	1.34	1.1057	2.15	1.251	2.38	0.1364	1.10
pou12	1.4514	2.73	0.367	1.29	1.3352	2.52	1.4161	2.67	0.185	1.14
dlx2a	1.447	2.73	0.4454	1.36	1.4447	2.72	1.3507	2.55	-0.0453	0.97
dbx1b	1.443	2.72	0.4465	1.36	1.367	2.58	0.6082	1.52	0.4201	1.34
hoxd13a	1.4425	2.72	0.5528	1.47	0.9923	1.99	1.6103	3.05	-0.041	0.97
hoxb4a	1.4411	2.72	0.3403	1.27	0.9331	1.91	1.2684	2.41	0.0806	1.06
hoxb2a	1.4396	2.71	0.4865	1.40	1.1386	2.20	1.065	2.09	0.1654	1.12
meis2.2	1.4394	2.71	0.5794	1.49	1.0577	2.08	1.0417	2.06	-0.2391	0.85
hoxb1a	1.4374	2.71	0.394	1.31	1.0449	2.06	1.27	2.41	0.2329	1.18
foxb1.1	1.4364	2.71	0.3724	1.29	1.0335	2.05	0.9462	1.93	0.3446	1.27
nkx2.5	1.4362	2.71	0.308	1.24	0.9461	1.93	0.4934	1.41	0.6204	1.54
hoxb1b	1.4349	2.70	0.2777	1.21	1.4793	2.79	1.1633	2.24	0.3143	1.24
ets1b	1.4337	2.70	0.2516	1.19	1.1121	2.16	0.6625	1.58	0.2896	1.22
dlx5a	1.4336	2.70	0.2788	1.21	1.0432	2.06	0.8976	1.86	0.194	1.14
her6	1.4332	2.70	0.3014	1.23	1.0545	2.08	0.4924	1.41	0.3055	1.24
zgc:110344 (six6b)	1.4294	2.69	0.5511	1.47	1.6616	3.16	0.493	1.41	0.3524	1.28
pcdh2ab10	1.4292	2.69	0.4285	1.35	0.9024	1.87	0.9327	1.91	-0.0701	0.95
pcdh2ab6	1.4292	2.69	0.2466	1.19	0.7662	1.70	1.3807	2.60	-0.2023	0.87
pcdh2ab7	1.4292	2.69	0.2466	1.19	0.7662	1.70	-0.5159	0.70	-0.2023	0.87
bhlhb5	1.4286	2.69	0.537	1.45	1.0541	2.08	1.1005	2.14	0.0332	1.02
hoxa3a	1.426	2.69	0.5076	1.42	1.5662	2.96	0.4347	1.35	0.4341	1.35
phox2a	1.4254	2.69	0.6704	1.59	1.3924	2.63	1.5677	2.96	-0.1188	0.92
og9x	1.4246	2.68	0.6055	1.52	1.321	2.50	1.1665	2.24	0.2362	1.18
wnt8-2	1.423	2.68	0.3562	1.28	1.1712	2.25	1.0698	2.10	0.4395	1.36
pcdh2ab9	1.4206	2.68	0.4285	1.35	0.8384	1.79	1.1078	2.16	-0.166	0.89
pcdh2ab3	1.4206	2.68	0.2465	1.19	0.7662	1.70	0.7549	1.69	-0.2022	0.87
pcdh2ab5	1.4206	2.68	0.136	1.10	0.6701	1.59	0.5908	1.51	-0.2948	0.82
nkx2.2b	1.4193	2.67	0.5264	1.44	1.2314	2.35	0.0321	1.02	0.0704	1.05
pou4f2	1.4183	2.67	0.4065	1.33	1.01	2.01	1.2294	2.34	0.0941	1.07
dlx4b	1.4174	2.67	0.3284	1.26	1.3252	2.51	0.6117	1.53	0.0937	1.07
fezf2	1.405	2.65	0.3457	1.27	1.1583	2.23	0.6567	1.58	0.1494	1.11
fgf4	1.4043	2.65	0.3727	1.29	0.8613	1.82	0.9119	1.88	0.0444	1.03
sp8	1.4037	2.65	0.5956	1.51	1.1624	2.24	0.7415	1.67	0.0468	1.03
LOC554876	1.3998	2.64	0.1596	1.12	1.2003	2.30	1.1	2.14	0.5808	1.50
zgc:113424 (contain	1.3998	2.64	0.1596	1.12	1.2003	2.30	1.095	2.14	0.5808	1.50
atoh2b	1.3981	2.64	0.4271	1.34	1.4514	2.73	1.095	2.14	0.3135	1.24
emx2	1.3976	2.63	0.4989	1.41	1.7486	3.36	0.7558	1.69	0.207	1.15
hoxa13b	1.3956	2.63	0.6576	1.58	1.3925	2.63	0.8278	1.77	0.0628	1.04
hoxa1a	1.3907	2.62	0.4832	1.40	1.7388	3.34	1.1144	2.17	0.4252	1.34
mafb	1.3906	2.62	0.407	1.33	1.2951	2.45	1.3548	2.56	-0.2642	0.83
nkx2.2a	1.3824	2.61	0.4368	1.35	0.9656	1.95	0.4559	1.37	0.4447	1.36
tbx20	1.3814	2.61	0.433	1.35	1.4975	2.82	0.4559	1.37	0.1254	1.09
foxg1	1.3799	2.60	0.4434	1.36	1.8608	3.63	1.0634	2.09	0.9114	1.88
tbx4	1.3799	2.60	0.4832	1.40	1.3539	2.56	1.2627	2.40	0.3899	1.31
dll4	1.3779	2.60	0.442	1.36	1.2466	2.37	1.0975	2.14	0.3974	1.32
nkx2.3	1.377	2.60	0.3507	1.28	1.0156	2.02	1.1375	2.20	-0.2275	0.85
slc17a6	1.3759	2.60	0.32	1.25	0.7077	1.63	0.6137	1.53	0.3129	1.24
hoxa10b	1.3744	2.59	0.5792	1.49	1.3005	2.46	0.3361	1.26	0.062	1.04
wnt10b	1.3738	2.59	0.0876	1.06	1.2079	2.31	0.5246	1.44	0.3119	1.24
hoxb5b	1.3734	2.59	0.3117	1.24	1.2848	2.44	1.0795	2.11	0.3398	1.27
pax3	1.3726	2.59	0.5818	1.50	1.6962	3.24	0.4765	1.39	0.1009	1.07
nrn1	1.3726	2.59	0.4878	1.40	0.8623	1.82	0.9433	1.92	-0.0074	0.99
tlx3a	1.3708	2.59	0.4585	1.37	0.9765	1.97	0.7838	1.72	-0.0041	1.00
bsx	1.3694	2.58	0.2436	1.18	1.417	2.67	0.4258	1.34	0.7323	1.66
zgc:64055 (prrx1a)	1.3649	2.58	0.3997	1.32	1.8427	3.59	0.8203	1.77	0.5217	1.44
pax2a	1.3644	2.57	0.5169	1.43	1.6134	3.06	-0.4454	0.73	0.3688	1.29
twist1a	1.364	2.57	0.5131	1.43	0.9937	1.99	0.0577	1.04	0.0872	1.06
ccnd1	1.3605	2.57	0.4207	1.34	1.1791	2.26	0.5427	1.46	-0.0618	0.96
neurod	1.3596	2.57	0.3782	1.30	1.4241	2.68	-0.4845	0.71	0.1391	1.10
hoxa11b	1.3547	2.56	0.5021	1.42	1.6128	3.06	1.1464	2.21	0.1471	1.11
lhx1a	1.3537	2.56	0.5066	1.42	1.3334	2.52	1.2607	2.40	0.434	1.35
nkx2.7	1.3533	2.55	0.3455	1.27	1.0751	2.11	0.639	1.56	-0.03	0.98
eomesa	1.353	2.55	0.7191	1.65	1.0435	2.06	0.7418	1.67	0.062	1.04
foxa3	1.3511	2.55	0.3948	1.31	1.2401	2.36	0.41	1.33	0.6006	1.52
znf503	1.351	2.55	0.4329	1.35	1.3606	2.57	0.9333	1.91	0.317	1.25
nkx3.2	1.351	2.55	0.5502	1.46	1.2063	2.31	0.6849	1.61	-0.0449	0.97
vsx2	1.3489	2.55	0.4556	1.37	1.7264	3.31	0.7	1.62	0.2711	1.21
nrp1a	1.3456	2.54	0.1818	1.13	0.5568	1.47	0.9628	1.95	-0.1441	0.90
zgc:136674	1.3456	2.54	0.1818	1.13	0.5568	1.47	0.9324	1.91	-0.1441	0.90
gfi1	1.3428	2.54	0.4328	1.35	1.4559	2.74	1.231	2.35	0.576	1.49

nr2f1	1.3391	2.53	0.2688	1.20	1.7332	3.32	1.3015	2.46	0.1513	1.11
neurog1	1.3363	2.53	0.2466	1.19	1.1503	2.22	1.1375	2.20	0.1925	1.14
zgc:92332 (six1a)	1.3351	2.52	0.5115	1.43	1.1739	2.26	1.0834	2.12	-0.1302	0.91
otx1l	1.3344	2.52	0.6244	1.54	1.5038	2.84	-0.1475	0.90	0.2996	1.23
gata2	1.3284	2.51	0.2216	1.17	1.3753	2.59	0.6709	1.59	0.1328	1.10
mmp14a	1.328	2.51	0.4948	1.41	0.9291	1.90	-0.2463	0.84	0.4303	1.35
bcor	1.3256	2.51	0.4957	1.41	1.6657	3.17	0.8209	1.77	0.4989	1.41
si:dkey-221h15.1	1.3244	2.50	0.5879	1.50	1.5138	2.86	0.6043	1.52	0.431	1.35
eng2a	1.3228	2.50	0.4419	1.36	2.1421	4.41	-0.712	0.61	0.4009	1.32
sox2	1.3212	2.50	0.5214	1.44	1.2098	2.31	0.6716	1.59	-0.1778	0.88
zgc:85869	1.3185	2.49	0.3547	1.28	1.1121	2.16	1.1133	2.16	0.051	1.04
foxd5	1.3178	2.49	0.4058	1.32	1.191	2.28	1.0868	2.12	-0.0439	0.97
zgc:153435 (btf3)	1.3153	2.49	0.4945	1.41	1.4613	2.75	-0.1712	0.89	0.3168	1.25
zgc:76875 (FoxD1)	1.3153	2.49	0.2917	1.22	1.4613	2.75	-0.1741	0.89	0.3168	1.25
sox21b	1.3148	2.49	0.3957	1.32	0.9882	1.98	0.6092	1.53	-0.0394	0.97
LOC567444	1.3144	2.49	0.4165	1.33	0.8281	1.78	0.3614	1.28	0.2313	1.17
zgc:77719 (hmga2)	1.3144	2.49	0.4165	1.33	0.8281	1.78	0.6206	1.54	0.2313	1.17
tfap2e	1.3142	2.49	0.3401	1.27	0.8285	1.78	0.225	1.17	0.1143	1.08
dmbx1a	1.3138	2.49	0.5816	1.50	1.5163	2.86	0.5265	1.44	0.0484	1.03
sim1	1.3118	2.48	0.5524	1.47	0.8353	1.78	0.7806	1.72	-0.0327	0.98
rx3	1.3113	2.48	0.741	1.67	1.4132	2.66	0.0072	1.01	0.3357	1.26
dlc	1.3111	2.48	0.2501	1.19	1.8667	3.65	0.0675	1.05	0.4792	1.39
cebpa	1.3077	2.48	0.4276	1.34	1.6488	3.14	0.5411	1.46	0.6425	1.56
cebpg	1.3077	2.48	0.4276	1.34	1.6488	3.14	0.5411	1.46	0.6425	1.56
lbx1	1.307	2.47	0.2778	1.21	0.8322	1.78	0.5411	1.46	-0.0937	0.94
eng2b	1.305	2.47	0.5097	1.42	2.0896	4.26	0.4188	1.34	0.4528	1.37
mab21l2	1.3048	2.47	0.4122	1.33	1.3015	2.46	-0.4899	0.71	0.2226	1.17
gata6	1.303	2.47	0.4751	1.39	1.1146	2.17	0.5452	1.46	-0.1968	0.87
fgf17b	1.3027	2.47	0.2281	1.17	0.4539	1.37	-0.0019	1.00	0.1941	1.14
hand2	1.3024	2.47	0.3822	1.30	1.5574	2.94	0.3244	1.25	0.1915	1.14
mab21l1	1.2996	2.46	0.4792	1.39	1.5223	2.87	0.3256	1.25	-0.1204	0.92
hoxc3a	1.2975	2.46	0.2861	1.22	1.3216	2.50	0.9285	1.90	0.3958	1.32
tlx1	1.2961	2.46	0.391	1.31	1.0162	2.02	1.3588	2.56	0.0103	1.01
hoxb9a	1.2935	2.45	0.3933	1.31	0.8522	1.81	1.168	2.25	-0.0562	0.96
gsc	1.2921	2.45	0.319	1.25	1.4291	2.69	-0.5004	0.71	0.2506	1.19
lhx9	1.2913	2.45	0.5529	1.47	1.1953	2.29	0.5277	1.44	-0.1053	0.93
six1	1.2896	2.44	0.2424	1.18	1.2879	2.44	0.778	1.71	-0.0442	0.97
meis4.1a	1.2893	2.44	0.617	1.53	1.4409	2.71	0.3013	1.23	0.0483	1.03
onecut1	1.2873	2.44	0.4605	1.38	1.2038	2.30	-0.1882	0.88	-0.0755	0.95
bmi1	1.2864	2.44	0.3825	1.30	2.2209	4.66	-0.1882	0.88	1.054	2.08
hoxa9b	1.2859	2.44	0.4903	1.40	1.3336	2.52	-0.1882	0.88	0.2592	1.20
lhx5	1.2852	2.44	0.4064	1.33	1.4434	2.72	-1.0105	0.50	0.0508	1.04
gata5	1.282	2.43	0.443	1.36	1.4113	2.66	0.1372	1.10	0.1476	1.11
zgc:158291 (contain l	1.2806	2.43	0.4237	1.34	1.0651	2.09	-0.0546	0.96	-0.0346	0.98
fgf18	1.2802	2.43	0.5022	1.42	0.2821	1.22	0.6391	1.56	0.1849	1.14
pdx1	1.2787	2.43	0.2683	1.20	1.1494	2.22	-0.1886	0.88	0.1911	1.14
mnx1	1.2781	2.43	0.4475	1.36	1.2295	2.34	-0.2424	0.85	0.4009	1.32
prox1	1.2697	2.41	0.4131	1.33	0.8634	1.82	-0.3734	0.77	0.2091	1.16
cdx4	1.2696	2.41	0.3822	1.30	0.9375	1.92	0.3507	1.28	0.1988	1.15
zgc:136976 (pitx1)	1.266	2.40	0.3261	1.25	1.0343	2.05	-0.3144	0.80	-0.284	0.82
shha	1.2639	2.40	0.2779	1.21	0.8596	1.81	-0.7612	0.59	0.0814	1.06
zgc:101766 (dmrt3)	1.2627	2.40	0.3871	1.31	1.2361	2.36	-0.4673	0.72	0.0317	1.02
ascl1a	1.262	2.40	0.4322	1.35	1.2496	2.38	0.4524	1.37	0.3363	1.26
lhx1b	1.2598	2.39	0.2683	1.20	1.2384	2.36	-0.0995	0.93	-0.0808	0.95
six3b	1.2596	2.39	0.3904	1.31	1.7777	3.43	0.1335	1.10	0.1968	1.15
zgc:77001 (tumor spe	1.2549	2.39	0.506	1.42	0.8804	1.84	0.1335	1.10	0.4139	1.33
hbaa1	1.2542	2.39	0.5626	1.48	1.1054	2.15	-0.3029	0.81	0.1924	1.14
ba1	1.2542	2.39	0.5626	1.48	1.0056	2.01	-0.9812	0.51	0.1191	1.09
ba2	1.2542	2.39	0.5626	1.48	1.0056	2.01	-0.9812	0.51	0.1191	1.09
si:xx-by187g17.1	1.2542	2.39	0.5626	1.48	1.0056	2.01	-0.9812	0.51	0.1191	1.09
hoxa4a	1.2526	2.38	0.1487	1.11	1.5512	2.93	0.7361	1.67	-0.0897	0.94
zgc:158781 (pbx1)	1.2486	2.38	0.5005	1.41	1.4401	2.71	-0.9812	0.51	0.0731	1.05
nr5a1b	1.2482	2.38	0.4096	1.33	0.9666	1.95	-0.5926	0.66	-0.1884	0.88
hoxc4a	1.2479	2.37	0.4	1.32	1.072	2.10	-1.0209	0.49	0.4809	1.40
diras1	1.2466	2.37	0.517	1.43	0.5103	1.42	-0.2076	0.87	0.4243	1.34
hmx3	1.2465	2.37	0.301	1.23	1.4194	2.67	-0.4149	0.75	0.2628	1.20
zgc:85969 (foxg1b)	1.2363	2.36	0.3551	1.28	0.6296	1.55	-0.4149	0.75	0.069	1.05
wnt8a	1.2348	2.35	0.1947	1.14	1.0664	2.09	0.7351	1.66	0.311	1.24
trh	1.2348	2.35	0.5865	1.50	0.4877	1.40	-0.1903	0.88	0.3138	1.24
tbx15	1.2334	2.35	0.4766	1.39	1.8334	3.56	-0.3836	0.77	0.2877	1.22
bmi1b	1.2292	2.34	0.3645	1.29	1.8527	3.61	-0.7394	0.60	0.2843	1.22
bmp2b	1.2276	2.34	0.4559	1.37	1.0724	2.10	-2.7095	0.15	0.2643	1.20
	K27me3		H2AFV		K4me3		K4me2		k14ac	
	fold in log2	fold	fold in log2	fold	fold in log2	fold	fold in log2	fold	fold in log2	fold
Average	1.42849651	2.70	0.44488897	1.36	1.2870477	2.44	1.01093925	2.02	0.2460754	1.19
Median	1.4193	2.67	0.4343	1.35	1.2305	2.35	0.9462	1.93	0.2226	1.17

Supplemental Table 4. H2AFV enriched top 250 genes in sperm.

si:dkey-7c18.18	1.4433
LOC557392	1.1433
zgc:136778	1.1433
mhc2dab	0.9705
zgc:152682	0.9705
zgc:123077	0.9705
si:busm1-266f07.1	0.9705
c15orf15	0.916
ddx54	0.9014
cat	0.8636
zgc:76869	0.8093
npffl	0.7867
eng1a	0.7635
rx3	0.741
zgc:85882	0.7309
barhl2	0.7296
LOC568664	0.7279
zgc:77499	0.7202
six3a	0.7201
eomesa	0.7191
zgc:112001	0.697
hoxa2b	0.6904
zgc:92225	0.6861
zgc:103670	0.6843
tlx3b	0.6751
phox2a	0.6704
vsx1	0.67
her3	0.6674
sept5a	0.6621
pcdh2ac	0.6621
pitx2a	0.6609
myca	0.6597
hoxa13b	0.6576
bxdc1	0.6571
slc11a2	0.6567
zgc:136699	0.6567
hoxa9a	0.6559
agps	0.6524
dlx1a	0.6521
foxd1	0.651
si:dkeyp-53d3.3	0.6509
zgc:56292	0.6476
zgc:152779	0.6368
msgn1	0.6328
si:ch211-51e12.7	0.6328
hoxa5a	0.6255
otx1l	0.6244
zgc:85979	0.6222
coe2	0.62
meis4.1a	0.617
eif2b1	0.6137
gtf2h3	0.6137
hoxa13a	0.6105
LOC566668	0.6104
zgc:136261	0.6104
zgc:112287	0.6104
og9x	0.6055
eno2	0.5995
hoxd4a	0.5993
zgc:92380	0.5981
sp8	0.5956
otx1	0.5903
hoxc12b	0.59
si:dkey-221h15.1	0.5879
rho	0.5878
commd3	0.5868
trh	0.5865
zgc:113324	0.5859
dlx3b	0.5853
zgc:64115	0.5847
tmcc3	0.5821
pax3	0.5818
dmbx1a	0.5816
dmbx1a	0.5816
irx1a	0.5812
irx1a	0.5812
evx2	0.5796
meis2.2	0.5794
hoxa10b	0.5792
ppp4r1	0.5783
si:ch211-103o12.1	0.5777
hoxc6b	0.5765
hoxc13a	0.5765
hoxc13a	0.5763

zgc:101598	0.5761
hoxb8a	0.5717
zgc:64213	0.5716
zgc:77397	0.5714
crygm4	0.5712
Tnni2	0.5664
tnni2	0.5664
si:xx-by187g17.1	0.5626
hbaa1	0.5626
ba2	0.5626
ba1	0.5626
zgc:110692	0.562
wbp2	0.5586
cbx8	0.557
zgc:63670	0.5549
zgc:77247	0.5543
zgc:101723	0.5539
zgc:55621	0.5533
lhx9	0.5529
lhx9	0.5529
hoxd13a	0.5528
zgc:111928	0.5525
msxe	0.5525
sim1	0.5524
emx1	0.5518
si:ch211-154o6.7	0.5516
zgc:110344	0.5511
nkx3.2	0.5502
rps9	0.5502
pax7	0.5495
pax7	0.5495
pax7	0.5495
pax7	0.5495
arpc1b	0.5489
lass5	0.5486
hel_dr3	0.5475
foxc1b	0.5472
rab13	0.5469
hspa4l	0.5461
zcchc10	0.5461
zgc:110567	0.5457
celsr2	0.5443
sox4a	0.5434
si:dkey-7c18.15	0.5422
LOC100003595	0.5411
zgc:63759	0.5405
zgc:103485	0.539
bhlhb5	0.537
zgc:63722	0.5368
zgc:162280	0.5365
vent	0.5345
pfdn5	0.5338
tfap2b	0.5338
tfap2b	0.5338
zgc:114196	0.533
nkx2.1b	0.5319
ppp2r2d	0.5302
zgc:92643	0.5292
rab14l	0.5292
fli1b	0.5282
zgc:173915	0.5279
zgc:77076	0.5279
zgc:171674	0.5279
serpinb1l3	0.5279
hoxd9a	0.5277
zgc:77816	0.5266
nkx2.2b	0.5264
pald	0.5244
zgc:66107	0.5241
pycard	0.5232
gnb2l1	0.5228
evx1	0.5218
sox2	0.5214
zgc:158376	0.5199
bysl	0.5194
slc25a10	0.5181
si:ch211-117l16.1	0.5181
hoxa11a	0.5176
diras1	0.517
pax2a	0.5169
zgc:171636	0.5153
zgc:92688	0.5153
pcdh2ab12	0.5148
zgc:73062	0.5145
hoxc6a	0.5132

hoxc6a	0.5132
twist1a	0.5131
si:ch211-153c20.4	0.5119
zgc:92332	0.5115
birc4	0.51
zgc:91873	0.51
eng2b	0.5097
zgc:101130	0.509
LOC554950	0.509
hoxa3a	0.5076
lhx1a	0.5066
zgc:63960	0.5066
zgc:77001	0.506
LOC791723	0.503
si:busm1-266f07.2	0.503
fgf18	0.5022
hoxa11b	0.5021
zgc:154123	0.5013
elovl1	0.5012
si:rp71-45k5.2	0.5009
zgc:158781	0.5005
emx2	0.4989
ldhd	0.498
ppapdc1b	0.4962
bcor	0.4957
cdca8l	0.4951
mmp14a	0.4948
zgc:153435	0.4945
vox	0.4939
zgc:55418	0.4915
si:dkey-7c18.11	0.4911
hoxa9b	0.4903
zgc:66036	0.4892
flh	0.489
robo2	0.489
nrn1	0.4878
aldoab	0.4876
six2.1	0.4871
lama4	0.4868
hoxb2a	0.4865
sox4b	0.4858
zgc:63466	0.4854
zgc:103479	0.4853
si:ch211-223m11.2	0.4849
zgc:92357	0.4847
chys1	0.4842
zgc:85889	0.4833
tbx4	0.4832
hoxa1a	0.4832
si:ch211-237l4.5	0.4821
slc10a4	0.482
LOC100000756	0.4819
ephb4a	0.4819
foxd3	0.4813
inhbaa	0.4808
esr1	0.4798
irx7	0.4797
mab21l1	0.4792
zgc:92360	0.479
hbaa1	0.4777
zgc:92429	0.4775
zgc:92871	0.4773
LOC566052	0.4773
LOC566052	0.4773
zgc:92871	0.4773
tbx15	0.4766
ptf1a	0.4763
arx	0.4758
pdyn	0.4752
pdyn	0.4752
gata6	0.4751
zgc:92004	0.4743
zgc:66442	0.4743
chd	0.4741
gnb1l	0.4738
zgc:73144	0.4736
LOC555053	0.4731
zgc:63514	0.4731
zgc:63721	0.4727
rs1	0.4703
zgc:91874	0.4688

	fold in log2	fold
Average	0.572124	1.48671
Median	0.545	1.45902

Supplemental Table 5. H2AFV GO

HYPERLINKED GO CATEGORY	TOTAL	GE CHANG	ENRICHMI	FALSE DISCOVERY RATE
GO:0035270_endocrine_system_development	31	14	6.358314	0
GO:0030902_hindbrain_development	38	15	5.557549	0
GO:0007420_brain_development	100	35	4.927694	0
GO:0007417_central_nervous_system_development	137	43	4.418995	0
GO:0022411_cellular_component_disassembly	312	90	4.061286	0
GO:0032984_macromolecular_complex_disassembly	312	90	4.061286	0
GO:0043241_protein_complex_disassembly	312	90	4.061286	0
GO:0043624_cellular_protein_complex_disassembly	312	90	4.061286	0
GO:0006353_transcription_termination	310	89	4.042071	0
GO:0031554_regulation_of_transcription_termination	310	89	4.042071	0
GO:0031555_transcriptional_attenuation	310	89	4.042071	0
GO:0031564_transcription_antitermination	310	89	4.042071	0
GO:0043244_regulation_of_protein_complex_disassembly	310	89	4.042071	0
GO:0048598_embryonic_morphogenesis	83	23	3.901444	0
GO:0032268_regulation_of_cellular_protein_metabolic_process	331	90	3.828161	0
GO:0051128_regulation_of_cellular_component_organization_and_b	349	91	3.671061	0
GO:0006355_regulation_of_transcription__DNA-dependent	747	188	3.543341	0
GO:0051252_regulation_of_RNA_metabolic_process	748	188	3.538604	0
GO:0006351_transcription__DNA-dependent	766	189	3.473831	0
GO:0032774_RNA_biosynthetic_process	769	189	3.460279	0
GO:0048646_anatomical_structure_formation	82	20	3.433933	0
GO:0051246_regulation_of_protein_metabolic_process	373	90	3.397108	0
GO:0045449_regulation_of_transcription	833	197	3.329637	0
GO:0019219_regulation_of_nucleobase__nucleoside__nucleotide_ar	837	197	3.313725	0
GO:0007399_nervous_system_development	236	55	3.281152	0
GO:0010468_regulation_of_gene_expression	857	199	3.269248	0
GO:0006350_transcription	859	198	3.245246	0
GO:0031323_regulation_of_cellular_metabolic_process	865	198	3.222736	0
GO:0019222_regulation_of_metabolic_process	908	198	3.070117	0
GO:0009887_organ_morphogenesis	172	37	3.028649	0
GO:0016070_RNA_metabolic_process	905	193	3.002509	0
GO:0048513_organ_development	482	100	2.92098	0
GO:0048731_system_development	571	111	2.736923	0
GO:0010467_gene_expression	1143	212	2.611351	0
GO:0048856_anatomical_structure_development	627	116	2.60475	0
GO:0050794_regulation_of_cellular_process	1269	232	2.573961	0
GO:0009790_embryonic_development	255	46	2.539764	0
GO:0007275_multicellular_organismal_development	725	129	2.505113	0
GO:0050789_regulation_of_biological_process	1345	238	2.491325	0
GO:0009653_anatomical_structure_morphogenesis	347	61	2.475005	0
GO:0032501_multicellular_organismal_process	844	147	2.45217	0
GO:0006139_nucleobase__nucleoside__nucleotide_and_nucleic_aci	1221	209	2.40994	0
GO:0007389_pattern_specification_process	170	29	2.401733	0
GO:0065007_biological_regulation	1594	263	2.322967	0
GO:0032502_developmental_process	869	137	2.219609	0
GO:0043283_biopolymer_metabolic_process	1699	225	1.86451	0
GO:0016043_cellular_component_organization_and_biogenesis	876	115	1.848287	0
GO:0043170_macromolecule_metabolic_process	2338	262	1.577729	0
GO:0044237_cellular_metabolic_process	2799	295	1.483866	0
GO:0044238_primary_metabolic_process	2744	288	1.477692	0
GO:0008152_metabolic_process	3336	316	1.333634	0
GO:0009987_cellular_process	4369	409	1.318005	0
GO:0044267_cellular_protein_metabolic_process	1486	142	1.345381	0.000159
GO:0002376_immune_system_process	121	22	2.559841	0.000161
GO:0009888_tissue_development	110	21	2.687833	0.000164
GO:0001708_cell_fate_specification	30	10	4.693042	0.000167
GO:0030901_midbrain_development	14	7	7.039562	0.000169
GO:0045165_cell_fate_commitment	47	13	3.894226	0.000172
GO:0030326_embryonic_limb_morphogenesis	13	7	7.581067	0.000175
GO:0035113_embryonic_appendage_morphogenesis	13	7	7.581067	0.000175
GO:0035115_embryonic_forelimb_morphogenesis	13	7	7.581067	0.000175
GO:0035118_embryonic_pectoral_fin_morphogenesis	13	7	7.581067	0.000175
GO:0003002_regionalization	128	24	2.639836	0.000189
GO:0048732_gland_development	21	8	5.363476	0.000312
GO:0019538_protein_metabolic_process	1572	148	1.325516	0.000588
GO:0033333_fin_development	40	11	3.871759	0.000597
GO:0048736_appendage_development	40	11	3.871759	0.000597
GO:0044260_cellular_macromolecule_metabolic_process	1504	143	1.33864	0.000615
GO:0042471_ear_morphogenesis	29	9	4.369383	0.000667
GO:0035295_tube_development	46	11	3.366747	0.000667
GO:0030154_cell_differentiation	394	47	1.679489	0.000674
GO:0048869_cellular_developmental_process	394	47	1.679489	0.000674
GO:0007423_sensory_organ_development	130	22	2.382621	0.000676

GO:0030097_hemopoiesis	48	12	3.519781	0.000685
GO:0031016_pancreas_development	25	8	4.50532	0.00069
GO:0015669_gas_transport	17	7	5.797287	0.000694
GO:0015671_oxygen_transport	17	7	5.797287	0.000694
GO:0033339_pectoral_fin_development	19	7	5.187046	0.000698
GO:0009952_anterior_posterior_pattern_formation	83	16	2.714048	0.000706
GO:0042472_inner_ear_morphogenesis	28	9	4.525433	0.000714
GO:0002520_immune_system_development	51	12	3.312735	0.000714
GO:0048534_hemopoietic_or_lymphoid_organ_development	51	12	3.312735	0.000714
GO:0035050_embryonic_heart_tube_development	34	10	4.140919	0.000725
GO:0030878_thyroid_gland_development	9	5	7.821736	0.000732
GO:0033334_fin_morphogenesis	36	10	3.910868	0.000741
GO:0035107_appendage_morphogenesis	36	10	3.910868	0.000741
GO:0035108_limb_morphogenesis	18	7	5.475215	0.000759
GO:0035136_forelimb_morphogenesis	18	7	5.475215	0.000759
GO:0035138_pectoral_fin_morphogenesis	18	7	5.475215	0.000759
GO:0060173_limb_development	18	7	5.475215	0.000759
GO:0031018_endocrine_pancreas_development	10	5	7.039562	0.000761
GO:0019882_antigen_processing_and_presentation	26	8	4.332038	0.000769
GO:0021575_hindbrain_morphogenesis	6	4	9.386083	0.000968
GO:0007507_heart_development	81	15	2.607245	0.001277
GO:0007422_peripheral_nervous_system_development	17	6	4.969103	0.002526
GO:0007186_G-protein_coupled_receptor_protein_signaling_pathwa	253	32	1.780759	0.003125
GO:0048592_eye_morphogenesis	38	9	3.33453	0.003402
GO:0001706_endoderm_formation	8	4	7.039562	0.004796
GO:0002009_morphogenesis_of_an_epithelium	56	11	2.765542	0.006364
GO:0035162_embryonic_hemopoiesis	21	6	4.022607	0.011
GO:0043049_otic_placode_formation	15	5	4.693042	0.012178
GO:0001654_eye_development	87	14	2.265606	0.012255
GO:0019748_secondary_metabolic_process	88	14	2.239861	0.01581
GO:0009611_response_to_wounding	44	9	2.879821	0.015865
GO:0030855_epithelial_cell_differentiation	5	3	8.447475	0.015922
GO:0048839_inner_ear_development	45	9	2.815825	0.017636
GO:0051216_cartilage_development	37	8	3.044135	0.017798
GO:0051090_regulation_of_transcription_factor_activity	10	4	5.63165	0.01787
GO:0051098_regulation_of_binding	10	4	5.63165	0.01787
GO:0051101_regulation_of_DNA_binding	10	4	5.63165	0.01787
GO:0043583_ear_development	46	9	2.754611	0.019279
GO:0007166_cell_surface_receptor_linked_signal_transduction	427	45	1.483748	0.020177
GO:0042060_wound_healing	38	8	2.964026	0.020357
GO:0001501_skeletal_development	56	10	2.514129	0.022174
GO:0030916_otic_vesicle_formation	17	5	4.140919	0.022193
GO:0001704_formation_of_primary_germ_layer	24	6	3.519781	0.02359
GO:0007492_endoderm_development	11	4	5.119682	0.023621
GO:0009953_dorsal_ventral_pattern_formation	48	9	2.639836	0.023644
GO:0006721_terpenoid_metabolic_process	6	3	7.039562	0.027317
GO:0006775_fat-soluble_vitamin_metabolic_process	6	3	7.039562	0.027317
GO:0006776_vitamin_A_metabolic_process	6	3	7.039562	0.027317
GO:0021546_rhombomere_development	6	3	7.039562	0.027317
GO:0022037_metencephalon_development	6	3	7.039562	0.027317
GO:0022008_neurogenesis	104	15	2.030643	0.027661
GO:0048514_blood_vessel_morphogenesis	49	9	2.585962	0.02768
GO:0048593_camera-type_eye_morphogenesis	18	5	3.910868	0.029206
GO:0033014_tetrapyrrole_biosynthetic_process	88	13	2.079871	0.033858
GO:0001666_response_to_hypoxia	19	5	3.705033	0.035
GO:0006783_heme_biosynthetic_process	79	12	2.138601	0.035271
GO:0009791_post-embryonic_development	7	3	6.033911	0.039769
GO:0003007_heart_morphogenesis	27	6	3.128694	0.040303
GO:0030900_forebrain_development	27	6	3.128694	0.040303
GO:0033013_tetrapyrrole_metabolic_process	90	13	2.033651	0.040451
GO:0048568_embryonic_organ_development	53	9	2.390795	0.041143
GO:0051093_negative_regulation_of_developmental_process	53	9	2.390795	0.041143
GO:0042168_heme_metabolic_process	81	12	2.085796	0.041667
GO:0007596_blood_coagulation	20	5	3.519781	0.041679
GO:0007599_hemostasis	20	5	3.519781	0.041679
GO:0050878_regulation_of_body_fluid_levels	20	5	3.519781	0.041679
GO:0007156_homophilic_cell_adhesion	44	8	2.559841	0.041866
GO:0009605_response_to_external_stimulus	82	12	2.06036	0.043077
GO:0046148_pigment_biosynthetic_process	82	12	2.06036	0.043077
GO:0001525_angiogenesis	28	6	3.016955	0.043404
GO:0050896_response_to_stimulus	348	36	1.456461	0.044
GO:0006779_porphyrin_biosynthetic_process	83	12	2.035536	0.044167
GO:0006631_fatty_acid_metabolic_process	21	5	3.352173	0.044589
GO:0031017_exocrine_pancreas_development	14	4	4.022607	0.04651
GO:0035272_exocrine_system_development	14	4	4.022607	0.04651

GO:0042445_hormone_metabolic_process	14	4	4.022607	0.04651
GO:0001568_blood_vessel_development	65	10	2.166019	0.050065
GO:0006633_fatty_acid_biosynthetic_process	8	3	5.279672	0.050195
GO:0042398_amino_acid_derivative_biosynthetic_process	8	3	5.279672	0.050195
GO:0043388_positive_regulation_of_DNA_binding	8	3	5.279672	0.050195
GO:0051091_positive_regulation_of_transcription_factor_activity	8	3	5.279672	0.050195
GO:0051099_positive_regulation_of_binding	8	3	5.279672	0.050195
GO:0006778_porphyrin_metabolic_process	85	12	1.987641	0.051019
GO:0042440_pigment_metabolic_process	85	12	1.987641	0.051019
GO:0050817_coagulation	22	5	3.199801	0.051835
GO:0001944_vasculature_development	66	10	2.133201	0.052767
GO:0007218_neuropeptide_signaling_pathway	15	4	3.754433	0.056125
GO:0050877_neurological_system_process	77	11	2.011304	0.057267
GO:0003008_system_process	108	14	1.825072	0.059383
GO:0016331_morphogenesis_of_embryonic_epithelium	23	5	3.060679	0.059877
GO:0006955_immune_response	68	10	2.070459	0.06061
GO:0002040_sprouting_angiogenesis	9	3	4.693042	0.064311
GO:0016053_organic_acid_biosynthetic_process	9	3	4.693042	0.064311
GO:0046394_carboxylic_acid_biosynthetic_process	9	3	4.693042	0.064311
GO:0065008_regulation_of_biological_quality	289	30	1.461501	0.06494
GO:0010001_glial_cell_differentiation	16	4	3.519781	0.06716
GO:0007601_visual_perception	41	7	2.403753	0.067719
GO:0050953_sensory_perception_of_light_stimulus	41	7	2.403753	0.067719
GO:0046483_heterocycle_metabolic_process	112	14	1.759891	0.071676
GO:0009880_embryonic_pattern_specification	33	6	2.559841	0.07186
GO:0043010_camera-type_eye_development	61	9	2.077248	0.072529
GO:0042063_gliogenesis	17	4	3.312735	0.075943
GO:0048547_gut_morphogenesis	10	3	4.223737	0.083977
GO:0015674_di-__tri-valent_inorganic_cation_transport	313	31	1.394418	0.099831
GO:0007368_determination_of_left_right_symmetry	45	7	2.190086	0.100955
GO:0001889_liver_development	11	3	3.839761	0.103132
GO:0030334_regulation_of_cell_migration	11	3	3.839761	0.103132
GO:0048546_digestive_tract_morphogenesis	11	3	3.839761	0.103132
GO:0051270_regulation_of_cell_motility	11	3	3.839761	0.103132
GO:0009799_determination_of_symmetry	55	8	2.047873	0.104649
GO:0009855_determination_of_bilateral_symmetry	55	8	2.047873	0.104649
GO:0016337_cell-cell_adhesion	55	8	2.047873	0.104649
GO:0006766_vitamin_metabolic_process	19	4	2.964026	0.109032
GO:0048699_generation_of_neurons	98	12	1.723974	0.129275
GO:0006308_DNA_catabolic_process	5	2	5.63165	0.129635
GO:0021548_pons_development	5	2	5.63165	0.129635
GO:0021953_central_nervous_system_neuron_differentiation	5	2	5.63165	0.129635
GO:0032835_glomerulus_development	5	2	5.63165	0.129635
GO:0045786_negative_regulation_of_cell_cycle	5	2	5.63165	0.129635
GO:0050935_iridophore_differentiation	5	2	5.63165	0.129635
GO:0007498_mesoderm_development	37	6	2.283101	0.130309
GO:0006826_iron_ion_transport	132	15	1.599901	0.134359
GO:0021536_diencephalon_development	12	3	3.519781	0.13731
GO:0042127_regulation_of_cell_proliferation	12	3	3.519781	0.13731
GO:0021532_neural_tube_patterning	20	4	2.815825	0.14005
GO:0021903_rostrocaudal_neural_tube_patterning	20	4	2.815825	0.14005
GO:0006873_cellular_ion_homeostasis	156	17	1.534264	0.140746
GO:0051188_cofactor_biosynthetic_process	122	14	1.615637	0.14075
GO:0048519_negative_regulation_of_biological_process	299	29	1.365534	0.14197
GO:0007600_sensory_perception	58	8	1.941948	0.14198
GO:0055082_cellular_chemical_homeostasis	158	17	1.514843	0.144902
GO:0048589_developmental_growth	21	4	2.681738	0.150439
GO:0050801_ion_homeostasis	159	17	1.505315	0.154757
GO:0006950_response_to_stress	160	17	1.495907	0.163961
GO:0006879_cellular_iron_ion_homeostasis	138	15	1.53034	0.183102
GO:0055072_iron_ion_homeostasis	138	15	1.53034	0.183102
GO:0007267_cell-cell_signaling	31	5	2.270827	0.184009
GO:0001505_regulation_of_neurotransmitter_levels	6	2	4.693042	0.184198
GO:0021983_pituitary_gland_development	6	2	4.693042	0.184198
GO:0021984_adenohypophysis_development	6	2	4.693042	0.184198
GO:0045597_positive_regulation_of_cell_differentiation	6	2	4.693042	0.184198
GO:0060030_dorsal_convergence	6	2	4.693042	0.184198
GO:0048878_chemical_homeostasis	161	17	1.486616	0.184346
GO:0030182_neuron_differentiation	82	10	1.716966	0.184789
GO:0021510_spinal_cord_development	14	3	3.016955	0.195045
GO:0021515_cell_differentiation_in_spinal_cord	14	3	3.016955	0.195045
GO:0060042_retina_morphogenesis_in_camera-type_eye	14	3	3.016955	0.195045
GO:0050793_regulation_of_developmental_process	141	15	1.497779	0.198054
GO:0030001_metal_ion_transport	940	78	1.168268	0.199955

Supplemental Table 6. DNA Hypomethylation GO

HYPERLINKED GO CATEGORY	TOTAL GE	CHANGED	ENRICHMI	FALSE DISCOVERY RATE
GO:0007417_central_nervous_system_development	157	32	3.015515	0
GO:0006355_regulation_of_transcription__DNA-dependent	539	85	2.333143	0
GO:0051252_regulation_of_RNA_metabolic_process	542	85	2.320229	0
GO:0032774_RNA_biosynthetic_process	563	88	2.31252	0
GO:0006351_transcription__DNA-dependent	561	87	2.294392	0
GO:0007399_nervous_system_development	282	43	2.255956	0
GO:0045449_regulation_of_transcription	719	105	2.160586	0
GO:0019219_regulation_of_nucleobase__nucleoside__nucleotide_an(	731	106	2.145358	0
GO:0051171_regulation_of_nitrogen_compound_metabolic_process	733	106	2.139504	0
GO:0031326_regulation_of_cellular_biosynthetic_process	747	108	2.139018	0
GO:0010556_regulation_of_macromolecule_biosynthetic_process	741	107	2.136372	0
GO:0009889_regulation_of_biosynthetic_process	749	108	2.133306	0
GO:0006350_transcription	751	108	2.127625	0
GO:0010468_regulation_of_gene_expression	766	109	2.105275	0
GO:0031323_regulation_of_cellular_metabolic_process	788	112	2.102824	0
GO:0080090_regulation_of_primary_metabolic_process	809	114	2.084815	0
GO:0060255_regulation_of_macromolecule_metabolic_process	825	115	2.062315	0
GO:0019222_regulation_of_metabolic_process	855	118	2.041865	0
GO:0016070_RNA_metabolic_process	721	94	1.928874	0
GO:0007275_multicellular_organismal_development	909	118	1.920566	0
GO:0032502_developmental_process	984	122	1.834324	0
GO:0034961_cellular_biopolymer_biosynthetic_process	989	122	1.82505	0
GO:0048513_organ_development	600	74	1.824701	0
GO:0048856_anatomical_structure_development	714	88	1.823458	0
GO:0043284_biopolymer_biosynthetic_process	993	122	1.817698	0
GO:0048731_system_development	684	84	1.816914	0
GO:0032501_multicellular_organismal_process	995	120	1.784306	0
GO:0034645_cellular_macromolecule_biosynthetic_process	1044	122	1.728903	0
GO:0010467_gene_expression	1087	127	1.728564	0
GO:0009059_macromolecule_biosynthetic_process	1049	122	1.720662	0
GO:0006139_nucleobase__nucleoside__nucleotide_and_nucleic_acid	1181	136	1.703728	0
GO:0044249_cellular_biosynthetic_process	1270	139	1.619281	0
GO:0006807_nitrogen_compound_metabolic_process	1287	140	1.609388	0
GO:0009058_biosynthetic_process	1318	140	1.571534	0
GO:0050794_regulation_of_cellular_process	1663	165	1.467922	0
GO:0034960_cellular_biopolymer_metabolic_process	1785	176	1.458766	0
GO:0050789_regulation_of_biological_process	1747	172	1.456622	0
GO:0044260_cellular_macromolecule_metabolic_process	1805	176	1.442602	0
GO:0065007_biological_regulation	1833	176	1.420566	0
GO:0043283_biopolymer_metabolic_process	2010	185	1.361717	0
GO:0043170_macromolecule_metabolic_process	2035	186	1.352259	0
GO:0044237_cellular_metabolic_process	2289	201	1.299157	0
GO:0044238_primary_metabolic_process	2445	208	1.258623	0.000233
GO:0009790_embryonic_development	320	42	1.941827	0.000682
GO:0015669_gas_transport	16	7	6.472756	0.000816
GO:0015671_oxygen_transport	16	7	6.472756	0.000816
GO:0048598_embryonic_morphogenesis	174	27	2.295756	0.000851
GO:0009653_anatomical_structure_morphogenesis	392	48	1.811617	0.00087
GO:0009887_organ_morphogenesis	262	36	2.032883	0.000889
GO:0045165_cell_fate_commitment	50	12	3.550769	0.002353
GO:0009987_cellular_process	3734	292	1.156964	0.0024
GO:0048523_negative_regulation_of_cellular_process	114	19	2.465812	0.00434
GO:0048519_negative_regulation_of_biological_process	131	21	2.371697	0.004423
GO:0022008_neurogenesis	147	22	2.214198	0.00537
GO:0031076_embryonic_camera-type_eye_development	16	6	5.548077	0.005818
GO:0043010_camera-type_eye_development	97	16	2.440391	0.007679
GO:0001708_cell_fate_specification	38	9	3.504049	0.007759
GO:0021522_spinal_cord_motor_neuron_differentiation	12	5	6.16453	0.007895
GO:0007420_brain_development	118	18	2.256845	0.008136
GO:0048699_generation_of_neurons	138	20	2.144184	0.008333
GO:0008152_metabolic_process	2951	232	1.163135	0.00918
GO:0021517_ventral_spinal_cord_development	13	5	5.690335	0.009355
GO:0007423_sensory_organ_development	173	23	1.966948	0.011587
GO:0021915_neural_tube_development	34	8	3.481146	0.012188
GO:0001654_eye_development	125	18	2.130462	0.015385
GO:0051129_negative_regulation_of_cellular_component_organizatio	9	4	6.575499	0.017121
GO:0021532_neural_tube_patterning	21	6	4.227106	0.0175
GO:0021903_rostrocaudal_neural_tube_patterning	21	6	4.227106	0.0175

GO:0030917_midbrain-hindbrain_boundary_development	15	5	4.931624	0.019855
GO:0030154_cell_differentiation	342	37	1.600615	0.021
GO:0003007_heart_morphogenesis	37	8	3.198891	0.021268
GO:0048869_cellular_developmental_process	355	38	1.583676	0.025556
GO:0010721_negative_regulation_of_cell_development	10	4	5.917949	0.026757
GO:0050768_negative_regulation_of_neurogenesis	10	4	5.917949	0.026757
GO:0030182_neuron_differentiation	122	17	2.06158	0.028421
GO:0021515_cell_differentiation_in_spinal_cord	16	5	4.623397	0.028533
GO:0048468_cell_development	212	25	1.744678	0.030909
GO:0021510_spinal_cord_development	17	5	4.351433	0.03141
GO:0006913_nucleocytoplasmic_transport	18	5	4.109687	0.04
GO:0051169_nuclear_transport	18	5	4.109687	0.04
GO:0051301_cell_division	59	10	2.507605	0.04
GO:0007492_endoderm_development	25	6	3.550769	0.040127
GO:0042472_inner_ear_morphogenesis	33	7	3.138306	0.040375
GO:0042471_ear_morphogenesis	34	7	3.046003	0.045833
GO:0009952_anterior_posterior_pattern_formation	90	13	2.137037	0.046235
GO:0033339_pectoral_fin_development	19	5	3.893387	0.046628
GO:0048839_inner_ear_development	53	9	2.512337	0.049663
GO:0009968_negative_regulation_of_signal_transduction	27	6	3.287749	0.049773
GO:0010648_negative_regulation_of_cell_communication	27	6	3.287749	0.049773
GO:0043583_ear_development	54	9	2.465812	0.062778
GO:0033365_protein_localization_in_organelle	21	5	3.522589	0.070549
GO:0006979_response_to_oxidative_stress	14	4	4.227106	0.076129
GO:0030901_midbrain_development	14	4	4.227106	0.076129
GO:0003002_regionalization	140	17	1.79652	0.078617
GO:0009792_embryonic_development_ending_in_birth_or_egg_hatch	108	14	1.917854	0.089375
GO:0043009_chordate_embryonic_development	108	14	1.917854	0.089375
GO:0006606_protein_import_into_nucleus	15	4	3.945299	0.100505
GO:0034504_protein_localization_in_nucleus	15	4	3.945299	0.100505
GO:0051170_nuclear_import	15	4	3.945299	0.100505
GO:0035270_endocrine_system_development	31	6	2.863524	0.1013
GO:0017038_protein_import	23	5	3.216276	0.104653
GO:0051128_regulation_of_cellular_component_organization	41	7	2.525954	0.108641
GO:0006605_protein_targeting	32	6	2.774038	0.109118
GO:0007369_gastrulation	82	11	1.984678	0.123302
GO:0048729_tissue_morphogenesis	82	11	1.984678	0.123302
GO:0007507_heart_development	92	12	1.929766	0.123365
GO:0007049_cell_cycle	115	14	1.801115	0.123796
GO:0051093_negative_regulation_of_developmental_process	52	8	2.276134	0.124393
GO:0035136_forelimb_morphogenesis	17	4	3.481146	0.129636
GO:0035138_pectoral_fin_morphogenesis	17	4	3.481146	0.129636
GO:0009126_purine_nucleoside_monophosphate_metabolic_process	10	3	4.438462	0.132845
GO:0009127_purine_nucleoside_monophosphate_biosynthetic_proce	10	3	4.438462	0.132845
GO:0009167_purine_ribonucleoside_monophosphate_metabolic_proc	10	3	4.438462	0.132845
GO:0009168_purine_ribonucleoside_monophosphate_biosynthetic_pr	10	3	4.438462	0.132845
GO:0043086_negative_regulation_of_catalytic_activity	10	3	4.438462	0.132845
GO:0048752_semicircular_canal_morphogenesis	10	3	4.438462	0.132845
GO:0050767_regulation_of_neurogenesis	35	6	2.536264	0.138814
GO:0051960_regulation_of_nervous_system_development	35	6	2.536264	0.138814
GO:0035108_limb_morphogenesis	18	4	3.287749	0.141333
GO:0060173_limb_development	18	4	3.287749	0.141333
GO:0002009_morphogenesis_of_an_epithelium	65	9	2.048521	0.141803
GO:0060429_epithelium_development	65	9	2.048521	0.141803
GO:0009888_tissue_development	228	23	1.492465	0.156508
GO:0048522_positive_regulation_of_cellular_process	110	13	1.748485	0.15752
GO:0040036_regulation_of_fibroblast_growth_factor_receptor_signalir	11	3	4.034965	0.15871
GO:0044092_negative_regulation_of_molecular_function	11	3	4.034965	0.15871
GO:0034621_cellular_macromolecular_complex_subunit_organization	100	12	1.775385	0.161473
GO:0033334_fin_morphogenesis	37	6	2.399168	0.161641
GO:0060284_regulation_of_cell_development	37	6	2.399168	0.161641
GO:0007169_transmembrane_receptor_protein_tyrosine_kinase_signa	47	7	2.203492	0.163615
GO:0006166_purine_ribonucleoside_salvage	5	2	5.917949	0.194118
GO:0032984_macromolecular_complex_disassembly	5	2	5.917949	0.194118
GO:0034623_cellular_macromolecular_complex_disassembly	5	2	5.917949	0.194118
GO:0043174_nucleoside_salvage	5	2	5.917949	0.194118
GO:0043241_protein_complex_disassembly	5	2	5.917949	0.194118
GO:0043624_cellular_protein_complex_disassembly	5	2	5.917949	0.194118
GO:0035107_appendage_morphogenesis	38	6	2.336032	0.196569

Supplemental Table 7. DNA hypomethylated top 250 genes in sperm.

zgc:85811	2.1896
zgc:162824	2.177
zgc:113443	2.0973
rac3	2.087
dmrt1	2.0849
dmrt1	2.0849
acvr1	2.036
zgc:173585	2.0341
zgc:136308	2.0296
zgc:113102	2.0295
zgc:56418	2.0042
zgc:112185	2.0042
zgc:153686	1.9959
irx3a	1.9958
zgc:110241	1.9879
meis1	1.9769
srrm1	1.9549
zgc:92607	1.9436
cha	1.9389
tpma	1.9374
zgc:103525	1.9355
zgc:110014	1.9355
zgc:55327	1.935
zgc:92027	1.9334
LOC571606	1.9317
zgc:113449	1.9299
zgc:103747	1.9286
LOC555925	1.9236
si:dkey-15j16.4	1.9236
dvl3	1.918
dll4	1.9143
zgc:110672	1.9128
anp32a	1.9108
hoxc12b	1.9096
zgc:92201	1.9092
glula	1.9071
hoxd10a	1.9049
zgc:92901	1.9034
zgc:158517	1.9033
LOC100000024	1.9018
MGC173577	1.9015
six1	1.8984
nkx6.1	1.895
LOC796505	1.8939
p4ha2	1.8894
zgc:65997	1.8779
nkx2.2b	1.8681
lmo4l	1.8674
si:dkey-185l3.3	1.8596
zgc:101053	1.8594
nkx1.2la	1.8498
phf16	1.8494
wwox	1.848
slit2	1.8467
slco2a1	1.8421
LOC798622	1.8298
zgc:86753	1.8298
zc3hc1	1.8259
ppp6c	1.8235
zgc:158781	1.8233
serac1	1.821
cebpg	1.8149
cebpa	1.8149
fst	1.8142
onecut1	1.8115
onecut1	1.8115
zgc:154123	1.8102
epn1	1.8095
hoxd9a	1.8084
mapk14a	1.8073
zgc:110406	1.8059
zgc:113200	1.8055
zgc:91896	1.8008
kctd10	1.8007
aacs	1.7996
lmo4	1.7992
c20orf20	1.7988
tkt	1.7934
zgc:91857	1.7934
robo2	1.7931
zgc:110711	1.7922
zgc:158246	1.7922
wipi1	1.7898
si:ch211-10j20.3	1.7894
si:dkey-217m5.9	1.7894
bmi1b	1.7874
rpp38	1.786
si:busm1-132m23.3	1.7834
gata2	1.7807

si:ch211-260g14.3	1.7799
zgc:56152	1.7756
lgals1l1	1.7708
psme2	1.7697
zgc:55317	1.7697
sfrs8	1.7666
zgc:86658	1.7647
si:dkey-14a7.4	1.7617
zgc:92393	1.7612
si:ch211-222k6.3	1.7611
tram2	1.7605
tram2	1.7605
zgc:56703	1.7602
zgc:63556	1.7589
ankrd6	1.7582
gcm2	1.7505
zgc:66241	1.7503
pax9	1.7502
cdx4	1.7494
bmi1	1.7464
wsb1	1.7459
igfbp5	1.7433
hif1a	1.743
zgc:110561	1.7407
nulf2	1.7407
rrm2	1.7407
alkbh6	1.7399
ube2h	1.7395
hoxc3a	1.7389
hoxc3a	1.7389
zgc:77862	1.7381
rpl9	1.7348
zgc:66080	1.7348
zgc:64055	1.7347
zgc:110821	1.7342
rab34	1.7336
cpt2	1.7326
vamp1	1.7313
pdcd8	1.7303
hoxa5a	1.7303
mtch2	1.7253
zgc:85611	1.7241
zgc:56409	1.7224
sec14l1	1.7209
snx9l	1.7207
LOC558917	1.7207
mc1r	1.7196
si:ch211-238e22.2	1.7183
zgc:92601	1.7176
dhps	1.7176
dhps	1.7176
wipi2	1.7175
dlx6a	1.7168
ddx39a	1.7165
zgc:101635	1.7139
zic5	1.7125
neurod	1.7117
igf1ra	1.7099
eif4a1b	1.7093
zgc:77593	1.701
anxa13	1.7002
zgc:55494	1.7
zgc:158437	1.7
zgc:113436	1.7
mapre1	1.698
zgc:101585	1.6965
rftn2	1.6929
tbx4	1.692
pbk	1.687
zgc:92115	1.6868
si:dkey-102f14.5	1.6842
sgta	1.682
thoc3	1.6809
si:dkey-183n20.16	1.6781
mrpl19	1.6781
glt8d3	1.678
zgc:92610	1.6778
ran	1.6778
etv5	1.675
hiat1a	1.6741
sec11a	1.6739
zgc:77449	1.6736
zgc:103474	1.6734
si:ch211-199m3.8	1.6727
si:dkey-222f8.3	1.6727
braf	1.6727
si:ch211-199m3.7	1.6727
eif5a	1.6721
rnf128	1.6702
lin9	1.6696

dlx2b		1.6689
ss18		1.6686
dmap1		1.6685
si:ch211-63o20.5		1.6651
LOC570343		1.6643
mobkl1a		1.6642
zgc:153305		1.6642
si:ch211-215m21.11		1.664
si:ch211-215m21.11		1.6639
hspa9		1.6615
zgc:92332		1.6613
zgc:91951		1.6606
foxl1		1.6602
map1lc3b		1.66
zgc:85736		1.6583
zgc:73351		1.6581
klf4		1.6577
zgc:103639		1.6537
thra		1.6526
MGC173792		1.6525
zgc:92822		1.6525
plekhk1		1.6522
usf2		1.652
bcl2l		1.6501
npc2		1.65
zgc:91960		1.6498
zgc:92662		1.6479
zgc:101107		1.6467
zgc:162630		1.6467
zgc:112374		1.6464
foxb1.2		1.6461
kptn		1.6445
rtn1a		1.6441
cdc16		1.6432
eng2b		1.6428
hoxc6a		1.6406
hoxc6a		1.6406
par1		1.6402
zgc:101867		1.64
faf1		1.6386
h3f3a		1.6373
ptgs1		1.6369
LOC558180		1.6369
si:ch211-212d10.2		1.6367
lhx9		1.6362
lhx9		1.6362
syncripl		1.6356
dhfr		1.633
zgc:92871		1.6325
LOC566052		1.6325
LOC566052		1.6325
zgc:92871		1.6325
cnot8		1.6318
zgc:113491		1.6318
calm2b		1.6315
evx1		1.6294
th2		1.6284
suz12		1.6275
pcdh2ab11		1.6272
pcdh2ab10		1.6272
pcdh2ab12		1.6272
acot7		1.6271
dyrk2		1.6266
zc3h10		1.6259
zgc:162358		1.6254
zgc:113397		1.6254
zgc:100911		1.6251
hlx1		1.6245
mapkapk2		1.6244
si:dkey-15h8.11		1.6243
txndc9		1.624
bactin1		1.6229
snap25b		1.6217
nkx2.1b		1.6216
si:ch211-217g15.2		1.62
lhx1a		1.6195
onecut1		1.6179
p2rx4a		1.6177
zgc:103736		1.6176
zgc:73273		1.6176
abcf2		1.6169
tpm3		1.6166
bsk146		1.6164
psme3		1.6157
		fold in log2 fold
	Average	1.752216 3.368756
	Median	1.7224 3.299849

Supplemental Table 8. DNA hypomethylated top 250 genes in sperm compared to muscle.

hoxb4a	2.9742
si:dkey-14a7.4	2.9002
six1	2.7385
LOC799904	2.7062
pax9	2.6507
si:dkey-202b22.4	2.6018
hoxa1a	2.5469
mab21l2	2.5157
hoxa3a	2.5061
dazl	2.4715
si:ch211-215m21.17	2.3837
hoxb1b	2.2627
hoxc1a	2.2473
hoxc1a	2.2473
hoxc1a	2.2473
zgc:92259	2.2343
hoxb5a	2.2267
tuba7l	2.2139
zgc:91918	2.2129
si:ch211-10j20.3	2.2078
si:dkey-217m5.9	2.2078
dvr1rbp	2.2063
hoxa5a	2.1857
si:ch211-215m21.11	2.1758
si:ch211-215m21.11	2.1754
hoxb5b	2.1709
hoxb1a	2.1695
zgc:92208	2.1416
tbx4	2.1205
dmrt1	2.0976
dmrt1	2.0976
pde6c	2.0759
zgc:86729	2.0092
irx3a	1.9949
hoxb2a	1.9909
si:ch211-51a19.5	1.9454
d4st1	1.9425
nr5a2	1.9372
pou5f1	1.9157
pdx1	1.9059
zar1	1.899
hoxc5a	1.8987
hoxc5a	1.8987
zgc:103502	1.8783
sox3	1.877
cdx4	1.8702
evx1	1.8626
bcor	1.8626
mao	1.8552
ldhd	1.8329
zic1	1.8165
zgc:162824	1.7856
hoxa11a	1.7786
cdkn1c	1.7633
hoxa4a	1.7425
foxd1	1.7371
LOC563808	1.7224
LOC100000024	1.7196
si:ch211-10j20.1	1.7078
efnb1	1.7053
rtn4r	1.6627
hoxc4a	1.657
hoxc4a	1.657
hoxc6a	1.6498
hoxc6a	1.6495
vox	1.6404
dmbx1a	1.6378
dmbx1a	1.6378
il1b	1.6372
brd8	1.6314
zgc:77439	1.585
tbx5	1.5639
gata2	1.5542
hoxd4a	1.5293
irx7	1.5216
pcdh2ab11	1.5174
pcdh2ab10	1.5174
pcdh2ab12	1.5174
rbp1b	1.5096
ntl	1.5066
cax1	1.5022
zgc:136271	1.5022
hoxb8a	1.4998
pcdh2ac	1.4998

zgc:85811	1.4756
zgc:113070	1.4733
zgc:110788	1.4526
zgc:56699	1.4353
irx1b	1.434
irx1b	1.4329
hoxc3a	1.4096
hoxc3a	1.4096
fam73a	1.4055
bmpr1a	1.4026
zgc:64055	1.4021
rbm35b	1.397
pias4l	1.3953
lft1	1.3931
zgc:64002	1.3913
zgc:77876	1.3906
zgc:66426	1.3884
zgc:111976	1.3884
rala	1.3884
hoxd9a	1.3838
disp2	1.3771
gfi1	1.3746
dharma	1.3722
LOC565439	1.3565
pcdh2ab10	1.3487
pcdh2ab9	1.3487
pcdh2ab11	1.3487
pcdh2ab9	1.3487
zgc:152667	1.3482
si:ch211-239e6.4	1.3482
ampd3	1.3275
twist1a	1.3177
zgc:114089	1.3171
zgc:110089	1.3163
tnrc4	1.3141
gata3	1.3008
gata3	1.3008
arrdc1	1.3008
fst	1.297
asz1	1.2942
bmi1	1.2889
foxe3	1.2889
hoxa2b	1.2842
hoxb6a	1.2649
foxi3b	1.2643
wnt11	1.2478
hoxa9a	1.2468
zgc:101674	1.2456
rtn1a	1.2405
igf2r	1.2404
tp53bp2	1.2351
meis1	1.2283
si:ch211-217g15.2	1.2273
cldnd	1.2256
entpd1	1.22
dll4	1.2055
zgc:63942	1.2038
zpcx	1.2038
LOC556137	1.1881
pou4f2	1.1861
hoxc8a	1.1821
hoxc8a	1.1816
zgc:103482	1.1805
zgc:101622	1.1799
ndr1	1.1798
foxi3a	1.1688
hey2	1.1685
gata5	1.1647
ccne	1.1596
zgc:162297	1.1596
snapc1	1.1579
dvl3	1.139
her6	1.1355
tnfb	1.1343
si:dkeyp-114f9.3	1.1302
zgc:101715	1.1299
pcdh10a	1.1284
cth1	1.127
hoxa13b	1.1264
h1m	1.1217
si:dkey-231l1.3	1.1182
pcdh2ab2	1.1165
mapk1	1.1155
pdzk1ip1l	1.1109
si:busm1-105l16.2	1.1078

si:busm1-105l16.2	1.1078
zgc:154123	1.1067
zgc:162824	1.1045
zgc:101639	1.1045
foxd5	1.1019
zgc:92332	1.1008
slc10a4	1.0914
zgc:77719	1.0795
LOC567444	1.0795
pvalb2	1.0702
lgals1l1	1.0636
tfap2b	1.0628
tfap2b	1.0628
zgc:77421	1.0594
zgc:153733	1.0582
cd2bp2	1.0582
zgc:66432	1.0574
fkbp9	1.054
crtap	1.054
zgc:113969	1.0539
zgc:66024	1.0539
zgc:92630	1.0506
zgc:91922	1.0495
zgc:55536	1.0437
zgc:100871	1.0408
mtr	1.04
zgc:158351	1.039
f11r	1.0336
tbx15	1.0306
zgc:122977	1.0302
fzd2	1.0206
arx	1.0195
si:dkey-246e3.3	1.0033
si:dkey-7c18.8	1.0033
si:dkey-7c18.8	1.0033
si:dkey-246e3.3	1.0033
cdx1a	1.0017
zgc:171679	0.9999
LOC100000024	0.996
MGC173425	0.996
ccdc106	0.9839
si:ch211-232m10.4	0.9839
foxg1	0.9808
fgf18	0.9743
spint1l	0.9738
zgc:123113	0.9711
zgc:158781	0.9701
gsx2	0.963
zdhhc5	0.958
zorba	0.9539
ccna1	0.9517
si:dkeyp-89c11.2	0.9428
si:dkey-171o17.7	0.921
LOC100003308	0.9178
MGC173425	0.9178
irx3b	0.9161
zgc:77542	0.9131
si:dkey-85n7.5	0.9124
zgc:64112	0.9111
neurog1	0.9057
LOC100001110	0.9057
LOC566773	0.9057
pcdh2ab11	0.904
pcdh2ab6	0.904
pcdh2ab7	0.904
pcdh2ab10	0.904
pcdh2ab9	0.904
pcdh2ab3	0.904
zgc:66241	0.898
sepw2b	0.897
zgc:91823	0.8967
si:dkey-88n24.5	0.8966
cyp2j21	0.8946
clic5	0.8942
popdc3	0.894
zgc:113924	0.8911
itih3	0.8911
tpr	0.89
zgc:77118	0.8897
zgc:101565	0.8864
hoxa10b	0.8774

	fold in log2	fold
Average	1.410299	2.657923
Median	1.2889	2.443417

Supplemental Table 9. H3K4me3 enriched top 250 genes in sperm.

plk1	2.6097
zgc:55448	2.4867
hprt1	2.4717
ppp6c	2.4672
dvl3	2.4637
zfand5a	2.4625
zgc:158610	2.4369
eif1b	2.4092
capza1	2.4062
LOC562052	2.3938
zgc:56126	2.3914
chst5	2.3906
gabarapl2	2.3906
ccnb1	2.3864
zgc:77849	2.3852
prkab1	2.3842
plekhk1	2.3768
stka	2.3737
chmp5	2.3735
zgc:73373	2.3718
zgc:92629	2.3705
zgc:92067	2.3705
zgc:56223	2.3689
zgc:56324	2.3682
vcp	2.3642
ift57	2.3633
zgc:123078	2.3632
smc4	2.3521
ift80	2.3521
si:dkey-86e18.1	2.3512
invs	2.3508
txndc4	2.3508
zgc:111863	2.35
unc119.1	2.35
zgc:101601	2.3451
brd3b	2.3369
bop1	2.3364
hsf1	2.3364
si:ch211-63o20.7	2.3313
ppp4c	2.3286
zgc:63497	2.3285
zgc:101608	2.3285
zgc:65884	2.3277
zgc:85700	2.3277
crat	2.3202
hnrpkl	2.3175
plaa	2.3163
zgc:55396	2.3148
ier5	2.3142
ddx41	2.3137
si:dkey-172o10.5	2.3137
anp32e	2.3088
wdr82	2.3075
eif4a1b	2.3066
zgc:153961	2.3063
dpagt1	2.3063
ndufa10	2.3043
zgc:92723	2.3043
fam46c	2.3028
zgc:76905	2.3019
st13	2.3019
rhoac	2.3003
rpl12	2.2999
LOC562066	2.2999
zgc:158262	2.2998
zgc:92606	2.2998
zgc:114143	2.2986
zgc:153930	2.2986
si:rp71-1p14.7	2.298
zgc:153619	2.298
cnot6	2.2957
ss18	2.2948
si:dkey-14a7.4	2.2914
mastl	2.2887
gmds	2.2881
gmds	2.2881
mapre1l	2.2881
zgc:92354	2.2872
mgrn1	2.2869
zgc:92858	2.2869
nek2	2.2838
cdc20	2.2836
zgc:162701	2.2832
eaf1	2.2832
usp25	2.2821
ck2a1	2.282
msh6	2.2818
eif6	2.2816

wdr51b	2.2811
tsga14	2.2811
epb41l5	2.2774
zgc:158424	2.2743
zgc:158424	2.2743
ccng2	2.2743
tm9sf2	2.2734
si:ch211-215m21.17	2.2715
bcat1	2.27
si:dkey-217m5.9	2.267
si:ch211-199l3.1	2.2664
rabgef1	2.2643
si:ch211-276e22.2	2.2637
zgc:152979	2.2637
sinup	2.2637
zgc:56005	2.2637
si:ch211-14a17.11	2.2615
zgc:92346	2.2613
snx9l	2.2603
LOC558917	2.2603
gmnn	2.2595
zgc:111986	2.2595
zgc:63654	2.2591
tex10	2.2583
si:dkey-121a11.2	2.2575
cacnb1	2.2573
foxm1l	2.256
cdc2	2.2557
zgc:113070	2.2554
csnk1dl	2.2553
uck2b	2.2543
zgc:55520	2.2542
LOC793774	2.2542
si:dkey-177p2.3	2.253
gpsm2	2.252
zgc:55461	2.2518
zgc:55664	2.2514
sfrs6	2.2505
zgc:76877	2.2493
arhgdia	2.2489
si:dkey-22l11.2	2.2471
zgc:91808	2.2455
kcnk5	2.2439
zgc:55327	2.2428
dlg7	2.2405
zgc:91918	2.2405
LOC563808	2.2405
trspap1	2.2401
trspap1	2.2401
zgc:100942	2.2399
hprt1l	2.2397
zgc:91814	2.2389
ncl1	2.2364
asb8	2.2363
taf3	2.2352
reep3	2.2332
tubb2c	2.232
zgc:101764	2.2302
zgc:66438	2.2288
suv420h1	2.2277
zgc:109719	2.2277
rgs12	2.2253
zgc:92169	2.2253
zgc:73223	2.2247
zgc:92867	2.224
zgc:123015	2.2225
zgc:153301	2.2225
bmi1	2.2209
katnb1	2.2207
zgc:56699	2.2192
dnah9	2.2181
zgc:63675	2.2178
zgc:113968	2.2174
zgc:77296	2.2169
cuedc2	2.216
strap	2.2158
zgc:73139	2.2153
zgc:112044	2.2153
zgc:77291	2.215
zgc:86657	2.2149
atp1b1a	2.2148
skiv2l2	2.2143
zgc:101711	2.2136
rsph3	2.2129
serinc1	2.2124
nono	2.2119
si:dkey-94n12.2	2.2113
zgc:65802	2.2112
actr2	2.2107

snip1	2.2104
ube2h	2.2101
rrm2	2.2095
zgc:63640	2.209
arl6ip1	2.2083
zgc:103612	2.2077
zgc:63557	2.2072
bat3	2.2071
hmmr	2.2069
rc3h1	2.2069
fbxl3a	2.2051
casp3	2.2051
zgc:92116	2.2041
ift52	2.204
vangl2	2.204
zgc:73324	2.2034
vrk1	2.2031
zgc:55466	2.2031
tdh	2.2031
si:dkey-65m5.3	2.2031
gtf2b	2.2027
phf23a	2.2014
atp6v1al	2.2014
zgc:92393	2.1996
zgc:63992	2.1987
tm2d1	2.1982
klf2a	2.1977
zgc:103692	2.1969
rhoad	2.1969
tmem161b	2.1966
atp6v1h	2.1965
zgc:73347	2.1961
zgc:101883	2.1948
si:dkey-42i9.5	2.1948
zgc:56418	2.1946
zgc:112185	2.1946
LOC571606	2.1937
bactin1	2.1932
bzw1	2.1931
abcg2b	2.1929
si:ch211-150c22.2	2.1928
styxl1	2.1926
cab39	2.192
zgc:92166	2.192
alg3	2.192
rpl18a	2.192
ppm1a	2.1918
ccna2	2.1916
zgc:110750	2.1915
si:ch211-240l14.1	2.1907
zgc:56682	2.1902
zgc:112182	2.1902
prpf38b	2.1897
hdac8	2.1879
g3bp1	2.1875
si:dkey-202b22.4	2.1864
zgc:76940	2.1857
pelo	2.1857
arl13b	2.1856
hspa5	2.1853
zgc:101845	2.1837
cul4a	2.1837
zgc:92611	2.1821
tardbpl	2.1814
zgc:55870	2.1811
tmf1	2.1804
zgc:85857	2.1801
zgc:63492	2.1798
zgc:55661	2.1793
yipf1	2.1783
lrrc42	2.1783
fam116b	2.1771
si:dkey-159a18.3	2.1771
mkks	2.1769
zgc:64090	2.1769
si:dkey-204f11.62	2.1762
zgc:110046	2.1762
zgc:154106	2.1757
LOC559969	2.1757
zgc:136620	2.1757
si:xx-by187g17.8	2.1757
prkar1a	2.1749
fxr1	2.1747

	fold in log2	fold
Average	2.2591535	4.787105
Median	2.2447	4.739385

Supplemental Table 10. H3K4me2 enriched top 250 genes in sperm.

ppib	2.5982
arhgdia	2.5864
zgc:92354	2.5612
si:dkey-235d18.4	2.5498
fam53b	2.5479
hnrpkl	2.5382
zgc:112345	2.5193
tcerg1	2.5193
zfand5a	2.5119
cdkn1b	2.5114
rhoac	2.4923
invs	2.486
txndc4	2.486
zgc:66100	2.4859
alkbh5	2.4856
sgsm3	2.4817
zgc:101024	2.4815
zgc:77285	2.4798
si:dkey-63j12.5	2.4784
ncl1	2.4766
zgc:136229	2.4744
zgc:136229	2.4744
kcnk5	2.4742
si:ch211-199l3.1	2.4675
eif5a	2.4627
LOC792168	2.4588
ing5a	2.4588
zgc:103672	2.4588
zgc:92393	2.4552
stka	2.4433
gldc	2.4427
tardbpl	2.4424
crsp7	2.4381
tob1b	2.4381
id1	2.4368
tkt	2.4348
zgc:136888	2.4341
pdcd6	2.4341
rpn1	2.428
fam76b	2.4269
zgc:92510	2.4269
zgc:101761	2.42
sp4	2.4198
zgc:114143	2.4167
zgc:153930	2.4167
ppp1r10	2.416
ier5	2.4143
klf2b	2.4109
zgc:91918	2.4097
LOC563808	2.4097
zgc:111863	2.4096
unc119.1	2.4096
zgc:101601	2.4087
zgc:56223	2.4083
stat1	2.4072
zgc:55520	2.4005
LOC793774	2.4005
zgc:153587	2.3985
zgc:65871	2.3985
pxk	2.3937
chst5	2.3935
gabarapl2	2.3935
plk1	2.3914
gtpbp4	2.3913
zgc:101867	2.3907
si:ch211-20b12.1	2.3901
zgc:103487	2.3897
fbxl14a	2.3895
zgc:162630	2.3874
zgc:112069	2.3843
taf8	2.3843
gtf2a1	2.383
6-Sep	2.3829
dvl3	2.3769
cdv3	2.3753
wrb	2.375
zgc:92169	2.3738
mrps18b	2.373
pgrmc1	2.3701
raf1	2.365
golph3	2.365
zgc:65884	2.3645
zgc:85700	2.3645
cyb561d2	2.3607
upf1	2.3594
zgc:153607	2.3589
si:dkey-30h14.2	2.3577
zgc:101644	2.3562

zgc:77665	2.3522
hprt1	2.3518
zgc:158610	2.3517
zgc:136614	2.3501
zgc:111893	2.3501
acvr1	2.3469
zgc:55661	2.3469
zgc:92257	2.3469
LOC562123	2.3466
LOC562741	2.3466
zgc:114170	2.3454
pms1	2.3445
ormdl1	2.3445
zgc:152901	2.3444
si:ch211-14a17.11	2.3437
zgc:55746	2.3411
tmem126a	2.3405
mapre1l	2.3398
zgc:85981	2.3393
si:ch211-212d10.2	2.3388
zgc:56112	2.3365
ythdf1	2.3365
rbm38	2.3358
LOC562052	2.3357
ptenb	2.335
sox4a	2.3347
cldna	2.3341
zgc:55396	2.3339
zgc:56418	2.3297
zgc:112185	2.3297
dbr1	2.3285
ptpn11	2.3262
zgc:77725	2.3262
mapk4	2.3257
zgc:73223	2.325
tpm3	2.3244
LOC554960	2.323
ubxd1	2.323
hdgfrp2	2.323
dnm2l	2.3223
zgc:153255	2.3218
tjp3	2.3205
h2afx	2.3185
si:dkey-22l11.2	2.3179
zgc:66241	2.3176
zgc:101883	2.3172
si:dkey-42i9.5	2.3172
zgc:73347	2.3159
zgc:152921	2.3149
atp1a1	2.3118
zgc:77929	2.3112
zgc:64185	2.3106
dad1	2.3103
abhd4	2.3103
ck2a1	2.3098
ckap5	2.3096
zgc:92873	2.3096
zgc:92379	2.3095
zgc:73187	2.3084
mos	2.308
LOC795055	2.308
zgc:92355	2.3077
ociad1	2.3075
zgc:77052	2.3073
bambi	2.307
aes	2.3067
zgc:92882	2.3052
zgc:92882	2.3052
mta3	2.3036
LOC555925	2.3007
si:dkey-15j16.4	2.3007
smox	2.3006
rps5	2.3002
zgc:63466	2.2993
zgc:55870	2.2991
vamp2	2.299
plaa	2.2985
rpl12	2.2977
LOC562066	2.2977
g3bp1	2.2961
vamp1	2.2951
mgrn1	2.2943
zgc:92858	2.2943
si:ch211-191i18.1	2.2937
LOC566423	2.2932
wdfy2	2.293
rpp38	2.2928
zgc:63666	2.2928
bactin1	2.2917

phf17	2.2901
zgc:92567	2.2891
si:ch211-199o1.5	2.2891
zgc:63675	2.289
smc4	2.2885
ift80	2.2885
ahcy	2.2885
si:busm1-79f24.1	2.2876
zgc:92208	2.2872
capza1	2.2869
zgc:92034	2.2852
ube2i2	2.2844
eef2k	2.2843
ube2g2	2.2842
vti1b	2.284
rdh12	2.284
si:dkey-121a11.2	2.2836
yipf1	2.2833
lrrc42	2.2833
zgc:55345	2.2812
kpna4	2.2811
gmfb	2.2804
axin1	2.279
anp32b	2.279
efnb2a	2.277
cbl	2.2766
si:busm1-105l16.2	2.2759
si:busm1-105l16.2	2.2759
hnrpab	2.2753
bop1	2.2748
hsf1	2.2748
crat	2.2745
zgc:92148	2.2742
yipf6	2.2733
ophn1	2.2733
scarb1	2.2732
fam60al	2.2729
plekhk1	2.2717
zgc:110561	2.2708
nulf2	2.2708
hprt1l	2.2706
zgc:85741	2.2693
ndufa10	2.269
zgc:92723	2.269
bcl2	2.2685
znf207b	2.2677
zgc:77306	2.2675
zgc:56218	2.2672
thoc2	2.2672
h3f3a	2.2669
bcat1	2.2668
zgc:56126	2.2662
cdk2	2.2661
zgc:109957	2.2661
wsb1	2.2655
nrarpa	2.2651
zgc:100871	2.2644
zgc:136620	2.2643
si:xx-by187g17.8	2.2643
si:ch211-132p20.4	2.2643
zgc:101650	2.2639
snx5	2.2639
zgc:154102	2.2623
hdlbp	2.2622
rap2c	2.262
si:ch211-63o20.7	2.262
bmi1b	2.2619
zgc:112417	2.2614
med14	2.2614
wee1	2.261
zgc:63470	2.2606
stard10	2.2605
p4ha2	2.2597
gng5	2.2587
atp6v1al	2.2586
rac1	2.2569
si:dkey-172o10.5	2.2569
anp32a	2.2564
zgc:56219	2.2562
zgc:101569	2.2559
rngtt	2.2554
si:dkey-77b17.2	2.2554
mycbp2	2.2547
tcf7l1a	2.2546

	fold in log2	fold
Average	2.3419536	5.069887168
Median	2.3185	4.988133233

Supplemental Table 11. H3K14ac enriched top 250 genes in sperm.

zgc:92354	1.8002
pplb	1.6787
pcf11	1.6155
zgc:113902	1.588
kpna2	1.588
zgc:85702	1.586
zgc:91808	1.5808
rab5al	1.575
si:dkey-177p2.3	1.5455
mdm1	1.5313
calua	1.5313
si:rp71-1f1.7	1.5195
plekhk1	1.4979
zgc:100801	1.4793
zgc:101774	1.4674
zgc:113355	1.4667
zgc:110008	1.4667
ndufa10	1.4604
zgc:92723	1.4604
pafah1b3	1.4603
cacnb1	1.4599
ift57	1.4497
fzr1	1.4396
zgc:92520	1.4292
prkar1a	1.4266
zgc:153587	1.4256
zgc:65871	1.4256
zgc:85857	1.4247
plk1	1.4231
si:busm1-79f24.1	1.4228
zgc:153412	1.4196
poll	1.4196
memo1	1.4094
zgc:123251	1.4094
zgc:56112	1.4039
si:dkey-65b13.8	1.3976
fam46c	1.3935
si:dkey-172o10.5	1.3863
zgc:56141	1.3855
zgc:56141	1.3855
LOC563289	1.3824
zgc:91821	1.3824
bxdc1	1.3802
ccdc65	1.3795
traf3ip1	1.3687
si:dkey-11n6.4	1.3667
ck2a1	1.3606
arl13b	1.343
snip1	1.3421
rc3h1	1.3415
LOC571606	1.3369
LOC407652	1.3362
zgc:123116	1.3362
vcp	1.335
si:ch211-199m3.1	1.3346
tacc3	1.33
si:dkey-14a7.4	1.3156
zgc:158610	1.312
zgc:55461	1.3103
calm3b	1.3073
ddx27	1.3039
bcat1	1.3007
zgc:103412	1.2968
gmnn	1.2952
zgc:111986	1.2952
ttc25	1.2897
hprt1	1.2896
zgc:158640	1.2894
smn1	1.2894
cab39	1.2859
zgc:92629	1.2856
zgc:92067	1.2856
zgc:158666	1.2855
zgc:101111	1.2855
ubtd2	1.2838
zgc:55664	1.2831
zgc:56093	1.2818
si:ch211-257i19.2	1.2818
zgc:91834	1.2799
zgc:153686	1.2793
tubb2c	1.2777
maf1	1.2727
zgc:56235	1.2723
si:ch211-215m21.11	1.2636
si:ch211-215m21.11	1.2635
zgc:112945	1.2604
si:ch211-101n13.4	1.2604
terfa	1.2579

zgc:92405	1.2575
smc4	1.2564
ift80	1.2564
zgc:55870	1.2556
zgc:101063	1.2543
zgc:91844	1.2543
LOC561143	1.2543
kifc1	1.2543
capza1	1.2514
zmpste24	1.2512
zgc:56199	1.2411
xrcc6	1.2411
si:dkey-7c18.18	1.2362
mgrn1	1.2355
zgc:92858	1.2355
gtpbp4	1.2341
zgc:123265	1.2302
ruvbl1	1.2302
zgc:123211	1.2298
zgc:56424	1.2276
polr3f	1.2211
zgc:103658	1.2211
zgc:103658	1.2211
zgc:92212	1.2205
chst5	1.2175
gabarapl2	1.2175
si:dkey-202b22.3	1.2162
zgc:73347	1.2074
zgc:55494	1.2066
ift52	1.2065
zgc:111863	1.2064
unc119.1	1.2064
zgc:101711	1.2035
rab5a	1.2032
zgc:100871	1.2023
LOC566423	1.2012
zgc:165341	1.1943
cdc20	1.192
mapre1l	1.1918
rsph3	1.191
zgc:153063	1.1891
nrarpa	1.1885
id1	1.1874
mospd1	1.1851
rcbtb1	1.1781
zgc:63648	1.1765
si:ch211-276e22.2	1.1764
zgc:152979	1.1764
sinup	1.1764
zgc:77052	1.1746
zgc:153219	1.1744
zgc:65845	1.1744
wdr51b	1.1731
tsga14	1.1731
sfrs5	1.1723
zgc:100912	1.1688
usp33	1.1661
tmem126a	1.164
rpl12	1.1639
LOC562066	1.1639
katnb1	1.1614
kif23	1.1592
abcb3l1	1.1583
arl6ip1	1.1563
mos	1.1546
LOC795055	1.1546
zgc:91814	1.1505
ube2h	1.1503
papolg	1.1473
rbm4l	1.1457
zgc:158262	1.1446
zgc:92606	1.1446
LOC100003308	1.1425
si:dkey-202b22.4	1.1422
riok3	1.142
fam116b	1.14
si:dkey-159a18.3	1.14
nphs2l	1.1373
zgc:55965	1.1353
ddx39b	1.1353
si:dkey-246a16.2	1.1322
zgc:92663	1.1322
zgc:153961	1.1321
dpagt1	1.1321
zgc:63497	1.1301
zgc:101608	1.1301
zgc:56418	1.1233
zgc:112185	1.1233
tkt	1.1222

zgc:110241	1.1221
nono	1.1211
zgc:101737	1.1207
tdh	1.1194
ddx26b	1.1163
si:rp71-1c10.3	1.1149
psmb9a	1.1144
zgc:162701	1.1126
eaf1	1.1126
LOC100000024	1.112
MGC173425	1.112
slc2a8l	1.1116
si:dkey-217m5.9	1.111
zgc:110113	1.1103
zgc:162824	1.1098
zgc:101639	1.1098
syncripl	1.1069
zgc:55327	1.1068
wdr82	1.1059
LOC565154	1.1055
zgc:56141	1.1041
hmmr	1.1038
dvl3	1.1024
fam60al	1.102
csnk1dl	1.0994
zgc:136474	1.0992
zgc:158387	1.0992
zgc:86657	1.0984
si:ch211-194d6.5	1.0968
rab5b	1.0968
arih1	1.0948
ift172	1.0948
slc20a1b	1.0926
otub1	1.0925
zgc:113305	1.0925
gmds	1.0918
gmds	1.0918
zgc:153910	1.0916
zgc:56200	1.0916
zgc:110741	1.0904
zgc:92307	1.0896
wee1	1.0868
zgc:85972	1.0855
mcm7	1.083
zgc:92664	1.0825
zgc:66474	1.0824
rnf113a	1.0814
snrp70	1.0814
zgc:56126	1.0812
si:ch211-10j20.1	1.0788
rbmx	1.0783
tubgcp2	1.0783
zgc:63666	1.0767
gpsm2	1.0765
zgc:66100	1.0763
zgc:162789	1.0755
zgc:154095	1.0739
slc30a1	1.0735
mapk15	1.0721
hnrpab	1.0721
rrm2	1.0707
rcan3	1.0705
ier5	1.0702
LOC563855	1.0692
zgc:154072	1.0672
zgc:64085	1.0648
cecr1	1.0645
cecr1	1.0645
calm2b	1.0609
zgc:162318	1.0602
cluap1	1.0602
dusp7	1.0594
clic4	1.0591
zgc:64050	1.0572
hel_dr1	1.0568
zgc:152681	1.056
dkfzp564o0523	1.056
hnrnpa0	1.0558
ccnb1	1.0552
zgc:109924	1.0551
polb	1.0551
zgc:153115	1.0549
si:ch211-215m21.17	1.0545
bmi1	1.054
psme3	1.0529

	fold in log2	fold
Average	1.22115649	2.331335
Median	1.18625	2.275605

Supplemental Table 12. H3K4me3 GO

HYPERLINKED GO CATEGORY	TOTAL	GE	CHANGED	ENRICHMI	FALSE DISCOVERY RATE
GO:0051301_cell_division	59		20	5.215819	0
GO:0007049_cell_cycle	115		22	2.943536	0
GO:0007018_microtubule-based_movement	31		10	4.963441	0
GO:0007017_microtubule-based_process	55		13	3.636848	0
GO:0000278_mitotic_cell_cycle	42		10	3.663492	0.01
GO:0022402_cell_cycle_process	49		11	3.45415	0.012
GO:0044257_cellular_protein_catabolic_process	113		17	2.314808	0.022
GO:0051603_proteolysis_involved_in_cellular_protein_catabolic_	113		17	2.314808	0.022
GO:0044267_cellular_protein_metabolic_process	817		75	1.412485	0.02375
GO:0048285_organelle_fission	32		8	3.846667	0.024167
GO:0022403_cell_cycle_phase	40		9	3.462	0.024615
GO:0019941_modification-dependent_protein_catabolic_process	101		16	2.437492	0.025455
GO:0043632_modification-dependent_macromolecule_catabolic_	101		16	2.437492	0.025455
GO:0016043_cellular_component_organization	373		41	1.691296	0.02625
GO:0000280_nuclear_division	30		8	4.103111	0.027143
GO:0000279_M_phase	39		9	3.550769	0.03
GO:0000087_M_phase_of_mitotic_cell_cycle	29		7	3.714023	0.048889
GO:0007067_mitosis	29		7	3.714023	0.048889
GO:0010970_microtubule-based_transport	5		3	9.232	0.059545
GO:0030705_cytoskeleton-dependent_intracellular_transport	5		3	9.232	0.059545
GO:0042073_intraflagellar_transport	5		3	9.232	0.059545
GO:0043064_flagellum_organization	5		3	9.232	0.059545
GO:0034962_cellular_biopolymer_catabolic_process	127		17	2.059633	0.07
GO:0051641_cellular_localization	169		21	1.911953	0.070435
GO:0051649_establishment_of_localization_in_cell	163		20	1.887935	0.076923
GO:0006996_organelle_organization	208		24	1.775385	0.078
GO:0044265_cellular_macromolecule_catabolic_process	131		17	1.996743	0.079259
GO:0051258_protein_polymerization	35		7	3.077333	0.119286
GO:0006413_translational_initiation	20		5	3.846667	0.137586
GO:0006974_response_to_DNA_damage_stimulus	65		10	2.367179	0.155
GO:0034984_cellular_response_to_DNA_damage_stimulus	65		10	2.367179	0.155
GO:0042384_cilium_assembly	13		4	4.734359	0.155667
GO:0043687_post-translational_protein_modification	372		36	1.489032	0.169091

Supplemental Table 13. H3K14ac GO

HYPERLINKED GO CATEGORY	TOTAL GE	CHANGED	ENRICHMI	FALSE DISCOVERY RATE
GO:0007017_microtubule-based_process	51	12	3.590812	0
GO:0046907_intracellular_transport	186	26	2.133251	0
GO:0051649_establishment_of_cellular_localization	217	30	2.109809	0
GO:0051641_cellular_localization	222	30	2.06229	0
GO:0006996_organelle_organization_and_biogenesis	246	32	1.985164	0
GO:0016043_cellular_component_organization_and_biogenesis	876	84	1.463379	0
GO:0006464_protein_modification_process	581	59	1.549735	0.007143
GO:0007067_mitosis	30	8	4.069586	0.01
GO:0000087_M_phase_of_mitotic_cell_cycle	31	8	3.938309	0.016667
GO:0000279_M_phase	39	9	3.521757	0.017273
GO:0022403_cell_cycle_phase	39	9	3.521757	0.017273
GO:0043412_biopolymer_modification	605	59	1.488258	0.025
GO:0043687_post-translational_protein_modification	455	46	1.542865	0.036923
GO:0006259_DNA_metabolic_process	121	17	2.1441	0.038125
GO:0007010_cytoskeleton_organization_and_biogenesis	102	15	2.244257	0.039412
GO:0007018_microtubule-based_movement	29	7	3.683677	0.04
GO:0030705_cytoskeleton-dependent_intracellular_transport	29	7	3.683677	0.04
GO:0010171_body_morphogenesis	5	3	9.156569	0.047778
GO:0022618_protein-RNA_complex_assembly	38	8	3.212831	0.051053
GO:0006974_response_to_DNA_damage_stimulus	57	10	2.677359	0.055217
GO:0019538_protein_metabolic_process	1572	128	1.242622	0.055909
GO:0051276_chromosome_organization_and_biogenesis	85	13	2.334027	0.058571
GO:0008104_protein_localization	217	25	1.758174	0.059583
GO:0006260_DNA_replication	39	8	3.130451	0.06
GO:0044267_cellular_protein_metabolic_process	1486	121	1.242648	0.060357
GO:0022402_cell_cycle_process	50	9	2.746971	0.061379
GO:0015031_protein_transport	207	24	1.769385	0.062222
GO:0045184_establishment_of_protein_localization	207	24	1.769385	0.062222
GO:0033036_macromolecule_localization	218	25	1.750109	0.0656
GO:0000278_mitotic_cell_cycle	42	8	2.906847	0.078065
GO:0022613_ribonucleoprotein_complex_biogenesis_and_assen	60	10	2.543491	0.078667
GO:0044260_cellular_macromolecule_metabolic_process	1504	121	1.227776	0.089688
GO:0006281_DNA_repair	55	9	2.497246	0.130606
GO:0007049_cell_cycle	77	11	2.180136	0.148824
GO:0051258_protein_polymerization	30	6	3.05219	0.152
GO:0009719_response_to_endogenous_stimulus	69	10	2.211732	0.166842
GO:0006468_protein_amino_acid_phosphorylation	276	28	1.548212	0.170541
GO:0065003_macromolecular_complex_assembly	156	18	1.760879	0.173333
GO:0006183_GTP_biosynthetic_process	9	3	5.086983	0.191087
GO:0006228_UTP_biosynthetic_process	9	3	5.086983	0.191087
GO:0006241_CTP_biosynthetic_process	9	3	5.086983	0.191087
GO:0009208_pyrimidine_ribonucleoside_triphosphate_metabolic_	9	3	5.086983	0.191087
GO:0009209_pyrimidine_ribonucleoside_triphosphate_biosynthet	9	3	5.086983	0.191087
GO:0046036_CTP_metabolic_process	9	3	5.086983	0.191087
GO:0046039_GTP_metabolic_process	9	3	5.086983	0.191087
GO:0046051_UTP_metabolic_process	9	3	5.086983	0.191087
GO:0006413_translational_initiation	33	6	2.774718	0.198936

Supplemental Table 14. 137 genes located within 12 kb of H3K36me3 top 2400 enriched loci.

acbd3
admr
bmi1b
calb2l
chmp7
coe2
commd3
crygm2d4
d4st1
ddx39b
dlx1a
dlx3b
dmrta2
emx2
faah2a
fam73a
foxd3
foxg1
foxo3a
gbx1
gpm6ab
hand2
hoxa11a
hoxa11b
hoxa1a
hoxa2b
hoxa3a
hoxa4a
hoxa5a
hoxa9a
hoxb5a
hoxb5b
hoxb8a
hoxc12b
hoxc6b
hoxc8a
hoxd4a
hoxd9a
irx5a
isl2a
lamb1
LOC559969
LOC561579
LOC572755
LOC573017
LOC794589
mab21l1
max
meis1
meis4.1a
mpp1
mynn
ndr2
ndufa6
nitr10a
nkx2.1b
nkx2.2a
nkx6.1
nola3
nr2f1l
ntn1a
or115-14
or129-1
otx1
otx2
pcdh2ab10
phf5a
pitx2a

pou4f2
ptgs1
ptpn2
si:ch211-119b12.5
si:ch211-125e6.12
si:ch211-282j17.10
si:ch73-189n23.1
si:dkey-220f10.7
si:dkey-236e20.7
si:dkey-239i20.2
si:dkey-27p7.2
si:dkey-88n24.7
si:dkey-88n24.8
sim2
six2.1
slc25a28
snrpfl
sox3
sp8l
sppl2
tbx1
tbx15
tfap2a
tomm20
tuba2
vox
zgc:100865
zgc:100971
zgc:101705
zgc:101774
zgc:101815
zgc:103448
zgc:110011
zgc:110344
zgc:111928
zgc:112028
zgc:112318
zgc:112350
zgc:114196
zgc:123296
zgc:123339
zgc:136371
zgc:136814
zgc:153035
zgc:153168
zgc:153222
zgc:153596
zgc:153630
zgc:154014
zgc:154100
zgc:154123
zgc:158397
zgc:158463
zgc:158706
zgc:158781
zgc:163013
zgc:173706
zgc:55696
zgc:56020
zgc:56526
zgc:66178
zgc:77327
zgc:77415
zgc:85611
zgc:85936
zgc:86775
zgc:91964
zgc:92883
zic1

Supplemental Table 15. H3K36me3 GO

HYPERLINKED GO CATEGORY	TOTAL GE	CHANGED	ENRICHMI	FALSE DISCOVERY RATE
GO:0006355_regulation_of_transcription__DNA-dependent	539	45	6.149686	0
GO:0051252_regulation_of_RNA_metabolic_process	542	45	6.115647	0
GO:0006351_transcription__DNA-dependent	561	46	6.039823	0
GO:0032774_RNA_biosynthetic_process	563	46	6.018367	0
GO:0007417_central_nervous_system_development	157	11	5.160862	0
GO:0045449_regulation_of_transcription	719	50	5.122363	0
GO:0019219_regulation_of_nucleobase__nucleoside__nucleotide_and_nucleic	731	50	5.038275	0
GO:0051171_regulation_of_nitrogen_compound_metabolic_process	733	50	5.024528	0
GO:0006350_transcription	751	51	5.002181	0
GO:0010556_regulation_of_macromolecule_biosynthetic_process	741	50	4.970282	0
GO:0031326_regulation_of_cellular_biosynthetic_process	747	50	4.93036	0
GO:0009889_regulation_of_biosynthetic_process	749	50	4.917195	0
GO:0010468_regulation_of_gene_expression	766	50	4.808066	0
GO:0016070_RNA_metabolic_process	721	47	4.801664	0
GO:0031323_regulation_of_cellular_metabolic_process	788	50	4.673831	0
GO:0080090_regulation_of_primary_metabolic_process	809	50	4.552508	0
GO:0060255_regulation_of_macromolecule_metabolic_process	825	50	4.464217	0
GO:0019222_regulation_of_metabolic_process	855	50	4.307577	0
GO:0007399_nervous_system_development	282	15	3.918062	0
GO:0034961_cellular_biopolymer_biosynthetic_process	989	51	3.798421	0
GO:0043284_biopolymer_biosynthetic_process	993	51	3.78312	0
GO:0034645_cellular_macromolecule_biosynthetic_process	1044	51	3.598313	0
GO:0009059_macromolecule_biosynthetic_process	1049	51	3.581161	0
GO:0007275_multicellular_organismal_development	909	44	3.56548	0
GO:0010467_gene_expression	1087	52	3.523733	0
GO:0032502_developmental_process	984	45	3.368578	0
GO:0032501_multicellular_organismal_process	995	45	3.331338	0
GO:0006139_nucleobase__nucleoside__nucleotide_and_nucleic_acid_metabo	1181	52	3.243267	0
GO:0006807_nitrogen_compound_metabolic_process	1287	52	2.976144	0
GO:0044249_cellular_biosynthetic_process	1270	51	2.957983	0
GO:0009058_biosynthetic_process	1318	52	2.906144	0
GO:0048731_system_development	684	25	2.692236	0
GO:0048856_anatomical_structure_development	714	26	2.682281	0
GO:0050794_regulation_of_cellular_process	1663	57	2.524712	0
GO:0050789_regulation_of_biological_process	1747	59	2.487644	0
GO:0065007_biological_regulation	1833	59	2.37093	0
GO:0034960_cellular_biopolymer_metabolic_process	1785	54	2.228357	0
GO:0044260_cellular_macromolecule_metabolic_process	1805	54	2.203666	0
GO:0043283_biopolymer_metabolic_process	2010	54	1.978914	0
GO:0043170_macromolecule_metabolic_process	2035	54	1.954603	0
GO:0044237_cellular_metabolic_process	2289	54	1.737709	0
GO:0044238_primary_metabolic_process	2445	55	1.656964	0
GO:0045165_cell_fate_commitment	50	6	8.839149	0.000227
GO:0048513_organ_development	600	22	2.700851	0.000233
GO:0008152_metabolic_process	2951	58	1.447731	0.000667
GO:0030154_cell_differentiation	342	14	3.015304	0.001064
GO:0009987_cellular_process	3734	68	1.341417	0.001087
GO:0048869_cellular_developmental_process	355	14	2.904885	0.002083
GO:0048598_embryonic_morphogenesis	174	9	3.809978	0.004694
GO:0035270_endocrine_system_development	31	4	9.504461	0.0048
GO:0022008_neurogenesis	147	8	4.008684	0.004902
GO:0007420_brain_development	118	7	4.369636	0.005769
GO:0030182_neuron_differentiation	122	7	4.226369	0.006604
GO:0001501_skeletal_system_development	63	5	5.845998	0.007037
GO:0001708_cell_fate_specification	38	4	7.753639	0.007636
GO:0007422_peripheral_nervous_system_development	18	3	12.2766	0.008036
GO:0050935_iridophore_differentiation	5	2	29.46383	0.010526
GO:0009653_anatomical_structure_morphogenesis	392	13	2.442792	0.012881
GO:0048468_cell_development	212	9	3.127057	0.012931
GO:0048699_generation_of_neurons	138	7	3.736355	0.015333
GO:0051216_cartilage_development	43	4	6.852053	0.01541
GO:0009792_embryonic_development_ending_in_birth_or_egg_hatching	108	6	4.092199	0.022857
GO:0043009_chordate_embryonic_development	108	6	4.092199	0.022857
GO:0009790_embryonic_development	320	11	2.532048	0.027656

GO:0043583_ear_development	54	4	5.456265	0.03697
GO:0048839_inner_ear_development	53	4	5.559213	0.037385
GO:0021782_glial_cell_development	9	2	16.36879	0.040299
GO:0031018_endocrine_pancreas_development	10	2	14.73192	0.050588
GO:0009887_organ_morphogenesis	262	9	2.530291	0.053333
GO:0021915_neural_tube_development	34	3	6.499374	0.056486
GO:0042471_ear_morphogenesis	34	3	6.499374	0.056486
GO:0021508_floor_plate_formation	11	2	13.39265	0.056761
GO:0021990_neural_plate_formation	11	2	13.39265	0.056761
GO:0042472_inner_ear_morphogenesis	33	3	6.696325	0.056944
GO:0007418_ventral_midline_development	12	2	12.2766	0.058625
GO:0030318_melanocyte_differentiation	12	2	12.2766	0.058625
GO:0030326_embryonic_limb_morphogenesis	12	2	12.2766	0.058625
GO:0035113_embryonic_appendage_morphogenesis	12	2	12.2766	0.058625
GO:0035115_embryonic_forelimb_morphogenesis	12	2	12.2766	0.058625
GO:0035118_embryonic_pectoral_fin_morphogenesis	12	2	12.2766	0.058625
GO:0001839_neural_plate_morphogenesis	14	2	10.5228	0.081975
GO:0030902_hindbrain_development	44	3	5.022244	0.10622
GO:0035136_forelimb_morphogenesis	17	2	8.665832	0.108353
GO:0035138_pectoral_fin_morphogenesis	17	2	8.665832	0.108353
GO:0050931_pigment_cell_differentiation	17	2	8.665832	0.108353
GO:0035108_limb_morphogenesis	18	2	8.184397	0.117471
GO:0060173_limb_development	18	2	8.184397	0.117471
GO:0048646_anatomical_structure_formation_involved_in_morphogenesis	122	5	3.018835	0.118068
GO:0001840_neural_plate_development	19	2	7.753639	0.120778
GO:0033339_pectoral_fin_development	19	2	7.753639	0.120778
GO:0007423_sensory_organ_development	173	6	2.554667	0.126452
GO:0010001_glial_cell_differentiation	20	2	7.365957	0.1275
GO:0048066_pigmentation_during_development	20	2	7.365957	0.1275
GO:0035239_tube_morphogenesis	21	2	7.015198	0.134105
GO:0042063_gliogenesis	21	2	7.015198	0.134105
GO:0009888_tissue_development	228	7	2.261478	0.136146
GO:0035295_tube_development	55	3	4.017795	0.14732
GO:0031175_neuron_projection_development	56	3	3.946049	0.152449
GO:0048514_blood_vessel_morphogenesis	58	3	3.809978	0.161313
GO:0016331_morphogenesis_of_embryonic_epithelium	25	2	5.892766	0.1648
GO:0000904_cell_morphogenesis_involved_in_differentiation	59	3	3.745402	0.165446
GO:0002009_morphogenesis_of_an_epithelium	65	3	3.399673	0.193204
GO:0060429_epithelium_development	65	3	3.399673	0.193204
GO:0014032_neural_crest_cell_development	29	2	5.079971	0.195905
GO:0031016_pancreas_development	29	2	5.079971	0.195905

Supplemental Table 16. Transcripts detected in zebrafish mature sperm (enriched over background, >5.8-fold)

GeneName	Description	values in log2
wu:fk34f03	fk34f03.y1 zebrafish fin day1 regeneration Danio rerio cDNA 5' similar to SW:COX1	16.20651143
TC278986	XB28SRRNA X.borealis 28S ribosomal RNA gene for 28S rRNA, partial (7%) [TC2	12.71784185
TC279053	Q6Q414 (Q6Q414) Acidic ribosomal protein P1, partial (32%) [TC279053]	12.36596256
vangl2	Danio rerio vang-like 2 (van gogh, Drosophila), mRNA (cDNA clone MGC:76845 IM	12.28864706
TC279055	NFU34338 Neoceratodus forsteri 28S ribosomal RNA gene, partial sequence, parti	12.11796913
TC279068	NFU34338 Neoceratodus forsteri 28S ribosomal RNA gene, partial sequence, parti	12.08504846
TC290305	Cyprinus carpio intergenic spacer region, partial sequence; 5' external transcribed s	11.98875155
TC279168	PAU34339 Protopterus aethiopicus 28S ribosomal RNA gene, partial sequence, pa	11.88970193
TC279240	Q6Q419 (Q6Q419) Ribosomal protein S29, partial (91%) [TC279240]	11.74151349
zgc:85811	Danio rerio zgc:85811 (zgc:85811), mRNA [NM_213284]	11.74078694
apoeb	Danio rerio apolipoprotein Eb (apoeb), mRNA [NM_131098]	11.65435251
ef1a	Danio rerio elongation factor 1-alpha (ef1a), mRNA [NM_131263]	11.57296506
TC290238	Cyprinus carpio intergenic spacer region, partial sequence; 5' external transcribed s	11.50222786
bactin2	Danio rerio bactin2 (bactin2), mRNA [NM_181601]	11.49125194
apoeb	Danio rerio apolipoprotein Eb (apoeb), mRNA [NM_131098]	11.44965077
TC290087	COX1_BRARE (Q9MIY8) Cytochrome c oxidase polypeptide I , partial (53%) [TC2	11.41330112
TC290296	Cyprinus carpio intergenic spacer region, partial sequence; 5' external transcribed s	11.41214154
TC290244	ARU34342 Anguilla rostrata 28S ribosomal RNA gene, partial sequence, partial (48	11.29023215
TC281691	BT007109 c-myc binding protein {Homo sapiens;} , partial (51%) [TC281691]	11.25933703
mtatp6	Danio rerio ATP synthase 6, mitochondrial (mtatp6), mRNA [NM_001007138]	11.21020909
vg1	Danio rerio vitellogenin 1 (vg1), mRNA [NM_170767]	11.0531073
vangl2	Danio rerio vang-like 2 (van gogh, Drosophila), mRNA (cDNA clone MGC:76845 IM	11.03916952
msh6	Danio rerio mutS homolog 6 (E. coli) (msh6), mRNA [NM_182860]	10.95421511
TC268919	Cyprinus carpio intergenic spacer region, partial sequence; 5' external transcribed s	10.65053642
TC290293	Cyprinus carpio intergenic spacer region, partial sequence; 5' external transcribed s	10.63585275
TC290346	Cyprinus carpio intergenic spacer region, partial sequence; 5' external transcribed s	10.55936394
zgc:66168	Danio rerio zgc:66168 (zgc:66168), mRNA [NM_200502]	10.54280423
TC268116	Q90YW4 (Q90YW4) Ribosomal protein L6 (Fragment), partial (37%) [TC268116]	10.24924744
TC290247	Cyprinus carpio intergenic spacer region, partial sequence; 5' external transcribed s	10.17216262
hnrpk	Danio rerio heterogeneous nuclear ribonucleoprotein K (hnrpk), mRNA [NM_21299	10.09217367
rpl7	Danio rerio ribosomal protein L7 (rpl7), mRNA [NM_213644]	10.07463679
zgc:66190	Danio rerio zgc:66190 (zgc:66190), mRNA [NM_213113]	10.02695572
rpl27	Danio rerio ribosomal protein L27 (rpl27), mRNA [NM_199724]	9.961406557
rpl7	Danio rerio ribosomal protein L7 (rpl7), mRNA [NM_213644]	9.954747664
psap	Danio rerio prosaposin (psap), mRNA [NM_131883]	9.943768408
zgc:76953	Danio rerio zgc:76953 (zgc:76953), mRNA [NM_214759]	9.943597699
bactin1	Danio rerio bactin1 (bactin1), mRNA [NM_131031]	9.939855428
TC267926	RLA2_HUMAN (P05387) 60S acidic ribosomal protein P2, partial (89%) [TC26792	9.931690723
tctp	Danio rerio translationally controlled tumor protein (tctp), mRNA [NM_198140]	9.918835396
fth1	Danio rerio ferritin, heavy polypeptide 1 (fth1), mRNA [NM_131585]	9.866069445
ckii	Danio rerio type II cytokeratin (ckii), mRNA [NM_131156]	9.802698575
rps8	Danio rerio ribosomal protein S8 (rps8), mRNA [NM_214793]	9.793445916
rps14	Danio rerio ribosomal protein S14 (rps14), mRNA [NM_200026]	9.77079477
zgc:66168	Danio rerio zgc:66168 (zgc:66168), mRNA [NM_200502]	9.763104825
zgc:85824	Danio rerio zgc:85824 (zgc:85824), mRNA [NM_213279]	9.723059979
zgc:92041	Danio rerio zgc:92041 (zgc:92041), mRNA [NM_001003737]	9.706642523
TC279257	Q9PUB5 (Q9PUB5) Type II cytokeratin, complete [TC279257]	9.697801009
wu:fa91f08	fa91f08.y1 zebrafish fin day1 regeneration Danio rerio cDNA 5' similar to gb:Y0036	9.625070963
rpl19	Danio rerio ribosomal protein L19 (rpl19), mRNA [NM_213208]	9.578269139
fth1	Danio rerio ferritin, heavy polypeptide 1 (fth1), mRNA [NM_131585]	9.573306304
hsp90b	Danio rerio heat shock protein hsp90beta mRNA, complete cds. [AF068772]	9.551634689
AI330993	fb04b10.y1 zebrafish fin day1 regeneration Danio rerio cDNA 5' similar to gb:Y0036	9.524620931
zgc:56640	Danio rerio zgc:56640 (zgc:56640), mRNA [NM_200028]	9.462725696
ckii	Danio rerio type II cytokeratin, mRNA (cDNA clone MGC:77647 IMAGE:6996972),	9.450076567
fau	Danio rerio Finkel-Biskis-Reilly murine sarcoma virus (FBR-MuSV) ubiquitously exp	9.416910292
eef2l	Danio rerio eukaryotic translation elongation factor 2, like (eef2l), mRNA [NM_2004	9.41021702
hspa8	Danio rerio heat shock 70kDa protein 8 (hspa8), mRNA [NM_131401]	9.403584485
BQ481378	faa75g05.y1 Gong zebrafish testis Danio rerio cDNA clone IMAGE:5899593 5', mR	9.39555488
zgc:92533	Danio rerio zgc:92533 (zgc:92533), mRNA [NM_001003445]	9.383152396
ns:zf-es43	AGENCOURT_22826715 NIH_ZGC_9 Danio rerio cDNA clone IMAGE:7279581 5'	9.36315197
hsp90b	Danio rerio heat shock protein 90-beta, mRNA (cDNA clone MGC:77433 IMAGE:69	9.331595195
rps15	Danio rerio ribosomal protein S15 (rps15), mRNA [NM_001001819]	9.284222292
TC280416	Q7ZV96 (Q7ZV96) Ribosomal protein L10, partial (98%) [TC280416]	9.263520077
rps15a	Danio rerio ribosomal protein S15a (rps15a), mRNA [NM_212762]	9.26177104
BC083506	Danio rerio cDNA clone IMAGE:6900534, partial cds. [BC083506]	9.246932676
rpl13a	Danio rerio ribosomal protein L13a (rpl13a), mRNA [NM_212784]	9.242820282
rps25	Danio rerio ribosomal protein S25 (rps25), mRNA [NM_200815]	9.224061846
rpl24	Danio rerio ribosomal protein L24 (rpl24), mRNA [NM_173235]	9.178023065
CO355067	DR_ATE_NRM04_B02 adult testis normalized (TLL) Danio rerio cDNA, mRNA seq	9.161356575
BC083506	Danio rerio cDNA clone IMAGE:6900534, partial cds. [BC083506]	9.156046662
rps3a	Danio rerio ribosomal protein S3A (rps3a), mRNA [NM_200059]	9.128794322
rpl7a	Danio rerio ribosomal protein L7a (rpl7a), mRNA [NM_200047]	9.105585447
zgc:92868	Danio rerio zgc:92868 (zgc:92868), mRNA [NM_001003434]	9.093861505
hsp90b	Danio rerio heat shock protein 90-beta (hsp90b), mRNA [NM_131310]	9.048797601
zgc:92076	Danio rerio zgc:92076 (zgc:92076), mRNA [NM_001005589]	9.045506876
BC091460	Q6Q418 (Q6Q418) Ribosomal protein L3, complete [TC279265]	9.03876314
rps9	Danio rerio ribosomal protein S9 (rps9), mRNA [NM_200852]	9.025226966
eef1b2	Danio rerio eukaryotic translation elongation factor 1 beta 2 (eef1b2), mRNA [NM_1	9.013436912
zgc:92371	Danio rerio zgc:92371 (zgc:92371), mRNA [NM_001002078]	9.005631189

zgc:92868	AGENCOURT_22402944 NIH_ZGC_9 Danio rerio cDNA clone IMAGE:7275020 5'	8.985647517
TC291444	RL39_ICTPU (Q90YS9) 60S ribosomal protein L39, complete [TC291444]	8.966029385
rpl23a	Danio rerio ribosomal protein L23a (rpl23a), mRNA [NM_001001593]	8.963941406
TC279348	Q6Y230 (Q6Y230) Ribosomal protein L18a (Fragment), partial (98%) [TC279348]	8.963060338
rps7	Danio rerio ribosomal protein S7 (rps7), mRNA [NM_200752]	8.93236208
wu:fb58g10	fb58g10.y1 Zebrafish WashU MPIMG EST Danio rerio cDNA clone IMAGE:371613	8.91348495
iclp1	Danio rerio invariant chain-like protein 1 (iclp1), mRNA [NM_131590]	8.888496097
ctsd	Danio rerio cathepsin D (ctsd), mRNA [NM_131710]	8.879229885
zgc:92789	Danio rerio zgc:92789 (zgc:92789), mRNA [NM_001002545]	8.876665094
rps5	Danio rerio ribosomal protein S5 (rps5), mRNA [NM_173232]	8.848366108
rpl9	Danio rerio ribosomal protein L9 (rpl9), mRNA [NM_001003861]	8.847610866
zgc:92859	Danio rerio zgc:92859 (zgc:92859), mRNA [NM_001002487]	8.842158383
ctrb1	Danio rerio chymotrypsinogen B1 (ctrb1), mRNA [NM_212618]	8.824171971
zgc:66382	Danio rerio zgc:66382 (zgc:66382), mRNA [NM_199605]	8.795262283
zgc:101846	Danio rerio zgc:101846 (zgc:101846), mRNA [NM_001005967]	8.77800869
zgc:101846	Danio rerio zgc:101846 (zgc:101846), mRNA [NM_001005967]	8.770437932
rpl3	Danio rerio ribosomal protein L3 (rpl3), mRNA [NM_001001590]	8.764941218
zgc:73380	Danio rerio zgc:73380 (zgc:73380), mRNA [NM_200811]	8.739964835
CO355975	DR_ATE_NRM14_E12 adult testis normalized (TLL) Danio rerio cDNA, mRNA seq	8.721320079
zgc:56455	Danio rerio zgc:56455 (zgc:56455), mRNA [NM_201122]	8.719744126
zgc:56642	Danio rerio zgc:56642 (zgc:56642), mRNA [NM_201191]	8.704137797
rpl23a	Danio rerio ribosomal protein L23a (rpl23a), mRNA [NM_001001593]	8.693965999
rps7	Danio rerio ribosomal protein S7 (rps7), mRNA [NM_200752]	8.675268885
rpl9	Danio rerio ribosomal protein L9 (rpl9), mRNA [NM_001003861]	8.670510207
zgc:101846	Danio rerio zgc:101846 (zgc:101846), mRNA [NM_001005967]	8.669139232
rps5	Danio rerio ribosomal protein S5 (rps5), mRNA [NM_173232]	8.663892354
rpl7	Danio rerio ribosomal protein L7 (rpl7), mRNA [NM_213644]	8.657419931
apoeb	Danio rerio apolipoprotein Eb (apoeb), mRNA [NM_131098]	8.638464298
zgc:56699	Danio rerio zgc:56699 (zgc:56699), mRNA [NM_212833]	8.62721538
ENSDART00(	END4_CHLTE (Q8KFL0) Probable endonuclease IV (Endodeoxyribonuclease IV)	8.614777723
zgc:92860	Danio rerio zgc:92860 (zgc:92860), mRNA [NM_001002486]	8.614154304
ctsc	Danio rerio cathepsin C (ctsc), mRNA [NM_214722]	8.603083534
CO355889	DR_ATE_NRM13_F06 adult testis normalized (TLL) Danio rerio cDNA, mRNA seq	8.589466276
naca	Danio rerio nascent polypeptide-associated complex alpha polypeptide (naca), mRI	8.586750329
rps3a	Danio rerio ribosomal protein S3A (rps3a), mRNA [NM_200059]	8.581599042
zgc:56699	Danio rerio cDNA clone IMAGE:6960324, partial cds. [BC067179]	8.579293199
zgc:91809	Danio rerio zgc:91809 (zgc:91809), mRNA [NM_001002079]	8.578205383
CO354313	DR_ATE_FL25_G03 adult testis full-length (TLL) Danio rerio cDNA, mRNA sequen	8.56023799
AW233060	fj27e11.y1 Zebrafish adult olfactory Danio rerio cDNA 5' similar to TR:O93238 O93	8.529160694
zgc:92114	Danio rerio zgc:92114 (zgc:92114), mRNA [NM_001003447]	8.527923219
zgc:65996	Danio rerio zgc:65996 (zgc:65996), mRNA [NM_212760]	8.526568248
TC282169	Q7SYV3 (Q7SYV3) MGC64464 protein, partial (59%) [TC282169]	8.525507614
zgc:85824	Danio rerio zgc:85824 (zgc:85824), mRNA [NM_213279]	8.524309863
ppia	Danio rerio peptidylprolyl isomerase A (cyclophilin A) (ppia), mRNA [NM_212758]	8.517563646
apoeb	Danio rerio apolipoprotein Eb (apoeb), mRNA [NM_131098]	8.512013805
oaz2	Danio rerio ornithine decarboxylase antizyme 2 (oaz2), mRNA [NM_194432]	8.506938427
rpl18a	Danio rerio ribosomal protein L18a (rpl18a), mRNA [NM_201060]	8.50582331
rpl35	Danio rerio ribosomal protein L35 (rpl35), mRNA [NM_173233]	8.484405852
zgc:77758	Danio rerio zgc:77758 (zgc:77758), mRNA [NM_213204]	8.447053405
zgc:92067	Danio rerio zgc:92067 (zgc:92067), mRNA [NM_001002377]	8.434941242
rpl13	Danio rerio ribosomal protein L13 (rpl13), mRNA [NM_198143]	8.432509166
cd163	Danio rerio Cd63 antigen (cd163), mRNA [NM_199543]	8.429878578
ENSDART00(	fj24a07.y1 Zebrafish adult olfactory Danio rerio cDNA 5' similar to gb:K03002 60S F	8.429321658
BM572617	fx55e04.y1 Zebrafish SJD 5 day embryo Danio rerio cDNA clone IMAGE:5627238 5	8.417129694
dct	Danio rerio dopachrome tautomerase (dct), mRNA [NM_131555]	8.416877192
zgc:86669	Danio rerio zgc:86669 (zgc:86669), mRNA [NM_001002155]	8.397591811
TC290329	Q8JHI0 (Q8JHI0) Solute carrier family 25 member 5 protein (Solute carrier family 2	8.387262484
TC277142	BC055187 ribosomal protein L36A {Danio rerio;} , partial (69%) [TC277142]	8.374463064
zgc:91809	Danio rerio zgc:91809 (zgc:91809), mRNA [NM_001002079]	8.348538453
rps12	Danio rerio ribosomal protein S12 (rps12), mRNA [NM_200046]	8.317824982
TC290333	Q6Q418 (Q6Q418) Ribosomal protein L3, partial (27%) [TC290333]	8.307997225
zgc:101745	Danio rerio zgc:101745 (zgc:101745), mRNA [NM_001006061]	8.305199727
rpl11	Danio rerio ribosomal protein L11 (rpl11), mRNA [NM_001002139]	8.303710426
AI330415	fa92d08.x1 zebrafish fin day1 regeneration Danio rerio cDNA 3', mRNA sequence [	8.292232251
zgc:73262	Danio rerio zgc:73262 (zgc:73262), mRNA [NM_200765]	8.291774283
TC290310	AF021880 Ictalurus punctatus 18S small subunit ribosomal RNA gene, complete se	8.284372623
wu:fb58g10	fb58g10.y1 Zebrafish WashU MPIMG EST Danio rerio cDNA clone IMAGE:371613	8.281906427
zgc:77702	Danio rerio zgc:77702 (zgc:77702), mRNA [NM_200845]	8.270123701
cox4i1	Danio rerio cytochrome c oxidase subunit IV isoform 1 (cox4i1), mRNA [NM_21470	8.268632863
rps5	Danio rerio ribosomal protein S5 (rps5), mRNA [NM_173232]	8.258012436
rplp0	Danio rerio ribosomal protein, large, P0 (rplp0), mRNA [NM_131580]	8.24368663
zgc:56493	Danio rerio zgc:56493 (zgc:56493), mRNA [NM_200023]	8.239690944
zgc:91997	Danio rerio zgc:91997 (zgc:91997), mRNA [NM_001004113]	8.231613229
zgc:103753	Danio rerio zgc:103753 (zgc:103753), mRNA [NM_205573]	8.228094989
zgc:86669	AGENCOURT_21855435 NIH_ZGC_8 Danio rerio cDNA clone IMAGE:7264014 5'	8.222954543
rpl9	Danio rerio ribosomal protein L9 (rpl9), mRNA [NM_001003861]	8.219411449
zgc:92533	Danio rerio zgc:92533 (zgc:92533), mRNA [NM_001003445]	8.213135582
zgc:91809	Danio rerio zgc:91809 (zgc:91809), mRNA [NM_001002079]	8.212743908
eef1g	Danio rerio eukaryotic translation elongation factor 1 gamma (eef1g), mRNA [NM_1	8.212649378
zgc:56493	Danio rerio zgc:56493 (zgc:56493), mRNA [NM_200023]	8.209738543
TC289321	APE_BRARE (O42364) Apolipoprotein E precursor (Apo-E), partial (62%) [TC2893	8.209077228

nme2	Danio rerio non-metastatic cells 2, protein (NM23B) expressed in (nme2), mRNA [N	8.20242414
ENSDART00(	IDLC_STRPU (Q26630) 33 kDa inner dynein arm light chain, axonemal (p33), parti	8.19686325
CN506336	AGENCOURT_22438073 NIH_ZGC_7 Danio rerio cDNA clone IMAGE:7267128 5'	8.19595558
TC267921	D86628 family-2 cystatin {Oncorhynchus keta;} , partial (61%) [TC267921]	8.188723665
zgc:65809	Danio rerio zgc:65809 (zgc:65809), mRNA [NM_213336]	8.175172814
zgc:66026	Danio rerio zgc:66026 (zgc:66026), mRNA [NM_200577]	8.172051845
zgc:66195	Danio rerio zgc:66195 (zgc:66195), mRNA [NM_200506]	8.15920183
iclp2	Danio rerio invariant chain-like protein 2 (iclp2), mRNA [NM_131372]	8.156712661
TC269177	BC044206 decorin {Danio rerio;} , complete [TC269177]	8.155292587
rps12	Danio rerio ribosomal protein S12 (rps12), mRNA [NM_200046]	8.155179624
rpl12	Danio rerio ribosomal protein L12 (rpl12), mRNA [NM_201584]	8.154179231
ENSDART00(	AGENCOURT_20193508 NIH_ZGC_14 Danio rerio cDNA clone IMAGE:7227504 5	8.143160673
apoeb	Danio rerio apolipoprotein Eb (apoeb), mRNA [NM_131098]	8.137967238
zgc:91930	Danio rerio zgc:91930 (zgc:91930), mRNA [NM_001003993]	8.130253992
krt8	Danio rerio keratin 8 (krt8), mRNA [NM_200080]	8.127722882
apoeb	Danio rerio apolipoprotein Eb (apoeb), mRNA [NM_131098]	8.116258287
TC273265	Q9JKX4 (Q9JKX4) Traube (Apoptosis antagonizing transcription factor), partial (26	8.09614948
TC293406	Q8R4T8 (Q8R4T8) Guanine deaminase, partial (76%) [TC293406]	8.092748118
zgc:55554	Danio rerio zgc:55554 (zgc:55554), mRNA [NM_213461]	8.086507546
bsg	Danio rerio basigin, mRNA (cDNA clone MGC:65810 IMAGE:6792452), complete c	8.079342103
TC287093	Q804H0 (Q804H0) Annexin 1c, partial (18%) [TC287093]	8.079072187
zgc:101846	AGENCOURT_22403018 NIH_ZGC_9 Danio rerio cDNA clone IMAGE:7272561 5'	8.073758095
CO353753	DR_ATE_FL19_D07 adult testis full-length (TLL) Danio rerio cDNA, mRNA sequen	8.067486639
zgc:55554	Danio rerio zgc:55554 (zgc:55554), mRNA [NM_213461]	8.043937972
zgc:91930	Danio rerio zgc:91930 (zgc:91930), mRNA [NM_001003993]	8.039618209
cetn2	DR_ATE_NRM02_B08 adult testis normalized (TLL) Danio rerio cDNA, mRNA seq	8.035721071
zgc:73232	Danio rerio zgc:73232 (zgc:73232), mRNA [NM_200072]	8.034983273
BM141616	ZFT480 Zebrafish Testis Danio rerio cDNA 5', mRNA sequence [BM141616]	8.014326204
TC290231	Q6PQG4 (Q6PQG4) Kazal-like serine protease inhibitor EPI9, partial (25%) [TC29(	8.002076833
TC268126	Q7R8P9 (Q7R8P9) Homeobox-containing protein (Fragment), partial (4%) [TC268	7.990240621
slc25a5	Danio rerio solute carrier family 25 alpha, member 5 (slc25a5), mRNA [NM_173247	7.983852364
CO355235	DR_ATE_NRM06_E05 adult testis normalized (TLL) Danio rerio cDNA, mRNA seq	7.982490191
ENSDART00(	Unknown	7.966245138
mhc1uea	Danio rerio major histocompatibility complex class I UEA gene (mhc1uea), mRNA [	7.95603401
krt4	Danio rerio keratin 4 (krt4), mRNA [NM_131509]	7.952748861
TC296972	Q8BU53 (Q8BU53) Mus musculus 2 days pregnant adult female oviduct cDNA, RIK	7.946265213
apoa	Danio rerio apolipoprotein A-I (apoa), mRNA [NM_131128]	7.939457408
apoeb	Danio rerio apolipoprotein Eb (apoeb), mRNA [NM_131098]	7.934680914
rpl12	Danio rerio ribosomal protein L12 (rpl12), mRNA [NM_201584]	7.925596706
ENSDART00(	fa96f07.y1 zebrafish fin day3 regeneration Danio rerio cDNA 5' similar to SW:RL22	7.906026658
CK397453	AGENCOURT_17391960 NIH_ZGC_4 Danio rerio cDNA clone IMAGE:7118686 5'	7.898333371
zgc:103753	Danio rerio zgc:103753 (zgc:103753), mRNA [NM_205573]	7.897051419
glula	Danio rerio glutamate-ammonia ligase (glutamine synthase) a (glula), mRNA [NM_	7.882136711
cirbp	Danio rerio cold inducible RNA binding protein (cirbp), mRNA [NM_200017]	7.869012268
TC268174	Q90YN8 (Q90YN8) Vitellogenin 1, partial (21%) [TC268174]	7.865084575
TC294291	Q71SZ1 (Q71SZ1) Cytochrome c oxidase subunit Vb, partial (75%) [TC294291]	7.852392927
zgc:92638	Danio rerio zgc:92638 (zgc:92638), mRNA [NM_001002438]	7.846564498
zgc:73149	Danio rerio zgc:73149 (zgc:73149), mRNA [NM_200732]	7.843827341
zgc:91813	Danio rerio zgc:91813 (zgc:91813), mRNA [NM_001002209]	7.841896062
zgc:101786	Danio rerio zgc:101786 (zgc:101786), mRNA [NM_001007398]	7.831365351
dtk	Danio rerio developmental receptor tyrosine kinase (dtk), mRNA [NM_131432]	7.820186873
TC269418	AY216591 phospholipid hydroperoxide glutathione peroxidase B {Danio rerio;} , cor	7.806846499
zgc:92638	Danio rerio zgc:92638 (zgc:92638), mRNA [NM_001002438]	7.804873134
b2m	Danio rerio beta-2-microglobulin (b2m), mRNA [NM_131163]	7.794512632
BE017569	fk79h08.x1 Zebrafish Research Genetics C32 fin Danio rerio cDNA 3', mRNA sequ	7.793211616
zgc:86681	Danio rerio zgc:86681 (zgc:86681), mRNA [NM_001001594]	7.782890623
mdh1a	Danio rerio malate dehydrogenase 1a, NAD (soluble) (mdh1a), mRNA [NM_19994	7.779907352
zgc:77877	Danio rerio zgc:77877 (zgc:77877), mRNA [NM_213011]	7.765008926
bysl	Danio rerio bystin-like (bysl), mRNA [NM_201106]	7.758858107
wu:fb11g12	Danio rerio wu:fb11g12 (wu:fb11g12), mRNA [NM_001001949]	7.757902796
zp2.3	Danio rerio zona pellucida glycoprotein 2.3 (zp2.3), mRNA [NM_131828]	7.752550111
TC290152	TCTP_BRARE (Q9DGK4) Translationally-controlled tumor protein (TCTP), partial (	7.734689633
rps8	Danio rerio ribosomal protein S8 (rps8), mRNA [NM_214793]	7.712634131
zgc:65840	Danio rerio zgc:65840 (zgc:65840), mRNA [NM_213133]	7.708379692
TC268079	NCS1_CHICK (P62167) Neuronal calcium sensor 1 (NCS-1) (Frequenin homolog)	7.708249827
coro1a	Danio rerio coronin, actin binding protein, 1A (coro1a), mRNA [NM_201114]	7.699407398
zgc:77449	Danio rerio zgc:77449 (zgc:77449), mRNA [NM_212899]	7.678217153
rps29	Danio rerio ribosomal protein S29 (rps29), mRNA [NM_212953]	7.677245324
rps3	Danio rerio ribosomal protein S3 (rps3), mRNA [NM_201153]	7.674124506
zgc:86828	Danio rerio zgc:86828 (zgc:86828), mRNA [NM_001002114]	7.66335775
fabp10	Danio rerio fatty acid binding protein 10, liver basic (fabp10), mRNA [NM_152960]	7.661474818
eef1g	Danio rerio eukaryotic translation elongation factor 1 gamma (eef1g), mRNA [NM_1	7.650683876
gstp1	Danio rerio glutathione S-transferase pi (gstp1), mRNA [NM_131734]	7.649412018
TC294969	Unknown	7.649025124
CO355783	DR_ATE_NRM12_E07 adult testis normalized (TLL) Danio rerio cDNA, mRNA seq	7.639879925
zgc:56640	AF401585 ribosomal protein L30 {Ictalurus punctatus;} , partial (98%) [TC279312]	7.633082555
b2m	Danio rerio beta-2-microglobulin (b2m), mRNA [NM_131163]	7.628166306
zgc:86681	Danio rerio zgc:86681 (zgc:86681), mRNA [NM_001001594]	7.621189727
zgc:66409	Danio rerio zgc:66409 (zgc:66409), mRNA [NM_212737]	7.61959762
ckb	Danio rerio creatine kinase, brain (ckb), mRNA [NM_173222]	7.618124757
TC268844	Q6PBZ5 (Q6PBZ5) Zgc:73179, complete [TC268844]	7.614651334

cndp2	Danio rerio CNDP dipeptidase 2 (metallopeptidase M20 family) (cndp2), mRNA [NM	7.600565759
TC280697	Q6PC06 (Q6PC06) S-adenosylhomocysteine hydrolase-like 2, complete [TC28069	7.592505926
zgc:63985	Danio rerio zgc:63985 (zgc:63985), mRNA [NM_199958]	7.585715297
ccni	Danio rerio cyclin I (ccni), mRNA [NM_212971]	7.584123557
zgc:77877	Danio rerio zgc:77877 (zgc:77877), mRNA [NM_213011]	7.573951754
gstp1	Danio rerio glutathione S-transferase pi (gstp1), mRNA [NM_131734]	7.573897018
rpl4	Danio rerio ribosomal protein L4 (rpl4), mRNA [NM_213107]	7.564332192
zgc:101069	Danio rerio zgc:101069 (zgc:101069), mRNA [NM_001003570]	7.564295277
eef2l	Danio rerio eukaryotic translation elongation factor 2, like (eef2l), mRNA [NM_2004	7.55938014
tuba8l4	Danio rerio tubulin, alpha 8 like 4 (tuba8l4), mRNA [NM_200185]	7.555754026
zgc:56334	Danio rerio zgc:56334 (zgc:56334), mRNA [NM_199568]	7.554343275
zgc:91809	Danio rerio zgc:91809 (zgc:91809), mRNA [NM_001002079]	7.55082585
zgc:91845	Danio rerio zgc:91845 (zgc:91845), mRNA [NM_001002199]	7.539423934
CO355080	DR_ATE_NRM04_C03 adult testis normalized (TLL) Danio rerio cDNA, mRNA seq	7.530610658
ahcy	Danio rerio S-adenosylhomocysteine hydrolase (ahcy), mRNA [NM_199218]	7.529660419
cfl2l	Danio rerio cofilin 2, like (cfl2l), mRNA [NM_213641]	7.529561218
gnb2l1	Danio rerio guanine nucleotide binding protein (G protein), beta polypeptide 2-like 1	7.529424318
krt8	Danio rerio keratin 8 (krt8), mRNA [NM_200080]	7.522671805
TC271103	Q7SXE0 (Q7SXE0) Wu:fj09e08 protein, complete [TC271103]	7.521093793
ENSDART00(	Q8JH37 (Q8JH37) Vitellogenin 1 (Fragment), partial (39%) [TC268135]	7.512832941
zgc:91947	Danio rerio zgc:91947 (zgc:91947), mRNA [NM_212783]	7.50953857
ccng1	Danio rerio cyclin G1 (ccng1), mRNA [NM_199481]	7.509359075
cndp2	Danio rerio CNDP dipeptidase 2 (metallopeptidase M20 family) (cndp2), mRNA [NM	7.50577407
TC293858	BC001022 PP protein {Homo sapiens;} , partial (75%) [TC293858]	7.503517213
zgc:101880	Danio rerio zgc:101880 (zgc:101880), mRNA [NM_001005961]	7.488040512
cox7c	Danio rerio cytochrome c oxidase, subunit VIIc (cox7c), mRNA [NM_199995]	7.485046886
glulb	Danio rerio glutamate-ammonia ligase (glutamine synthase) b (glulb), mRNA [NM_	7.475393146
zgc:85951	Danio rerio zgc:85951 (zgc:85951), mRNA [NM_213233]	7.469242235
myl9l	Danio rerio myosin, light polypeptide 9, like (myl9l), mRNA [NM_214699]	7.464102592
TC269128	CR457344 FLJ21827 {Homo sapiens;} , partial (84%) [TC269128]	7.460883716
TC291359	Q6JZV5 (Q6JZV5) Cathepsin Z, partial (97%) [TC291359]	7.460851452
CO355043	DR_ATE_NRM03_H01 adult testis normalized (TLL) Danio rerio cDNA, mRNA seq	7.459106241
atp5g	Danio rerio ATP synthase, H+ transporting, mitochondrial F0 complex, subunit c (su	7.455681207
arl6ip	Danio rerio ADP-ribosylation factor-like 6 interacting protein (arl6ip), mRNA [NM_20	7.454628333
si:busm1-202l	Danio rerio si:busm1-202l16.3 (si:busm1-202l16.3), mRNA [NM_001002603]	7.446627827
oaz1	Danio rerio ornithine decarboxylase antizyme 1 (oaz1), mRNA [NM_194264]	7.443698701
ENSDART00(	DR_ATE_NRM02_G02 adult testis normalized (TLL) Danio rerio cDNA, mRNA seq	7.439344042
rpl3	Danio rerio ribosomal protein L3 (rpl3), mRNA [NM_001001590]	7.422672503
zgc:85774	Danio rerio zgc:85774 (zgc:85774), mRNA [NM_212688]	7.422333844
CK867885	AGENCOURT_19703640 NIH_ZGC_6 Danio rerio cDNA clone IMAGE:7218721 5'	7.409521701
rps26	Danio rerio ribosomal protein S26 (rps26), mRNA [NM_200025]	7.407632762
ppial	Danio rerio peptidylprolyl isomerase A, like (ppial), mRNA [NM_199957]	7.406609397
atp6v1g1	Danio rerio ATPase, H+ transporting, V1 subunit G isoform 1 (atp6v1g1), mRNA [N	7.405335793
ndufb4	Danio rerio NADH dehydrogenase (ubiquinone) 1 beta subcomplex, 4 (ndufb4), mR	7.405028051
slc25a5	Danio rerio solute carrier family 25 alpha, member 5 (slc25a5), mRNA [NM_17324	7.397650807
rpl8	Danio rerio ribosomal protein L8 (rpl8), mRNA [NM_200713]	7.389552103
TC279375	Q6Q421 (Q6Q421) Ribosomal protein S15, complete [TC279375]	7.384300202
etfb	Danio rerio electron-transfer-flavoprotein, beta polypeptide (etfb), mRNA [NM_212	7.369563171
ENSDART00(	DR_ATE_NRM02_G02 adult testis normalized (TLL) Danio rerio cDNA, mRNA seq	7.361591268
tfa	Danio rerio transferrin-a, mRNA (cDNA clone IMAGE:3815706), partial cds. [BC05	7.355454037
zgc:103420	Danio rerio zgc:103420 (zgc:103420), mRNA [NM_001006043]	7.349881251
arpc1b	Danio rerio actin related protein 2/3 complex, subunit 1B (arpc1b), mRNA [NM_213	7.337897356
zgc:64051	Danio rerio zgc:64051 (zgc:64051), mRNA [NM_200371]	7.331648431
ENSDART00(	TSR6_HUMAN (P59910) Testis spermatocyte apoptosis-related gene 6 protein (Te	7.317132725
ldhb	Danio rerio lactate dehydrogenase B4, mRNA (cDNA clone MGC:76941 IMAGE:65	7.309901452
zgc:92891	Danio rerio zgc:92891 (zgc:92891), mRNA [NM_001002468]	7.308628392
fbxo42	Danio rerio F-box protein 42 (fbxo42), mRNA [NM_212739]	7.307287735
wu:fe14c05	AGENCOURT_16619450 NIH_ZGC_7 Danio rerio cDNA clone IMAGE:7053065 5'	7.300719922
LOC402797	Danio rerio similar to synaptonemal complex protein 1, mRNA (cDNA clone IMAGE	7.293649218
glulb	Danio rerio glutamate-ammonia ligase (glutamine synthase) b (glulb), mRNA [NM_	7.28622772
zgc:103764	Danio rerio zgc:103764 (zgc:103764), mRNA [NM_001005593]	7.283186645
ENSDART00(	HG15_CHICK (P12902) Nonhistone chromosomal protein HMG-14A, partial (43%)	7.281950352
sars	Danio rerio seryl-tRNA synthetase (sars), mRNA [NM_001003882]	7.280098188
TC291549	BC045970 proteasome (prosome, macropain) subunit, alpha type, 4 {Danio rerio;}	7.268960558
cdkn1bl	Danio rerio cyclin-dependent kinase inhibitor 1b, like, mRNA (cDNA clone IMAGE:6	7.267868883
zgc:56335	AGENCOURT_22422823 NIH_ZGC_9 Danio rerio cDNA clone IMAGE:7275163 5'	7.261141891
tubb2	Danio rerio tubulin, beta, 2 (tubb2), mRNA [NM_198809]	7.25670286
zgc:76908	Danio rerio zgc:76908 (zgc:76908), mRNA [NM_213094]	7.250424375
zgc:91810	Danio rerio zgc:91810 (zgc:91810), mRNA [NM_001003482]	7.248821044
atp5l	Danio rerio ATP synthase, H+ transporting, mitochondrial F0 complex, subunit g (al	7.244978729
zgc:56193	Danio rerio zgc:56193 (zgc:56193), mRNA [NM_212996]	7.241896014
wu:fd55c07	AGENCOURT_16624123 NIH_ZGC_7 Danio rerio cDNA clone IMAGE:7052466 5'	7.234648341
hdlbp	Danio rerio high density lipoprotein-binding protein (vigilin) (hdlbp), mRNA [NM_20	7.234443228
mg:bb02h10	bb02h10_p1 ZF adult heart library Danio rerio cDNA 5 prime similar to 5' end of rib	7.231667775
ndufa6	Danio rerio NADH dehydrogenase (ubiquinone) 1 alpha subcomplex, 6, 14kDa (ndu	7.229249696
TC291464	Q9W672 (Q9W672) CCCH zinc finger protein C3H-2, partial (75%) [TC291464]	7.227856472
BC067158	Danio rerio cDNA clone IMAGE:6525439. [BC067158]	7.220498902
ENSDART00(	IF35_HUMAN (O00303) Eukaryotic translation initiation factor 3 subunit 5 (eIF-3 ep	7.216066238
rps8	Danio rerio ribosomal protein S8 (rps8), mRNA [NM_214793]	7.214014439
zgc:86773	Danio rerio zgc:86773 (zgc:86773), mRNA [NM_001002129]	7.213919222
wu:fb15g10	fj22h01.y1 Zebrafish adult olfactory Danio rerio cDNA 5', mRNA sequence [AW202	7.213887183

zgc:55524	Danio rerio zgc:55524 (zgc:55524), mRNA [NM_200960]	7.208739017
lcp1	Danio rerio lymphocyte cytosolic plastin 1 (lcp1), mRNA [NM_131320]	7.206161857
TC269495	STB1_BOVIN (P61763) Syntaxin binding protein 1 (Unc-18 homolog) (Unc-18A) (U	7.196711648
mylz2	Danio rerio myosin, light polypeptide 2, skeletal muscle (mylz2), mRNA [NM_1311E	7.196404649
zgc:56090	Danio rerio zgc:56090 (zgc:56090), mRNA [NM_199693]	7.194858056
ywhab	Danio rerio tyrosine 3-monooxygenase/tryptophan 5-monooxygenase activation prc	7.191340008
zgc:77315	Danio rerio zgc:77315 (zgc:77315), mRNA [NM_205667]	7.190798488
TC293950	Q6NX86 (Q6NX86) High mobility group box 1, partial (70%) [TC293950]	7.190648992
TC291339	Unknown	7.181042504
mhc1uba	Danio rerio major histocompatibility complex class I UBA gene (mhc1uba), mRNA [	7.175709008
icn	Danio rerio ictacalcin (icn), mRNA [NM_212761]	7.174935668
pabpc1	Danio rerio poly A binding protein, cytoplasmic 1 (pabpc1), mRNA [NM_200882]	7.17346035
gpm6ba	Danio rerio glycoprotein M6Ba (gpm6ba), mRNA [NM_203427]	7.166654709
BQ479592	faa70b02.y1 Gong zebrafish testis Danio rerio cDNA clone IMAGE:5898962 5' simi	7.16652985
eif2b3	Danio rerio eukaryotic translation initiation factor 2B, subunit 3 gamma, 58kDa (eif2	7.163342361
ENSDART00(	AP001753 HES1 protein {Homo sapiens;} , partial (68%) [TC292484]	7.161203233
rps3a	Danio rerio ribosomal protein S3A (rps3a), mRNA [NM_200059]	7.144715049
ENSDART00(	AGENCOURT_22404247 NIH_ZGC_9 Danio rerio cDNA clone IMAGE:7272744 5'	7.139105473
zgc:86752	Danio rerio proto galectin Gal1-L2 (LOC405830), mRNA [NM_212894]	7.137271208
wu:fc19f04	fc19f04.x1 Zebrafish WashU MPIMG EST Danio rerio cDNA clone IMAGE:372185E	7.136043054
zgc:55489	Danio rerio zgc:55489 (zgc:55489), mRNA [NM_214714]	7.134489238
TC292167	NU93_BRARE (Q7ZU29) Nuclear pore complex protein Nup93 (Nucleoporin Nup9:	7.133458858
oaz1	Danio rerio ornithine decarboxylase antizyme 1 (oaz1), mRNA [NM_194264]	7.132639372
nsep1	Danio rerio nuclease sensitive element binding protein 1, mRNA (cDNA clone MGC	7.132503026
slc25a3	Danio rerio solute carrier family 25 (mitochondrial carrier; phosphate carrier), memb	7.123011892
zgc:92523	Danio rerio zgc:92523 (zgc:92523), mRNA [NM_001003449]	7.122876127
zgc:92891	Danio rerio zgc:92891 (zgc:92891), mRNA [NM_001002468]	7.119406608
atp6ap2	Danio rerio ATPase, H+ transporting, lysosomal accessory protein 2 (atp6ap2), mR	7.117969658
zgc:56189	Danio rerio zgc:56189 (zgc:56189), mRNA [NM_199914]	7.117359376
TC291063	Q7ZU67 (Q7ZU67) Eukaryotic translation initiation factor 4A, isoform 1B, complete	7.116517326
cndp2	Danio rerio CNDP dipeptidase 2 (metallopeptidase M20 family) (cndp2), mRNA [NM	7.115807201
si:rp71-1o1.2	Danio rerio si:rp71-1o1.2 (si:rp71-1o1.2), mRNA [NM_001004643]	7.112942056
gnb1	Danio rerio guanine nucleotide binding protein (G protein), beta polypeptide 1 (gnb	7.111334052
atp6ap2	Danio rerio ATPase, H+ transporting, lysosomal accessory protein 2 (atp6ap2), mR	7.106117933
zgc:73269	Danio rerio zgc:73269 (zgc:73269), mRNA [NM_200769]	7.105121999
TC269419	AY216591 phospholipid hydroperoxide glutathione peroxidase B {Danio rerio:} , cor	7.09716082
TC281969	BC021603 D11Bwg0434e protein {Mus musculus;} , partial (82%) [TC281969]	7.081716928
nsep1	Danio rerio nuclease sensitive element binding protein 1 (nsep1), mRNA [NM_1316	7.07976317
zgc:103482	Danio rerio zgc:103482 (zgc:103482), mRNA [NM_001006022]	7.07584671
zgc:92053	Danio rerio zgc:92053 (zgc:92053), mRNA [NM_205575]	7.075067171
eif3s8	Danio rerio eukaryotic translation initiation factor 3, subunit 8 (eif3s8), mRNA [NM_	7.07320571
CN836761	AGENCOURT_25020868 NIH_ZGC_4 Danio rerio cDNA clone IMAGE:7289896 5'	7.06880374
zgc:73152	Danio rerio zgc:73152 (zgc:73152), mRNA [NM_212722]	7.065650067
cygb	Danio rerio cytoglobin (cygb), mRNA [NM_152952]	7.065357198
ndufb4	Danio rerio NADH dehydrogenase (ubiquinone) 1 beta subcomplex, 4 (ndufb4), mR	7.063756896
zgc:101854	Danio rerio zgc:101854 (zgc:101854), mRNA [NM_001004674]	7.060495971
ucp4	Danio rerio uncoupling protein 4 (ucp4), mRNA [NM_199523]	7.057317236
zgc:100919	Danio rerio zgc:100919 (zgc:100919), mRNA [NM_001002748]	7.054557284
zgc:101682	Danio rerio zgc:101682 (zgc:101682), mRNA [NM_001006075]	7.050263772
zgc:73293	Danio rerio zgc:73293 (zgc:73293), mRNA [NM_213028]	7.048723246
zgc:103587	Danio rerio zgc:103587 (zgc:103587), mRNA [NM_001004682]	7.048385367
TC270083	BC023434 Stard8 protein {Mus musculus;} , partial (20%) [TC270083]	7.048107713
wu:fe37g01	Danio rerio wu:fe37g01 (wu:fe37g01), mRNA [NM_001003838]	7.048061447
rps26	Danio rerio ribosomal protein S26 (rps26), mRNA [NM_200025]	7.045897127
ndpkz2	Danio rerio nucleoside diphosphate kinase-Z2 (ndpkz2), mRNA [NM_130927]	7.044570811
zgc:56107	Danio rerio zgc:56107 (zgc:56107), mRNA [NM_201013]	7.042139773
rrm1	ribonucleotide reductase M1 polypeptide [Source:ZFIN;Acc:ZDB-GENE-990415-24	7.041409103
zgc:73161	Danio rerio zgc:73161 (zgc:73161), mRNA [NM_200043]	7.039019099
TC290974	Q7T3L6 (Q7T3L6) Cyclin A1, complete [TC290974]	7.036632947
CN023237	AGENCOURT_20193220 NIH_ZGC_14 Danio rerio cDNA clone IMAGE:7227486 5	7.035248628
zgc:92114	Danio rerio zgc:92114 (zgc:92114), mRNA [NM_001003447]	7.029122081
zgc:76908	Danio rerio zgc:76908 (zgc:76908), mRNA [NM_213094]	7.018683127
zgc:56107	Danio rerio zgc:56107 (zgc:56107), mRNA [NM_201013]	7.018552661
zgc:77704	Danio rerio zgc:77704, mRNA (cDNA clone MGC:56505 IMAGE:5913495), comple	7.014287534
thy1	Danio rerio Thy-1 cell surface antigen (thy1), mRNA [NM_198065]	7.013213667
zgc:77517	Danio rerio zgc:77517 (zgc:77517), mRNA [NM_200568]	7.009874822
slc25a3	Danio rerio solute carrier family 25 (mitochondrial carrier; phosphate carrier), memb	7.008850257
eno3	Danio rerio enolase 3, (beta, muscle) (eno3), mRNA [NM_214723]	7.007986857
tubb2	Danio rerio tubulin, beta, 2 (tubb2), mRNA [NM_198809]	7.004682831
ENSDART00(	Q6T3V3 (Q6T3V3) Activating transcription factor 4, partial (41%) [TC289897]	7.001287187
eif3s8	Danio rerio eukaryotic translation initiation factor 3, subunit 8 (eif3s8), mRNA [NM_	6.999572577
wu:fw32f02	fw32f02.y1 Zebrafish C32 14 somite embryo Danio rerio cDNA clone IMAGE:5566E	6.999450417
s100a1	Danio rerio S100 calcium binding protein A1, mRNA (cDNA clone IMAGE:5411703	6.994639474
fech	Danio rerio ferrochelatase (fech), mRNA [NM_131631]	6.992922539
zgc:92379	Danio rerio zgc:92379 (zgc:92379), mRNA [NM_001002077]	6.991155146
TC292993	1KTB_A Chain A, The Structure Of Alpha-N-Acetylgalactosaminidase. {Gallus gallu	6.988681372
zgc:64137	Danio rerio zgc:64137 (zgc:64137), mRNA [NM_199645]	6.985542736
zgc:85963	Danio rerio zgc:85963 (zgc:85963), mRNA [NM_214812]	6.985508029
zgc:55362	Danio rerio zgc:55362 (zgc:55362), mRNA [NM_199832]	6.984469109
zgc:77718	Danio rerio zgc:77718 (zgc:77718), mRNA [NM_200855]	6.984262546
CO355420	DR_ATE_NRM08_E07 adult testis normalized (TLL) Danio rerio cDNA, mRNA seq	6.982098911

tubb2	Danio rerio tubulin, beta, 2 (tubb2), mRNA [NM_198809]	6.98142875
gpd1	Danio rerio glycerol-3-phosphate dehydrogenase 1 (soluble) (gpd1), mRNA [NM_2	6.979196076
ba2	Danio rerio ba2 globin (ba2), mRNA [NM_131021]	6.977677293
zgc:77820	BC034787 NADH dehydrogenase (ubiquinone) 1 beta subcomplex, 7 {Mus muscul	6.977501599
TC270103	Q7ZYS8 (Q7ZYS8) Rpl10a-prov protein, partial (97%) [TC270103]	6.977142955
zgc:77517	Danio rerio zgc:77517 (zgc:77517), mRNA [NM_200568]	6.974564889
chchd2l	Danio rerio coiled-coil-helix-coiled-coil-helix domain containing 2-like (chchd2l), mR	6.965843057
zgc:73093	Danio rerio zgc:73093 (zgc:73093), mRNA [NM_200117]	6.965702773
zgc:92656	Danio rerio zgc:92656 (zgc:92656), mRNA [NM_001002427]	6.962254959
zgc:56217	Danio rerio zgc:56217 (zgc:56217), mRNA [NM_200212]	6.961721883
BC055643	Danio rerio cDNA clone MGC:66406 IMAGE:5915478, complete cds. [BC055643]	6.959406253
BI702854	fr63d12.y1 Zebrafish SJD day 8 fin regeneration Danio rerio cDNA clone IMAGE:49	6.959086428
hspa5	Danio rerio heat shock 70kDa protein 5 (glucose-regulated protein) (hspa5), mRNA	6.956367171
zgc:65782	Danio rerio zgc:65782 (zgc:65782), mRNA [NM_200548]	6.953138301
eif2s3	Danio rerio eukaryotic translation initiation factor 2, subunit 3 gamma (eif2s3), mRN	6.947231759
sb:cb890	Danio rerio sb:cb890 (sb:cb890), mRNA [NM_198824]	6.946701193
TC280535	BC070025 zgc:85963 {Danio rerio;} , complete [TC280535]	6.945861184
zgc:66488	Danio rerio zgc:66488 (zgc:66488), mRNA [NM_200431]	6.945767673
TC290717	Q9D4I5 (Q9D4I5) Mus musculus adult male testis cDNA, RIKEN full-length enriche	6.941656385
idh2	Danio rerio isocitrate dehydrogenase 2 (NADP+), mitochondrial (idh2), mRNA [NM_	6.941113366
cotl1	Danio rerio coactosin-like 1 (Dictyostelium) (cotl1), mRNA [NM_200012]	6.940796701
cct5	Danio rerio chaperonin containing TCP1, subunit 5 (epsilon) (cct5), mRNA [NM_21	6.939862687
TC293276	Q6VEU9 (Q6VEU9) H+ transporting F1 ATP synthase epsilon subunit, partial (96%	6.937647206
itgb4bp4	Danio rerio integrin beta 4 binding protein (itgb4bp4), mRNA [NM_200944]	6.936923252
BC090911	AGENCOURT_22403115 NIH_ZGC_9 Danio rerio cDNA clone IMAGE:7272371 5'	6.934810161
ENSDART00(	MIBTCIB22 NADH-ubiquinone oxidoreductase complex B22 subunit {Bos taurus;} ,	6.933199049
zgc:101737	Danio rerio zgc:101737 (zgc:101737), mRNA [NM_001007408]	6.930634405
prdx6	Danio rerio peroxiredoxin 6 (prdx6), mRNA [NM_200805]	6.928970356
eif3s7	Danio rerio eukaryotic translation initiation factor 3, subunit 7 zeta (eif3s7), mRNA [	6.926623333
dnaja2	Danio rerio DnaJ (Hsp40) homolog, subfamily A, member 2 (dnaja2), mRNA [NM_2	6.924007464
gnb2l1	Danio rerio guanine nucleotide binding protein (G protein), beta polypeptide 2-like 1	6.922024764
zgc:56271	Danio rerio zgc:56271 (zgc:56271), mRNA [NM_200251]	6.919700526
zgc:55760	Danio rerio zgc:55760 (zgc:55760), mRNA [NM_214770]	6.917527474
rps11	Danio rerio ribosomal protein S11 (rps11), mRNA [NM_213377]	6.913438439
zgc:65802	Danio rerio zgc:65802 (zgc:65802), mRNA [NM_200550]	6.909849574
TC269498	CATK_PIG (Q9GLE3) Cathepsin K precursor , partial (61%) [TC269498]	6.906828277
psma5	Danio rerio proteasome (prosome, macropain) subunit, alpha type,5 (psma5), mRN	6.904322033
zgc:56335	Danio rerio zgc:56335 (zgc:56335), mRNA [NM_201188]	6.90103767
idh2	Danio rerio isocitrate dehydrogenase 2 (NADP+), mitochondrial (idh2), mRNA [NM_	6.892124398
junb	Danio rerio jun B proto-oncogene (junb), mRNA [NM_213556]	6.891226695
ifi30	Danio rerio interferon gamma inducible protein 30 (ifi30), mRNA [NM_001006057]	6.890045611
TC279408	Q6TNV4 (Q6TNV4) Chaperonin containing TCP1, subunit 8 (Theta), complete [TC2	6.88960937
sars	Danio rerio seryl-tRNA synthetase (sars), mRNA [NM_001003882]	6.887654409
BC080245	Danio rerio cDNA clone IMAGE:7042113, partial cds. [BC080245]	6.887319195
zgc:77820	Danio rerio zgc:77820 (zgc:77820), mRNA [NM_200848]	6.881315604
TC292781	BC007087 upregulated during skeletal muscle growth 5 {Homo sapiens;} , partial (8	6.878863348
erh	Danio rerio enhancer of rudimentary homolog (Drosophila) (erh), mRNA [NM_1312	6.874523132
rplp0	Danio rerio ribosomal protein, large, P0 (rplp0), mRNA [NM_131580]	6.874337536
zgc:85681	Danio rerio zgc:85681 (zgc:85681), mRNA [NM_214698]	6.874076937
wu:fj49a01	AGENCOURT_22423182 NIH_ZGC_9 Danio rerio cDNA clone IMAGE:7273025 5'	6.873744631
zgc:101737	Danio rerio zgc:101737 (zgc:101737), mRNA [NM_001007408]	6.873707124
H2AV	Danio rerio similar to H2A histone family, member V, mRNA (cDNA clone IMAGE:6	6.871848285
krtl	AGENCOURT_21610442 NIH_ZGC_19 Danio rerio cDNA clone IMAGE:7252092 5	6.867792681
zgc:77291	Danio rerio zgc:77291 (zgc:77291), mRNA [NM_213231]	6.866221527
cebpb	Danio rerio CCAAT/enhancer binding protein (C/EBP), beta (cebpb), mRNA [NM_1	6.864492274
zgc:85681	Danio rerio zgc:85681 (zgc:85681), mRNA [NM_214698]	6.863718274
wasl	Danio rerio Wiskott-Aldrich syndrome, like (wasl), mRNA [NM_201059]	6.862140728
ENSDART00(	AGENCOURT_24291173 NIH_ZGC_4 Danio rerio cDNA clone IMAGE:7288018 5'	6.861225844
TC301128	Q6PBV8 (Q6PBV8) Zgc:73224 protein, partial (80%) [TC301128]	6.860709077
TC270598	Q6P0E4 (Q6P0E4) Type I cytokeratin, enveloping layer, partial (85%) [TC270598]	6.860206086
ENSDART00(	fd05d01.y1 Zebrafish WashU MPIMG EST Danio rerio cDNA clone IMAGE:372998	6.854441113
TC268925	Q7ZTH6 (Q7ZTH6) Dehydrogenase/3-ketoacyl-Coenzyme A thiolase, complete [TC	6.852310203
zgc:55760	Danio rerio zgc:55760 (zgc:55760), mRNA [NM_214770]	6.850415517
ccnb2	Danio rerio cyclin B2 (ccnb2), mRNA [NM_199430]	6.846459271
zgc:55603	Danio rerio zgc:55603 (zgc:55603), mRNA [NM_200260]	6.846251213
TC281840	HUAC002425 Gene product with similarity to Rat P8 {Homo sapiens;} , partial (38%	6.844193075
ef1	Danio rerio ETS-related factor1 (ef1), mRNA [NM_131159]	6.843307991
gpx1	Danio rerio glutathione peroxidase 1 (gpx1), mRNA [NM_001007281]	6.84195328
zgc:85790	Danio rerio zgc:85790 (zgc:85790), mRNA [NM_213299]	6.841925547
slc3a2	Danio rerio solute carrier family 3, member 2 (slc3a2), mRNA [NM_131601]	6.837691556
zgc:65921	Danio rerio zgc:65921 (zgc:65921), mRNA [NM_200546]	6.824478178
smn	Danio rerio survival motor neuron 1 (smn1), mRNA [NM_131191]	6.819381223
LOC402854	Danio rerio hypothetical protein LOC402854, mRNA (cDNA clone IMAGE:6795258	6.815317781
zgc:92379	AGENCOURT_17113629 NIH_ZGC_4 Danio rerio cDNA clone IMAGE:7090701 5'	6.814354979
LOC402833	Danio rerio hypothetical protein LOC402833, mRNA (cDNA clone IMAGE:2601258	6.809490503
CO359542	DR_ATE_SU06_G03 adult testis subtracted 1 (TLL) Danio rerio cDNA, mRNA sequ	6.80874622
zgc:63939	Danio rerio zgc:63939 (zgc:63939), mRNA [NM_213350]	6.805315143
TC271723	Q7ZWJ8 (Q7ZWJ8) LOC402796 protein (Fragment), complete [TC271723]	6.803241666
zgc:66160	Danio rerio zgc:66160 (zgc:66160), mRNA [NM_199781]	6.801530066
TC296296	Q6TGU1 (Q6TGU1) Serine proteinase inhibitor, clade B, member 1, partial (68%) [	6.798809957
TC279086	NFU34338 Neoceratodus forsteri 28S ribosomal RNA gene, partial sequence, parti	6.795662187

BM181130	fv94f05.y1 Zebrafish SJD adult male II Danio rerio cDNA clone IMAGE:5544729 5',	6.794753383
c20orf149l	Danio rerio chromosome 20 open reading frame 149, like (c20orf149l), mRNA [NM_	6.79402055
wu:fj06d11	fj06d11.y1 Zebrafish adult olfactory Danio rerio cDNA 5', mRNA sequence [AW174	6.79264853
ctsd	Danio rerio cathepsin D (ctsd), mRNA [NM_131710]	6.792605709
gpia	Danio rerio glucose phosphate isomerase a (gpia), mRNA [NM_144763]	6.791552922
zgc:101768	Danio rerio zgc:101768 (zgc:101768), mRNA [NM_001006055]	6.79003223
zgc:92744	Danio rerio zgc:92744 (zgc:92744), mRNA [NM_001002573]	6.789470819
TC290342	AF021880 Ictalurus punctatus 18S small subunit ribosomal RNA gene, complete se	6.788581001
fth1	Danio rerio ferritin, heavy polypeptide 1 (fth1), mRNA [NM_131585]	6.787610243
TC268871	Q9W7Q4 (Q9W7Q4) Chymotrypsinogen 1, partial (83%) [TC268871]	6.786673803
LOC402823	Danio rerio hypothetical protein LOC402823, mRNA (cDNA clone IMAGE:6789379	6.784389227
eif3s7	Danio rerio eukaryotic translation initiation factor 3, subunit 7 zeta (eif3s7), mRNA [	6.784014695
mef2a	Danio rerio myocyte enhancer factor 2a (mef2a), mRNA [NM_131301]	6.783411959
wu:fb83a09	fb83a09.x1 Zebrafish WashU MPIMG EST Danio rerio cDNA clone IMAGE:371845	6.783410189
pkm2	Danio rerio pyruvate kinase, muscle (pkm2), mRNA [NM_199333]	6.781108978
zgc:56053	Danio rerio zgc:56053 (zgc:56053), mRNA [NM_213050]	6.77582483
zgc:91805	Danio rerio zgc:91805 (zgc:91805), mRNA [NM_001002210]	6.775385594
ywhaq	Danio rerio tyrosine 3-monooxygenase/tryptophan 5-monooxygenase activation prc	6.772937248
BC091458	Q72I65 (Q72I65) TRNA pseudouridine synthase A , partial (7%) [TC269223]	6.769793779
zp2	Danio rerio zona pellucida glycoprotein 2 (zp2), mRNA [NM_131330]	6.761386414
wu:fk49e04	AGENCOURT_17388047 NIH_ZGC_4 Danio rerio cDNA clone IMAGE:7120001 5'	6.759928866
zgc:64125	Danio rerio zgc:64125 (zgc:64125), mRNA [NM_200380]	6.75980422
oazin	Danio rerio ornithine decarboxylase antizyme inhibitor (oazin), mRNA [NM_001007	6.755767313
CN326479	AGENCOURT_21848960 NIH_ZGC_8 Danio rerio cDNA clone IMAGE:7261479 5'	6.755646074
id6	Danio rerio inhibitor of DNA binding 6 (id6), mRNA [NM_131245]	6.751639611
itm2bl	Danio rerio integral membrane protein 2B, like (itm2bl), mRNA [NM_212976]	6.749882994
TC289098	Q8TB05 (Q8TB05) LOC124402, partial (48%) [TC289098]	6.747149944
ENSDART00(	Q7QTP3 (Q7QTP3) GLP_0_6355_7056, partial (37%) [TC293251]	6.745970063
ENSDART00(	AGENCOURT_16542615 NIH_ZGC_7 Danio rerio cDNA clone IMAGE:7037034 5'	6.743793851
zgc:56189	Danio rerio zgc:56189 (zgc:56189), mRNA [NM_199914]	6.743198269
15-Sep	Danio rerio selenoprotein, 15 kDa (sep15), mRNA [NM_178294]	6.74286413
zgc:92848	Danio rerio zgc:92848 (zgc:92848), mRNA [NM_001002495]	6.739319934
zgc:73107	Danio rerio zgc:73107 (zgc:73107), mRNA [NM_200714]	6.739237345
TC268327	Q90YN8 (Q90YN8) Vitellogenin 1, partial (20%) [TC268327]	6.737493197
BC061452	Danio rerio cDNA clone IMAGE:5603807, partial cds. [BC061452]	6.735594841
rdh1l	Danio rerio retinol dehydrogenase 1, like (rdh1l), mRNA [NM_199609]	6.733667796
ENSDART00(	Q9PW25 (Q9PW25) Pendulin, partial (17%) [TC275874]	6.733047583
BC067619	Danio rerio cDNA clone IMAGE:6960784, partial cds. [BC067619]	6.729489727
zgc:66068	Danio rerio zgc:66068 (zgc:66068), mRNA [NM_213093]	6.729143098
eif3s6	Danio rerio eukaryotic translation initiation factor 3, subunit 6 (eif3s6), mRNA [NM_	6.728187439
zgc:63495	Danio rerio zgc:63495 (zgc:63495), mRNA [NM_201133]	6.726519096
tuba8l	Danio rerio tubulin, alpha 8 like (tuba8l), mRNA [NM_212772]	6.725889851
smad5	Danio rerio MAD homolog 5 (Drosophila) (smad5), mRNA [NM_131368]	6.724855068
bcat2	Danio rerio branched chain aminotransferase 2, mitochondrial (bcat2), mRNA [NM_	6.711245709
zgc:73358	Danio rerio zgc:73358 (zgc:73358), mRNA [NM_213045]	6.709529731
TC294040	NTC1_BRARE (P46530) Neurogenic locus notch homolog protein 1 precursor, cor	6.709498127
si:busm1-266f	Danio rerio si:busm1-266f07.1 (si:busm1-266f07.1), mRNA [NM_001007167]	6.704703245
ENSDART00(	Q9PVU3 (Q9PVU3) Alpha-2-macroglobulin-3 (Fragment), partial (22%) [TC267933	6.702736073
BC071456	Danio rerio cDNA clone IMAGE:6900672, partial cds. [BC071456]	6.702502472
TC279473	H2B_SALTR (P02282) Histone H2B, partial (98%) [TC279473]	6.700160679
TC268325	Q8JH37 (Q8JH37) Vitellogenin 1 (Fragment), partial (14%) [TC268325]	6.699000973
zgc:100829	Danio rerio zgc:100829 (zgc:100829), mRNA [NM_001003543]	6.698337049
mcm7	Danio rerio MCM7 minichromosome maintenance deficient 7 (S. cerevisiae) (mcm7	6.698066695
edf1	Danio rerio endothelial differentiation-related factor 1 (edf1), mRNA [NM_200745]	6.697938579
zgc:92848	Danio rerio zgc:92848 (zgc:92848), mRNA [NM_001002495]	6.697895802
zgc:77263	Danio rerio zgc:77263 (zgc:77263), mRNA [NM_199820]	6.69521658
zp3b	Danio rerio zona pellucida glycoprotein 3 b (zp3b), mRNA [NM_131696]	6.695002222
dlst	Danio rerio dihydrolipoamide S-succinyltransferase (dlst), mRNA [NM_201487]	6.692249573
TC272246	BC028164 ACK1 protein {Homo sapiens;} , partial (51%) [TC272246]	6.687594135
zgc:63803	Danio rerio zgc:63803 (zgc:63803), mRNA [NM_213441]	6.687541464
ENSDART00(	Q6IN37 (Q6IN37) GM2 ganglioside activator protein, partial (79%) [TC269235]	6.686933458
sb:cb653	STR00646 oligo dT primed shield stage Danio rerio cDNA clone CB653 5', mRNA s	6.686866093
zgc:56141	Danio rerio zgc:56141 (zgc:56141), mRNA [NM_213004]	6.685883779
zgc:55683	Danio rerio zgc:55683 (zgc:55683), mRNA [NM_213435]	6.685749968
zgc:86902	Danio rerio zgc:86902 (zgc:86902), mRNA [NM_001002677]	6.683488883
zgc:66448	Danio rerio zgc:66448 (zgc:66448), mRNA [NM_199800]	6.683357358
rnpc2	Danio rerio RNA-binding region (RNP1, RRM) containing 2 (rnpc2), mRNA [NM_00	6.683017322
poldip2	Danio rerio polymerase (DNA-directed), delta interacting protein 2 (poldip2), mRNA	6.681322751
zgc:73358	Danio rerio zgc:73358 (zgc:73358), mRNA [NM_213045]	6.677012443
zgc:55809	Danio rerio zgc:55809, mRNA (cDNA clone MGC:55809 IMAGE:3817677), comple	6.676907037
TC290100	BC006598 proline-rich nuclear receptor coactivator 2 {Mus musculus;} , partial (36	6.67062339
TC293449	Q6PBF2 (Q6PBF2) Cell death-regulatory protein GRIM19, complete [TC293449]	6.668300319
zgc:64065	Danio rerio zgc:64065 (zgc:64065), mRNA [NM_201334]	6.667200132
zgc:103597	Danio rerio zgc:103597 (zgc:103597), mRNA [NM_001005976]	6.664999102
zgc:66488	Danio rerio zgc:66488 (zgc:66488), mRNA [NM_200431]	6.660347618
TC295809	Q7T1B0 (Q7T1B0) Embryonic globin beta e2, complete [TC295809]	6.659382736
zgc:55573	Danio rerio zgc:55573 (zgc:55573), mRNA [NM_213455]	6.658365112
zgc:55529	Danio rerio zgc:55529 (zgc:55529), mRNA [NM_200161]	6.658307793
zgc:56081	Danio rerio zgc:56081 (zgc:56081), mRNA [NM_200192]	6.657381057
CK361216	AGENCOURT_17114242 NIH_ZGC_4 Danio rerio cDNA clone IMAGE:7089227 5'	6.65728792
zgc:63631	Danio rerio zgc:63631 (zgc:63631), mRNA [NM_200468]	6.655768635

pa2g4a	Danio rerio proliferation-associated 2G4, a (pa2g4a), mRNA [NM_001002070]	6.655087068
TC279380	IR1902571 GLTSCR2, glioma tumor suppressor candidate region protein 2 (AF182	6.654754406
BC071456	Danio rerio cDNA clone IMAGE:6900672, partial cds. [BC071456]	6.654439188
zgc:55507	Danio rerio zgc:55507 (zgc:55507), mRNA [NM_199598]	6.653962681
tpd52l2	Danio rerio tumor protein D52-like 2 (tpd52l2), mRNA [NM_199582]	6.653926552
zgc:86686	Danio rerio zgc:86686 (zgc:86686), mRNA [NM_001002061]	6.653868109
hbbe2	Danio rerio hemoglobin beta embryonic-2 (hbbe2), mRNA [NM_212846]	6.652360748
AL916914	AL916914 PJR-Z1+Z2 Danio rerio cDNA clone 024-A11-2, mRNA sequence [AL91	6.645928013
zgc:56504	Danio rerio zgc:56504, mRNA (cDNA clone MGC:56504 IMAGE:5777534), comple	6.645833532
dap1a	Danio rerio death associated protein 1a (dap1a), mRNA [NM_131572]	6.645028056
stxbp3	Danio rerio syntaxin binding protein 3 (stxbp3), mRNA [NM_213471]	6.643294811
ssr1	Danio rerio signal sequence receptor, alpha (ssr1), mRNA [NM_201327]	6.642284033
si:ch211-14a1	Danio rerio si:ch211-14a17.7 (si:ch211-14a17.7), mRNA [NM_001007180]	6.64223803
TC282180	RT28_MOUSE (Q9CY16) Mitochondrial 28S ribosomal protein S28 (S28mt) (MRP-	6.641705079
ENSDART00(	AGENCOURT_21844715 NIH_ZGC_10 Danio rerio cDNA clone IMAGE:7260566 5	6.641375822
ddx39	Danio rerio DEAD (Asp-Glu-Ala-Asp) box polypeptide 39 (ddx39), mRNA [NM_212	6.640795797
pane1	proliferation associated nuclear element [Source:ZFIN;Acc:ZDB-GENE-040611-4] [	6.637651587
BC057521	Danio rerio cDNA clone IMAGE:5604666, partial cds. [BC057521]	6.631079681
ndufa4l	Danio rerio NADH dehydrogenase (ubiquinone) 1 alpha subcomplex 4, like (ndufa4	6.62936119
ENSDART00(	GIN4_YEAST (Q12263) Serine/threonine-protein kinase GIN4 , partial (9%) [TC29	6.629095458
zgc:85975	Danio rerio zgc:85975 (zgc:85975), mRNA [NM_213265]	6.628069043
zgc:86945	Danio rerio zgc:86945 (zgc:86945), mRNA [NM_001002335]	6.627300872
wu:fl24a12	AGENCOURT_20754282 NIH_ZGC_14 Danio rerio cDNA clone IMAGE:7229249 5	6.621306758
crabp1	Danio rerio cellular retinoic acid binding protein 1 (crabp1), mRNA [NM_182858]	6.620409581
TC268543	Q6TH32 (Q6TH32) Muscle cofilin 2, complete [TC268543]	6.620165438
TC269505	AF353634S2 bHLH transcription factor DEC1 {Homo sapiens;} , partial (46%) [TC2	6.62013572
zgc:56330	Danio rerio zgc:56330 (zgc:56330), mRNA [NM_199683]	6.618359002
zgc:77221	Danio rerio zgc:77221 (zgc:77221), mRNA [NM_205657]	6.617767664
arcn1l	Danio rerio archain 1 like (arcn1l), mRNA [NM_201993]	6.617729417
TC290365	BC055209 zgc:63694 {Danio rerio;} , partial (43%) [TC290365]	6.616582978
atp6v1f	Danio rerio ATPase, H+ transporting, lysosomal 14kDa, V1 subunit F (atp6v1f), mR	6.615866935
zgc:64130	Danio rerio zgc:64130 (zgc:64130), mRNA [NM_201209]	6.614681162
ENSDART00(	Q91480 (Q91480) Apolipoprotein B (Fragment), partial (31%) [TC279319]	6.614338624
mcm7	Danio rerio MCM7 minichromosome maintenance deficient 7 (S. cerevisiae) (mcm7	6.61319628
sod1	Danio rerio superoxide dismutase 1, soluble (sod1), mRNA [NM_131294]	6.613060898
zgc:55795	Danio rerio zgc:55795 (zgc:55795), mRNA [NM_199585]	6.607454695
zgc:65913	Danio rerio zgc:65913 (zgc:65913), mRNA [NM_212655]	6.607224551
mapk14b	Danio rerio mitogen-activated protein kinase 14b (mapk14b), mRNA [NM_178223]	6.606004279
rab5c	Danio rerio RAB5C, member RAS oncogene family, mRNA (cDNA clone MGC:772	6.603418224
zgc:92848	Danio rerio zgc:92848 (zgc:92848), mRNA [NM_001002495]	6.603136372
zgc:85671	Danio rerio zgc:85671 (zgc:85671), mRNA [NM_212811]	6.601800965
zgc:64103	Danio rerio zgc:64103 (zgc:64103), mRNA [NM_200639]	6.60029737
ENSDART00(	Unknown	6.599794391
zgc:101895	Danio rerio zgc:101895 (zgc:101895), mRNA [NM_001005958]	6.599750074
ENSDART00(	IF39_HUMAN (P55884) Eukaryotic translation initiation factor 3 subunit 9 (eIF-3 eta	6.599660987
uros	Danio rerio uroporphyrinogen III synthase (uros), mRNA [NM_212828]	6.599485255
BQ479659	faa71c12.y1 Gong zebrafish testis Danio rerio cDNA clone IMAGE:5899031 5', mR	6.596639076
zgc:56010	Danio rerio zgc:56010 (zgc:56010), mRNA [NM_201081]	6.595315986
pfn2l	Danio rerio profilin 2 like (pfn2l), mRNA [NM_201466]	6.591340169
ccnb1	Danio rerio cyclin B1 (ccnb1), mRNA [NM_131513]	6.590558566
ENSDART00(	Q6P7G4 (Q6P7G4) MGC68811 protein, partial (51%) [TC294705]	6.589379712
tegt	fb04h02.y1 zebrafish fin day1 regeneration Danio rerio cDNA 5', mRNA sequence [	6.588034058
zgc:86939	Danio rerio zgc:86939 (zgc:86939), mRNA [NM_205572]	6.587120116
TC268992	BC047800 zgc:55996 {Danio rerio;} , complete [TC268992]	6.586385816
zgc:56274	Danio rerio zgc:56274 (zgc:56274), mRNA [NM_200019]	6.584544701
zgc:56010	Danio rerio zgc:56010 (zgc:56010), mRNA [NM_201081]	6.584535321
TC269025	Q6NYM6 (Q6NYM6) Zgc:77481, complete [TC269025]	6.582101413
TC280762	DRR1_HUMAN (O95990) DRR1 protein (Down regulated in renal cell carcinoma 1)	6.580613692
ENSDART00(	IDLC_STRPU (Q26630) 33 kDa inner dynein arm light chain, axonemal (p33), parti	6.578897641
BQ262361	fz85c11.x1 Sugano SJD adult male Danio rerio cDNA clone IMAGE:5915156 3', mI	6.577175312
TC268461	BC053272 zgc:64133 {Danio rerio;} , complete [TC268461]	6.57705174
hig1	Danio rerio hypoxia induced gene 1 (hig1), mRNA [NM_200100]	6.575914054
ns:zf-e239	ZF-E239 zebrafish embryonic Danio rerio cDNA clone ZF-E239 5', mRNA sequenc	6.574852096
TC267994	TPP1_MOUSE (O89023) Tripeptidyl-peptidase I precursor (TPP-I) (Tripeptidyl ami	6.574293684
zgc:77279	Danio rerio zgc:77279 (zgc:77279), mRNA [NM_207072]	6.574242662
dldh	Danio rerio dihydrolipoamide dehydrogenase (dldh), mRNA [NM_201506]	6.573232319
LOC402883	Danio rerio hypothetical protein LOC402883, mRNA (cDNA clone IMAGE:4788333	6.573082859
AI964259	EST269373 zebrafish T0315, Steve Ekker Danio rerio cDNA clone RZBDA55, mR	6.573048288
TC279701	Q7SZ52 (Q7SZ52) FXYD domain containing ion transport regulator 6, partial (35%)	6.572939231
zgc:92762	Danio rerio zgc:92762 (zgc:92762), mRNA [NM_001002561]	6.572370816
zgc:55307	Danio rerio zgc:55307 (zgc:55307), mRNA [NM_201129]	6.572051607
TC279409	Q7T2D1 (Q7T2D1) Retinol dehydrogenase 10, complete [TC279409]	6.57202539
zgc:85645	Danio rerio zgc:85645 (zgc:85645), mRNA [NM_213312]	6.571717442
LOC402883	Danio rerio hypothetical protein LOC402883, mRNA (cDNA clone IMAGE:4788333	6.571688705
tpd52l2	Danio rerio tumor protein D52-like 2 (tpd52l2), mRNA [NM_199582]	6.571531031
vg1	Danio rerio vitellogenin 1 (vg1), mRNA [NM_170767]	6.571201157
zgc:101797	Danio rerio zgc:101797 (zgc:101797), mRNA [NM_001007397]	6.571119426
pgam1	Danio rerio phosphoglycerate mutase 1 (pgam1), mRNA [NM_198804]	6.571114019
BC076035	Danio rerio cDNA clone IMAGE:7046318, partial cds. [BC076035]	6.570863087
BI842184	fq82h05.x1 Zebrafish neuronal Danio rerio cDNA clone IMAGE:4887008 3', mRNA	6.566885247
BC076359	Danio rerio cDNA clone IMAGE:7119330, partial cds. [BC076359]	6.56658253

tuba4l	Danio rerio tubulin, alpha 4 like (tuba4l), mRNA [NM_199795]	6.566477927
zgc:86923	Danio rerio zgc:86923 (zgc:86923), mRNA [NM_001002091]	6.565874874
fabp7a	Danio rerio fatty acid binding protein 7, brain, a (fabp7a), mRNA [NM_131605]	6.560834101
zgc:101887	Danio rerio zgc:101887 (zgc:101887), mRNA [NM_001005960]	6.55937455
IRF1	Danio rerio interferon regulatory factor 1 (IRF1), mRNA [NM_205747]	6.557864975
zgc:55461	Danio rerio zgc:55461 (zgc:55461), mRNA [NM_213490]	6.556870629
pkm2	Danio rerio pyruvate kinase, muscle (pkm2), mRNA [NM_199333]	6.556304445
si:rp71-1f1.7	Danio rerio si:rp71-1f1.7 (si:rp71-1f1.7), mRNA [NM_001004624]	6.55450239
nsep1	Danio rerio nuclease sensitive element binding protein 1 (nsep1), mRNA [NM_1316	6.553869392
bzw1l	Danio rerio basic leucine zipper and W2 domains 1, like (bzw1l), mRNA [NM_2130	6.550707043
zgc:55461	Danio rerio zgc:55461 (zgc:55461), mRNA [NM_213490]	6.550363431
TC268139	O93584 (O93584) ZfY1, partial (49%) [TC268139]	6.549986925
ppan	Danio rerio peter pan homolog (Drosophila) (ppan), mRNA [NM_201463]	6.549950011
zgc:92795	Danio rerio zgc:92795 (zgc:92795), mRNA [NM_001002539]	6.549941557
g12l	Danio rerio MID1 interacting protein 1 (mid1ip1), mRNA [NM_213439]	6.54920951
arl2bp	Danio rerio ADP-ribosylation factor-like 2 binding protein (arl2bp), mRNA [NM_201	6.545173923
zgc:56517	Danio rerio zgc:56517 (zgc:56517), mRNA [NM_200278]	6.541632942
zgc:63948	Danio rerio zgc:63948 (zgc:63948), mRNA [NM_213347]	6.541060119
zgc:92053	Danio rerio troponin mRNA, complete cds. [AF539738]	6.5409473
zgc:64115	Danio rerio zgc:64115 (zgc:64115), mRNA [NM_213136]	6.5406549
anp32b	EST269374 zebrafish T0315, Steve Ekker Danio rerio cDNA clone RZBDA58, mRN	6.539023928
TC290034	Q9PTT9 (Q9PTT9) Homeobox protein, partial (39%) [TC290034]	6.533703067
TC288191	TCE3_HUMAN (O75764) Transcription elongation factor A protein 3 (Transcription	6.532841812
arpc4	Danio rerio actin related protein 2/3 complex, subunit 4 (arpc4), mRNA [NM_20553	6.532816238
tfg	Danio rerio TRK-fused gene (tfg), mRNA [NM_200015]	6.530851861
TC283498	Q86XW2 (Q86XW2) KRTCAP2 protein (Fragment), partial (82%) [TC283498]	6.530292654
snrpd1	Danio rerio small nuclear ribonucleoprotein D1 polypeptide (snrpd1), mRNA [NM_1	6.52861538
zgc:92576	Danio rerio zgc:92576 (zgc:92576), mRNA [NM_001002729]	6.52338397
seph	Danio rerio selenoprotein H, mRNA (cDNA clone MGC:55775 IMAGE:3817133), cc	6.522989946
zgc:56336	Danio rerio zgc:56336 (zgc:56336), mRNA [NM_213369]	6.522233932
TC291689	O57332 (O57332) Proteasome subunit Y, complete [TC291689]	6.520060837
rpl13a	Danio rerio ribosomal protein L13a (rpl13a), mRNA [NM_212784]	6.519299487
yy1l	Danio rerio YY1 transcription factor, like (yy1l), mRNA [NM_213120]	6.518270014
zgc:64118	Danio rerio zgc:64118 (zgc:64118), mRNA [NM_200070]	6.51661297
zgc:55795	Danio rerio zgc:55795 (zgc:55795), mRNA [NM_199585]	6.51639537
capzb	Danio rerio capping protein (actin filament) muscle Z-line, beta (capzb), mRNA [NM	6.51580787
TC288450	Q15407 (Q15407) RTSbeta, partial (30%) [TC288450]	6.515311873
TC273750	Q9CVC5 (Q9CVC5) Mus musculus adult male stomach cDNA, RIKEN full-length en	6.515203046
wu:fl24a12	AGENCOURT_20754282 NIH_ZGC_14 Danio rerio cDNA clone IMAGE:7229249 5	6.513933287
zgc:91896	Danio rerio zgc:91896 (zgc:91896), mRNA [NM_001003460]	6.513016572
rdh10	Danio rerio retinol dehydrogenase 10 (rdh10), mRNA [NM_201331]	6.512915291
zgc:56211	Danio rerio zgc:56211 (zgc:56211), mRNA [NM_212990]	6.511929038
zgc:92246	Danio rerio zgc:92246 (zgc:92246), mRNA [NM_001002625]	6.511824162
atp6v1e1	Danio rerio ATPase, H+ transporting, lysosomal, V1 subunit E isoform 1 (atp6v1e1)	6.511564071
ENSDART00(	Q8UW23 (Q8UW23) GCN5-like protein, partial (98%) [TC296494]	6.51086512
fbxw1b	Danio rerio F-box and WD-40 domain protein 11 (fbxw11), mRNA [NM_201310]	6.510758389
si:ch211-14a1	Danio rerio si:ch211-14a17.7 (si:ch211-14a17.7), mRNA [NM_001007180]	6.510259987
zgc:77853	Danio rerio zgc:77853 (zgc:77853), mRNA [NM_205688]	6.509142649
wu:fb38g09	Danio rerio wu:fb38g09 (wu:fb38g09), mRNA [NM_214682]	6.509116704
zgc:56517	Danio rerio zgc:56517 (zgc:56517), mRNA [NM_200278]	6.508720388
plxnd1	Danio rerio plexin D1 (plxnd1), mRNA [NM_205697]	6.506316897
zgc:56202	Danio rerio zgc:56202 (zgc:56202), mRNA [NM_212993]	6.505321411
eva1	Danio rerio epithelial V-like antigen 1 (eva1), mRNA [NM_212763]	6.504683635
CK363440	AGENCOURT_17170766 NIH_ZGC_4 Danio rerio cDNA clone IMAGE:7086541 5'	6.503602798
zgc:91831	Danio rerio zgc:91831 (zgc:91831), mRNA [NM_001002203]	6.502474708
wu:fk86d05	Danio rerio wu:fk86d05 (wu:fk86d05), mRNA [NM_001003843]	6.502304013
zgc:92840	Danio rerio zgc:92840 (zgc:92840), mRNA [NM_001002499]	6.502009289
arrb2	Danio rerio arrestin, beta 2 (arrb2), mRNA [NM_201124]	6.501520922
xbp1	Danio rerio X-box binding protein 1 (xbp1), mRNA [NM_131874]	6.500556241
wu:fb06h05	AGENCOURT_17391282 NIH_ZGC_4 Danio rerio cDNA clone IMAGE:7120780 5'	6.497489344
ENSDART00(	Unknown	6.496843411
zgc:73376	Danio rerio zgc:73376 (zgc:73376), mRNA [NM_200809]	6.496011659
wu:fi35e03	AGENCOURT_21835355 NIH_ZGC_10 Danio rerio cDNA clone IMAGE:7257497 5	6.494865617
provisionalck7	EA0189 Danio rerio one-day regenerating caudal fin subtracted cDNA Danio rerio c	6.494345192
CN508670	AGENCOURT_22402475 NIH_ZGC_9 Danio rerio cDNA clone IMAGE:7274378 5'	6.494165828
TC290860	Q7ZUQ9 (Q7ZUQ9) Cold inducible RNA binding protein, complete [TC290860]	6.493469831
zgc:101013	Danio rerio zgc:101013 (zgc:101013), mRNA [NM_001003598]	6.492760339
IRF1	Danio rerio interferon regulatory factor 1 (IRF1), mRNA [NM_205747]	6.491904065
CO355671	DR_ATE_NRM11_C12 adult testis normalized (TLL) Danio rerio cDNA, mRNA seq	6.490451616
zgc:76975	Danio rerio zgc:76975 (zgc:76975), mRNA [NM_214713]	6.489583649
TC279995	Unknown	6.489330575
fgfr1	Danio rerio fibroblast growth factor receptor 1 (fgfr1), mRNA [NM_152962]	6.488483436
dct	Danio rerio dopachrome tautomerase (dct), mRNA [NM_131555]	6.488154814
BG307343	fm03a06.y1 Zebrafish adult retina cDNA Danio rerio cDNA clone IMAGE:4145170 5	6.486994407
TC274435	Q7ZYN5 (Q7ZYN5) LOC398528 protein (Fragment), partial (25%) [TC274435]	6.486972964
CO918378	AGENCOURT_30538312 NIH_ZGC_15 Danio rerio cDNA clone IMAGE:7431891 5	6.48644909
try	Danio rerio trypsin (try), mRNA [NM_131708]	6.484644377
strap	Danio rerio serine/threonine kinase receptor associated protein (strap), mRNA [NM	6.483856043
ripk5	Danio rerio receptor interacting protein kinase 5 (ripk5), mRNA [NM_205627]	6.483665336
si:ch211-191d	Danio rerio si:ch211-191d15.2 (si:ch211-191d15.2), mRNA [NM_001003632]	6.483007242
wu:fb33c08	fb33c08.y1 Zebrafish WashU MPIMG EST Danio rerio cDNA clone IMAGE:371367	6.480978919

xbp1	Danio rerio X-box binding protein 1 (xbp1), mRNA [NM_131874]	6.479801431
wu:fl24a12	AGENCOURT_20754282 NIH_ZGC_14 Danio rerio cDNA clone IMAGE:7229249 5	6.479726613
zgc:55962	Danio rerio zgc:55962 (zgc:55962), mRNA [NM_199579]	6.47948053
TC279378	Unknown	6.478196167
TC268283	Q90YN8 (Q90YN8) Vitellogenin 1, partial (25%) [TC268283]	6.477932559
apoeb	Danio rerio apolipoprotein Eb (apoeb), mRNA [NM_131098]	6.476424079
eva1	epithelial V-like antigen 1 [Source:ZFIN;Acc:ZDB-GENE-030131-8774] [ENSDART	6.476031781
wu:fk66c03	fk66c03.y1 Zebrafish Research Genetics C32 fin Danio rerio cDNA 5', mRNA sequ	6.47451819
zgc:77891	Danio rerio zgc:77891 (zgc:77891), mRNA [NM_205693]	6.474266462
ENSDART00(	R18A_HUMAN (Q9NVS2) 28S ribosomal protein S18a, mitochondrial precursor (M	6.471989708
zgc:92784	Danio rerio zgc:92784 (zgc:92784), mRNA [NM_001002548]	6.467128634
bcl2l	Danio rerio bcl2-like (bcl2l), mRNA [NM_131807]	6.466683769
zgc:55842	Danio rerio zgc:55842 (zgc:55842), mRNA [NM_200988]	6.466338806
CO960157	AGENCOURT_30802604 NIH_ZGC_19 Danio rerio cDNA clone IMAGE:7427007 5	6.464296779
zgc:86940	Danio rerio zgc:86940 (zgc:86940), mRNA [NM_001002082]	6.463261471
ppp2r5e1	Danio rerio protein phosphatase 2, regulatory subunit B (B56) (ppp2r5e1), mRNA [I	6.462699005
rpn1	Danio rerio ribophorin I (rpn1), mRNA [NM_197934]	6.462088374
zgc:56451	Danio rerio zgc:56451 (zgc:56451), mRNA [NM_213110]	6.461992539
gng5	AGENCOURT_16540949 NIH_ZGC_10 Danio rerio cDNA clone IMAGE:7042809 5	6.461219417
TC279629	BC054585 zgc:63980 {Danio rerio;} , complete [TC279629]	6.460542366
hig1	Danio rerio hypoxia induced gene 1 (hig1), mRNA [NM_200100]	6.457860344
zgc:92707	Danio rerio zgc:92707 (zgc:92707), mRNA [NM_001002398]	6.454831078
adh8a	Danio rerio alcohol dehydrogenase 8a (adh8a), mRNA [NM_001001946]	6.454369636
zgc:63709	Danio rerio zgc:63709 (zgc:63709), mRNA [NM_199750]	6.45306758
zgc:103512	Danio rerio zgc:103512 (zgc:103512), mRNA [NM_001006016]	6.452800578
tpi1b	Danio rerio triosephosphate isomerase 1b (tpi1b), mRNA [NM_153668]	6.45251914
tlx3a	Danio rerio T-cell leukemia, homeobox 3a (tlx3a), mRNA [NM_153651]	6.452109208
anxa1a	Danio rerio annexin A1a (anxa1a), mRNA [NM_181758]	6.45176904
kars	Danio rerio lysyl-tRNA synthetase (kars), mRNA [NM_001002386]	6.45017774
BQ259133	fz95g05.y1 zebrafish fin day1 regeneration Danio rerio cDNA clone IMAGE:590840	6.450162845
g12l	Danio rerio MID1 interacting protein 1 (mid1ip1), mRNA [NM_213439]	6.450133444
BQ093890	fz53a02.y1 zebrafish fin day1 regeneration Danio rerio cDNA clone IMAGE:590659	6.448846367
TC267911	Q9DFT6 (Q9DFT6) Beta tubulin, complete [TC267911]	6.448618763
ncl	Danio rerio nucleolin (ncl), mRNA [NM_001003839]	6.445865145
TC270569	S68134 cyclic AMP-responsive element modulator beta isoform {Homo sapiens;} ,	6.445836719
TC269191	ADR2_MOUSE (Q8BQS5) Adiponectin receptor protein 2, partial (38%) [TC269191	6.44486123
zgc:77650	Danio rerio zgc:77650 (zgc:77650), mRNA [NM_199876]	6.443062783
wu:fb12g11	fc43b09.y1 Zebrafish WashU MPIMG EST Danio rerio cDNA clone IMAGE:372412	6.442102007
zgc:100853	Danio rerio 6-phosphogluconolactonase (pgls), mRNA [NM_001004117]	6.441827523
TC268167	CR457185 LSM3 {Homo sapiens;} , complete [TC268167]	6.441503573
zgc:92665	Danio rerio zgc:92665 (zgc:92665), mRNA [NM_001002421]	6.438847511
smyd1	Danio rerio SET and MYND domain containing 1 (smyd1), mRNA [NM_205540]	6.438011168
mapk14a	Danio rerio mitogen-activated protein kinase 14a (mapk14a), mRNA [NM_131722]	6.437989885
zgc:77882	Danio rerio zgc:77882 (zgc:77882), mRNA [NM_199649]	6.437613448
psmd12	Danio rerio proteasome (prosome, macropain) 26S subunit, non-ATPase, 12 (psmc	6.437447515
zgc:63907	Danio rerio zgc:63907 (zgc:63907), mRNA [NM_201137]	6.437338335
zgc:56034	Danio rerio zgc:56034 (zgc:56034), mRNA [NM_199956]	6.436243184
ap1s1	Danio rerio adaptor-related protein complex 1, sigma 1 subunit (ap1s1), mRNA [NM	6.435924813
pgam1	Danio rerio phosphoglycerate mutase 1 (pgam1), mRNA [NM_198804]	6.435058417
tram	Danio rerio translocating chain-associating membrane protein (tram), mRNA [NM_1	6.433608901
rpn1	Danio rerio ribophorin I (rpn1), mRNA [NM_197934]	6.433082381
zgc:86762	Danio rerio zgc:86762 (zgc:86762), mRNA [NM_001002131]	6.433074811
zgc:92329	Danio rerio zgc:92329 (zgc:92329), mRNA [NM_001007313]	6.432684041
TC290166	Q804H0 (Q804H0) Annexin 1c, partial (74%) [TC290166]	6.432314217
jup	Danio rerio junction plakoglobin (jup), mRNA [NM_131177]	6.430903553
g10	Danio rerio maternal G10 transcript (g10), mRNA [NM_001003860]	6.430411825
hsp90b	Danio rerio heat shock protein 90-beta (hsp90b), mRNA [NM_131310]	6.429628937
calm1b	Danio rerio calmodulin 1b (calm1b), mRNA [NM_200082]	6.428523045
slc31a1	Danio rerio solute carrier family 31 (copper transporters), member 1 (slc31a1), mR	6.428017501
CO354952	DR_ATE_NRM02_G08 adult testis normalized (TLL) Danio rerio cDNA, mRNA seq	6.427293445
rab5a	Danio rerio RAB5A, member RAS oncogene family (rab5a), mRNA [NM_201485]	6.427257866
ENSDART00(	AGENCOURT_22438073 NIH_ZGC_7 Danio rerio cDNA clone IMAGE:7267128 5'	6.426763575
sas	Danio rerio sarcoma amplified sequence (sas), mRNA [NM_200281]	6.424985206
AL922014	AL922014 PJR-Z1+Z2 Danio rerio cDNA clone 104-F02-2, mRNA sequence [AL92	6.421165966
ap1s1	Danio rerio adaptor-related protein complex 1, sigma 1 subunit (ap1s1), mRNA [NM	6.4202927
TC268487	BC055209 zgc:63694 {Danio rerio;} , partial (25%) [TC268487]	6.419332705
zgc:65772	Danio rerio zgc:65772 (zgc:65772), mRNA [NM_200533]	6.419208671
TC278192	PIM1_BOVIN (Q9N0P9) Proto-oncogene serine/threonine-protein kinase pim-1 , p	6.418871227
gnl2	Danio rerio guanine nucleotide binding protein-like 2 (nucleolar) (gnl2), mRNA [NM_	6.418382539
stxbp3	Danio rerio syntaxin binding protein 3 (stxbp3), mRNA [NM_213471]	6.417899866
npm1	Danio rerio nucleophosmin 1 (npm1), mRNA [NM_199428]	6.417670261
zgc:92282	Danio rerio zgc:92282 (zgc:92282), mRNA [NM_001002609]	6.417569753
tmem32	Danio rerio transmembrane protein 32 (tmem32), mRNA [NM_205599]	6.413329336
TC292096	Q7ZXY7 (Q7ZXY7) Flj20436-prov protein, partial (72%) [TC292096]	6.412388206
TC290362	BC055209 zgc:63694 {Danio rerio;} , partial (43%) [TC290362]	6.412331404
fgfr2	Danio rerio fibroblast growth factor receptor 2 (fgfr2), mRNA [NM_178303]	6.41214383
ENSDART00(	BC004499 MOV10 protein {Homo sapiens;} , partial (37%) [TC271246]	6.411465458
zgc:66175	Danio rerio zgc:66175 (zgc:66175), mRNA [NM_213383]	6.411309065
ddx39	Danio rerio DEAD (Asp-Glu-Ala-Asp) box polypeptide 39 (ddx39), mRNA [NM_212	6.409671768
si:busm1-266f	Danio rerio si:busm1-266f07.2 (si:busm1-266f07.2), mRNA [NM_001004521]	6.409613322
cct8	Danio rerio chaperonin containing TCP1, subunit 8 (theta) (cct8), mRNA [NM_2010	6.409008021

serpina1	Danio rerio serine (or cysteine) proteinase inhibitor, clade A (alpha-1 antiproteinase	6.407173711
AW018556	fd48d09.y1 Zebrafish WashU MPIMG EST Danio rerio cDNA clone IMAGE:373297	6.406927052
c4orf9	Danio rerio chromosome 4 open reading frame 9 (H. sapiens) (c4orf9), mRNA [NM_	6.406699129
TC279845	Q6NYN6 (Q6NYN6) Wu:fc22d10 protein, complete [TC279845]	6.405485394
TC271399	BC069228 phosphatidylinositol glycan class S {Homo sapiens;} , partial (57%) [TC2	6.403990774
snd1	Danio rerio staphylococcal nuclease domain containing 1 (snd1), mRNA [NM_1828	6.403205134
clic4	Danio rerio chloride intracellular channel 4 (clic4), mRNA [NM_201486]	6.402999614
zgc:63624	Danio rerio zgc:63624 (zgc:63624), mRNA [NM_200611]	6.402439434
zgc:56134	Danio rerio zgc:56134 (zgc:56134), mRNA [NM_200014]	6.402197037
ENSDART00(	AGENCOURT_21835355 NIH_ZGC_10 Danio rerio cDNA clone IMAGE:7257497 5	6.400974364
zgc:92534	Danio rerio zgc:92534 (zgc:92534), mRNA [NM_001003444]	6.400202458
zff9	Danio rerio zinc finger protein 9 (zff9), mRNA [NM_199749]	6.39969946
ube2i	Danio rerio ubiquitin-conjugating enzyme E2I (ube2i), mRNA [NM_131351]	6.398852935
LOC402840	Danio rerio hypothetical protein LOC402840, mRNA (cDNA clone IMAGE:5605364	6.397886607
zgc:66077	Danio rerio zgc:66077 (zgc:66077), mRNA [NM_200579]	6.395460025
wu:fk84g05	AGENCOURT_20186052 NIH_ZGC_15 Danio rerio cDNA clone IMAGE:7226726 5	6.395419162
CK864691	AGENCOURT_19725966 NIH_ZGC_6 Danio rerio cDNA clone IMAGE:7219299 5'	6.394716305
zgc:64040	Danio rerio zgc:64040 (zgc:64040), mRNA [NM_200369]	6.3946739
CO354299	DR_ATE_FL25_E12 adult testis full-length (TLL) Danio rerio cDNA, mRNA sequen	6.394498617
pim1	Danio rerio pim-1 oncogene (pim1), mRNA [NM_131539]	6.394466629
zgc:55525	Danio rerio zgc:55525 (zgc:55525), mRNA [NM_213468]	6.394199823
tnnt3b	Danio rerio troponin T3b, skeletal, fast (tnnt3b), mRNA [NM_181653]	6.393620794
2-Sep	Danio rerio cDNA clone IMAGE:6996377, partial cds. [BC065465]	6.392836186
zgc:63796	Danio rerio zgc:63796 (zgc:63796), mRNA [NM_199922]	6.390695318
BM572257	fx08g03.y1 Gong zebrafish ovary Danio rerio cDNA clone IMAGE:5619269 5', mRN	6.390551604
TC283776	BC000219 MRPS5 protein {Homo sapiens;} , partial (42%) [TC283776]	6.389035094
zgc:66388	Danio rerio zgc:66388 (zgc:66388), mRNA [NM_201141]	6.388532118
hsp90b	Danio rerio heat shock protein 90-beta (hsp90b), mRNA [NM_131310]	6.388381063
zgc:92169	Danio rerio zgc:92169 (zgc:92169), mRNA [NM_001004553]	6.387991453
pafah1b3	Danio rerio platelet-activating factor acetylhydrolase, isoform Ib, gamma subunit (p	6.387681519
AJ245492	Danio rerio mRNA for hypothetical protein, clone sd50. [AJ245492]	6.386935135
zgc:92511	Danio rerio zgc:92511 (zgc:92511), mRNA [NM_001003450]	6.386932348
zgc:91894	Danio rerio zgc:91894 (zgc:91894), mRNA [NM_001004116]	6.386860733
rpl5	Danio rerio ribosomal protein L5 (rpl5), mRNA [NM_001002106]	6.386009398
TC293027	AKA1_HUMAN (P14550) Alcohol dehydrogenase [NADP+] (Aldehyde reductase) (	6.385183592
A_15_P11940	Unknown	6.384876211
slc6a9	Danio rerio GLYT1 mRNA for glycine transporter 1, partial cds. [AB183388]	6.384009707
AW777390	fk44b01.x1 Zebrafish 15-19hr embryonic cDNA Danio rerio cDNA 3', mRNA sequer	6.383053512
cdc42	Danio rerio cell division cycle 42 (cdc42), mRNA [NM_200632]	6.382154263
ENSDART00(	AY221262 selenoprotein N {Danio rerio;} , complete [TC270039]	6.381875342
zgc:86800	EST269390 zebrafish T0315, Steve Ekker Danio rerio cDNA clone RZBDA82 simil	6.381147143
fkbp4	Danio rerio FK506 binding protein 4 (fkbp4), mRNA [NM_201469]	6.380882103
sb:cb551	Danio rerio sb:cb551, mRNA (cDNA clone IMAGE:2601514), partial cds. [BC04456	6.380161204
zgc:92765	Danio rerio zgc:92765 (zgc:92765), mRNA [NM_001002559]	6.379882936
TC279489	Q6IA63 (Q6IA63) C6orf62 protein, complete [TC279489]	6.379287635
ENSDART00(	AF498951 small GTP binding protein RAB23 {Homo sapiens;} , partial (81%) [TC2	6.378606179
zgc:73376	Danio rerio zgc:73376 (zgc:73376), mRNA [NM_200809]	6.37841611
ctsla	Danio rerio cathepsin L, a (ctsla), mRNA [NM_212584]	6.378371097
BQ074893	fz23h04.y1 Gong zebrafish testis Danio rerio cDNA 5', mRNA sequence [BQ07489	6.377866491
zgc:65794	Danio rerio zgc:65794 (zgc:65794), mRNA [NM_213349]	6.37713839
copz2	Danio rerio zeta2-cop (copz2), mRNA [NM_131507]	6.374270993
nsep1	Danio rerio nuclease sensitive element binding protein 1 (nsep1), mRNA [NM_1316	6.371742709
ENSDART00(	MMU92704 Olf-1/EBF-like-2(OS) transcription factor {Mus musculus;} , partial (51%	6.37139374
zgc:63926	Danio rerio zgc:63926 (zgc:63926), mRNA [NM_213351]	6.370904532
cpne3	Danio rerio copine III (cpne3), mRNA [NM_199699]	6.370589871
egr2b	Danio rerio early growth response 2b (egr2b), mRNA [NM_130997]	6.370390887
zgc:92022	Danio rerio zgc:92022 (zgc:92022), mRNA [NM_001002305]	6.369809334
zgc:92237	Danio rerio zgc:92237 (zgc:92237), mRNA [NM_001003728]	6.369771617
TC287937	Q9W3T5 (Q9W3T5) CG32736-PA (Cg32736-pb) (RE60462p), partial (35%) [TC28	6.368823875
TC270311	Q8CFK3 (Q8CFK3) Paraoxonase 2, partial (66%) [TC270311]	6.368791244
TC281853	FGL2_HUMAN (Q14314) Fibroleukin precursor (Fibrinogen-like protein 2) (pT49), p	6.366725049
glo1	Danio rerio glyoxalase 1 (glo1), mRNA [NM_213151]	6.366346463
TC291664	Q8QFS3 (Q8QFS3) H01CJC protein, partial (81%) [TC291664]	6.365842401
TC290492	MUSIGHV01B Ig heavy chain precursor {Mus musculus;} , partial (34%) [TC29049	6.365808906
zgc:63910	Danio rerio zgc:63910 (zgc:63910), mRNA [NM_200686]	6.365473319
calm1b	Danio rerio calmodulin 1b (calm1b), mRNA [NM_200082]	6.365316899
zgc:56335	Danio rerio zgc:56335 (zgc:56335), mRNA [NM_201188]	6.364777128
zgc:77650	Danio rerio zgc:77650 (zgc:77650), mRNA [NM_199876]	6.362558792
TC291456	Q70Q12 (Q70Q12) Phospholemman-like protein precursor, partial (43%) [TC29145	6.362306644
TC296590	IF2M_BOVIN (P46198) Translation initiation factor IF-2, mitochondrial precursor (IF	6.361667819
BC071437	Danio rerio cDNA clone IMAGE:6899804, partial cds. [BC071437]	6.361268819
zgc:73206	Danio rerio zgc:73206 (zgc:73206), mRNA [NM_200748]	6.359914746
gabarap	Danio rerio GABA(A) receptor-associated protein, mRNA (cDNA clone IMAGE:679	6.358074498
atp6v1c1	Danio rerio ATPase, H+ transporting, lysosomal, V1 subunit C, isoform 1 (atp6v1c1	6.357815729
u2af1	Danio rerio U2(RNU2) small nuclear RNA auxiliary factor 1 (u2af1), mRNA [NM_17	6.356039316
mfng	Danio rerio manic fringe homolog (mfng), mRNA [NM_001007788]	6.355841405
TC293078	E2BG_RAT (P70541) Translation initiation factor eIF-2B gamma subunit (eIF-2B G	6.355306577
ENSDART00(	zfshTOP10000080 Zebrafish shield stage whole embryo Danio rerio cDNA clone S	6.354011808
BC074029	Danio rerio cDNA clone IMAGE:7001722, partial cds. [BC074029]	6.353588638
psmb10	Danio rerio proteasome subunit beta 12 (PSMB12) mRNA, partial cds. [AF155577]	6.352716686
zgc:56708	Danio rerio zgc:56708 (zgc:56708), mRNA [NM_200310]	6.352612833

TC294394	Q803X5 (Q803X5) AMP deaminase 3, complete [TC294394]	6.352055559
AI584617	fb81c08.y1 Zebrafish WashU MPIMG EST Danio rerio cDNA clone IMAGE:371828	6.351624199
was	Danio rerio Wiskott-Aldrich syndrome (eczema-thrombocytopenia) (was), mRNA [N	6.351438699
arl2l1	Danio rerio ADP-ribosylation factor-like 2-like 1 (arl2l1), mRNA [NM_173272]	6.35136373
TC291819	Q9QX82 (Q9QX82) Endolyn precursor, partial (26%) [TC291819]	6.350373147
zgc:56296	Danio rerio zgc:56296 (zgc:56296), mRNA [NM_213376]	6.350064344
ENSDART00(	Q7T0Q2 (Q7T0Q2) MGC69100 protein, partial (85%) [TC290370]	6.348727698
ENSDART00(	fab03g11.y1 Sugano SJD adult male Danio rerio cDNA clone IMAGE:6034388 5' si	6.348573608
tram	Danio rerio translocating chain-associating membrane protein (tram), mRNA [NM_1	6.34843049
zgc:92593	Danio rerio zgc:92593 (zgc:92593), mRNA [NM_001005929]	6.347719544
BM316101	fw69d04.x1 Gong zebrafish testis Danio rerio cDNA clone IMAGE:5615647 3', mR	6.346794522
TC291230	FRIM_SALSA (P49947) Ferritin, middle subunit (Ferritin M), partial (97%) [TC2912	6.346486483
TC279559	BI1_PAROL (Q9IA79) Probable Bax inhibitor-1 (BI-1), partial (70%) [TC279559]	6.345666108
gtpbp4	Danio rerio GTP binding protein 4 (gtpbp4), mRNA [NM_199851]	6.344955278
TC269175	Q7T2C2 (Q7T2C2) Wu:fb52d04 protein, complete [TC269175]	6.344945879
TC292799	BC066453 zgc:77417 protein {Danio rerio;} , complete [TC292799]	6.344648857
zgc:63986	Danio rerio zgc:63986 (zgc:63986), mRNA [NM_213332]	6.34387798
zgc:103594	Danio rerio zgc:103594 (zgc:103594), mRNA [NM_001004680]	6.342204456
TC269846	Q6P0G5 (Q6P0G5) Tfg protein, complete [TC269846]	6.340269207
slc31a1	Danio rerio solute carrier family 31 (copper transporters), member 1 (slc31a1), mR	6.340193202
zgc:77806	Danio rerio zgc:77806 (zgc:77806), mRNA [NM_205691]	6.339511172
zgc:73396	Danio rerio zgc:73396 (zgc:73396), mRNA [NM_200817]	6.336669979
tmed5	Danio rerio transmembrane emp24 protein transport domain containing 5 (tmed5),	6.335725662
rplp0	Danio rerio ribosomal protein, large, P0, mRNA (cDNA clone MGC:77791 IMAGE:7	6.335669724
zgc:92775	Danio rerio zgc:92775 (zgc:92775), mRNA [NM_001003424]	6.333505301
zgc:92282	Danio rerio zgc:92282 (zgc:92282), mRNA [NM_001002609]	6.332237202
cat	Danio rerio catalase (cat), mRNA [NM_130912]	6.332147132
rps3a	Danio rerio ribosomal protein S3A (rps3a), mRNA [NM_200059]	6.331882824
zgc:66058	Danio rerio zgc:66058 (zgc:66058), mRNA [NM_213137]	6.331183532
zgc:55813	Danio rerio zgc:55813 (zgc:55813), mRNA [NM_201514]	6.330448985
TC269084	CLH1_HUMAN (Q00610) Clathrin heavy chain 1 (CLH-17), complete [TC269084]	6.330012817
zgc:92893	Danio rerio zgc:92893 (zgc:92893), mRNA [NM_001002467]	6.329933872
CN510123	AGENCOURT_22403482 NIH_ZGC_9 Danio rerio cDNA clone IMAGE:7273369 5'	6.329249144
ENSDART00(	Q98TC8 (Q98TC8) XP8, partial (71%) [TC282051]	6.328855003
atp5c1	Danio rerio ATP synthase, H+ transporting, mitochondrial F1 complex, gamma poly	6.326979176
BC067693	Danio rerio cDNA clone IMAGE:6960489, partial cds. [BC067693]	6.32546856
snd1	Danio rerio staphylococcal nuclease domain containing 1 (snd1), mRNA [NM_1828	6.325429276
zgc:92542	Danio rerio zgc:92542 (zgc:92542), mRNA [NM_001003442]	6.323814924
zgc:92355	Danio rerio zgc:92355 (zgc:92355), mRNA [NM_001007311]	6.323196429
BG305285	fm11b07.x1 Zebrafish adult retina cDNA Danio rerio cDNA clone IMAGE:4145988	6.323017898
zgc:63722	Danio rerio zgc:63722 (zgc:63722), mRNA [NM_201300]	6.322216483
tcp1	Danio rerio t-complex polypeptide 1 (tcp1), mRNA [NM_131230]	6.321645134
zorba	Danio rerio Orb/CPEB-related RNA-binding protein (zorba), mRNA [NM_131427]	6.320891961
im:7138714	ZF101-P00012-DEPE-F_D08 GISZF101 Danio rerio cDNA clone IMAGE:7138714	6.320478526
ENSDART00(	BOVNADHURA NADH dehydrogenase (ubiquinone) {Bos taurus;} , partial (81%) [T	6.320384718
zgc:73206	Danio rerio zgc:73206 (zgc:73206), mRNA [NM_200748]	6.318960703
LOC402861	Danio rerio hypothetical protein LOC402861, mRNA (cDNA clone IMAGE:5605410	6.31815169
zgc:77778	Danio rerio zgc:77778 (zgc:77778), mRNA [NM_213203]	6.316694013
TC291927	AXU1_HUMAN (Q96S65) Axin-1 up-regulated gene 1 protein (TGF-beta induced a	6.316405817
zgc:92831	Danio rerio zgc:92831 (zgc:92831), mRNA [NM_001002505]	6.316243602
zgc:73355	Danio rerio zgc:73355 (zgc:73355), mRNA [NM_200803]	6.31553761
pepd	Danio rerio peptidase D (pepd), mRNA [NM_198912]	6.314366789
TC280445	Q90ZF4 (Q90ZF4) V-ATPase subunit A, complete [TC280445]	6.313167383
TC280392	Q803I8 (Q803I8) Wu:fk91f10 protein, complete [TC280392]	6.312441909
ppaa	Danio rerio F-box and leucine-rich repeat protein 14a (fbxl14a), mRNA [NM_20148	6.311853352
atp6v1c1	Danio rerio ATPase, H+ transporting, lysosomal, V1 subunit C, isoform 1 (atp6v1c1	6.310573886
zgc:56537	Danio rerio zgc:56537 (zgc:56537), mRNA [NM_199950]	6.309681638
nedd5	Danio rerio neural precursor cell expressed, developmentally down-regulated 5, mR	6.308738041
15-Sep	Danio rerio selenoprotein, 15 kDa (sep15), mRNA [NM_178294]	6.306173764
zgc:77115	Danio rerio zgc:77115 (zgc:77115), mRNA [NM_213176]	6.305538366
zgc:64161	Danio rerio zgc:64161 (zgc:64161), mRNA [NM_213126]	6.305396018
TC290674	Q7ZX32 (Q7ZX32) Homer3-prov protein, partial (23%) [TC290660]	6.304207682
slc11a2	Danio rerio solute carrier family 11 (proton-coupled divalent metal ion transporters),	6.30395483
gosr2	Danio rerio golgi SNAP receptor complex member 2 (gosr2), mRNA [NM_199688]	6.302060937
zgc:92770	Danio rerio zgc:92770 (zgc:92770), mRNA [NM_001002556]	6.301799743
pl10	Danio rerio pl10 (pl10), mRNA [NM_130941]	6.301233379
TC297861	Q6W8Q3 (Q6W8Q3) Purkinje cell protein 4-like 1, partial (38%) [TC297861]	6.300180505
wu:fk18g10	fk18g10.y1 zebrafish fin day1 regeneration Danio rerio cDNA 5', mRNA sequence [	6.298878004
gabbr1	Danio rerio gamma-aminobutyric acid B receptor mRNA, partial cds. [AY050509]	6.298332641
psmd7	Danio rerio proteasome (prosome, macropain) 26S subunit, non-ATPase, 7 (Mov34	6.298084906
hm13	Danio rerio histocompatibility (minor) 13 (hm13), mRNA [NM_212572]	6.296767766
TC281048	VE5_PAPVR (P21403) E5 protein, partial (30%) [TC281048]	6.296411305
rer1	Danio rerio RER1 retention in endoplasmic reticulum 1 homolog (S. cerevisiae), mR	6.294974807
TC267920	Q8AXN3 (Q8AXN3) Carboxypeptidase B (Fragment), partial (93%) [TC267920]	6.294578848
wu:fc51f04	fb55b02.x1 Zebrafish WashU MPIMG EST Danio rerio cDNA clone IMAGE:371575	6.293945183
CK869940	AGENCOURT_19703459 NIH_ZGC_6 Danio rerio cDNA clone IMAGE:7218939 5'	6.292976422
zgc:77202	Danio rerio zgc:77202 (zgc:77202), mRNA [NM_214745]	6.292791779
TC290696	Q6NYR4 (Q6NYR4) Hsc70 protein, complete [TC290696]	6.292521793
gnb1	guanine nucleotide binding protein (G protein), beta polypeptide 1 [Source:ZFIN;Ac	6.292516786
ENSDART00(	Q7Z4H3 (Q7Z4H3) NS5ATP2, partial (79%) [TC281519]	6.291662305
calm2b	Danio rerio calmodulin 2, beta (phosphorylase kinase, delta) (calm2b), mRNA [NM_	6.291122199

TC290452	Q6NVT5 (Q6NVT5) MGC69489 protein, partial (28%) [TC290452]	6.290700769
smox	Danio rerio spermine oxidase, mRNA (cDNA clone MGC:77167 IMAGE:6961486),	6.290578391
BC061452	Danio rerio cDNA clone IMAGE:5603807, partial cds. [BC061452]	6.290455591
zgc:92091	Danio rerio zgc:92091 (zgc:92091), mRNA [NM_205720]	6.290192046
zgc:56603	Danio rerio zgc:56603 (zgc:56603), mRNA [NM_199946]	6.289898321
TC292616	DPM1_CRIGR (Q9WU83) Dolichol-phosphate mannosyltransferase (Dolichol-phos	6.28937154
zgc:92513	Danio rerio zgc:92513 (zgc:92513), mRNA [NM_001002363]	6.289341938
slc31a1	Danio rerio solute carrier family 31 (copper transporters), member 1 (slc31a1), mR	6.289010094
zgc:92848	Danio rerio zgc:92848 (zgc:92848), mRNA [NM_001002495]	6.288832538
zgc:63980	Danio rerio zgc:63980 (zgc:63980), mRNA [NM_213335]	6.288719023
pim1	Danio rerio pim-1 oncogene (pim1), mRNA [NM_131539]	6.288348753
anxa11b	Danio rerio annexin A11b (anxa11b), mRNA [NM_181766]	6.288164441
pepd	Danio rerio peptidase D (pepd), mRNA [NM_198912]	6.287688379
zgc:73329	Danio rerio zgc:73329 (zgc:73329), mRNA [NM_200791]	6.287676761
TC294095	Q7ZT82 (Q7ZT82) RNA-binding protein, complete [TC294095]	6.286727672
wu:fb01d02	AGENCOURT_20193737 NIH_ZGC_14 Danio rerio cDNA clone IMAGE:7227944 5	6.286362427
wu:fb16h02	AGENCOURT_22822120 NIH_ZGC_9 Danio rerio cDNA clone IMAGE:7280302 5'	6.286067399
hm13	Danio rerio histocompatibility (minor) 13 (hm13), mRNA [NM_212572]	6.285823562
scap2	Danio rerio src family associated phosphoprotein 2 (scap2), mRNA [NM_200628]	6.284750337
zgc:91981	Danio rerio zgc:91981 (zgc:91981), mRNA [NM_001002653]	6.283651133
zgc:77725	Danio rerio zgc:77725 (zgc:77725), mRNA [NM_199548]	6.281925073
zgc:56344	Danio rerio zgc:56344 (zgc:56344), mRNA [NM_212632]	6.281641175
wu:fc04a02	fc04a02.x1 Zebrafish WashU MPIMG EST Danio rerio cDNA clone IMAGE:372036	6.281140773
TC279018	Q9PWD8 (Q9PWD8) Type I cytokeratin, partial (98%) [TC279018]	6.281042152
zgc:92557	Danio rerio zgc:92557 (zgc:92557), mRNA [NM_001008573]	6.280791831
zgc:100815	Danio rerio zgc:100815 (zgc:100815), mRNA [NM_001003758]	6.278949176
cdk8	Danio rerio, Similar to cyclin-dependent kinase 8, clone IMAGE:3820094, mRNA. [I	6.277316322
zgc:101101	Danio rerio zgc:101101 (zgc:101101), mRNA [NM_214712]	6.276610221
rab14	Danio rerio RAB14, member RAS oncogene family (rab14), mRNA [NM_201495]	6.276157419
zgc:77741	Danio rerio zgc:77741 (zgc:77741), mRNA [NM_199644]	6.275835472
lmnb1	Danio rerio lamin B1 (lmnb1), mRNA [NM_152972]	6.275015216
Ubi-p63E	Danio rerio similar to ubiquitin C, mRNA (cDNA clone IMAGE:5913895), partial cds	6.274882967
txnip	Danio rerio thioredoxin interacting protein (txnip), mRNA [NM_200087]	6.274494059
hsp90a	Danio rerio heat shock protein 90-alpha (hsp90a), mRNA [NM_131328]	6.274476075
zgc:73350	Danio rerio zgc:73350 (zgc:73350), mRNA [NM_200800]	6.274047002
psmc1	Danio rerio proteasome (prosome, macropain) 26S subunit, ATPase, 1 (psmc1), m	6.273991437
zgc:85809	Danio rerio zgc:85809 (zgc:85809), mRNA [NM_213286]	6.273375942
zgc:55695	Danio rerio zgc:55695 (zgc:55695), mRNA [NM_201089]	6.273368214
AJ243959	Danio rerio mRNA for hypothetical protein, clone sd29. [AJ243959]	6.273156185
zgc:56504	Danio rerio zgc:56504, mRNA (cDNA clone MGC:56504 IMAGE:5777534), comple	6.272501269
casc3	Danio rerio cancer susceptibility candidate 3 (casc3), mRNA [NM_205716]	6.271649301
zgc:101101	Danio rerio zgc:101101 (zgc:101101), mRNA [NM_214712]	6.271475606
ENSDART00(	AGENCOURT_19459329 NIH_ZGC_16 Danio rerio cDNA clone IMAGE:7214692 5	6.271232207
odc1	Danio rerio ornithine decarboxylase 1 (odc1), mRNA [NM_131801]	6.271137276
zgc:56134	Danio rerio zgc:56134 (zgc:56134), mRNA [NM_200014]	6.270887595
zgc:55902	Danio rerio zgc:55902 (zgc:55902), mRNA [NM_213068]	6.270054609
zgc:92362	Danio rerio zgc:92362 (zgc:92362), mRNA [NM_001002213]	6.269293213
TC281848	TAFA_HUMAN (Q12962) Transcription initiation factor TFIID subunit 10 (Transcripl	6.269187684
zgc:103708	Danio rerio zgc:103708 (zgc:103708), mRNA [NM_001005941]	6.268777993
zgc:56330	Danio rerio zgc:56330 (zgc:56330), mRNA [NM_199683]	6.268614636
anxa1a	Danio rerio annexin A1a (anxa1a), mRNA [NM_181758]	6.268114241
ptplb	Danio rerio protein tyrosine phosphatase-like (proline instead of catalytic arginine),	6.2680131
hm13	Danio rerio histocompatibility (minor) 13 (hm13), mRNA [NM_212572]	6.267894802
TC292921	CU4B_HUMAN (Q13620) Cullin homolog 4B (CUL-4B), partial (95%) [TC292921]	6.26735142
dusp6	Danio rerio dual specificity phosphatase 6 (dusp6), mRNA [NM_194380]	6.26728961
cpvl	Danio rerio carboxypeptidase, vitellogenic-like (cpvl), mRNA [NM_199278]	6.264765224
TC281703	NISM_BOVIN (Q02380) NADH-ubiquinone oxidoreductase SGDH subunit, mitochc	6.2646468
ndufb10	Danio rerio NADH dehydrogenase (ubiquinone) 1 beta subcomplex, 10 (ndufb10), r	6.263266032
ENSDART00(	Q7T2W9 (Q7T2W9) Complement protein component C7, partial (48%) [TC271593]	6.262253799
TC290463	Q9PUK9 (Q9PUK9) High mobility group protein HMG1, partial (22%) [TC290463]	6.262037007
zgc:55580	Danio rerio zgc:55580 (zgc:55580), mRNA [NM_200918]	6.260605894
zgc:92432	Danio rerio zgc:92432 (zgc:92432), mRNA [NM_001002175]	6.260514277
zgc:73355	Danio rerio zgc:73355 (zgc:73355), mRNA [NM_200803]	6.260188913
wu:fb63g02	Danio rerio wu:fb63g02 (wu:fb63g02), mRNA [NM_212622]	6.260078772
zgc:73197	Danio rerio zgc:73197 (zgc:73197), mRNA [NM_200058]	6.259955405
ENSDART00(	AF086645 metastasis suppressor protein {Homo sapiens;} , partial (21%) [TC2835]	6.257999133
brd8	Danio rerio bromodomain containing 8 (brd8), mRNA [NM_212777]	6.257789603
zgc:55615	Danio rerio zgc:55615 (zgc:55615), mRNA [NM_200927]	6.257699417
zgc:63962	Danio rerio zgc:63962 (zgc:63962), mRNA [NM_199748]	6.256595708
evx1	Danio rerio even-skipped homeobox 1 (evx1), mRNA [NM_131249]	6.25642883
zp3b	Danio rerio zona pellucida glycoprotein 3 b (zp3b), mRNA [NM_131696]	6.256209639
BC056551	Danio rerio cDNA clone IMAGE:6794135, partial cds. [BC056551]	6.256183735
zgc:85807	Danio rerio zgc:85807 (zgc:85807), mRNA [NM_213289]	6.256075196
ENSDART00(	T00742 ubiquitin-binding protein homolog A-735G6.2 - human {Homo sapiens;} , pa	6.255691357
CF543835	DRerAM-52400053 zebrafish late somitogenesis cDNA library ICRFp524 Danio rer	6.254798951
zgc:101532	Danio rerio zgc:101532 (zgc:101532), mRNA [NM_214718]	6.254737034
TC267956	Q8JH37 (Q8JH37) Vitellogenin 1 (Fragment), partial (83%) [TC267956]	6.251614131
zgc:56296	Danio rerio zgc:56296 (zgc:56296), mRNA [NM_213376]	6.251159545
wu:fi15g04	Danio rerio wu:fi15g04, mRNA (cDNA clone IMAGE:5915397), partial cds. [BC057	6.251004507
zgc:92421	Danio rerio zgc:92421 (zgc:92421), mRNA [NM_001002076]	6.250580448
zgc:92757	Danio rerio zgc:92757 (zgc:92757), mRNA [NM_001002566]	6.249895093

TC290892	Q9UEX4 (Q9UEX4) Zinc finger protein, partial (26%) [TC290892]	6.248511197
TC269112	Q7ZVY8 (Q7ZVY8) DnaJ (Hsp40) homolog, subfamily B, member 1, complete [TC:	6.24641526
mg:ab04g06	ab04g06_p1 ZF adult heart library Danio rerio cDNA 5 prime, mRNA sequence [AI1	6.244446463
txnip	Danio rerio thioredoxin interacting protein (txnip), mRNA [NM_200087]	6.242210705
TC299442	PIM3_XENLA (Q91822) Serine/threonine-protein kinase Pim-3 (Pim-1) , partial (29	6.242063614
amfr	Danio rerio autocrine motility factor receptor (amfr), mRNA [NM_213163]	6.241614047
ndufb10	Danio rerio NADH dehydrogenase (ubiquinone) 1 beta subcomplex, 10 (ndufb10), r	6.241111135
zgc:77793	Danio rerio zgc:77793 (zgc:77793), mRNA [NM_200889]	6.240252761
zgc:56116	Danio rerio zgc:56116 (zgc:56116), mRNA [NM_200196]	6.239925036
zgc:66039	Danio rerio zgc:66039 (zgc:66039), mRNA [NM_213148]	6.238830631
TC280763	Q801W1 (Q801W1) SI:dZ262K18.6 (Proteasome (Prosome, macropain) subunit, b	6.238714643
alas1	Danio rerio aminolevulinate, delta-, synthetase 1 (alas1), mRNA [NM_201287]	6.238300253
TC290818	Q6P0Y9 (Q6P0Y9) Hsp90b protein, partial (25%) [TC290818]	6.236934295
zgc:55870	Danio rerio zgc:55870 (zgc:55870), mRNA [NM_200143]	6.236284024
zgc:63767	Danio rerio zgc:63767 (zgc:63767), mRNA [NM_200957]	6.236267219
atp6v1ba	Danio rerio ATPase, H+ transporting, lysosomal, V1 subunit B, member a (atp6v1b	6.236209326
zgc:103725	Danio rerio zgc:103725 (zgc:103725), mRNA [NM_001005938]	6.235503682
zgc:86676	Danio rerio zgc:86676 (zgc:86676), mRNA [NM_001002152]	6.235397731
add3	Danio rerio adducin 3 (gamma) (add3), mRNA [NM_199663]	6.234389578
pdcd10	Danio rerio programmed cell death 10 (pdcd10), mRNA [NM_200555]	6.234338937
TC290299	Cyprinus carpio intergenic spacer region, partial sequence; 5' external transcribed s	6.234154428
zgc:91930	AGENCOURT_22437750 NIH_ZGC_7 Danio rerio cDNA clone IMAGE:7267060 5'	6.233575018
BI881813	fn09h04.x1 Zebrafish WashU MPIMG EST Danio rerio cDNA clone IMAGE:448995	6.233342149
CF996856	AGENCOURT_16393148 NIH_ZGC_7 Danio rerio cDNA clone IMAGE:7037315 5'	6.232756745
zgc:65772	Danio rerio zgc:65772 (zgc:65772), mRNA [NM_200533]	6.232705957
cp	Danio rerio ceruloplasmin (cp), mRNA [NM_131802]	6.232512209
tra2a	Danio rerio transformer-2 alpha (tra2a), mRNA [NM_200416]	6.232508867
zgc:92840	AGENCOURT_21855487 NIH_ZGC_8 Danio rerio cDNA clone IMAGE:7264113 5'	6.23096617
ddx5	Danio rerio DEAD (Asp-Glu-Ala-Asp) box polypeptide 5 (ddx5), mRNA [NM_21261:	6.230916641
wu:fb01d11	AGENCOURT_22422688 NIH_ZGC_9 Danio rerio cDNA clone IMAGE:7275394 5'	6.228423985
fgb	fibrinogen, B beta polypeptide [Source:ZFIN;Acc:ZDB-GENE-030131-9261] [ENSD	6.227859936
TC294580	NUPL_XENLA (P05221) Nucleoplasmin, partial (31%) [TC294580]	6.226149629
zgc:101775	Danio rerio zgc:101775 (zgc:101775), mRNA [NM_001008624]	6.224801538
zgc:66107	Danio rerio zgc:66107 (zgc:66107), mRNA [NM_199903]	6.223805151
eif2s1l	Danio rerio eukaryotic translation initiation factor 2, subunit 1 alpha, like (eif2s1l), m	6.223644768
yars	Danio rerio tyrosyl-tRNA synthetase (yars), mRNA [NM_201316]	6.223457385
fads2	Danio rerio fatty acid desaturase 2 (fads2), mRNA [NM_131645]	6.223414032
TC278959	BC052129 LOC407640 protein {Danio rerio;} , partial (21%) [TC278959]	6.22322855
wu:fk86d05	Danio rerio wu:fk86d05 (wu:fk86d05), mRNA [NM_001003843]	6.222437797
TC300287	Q9K3D3 (Q9K3D3) Biphenyl-2,3-diol 1,2-dioxygenase III-related protein, partial (86	6.221515747
zgc:92355	Danio rerio zgc:92355 (zgc:92355), mRNA [NM_001007311]	6.221246575
TC291234	FRIM_SALSA (P49947) Ferritin, middle subunit (Ferritin M), partial (97%) [TC2912:	6.21951706
zgc:63792	Danio rerio zgc:63792 (zgc:63792), mRNA [NM_200446]	6.219086917
scap2	Danio rerio src family associated phosphoprotein 2 (scap2), mRNA [NM_200628]	6.218447697
atp1a1b	Danio rerio ATPase, Na+/K+ transporting, alpha 1b polypeptide (atp1a1b), mRNA [	6.217900828
nxf1	Danio rerio nuclear RNA export factor 1 mRNA, partial cds. [AY648819]	6.217617359
zgc:55769	Danio rerio zgc:55769 (zgc:55769), mRNA [NM_214769]	6.217482872
vps26	Danio rerio vacuolar protein sorting 26 (yeast) (vps26), mRNA [NM_200907]	6.217422449
wu:fj44c03	fj44c03.y1 zebrafish adult brain Danio rerio cDNA 5' similar to contains element TA	6.216208002
tcp1	Danio rerio t-complex polypeptide 1 (tcp1), mRNA [NM_131230]	6.215553274
zgc:101883	Danio rerio zgc:101883 (zgc:101883), mRNA [NM_001007375]	6.215173156
zgc:65942	Danio rerio zgc:65942 (zgc:65942), mRNA [NM_200678]	6.214754955
zgc:92866	Danio rerio zgc:92866 (zgc:92866), mRNA [NM_001002482]	6.214424623
zgc:56095	Danio rerio zgc:56095 (zgc:56095), mRNA [NM_213013]	6.213998692
fabp7b	Danio rerio fatty acid binding protein 7, brain, b (fabp7b), mRNA [NM_214807]	6.213937096
BM533115	fx68b05.y1 Zebrafish SJD 5 day embryo Danio rerio cDNA clone IMAGE:5628249 :	6.213886505
TC269662	Q98TQ8 (Q98TQ8) Connective tissue growth factor precursor (Connective tissue g	6.21370989
TC290036	RIR2_BRARE (P79733) Ribonucleoside-diphosphate reductase M2 chain (Ribonu	6.212176478
eif2s1l	Danio rerio eukaryotic translation initiation factor 2, subunit 1 alpha, like (eif2s1l), m	6.212096289
AI641052	fc18d10.x1 Zebrafish WashU MPIMG EST Danio rerio cDNA clone IMAGE:372174	6.21092677
zgc:77112	Danio rerio zgc:77112 (zgc:77112), mRNA [NM_213180]	6.210042951
chordc1	Danio rerio cysteine and histidine-rich domain (CHORD)-containing, zinc binding pr	6.209781127
psen2	Danio rerio presenilin2 (psen2), mRNA [NM_131514]	6.209767209
add3	Danio rerio adducin 3 (gamma) (add3), mRNA [NM_199663]	6.209643199
h2afx	AGENCOURT_22823111 NIH_ZGC_9 Danio rerio cDNA clone IMAGE:7278708 5'	6.209222388
zgc:86806	Danio rerio zgc:86806 (zgc:86806), mRNA [NM_001002121]	6.209126559
TC270231	Q9YHZ8 (Q9YHZ8) Pax-family transcription factor 6.2, partial (95%) [TC270231]	6.208868313
BC056568	Danio rerio cDNA clone IMAGE:6799414, partial cds. [BC056568]	6.20824351
slc16a3	Danio rerio solute carrier family 16 (monocarboxylic acid transporters), member 3 (:	6.207546039
mcl1b	Danio rerio myeloid cell leukemia sequence 1b (mcl1b), mRNA [NM_194394]	6.207530423
h2afx	Danio rerio H2A histone family, member X (h2afx), mRNA [NM_201073]	6.20727478
zgc:92066	Danio rerio zgc:92066 (zgc:92066), mRNA [NM_001002378]	6.206837083
zgc:55902	Danio rerio zgc:55902 (zgc:55902), mRNA [NM_213068]	6.206650521
eef2l	Danio rerio eukaryotic translation elongation factor 2, like (eef2l), mRNA [NM_2004	6.206219326
TC281441	Q801N1 (Q801N1) MGC53150 protein, partial (28%) [TC281441]	6.205709453
rap2b	Danio rerio RAP2B, member of RAS oncogene family (rap2b), mRNA [NM_001001	6.20519163
TC295900	MUSPIM2M protein-serine/threonine kinase {Mus musculus;} , partial (23%) [TC29:	6.204594169
zgc:92251	Danio rerio zgc:92251 (zgc:92251), mRNA [NM_001003420]	6.204469773
BM183382	fv63a05.y1 Sugano SJD adult male Danio rerio cDNA clone IMAGE:5413136 5' sim	6.204048096
TC269062	Q6P736 (Q6P736) Ptb protein, partial (89%) [TC269062]	6.203880528
TC270545	ZM11_MOUSE (Q8R5C8) Zinc finger MYND domain containing protein 11, partial (	6.203276152

ENSDART00(	Q719H9 (Q719H9) Potassium channel tetramerization domain-containing 1 (KCTD	6.203151169
ndrg3a	Danio rerio N-myc downstream regulated family member 3a (ndrg3a), mRNA [NM_	6.202468868
TC277748	Q6P3J5 (Q6P3J5) Eukaryotic translation elongation factor 2, like, partial (40%) [TC	6.20077006
mibp2	Danio rerio muscle-specific beta 1 integrin binding protein 2 (mibp2), mRNA [NM_1	6.20050632
psen2	Danio rerio presenilin2 (psen2), mRNA [NM_131514]	6.200206476
chordc1	Danio rerio cysteine and histidine-rich domain (CHORD)-containing, zinc binding pr	6.199869952
zgc:56225	AW202851 fj23b04.y1 Zebrafish adult olfactory Danio rerio cDNA 5', mRNA sequer	6.199726558
BC056779	Danio rerio cDNA clone IMAGE:3816160, partial cds. [BC056779]	6.19910273
zgc:103451	Danio rerio zgc:103451 (zgc:103451), mRNA [NM_001008614]	6.198879708
zgc:73238	Q8AVU5 (Q8AVU5) MGC52819 protein, partial (72%) [TC293116]	6.197833042
rac1	Danio rerio ras-related C3 botulinum toxin substrate 1 (rho family, small GTP bindir	6.197349996
atp6v0d1	Danio rerio ATPase, H+ transporting, V0 subunit D isoform 1 (atp6v0d1), mRNA [N	6.195683783
ENSDART00(	BTCIB8 NADH dehydrogenase {Bos taurus;} , partial (80%) [TC290547]	6.195361665
BI326630	fp37h02.x3 zebrafish gridded kidney Danio rerio cDNA clone IMAGE:4759130 3', m	6.194546225
zgc:77637	Danio rerio zgc:77637 (zgc:77637), mRNA [NM_199990]	6.193901043
zgc:77197	Danio rerio zgc:77197 (zgc:77197), mRNA [NM_207075]	6.192734187
zgc:64162	Danio rerio zgc:64162 (zgc:64162), mRNA [NM_200385]	6.192610239
zgc:64102	Danio rerio zgc:64102 (zgc:64102), mRNA [NM_201208]	6.192272358
han11l	Danio rerio HAN11-like (han11l), mRNA [NM_200069]	6.191976517
CO355761	DR_ATE_NRM12_C08 adult testis normalized (TLL) Danio rerio cDNA, mRNA seq	6.190921207
zgc:73214	Danio rerio zgc:73214 (zgc:73214), mRNA [NM_213019]	6.190104244
ENSDART00(	Q9VVW8 (Q9VVW8) CG10424-PA (GH09035p), partial (42%) [TC293617]	6.189501032
zgc:92864	Danio rerio zgc:92864 (zgc:92864), mRNA [NM_001005924]	6.189076475
zgc:77299	Danio rerio zgc:77299 (zgc:77299), mRNA [NM_205637]	6.18872924
LOC445395	Danio rerio RIKEN cDNA 2410004I17-like (LOC445395), mRNA [NM_001003872]	6.188429734
tnfsf5ip1	Danio rerio tumor necrosis factor superfamily, member 5-induced protein 1 (tnfsf5ip	6.187774098
zgc:56363	Danio rerio zgc:56363 (zgc:56363), mRNA [NM_201128]	6.187247293
tfpia	Danio rerio tissue factor pathway inhibitor a (tfpia), mRNA [NM_182872]	6.18714454
TC283697	Q91ZY6 (Q91ZY6) Nuclear receptor coactivator GT198, partial (36%) [TC283697]	6.186148341
zgc:103709	Danio rerio zgc:103709 (zgc:103709), mRNA [NM_001005940]	6.185994441
wu:fa18c12	fa18c12.s1 Ekkerearly gastrulation zebrafish embryo Danio rerio cDNA clone 1036	6.185781399
her6	Danio rerio hairy-related 6 (her6), mRNA [NM_131079]	6.185768726
TC271295	HSEXPORTI Exportin(tRNA) {Homo sapiens;} , partial (9%) [TC271295]	6.184140266
zgc:63767	Danio rerio zgc:63767, mRNA (cDNA clone MGC:63767 IMAGE:2641824), comple	6.184047544
pald	Danio rerio paladin (pald), mRNA [NM_198811]	6.182401083
zgc:56116	Danio rerio zgc:56116 (zgc:56116), mRNA [NM_200196]	6.181767886
uqcrfs1	Danio rerio ubiquinol-cytochrome c reductase, Rieske iron-sulfur polypeptide 1 (uqc	6.181664324
znf207	Danio rerio zinc finger protein 207 (znf207), mRNA [NM_199665]	6.181216318
MAP3K7IP1	Danio rerio TAK1-binding protein 1, mRNA (cDNA clone IMAGE:6971404), partial c	6.179261369
zgc:56101	Danio rerio zgc:56101 (zgc:56101), mRNA [NM_213010]	6.178684672
CK703042	CK703042 ZF101-P00002-DEPE-R_D14 GISZF001_ra Danio rerio cDNA clone IM	6.178670391
zgc:77147	Danio rerio zgc:77147 (zgc:77147), mRNA [NM_205646]	6.17820926
rpl4	Danio rerio ribosomal protein L4 (rpl4), mRNA [NM_213107]	6.176572775
zgc:56471	Danio rerio zgc:56471 (zgc:56471), mRNA [NM_200291]	6.176514115
si:ch211-150c	Danio rerio si:ch211-150c22.2 (si:ch211-150c22.2), mRNA [NM_001006019]	6.175214782
bzw1	Danio rerio basic leucine zipper and W2 domains 1 (bzw1), mRNA [NM_199708]	6.174860678
zgc:77146	Danio rerio zgc:77146 (zgc:77146), mRNA [NM_213298]	6.174852134
sf3b5	Danio rerio splicing factor 3b, subunit 5 (sf3b5), mRNA [NM_001002478]	6.174133517
TC294699	Q8WWL7 (Q8WWL7) Fetal globin inducing factor, partial (69%) [TC294699]	6.171647092
zgc:92057	Danio rerio zgc:92057 (zgc:92057), mRNA [NM_001007323]	6.170797596
TC290737	SFR9_HUMAN (Q13242) Splicing factor, arginine/serine-rich 9 (Pre-mRNA splicing	6.170737666
arl2bp	Danio rerio ADP-ribosylation factor-like 2 binding protein (arl2bp), mRNA [NM_201(	6.170282177
zgc:86853	Danio rerio zgc:86853 (zgc:86853), mRNA [NM_001009896]	6.169028843
seh1l	Danio rerio SEH1-like (S. cerevisiae) (seh1l), mRNA [NM_199923]	6.168882719
zgc:103782	Danio rerio zgc:103782 (zgc:103782), mRNA [NM_001005592]	6.168796272
sdcbp	Danio rerio syndecan binding protein (syntenin) (sdcbp), mRNA [NM_212691]	6.16850043
TC279019	Unknown	6.167848757
zgc:85694	Danio rerio zgc:85694 (zgc:85694), mRNA [NM_214746]	6.167777128
h1m	Danio rerio linker histone H1M (h1m), mRNA [NM_183071]	6.166522368
rac1	Danio rerio ras-related C3 botulinum toxin substrate 1 (rho family, small GTP bindir	6.166347716
wu:fj61b01	fj61b01.x1 zebrafish adult brain Danio rerio cDNA 3', mRNA sequence [AW282020	6.166161397
zgc:103488	Danio rerio zgc:103488 (zgc:103488), mRNA [NM_001007345]	6.164788553
CO920034	AGENCOURT_30419550 NIH_ZGC_17 Danio rerio cDNA clone IMAGE:7425636 5	6.16454301
TC269288	Q8UVE6 (Q8UVE6) Transcription factor AP2 alpha 1, complete [TC269288]	6.164129602
CD605735	RK058A1E12.T7 Zebrafish Kidney Marrow cDNA library Danio rerio cDNA clone RI	6.163348952
pcbp2	Danio rerio poly(rC) binding protein 2 (pcbp2), mRNA [NM_201192]	6.163329129
psmb1	Danio rerio proteasome (prosome, macropain) subunit, beta type, 1 (psmb1), mRN	6.163279699
zgc:64222	Q6KCE3 (Q6KCE3) Histone H3.3, complete [TC291777]	6.160558112
TC272645	RT14_HUMAN (O60783) Mitochondrial 28S ribosomal protein S14 (S14mt) (MRP-S	6.159175527
CO920252	AGENCOURT_30429352 NIH_ZGC_17 Danio rerio cDNA clone IMAGE:7417404 5	6.158854107
mg:ab04g06	ab04g06_p1 ZF adult heart library Danio rerio cDNA 5 prime, mRNA sequence [AI1	6.158771592
LOC407641	Danio rerio hypothetical protein LOC407641, mRNA (cDNA clone IMAGE:5915890	6.158308558
zgc:92671	Danio rerio zgc:92671 (zgc:92671), mRNA [NM_001003439]	6.158100768
LOC445395	Danio rerio RIKEN cDNA 2410004I17-like (LOC445395), mRNA [NM_001003872]	6.157859452
TC282119	ATTY_MOUSE (Q8QZR1) Tyrosine aminotransferase (L-tyrosine:2-oxoglutarate a	6.157736337
cct7	Danio rerio chaperonin containing TCP1, subunit 7 (eta) (cct7), mRNA [NM_17324	6.157513533
zgc:64050	Danio rerio zgc:64050 (zgc:64050), mRNA [NM_001007186]	6.157160629
zgc:55982	Danio rerio zgc:55982 (zgc:55982), mRNA [NM_213061]	6.156872364
zgc:77187	Danio rerio zgc:77187 (zgc:77187), mRNA [NM_205566]	6.156465008
zgc:55712	Danio rerio zgc:55712 (zgc:55712), mRNA [NM_199575]	6.155978182
TC287951	Q7PKG0 (Q7PKG0) ENSANGP00000024462 (Fragment), partial (30%) [TC287951	6.1554919

rtn4ip1	Danio rerio reticulon 4 interacting protein 1 (rtn4ip1), mRNA [NM_200352]	6.153551147
TC279552	Q7SZ26 (Q7SZ26) Ppib-prov protein, complete [TC279552]	6.152483379
zgc:63489	Danio rerio zgc:63489 (zgc:63489), mRNA [NM_200629]	6.152459872
glud1a	Danio rerio glutamate dehydrogenase 1a (glud1a), mRNA [NM_212576]	6.15244047
zgc:101667	Danio rerio zgc:101667 (zgc:101667), mRNA [NM_001006083]	6.151977874
zgc:55510	Danio rerio zgc:55510 (zgc:55510), mRNA [NM_200507]	6.151958314
zgc:55919	Danio rerio zgc:55919 (zgc:55919), mRNA [NM_199655]	6.151925291
mapre1l	Danio rerio microtubule-associated protein, RP/EB family, member 1, like (mapre1l	6.151862893
TC281102	GNPI_HUMAN (P46926) Glucosamine-6-phosphate isomerase (Glucosamine-6-pl	6.151741943
arpc1a	Danio rerio actin related protein 2/3 complex, subunit 1A (arpc1a), mRNA [NM_201	6.150558004
CO928404	AGENCOURT_30540916 NIH_ZGC_19 Danio rerio cDNA clone IMAGE:7427968 5	6.15028946
zgc:92087	Danio rerio zgc:92087 (zgc:92087), mRNA [NM_001007299]	6.149403878
wu:fb63g02	Danio rerio wu:fb63g02 (wu:fb63g02), mRNA [NM_212622]	6.148837475
ENSDART00(	BC009610 activated RNA polymerase II transcription cofactor 4 {Homo sapiens;} , I	6.147975783
zgc:66337	Danio rerio zgc:66337 (zgc:66337), mRNA [NM_200520]	6.147378564
CO360641	DR_ATE_SUL17_D09 adult testis subtracted 2 (TLL) Danio rerio cDNA, mRNA sec	6.145801708
BC061452	Danio rerio cDNA clone IMAGE:5603807, partial cds. [BC061452]	6.145183354
eif2s2	Danio rerio eukaryotic translation initiation factor 2, subunit 2 beta (eif2s2), mRNA [	6.14510966
zgc:55982	Danio rerio zgc:55982 (zgc:55982), mRNA [NM_213061]	6.143966486
rps10	Danio rerio ribosomal protein S10 (rps10), mRNA [NM_201146]	6.143702906
id:ibd1247	1247t3 NICHD Zebrafish normalized I Danio rerio cDNA clone 1247, mRNA sequer	6.143003364
TC291107	Q7ZU04 (Q7ZU04) Creatine kinase, brain, partial (51%) [TC291107]	6.140749122
sec61a	Danio rerio SEC61, alpha subunit (sec61a), mRNA [NM_153659]	6.140395143
prps1a	Danio rerio phosphoribosyl pyrophosphate synthetase 1A (prps1a), mRNA [NM_21	6.140162779
ndrg1	Danio rerio zgc:63944, mRNA (cDNA clone MGC:63944 IMAGE:6791251), comple	6.139725645
zgc:92009	Danio rerio zgc:92009 (zgc:92009), mRNA [NM_001003738]	6.138935261
gnaia	Danio rerio guanine nucleotide binding protein (G protein), alpha inhibiting activity p	6.13876906
arpc1a	Danio rerio actin related protein 2/3 complex, subunit 1A (arpc1a), mRNA [NM_201	6.136486353
TC290216	THO4_MOUSE (O08583) THO complex subunit 4 (Tho4) (RNA and export factor b	6.135677686
gart	Danio rerio phosphoribosylglycinamide formyltransferase (gart), mRNA [NM_13161	6.134946976
TC295435	GCDH_HUMAN (Q92947) Glutaryl-CoA dehydrogenase, mitochondrial precursor (	6.134093818
cct7	Danio rerio chaperonin containing TCP1, subunit 7 (eta) (cct7), mRNA [NM_17324	6.133829381
tnnt3b	AGENCOURT_16620514 NIH_ZGC_7 Danio rerio cDNA clone IMAGE:7055650 5'	6.132898505
rab1a	Danio rerio RAB1A, member RAS oncogene family (rab1a), mRNA [NM_00100716	6.132878844
zgc:56007	Danio rerio zgc:56007 (zgc:56007), mRNA [NM_199782]	6.132664809
tial1	Danio rerio TIA1 cytotoxic granule-associated RNA binding protein-like 1 (tial1), mF	6.130359579
txnrd1	Danio rerio thioredoxin reductase 1 (txnrd1), mRNA [NM_183072]	6.130292068
TC272858	AF082658 Era GTPase B protein {Homo sapiens;} , partial (27%) [TC272858]	6.129021528
zgc:63831	Danio rerio zgc:63831 (zgc:63831), mRNA [NM_200031]	6.128506104
zgc:92208	Danio rerio zgc:92208 (zgc:92208), mRNA [NM_001007308]	6.127777884
AB055682	Danio rerio D254 mRNA, 3'UTR, partial sequence. [AB055682]	6.127194163
zgc:101894	Danio rerio zgc:101894 (zgc:101894), mRNA [NM_001004671]	6.127055085
wu:fd54d09	fd54d09.x1 Zebrafish WashU MPIMG EST Danio rerio cDNA clone IMAGE:373355	6.126676564
btg4	Danio rerio B-cell translocation gene 4, mRNA (cDNA clone MGC:64080 IMAGE:67	6.126281261
zgc:55515	Danio rerio zgc:55515 (zgc:55515), mRNA [NM_199576]	6.125306196
zgc:55569	Danio rerio zgc:55569 (zgc:55569), mRNA [NM_200935]	6.125268049
aldoc	Danio rerio aldolase c, fructose-bisphosphate (aldoc), mRNA [NM_194384]	6.125239616
zgc:56592	Danio rerio zgc:56592 (zgc:56592), mRNA [NM_213408]	6.125182609
zgc:55566	Danio rerio zgc:55566 (zgc:55566), mRNA [NM_213457]	6.124529092
TC280553	IF2P_HUMAN (O60841) Eukaryotic translation initiation factor 5B (eIF-5B) (Transla	6.124211451
zgc:100902	Danio rerio zgc:100902 (zgc:100902), mRNA [NM_001003520]	6.124206865
TC292661	Q6PF51 (Q6PF51) MGC68893 protein, partial (26%) [TC292661]	6.122801751
wu:fa12g02	AGENCOURT_30541555 NIH_ZGC_19 Danio rerio cDNA clone IMAGE:7434824 5	6.122754352
ENSDART00(	Q8IZM9 (Q8IZM9) N system amino acid transporter NAT-1, partial (65%) [TC2945	6.122721476
her6	Danio rerio hairy-related 6 (her6), mRNA [NM_131079]	6.122456977
si:rp71-71m17	Danio rerio si:rp71-71m17.1 (si:rp71-71m17.1), mRNA [NM_001007031]	6.122197215
zgc:63982	Danio rerio zgc:63982 (zgc:63982), mRNA [NM_200061]	6.121893619
TC292329	Q7ZVH8 (Q7ZVH8) Id:ibd1103 protein, complete [TC292329]	6.121185792
BM155183	fw10c02.y1 SJD adult pectoral fin Danio rerio cDNA clone IMAGE:5546114 5', mR	6.121059273
zgc:101686	Danio rerio zgc:101686 (zgc:101686), mRNA [NM_001007432]	6.120694293
TC291478	Unknown	6.120216969
si:dkey-61p9.(	AGENCOURT_16393796 NIH_ZGC_7 Danio rerio cDNA clone IMAGE:7036605 5'	6.116969625
CK360756	AGENCOURT_17113711 NIH_ZGC_4 Danio rerio cDNA clone IMAGE:7090730 5'	6.116885878
snx12	Danio rerio sorting nexin 12, variation 2 (SNX12-var2) mRNA, complete cds. [AY39	6.115720957
zgc:76914	Danio rerio zgc:76914 (zgc:76914), mRNA [NM_213088]	6.113736329
wu:fl22c07	fl22a09.y1 Zebrafish Research Genetics C32 fin Danio rerio cDNA 5', mRNA seque	6.113271391
TC290341	Q6NYN8 (Q6NYN8) Eef1g protein (Fragment), partial (49%) [TC290341]	6.112291778
ppia	Danio rerio peptidylprolyl isomerase A (cyclophilin A) (ppia), mRNA [NM_212758]	6.111858313
TC273264	Q6QPX3 (Q6QPX3) Cell division cycle 14 alpha protein, partial (66%) [TC273264]	6.111463319
CO352814	DR_ATE_FL05_B04 adult testis full-length (TLL) Danio rerio cDNA, mRNA sequen	6.110362811
wu:fc16c02	fc16c02.x1 Zebrafish WashU MPIMG EST Danio rerio cDNA clone IMAGE:372153	6.110284793
smad7	Danio rerio MAD, mothers against decapentaplegic homolog 7 (Drosophila) (smad7	6.109530424
pknox1.1	Danio rerio pbx/knotted 1 homeobox 1.1 (pknox1.1), mRNA [NM_131891]	6.108575696
TC297159	Q6T937 (Q6T937) Gremlin, complete [TC297159]	6.108528225
TC273544	CHKCETSS9 c-ets protein {Gallus gallus;} , partial (21%) [TC273544]	6.108312486
zgc:92169	Danio rerio zgc:92169 (zgc:92169), mRNA [NM_001004553]	6.106162847
zgc:101527	Danio rerio zgc:101527 (zgc:101527), mRNA [NM_001005574]	6.105399113
TC284560	Q7QAJ1 (Q7QAJ1) AgCP7750 (Fragment), partial (10%) [TC284560]	6.105369532
zgc:66321	Danio rerio zgc:66321 (zgc:66321), mRNA [NM_201118]	6.105101877
zgc:63640	Danio rerio zgc:63640 (zgc:63640), mRNA [NM_200471]	6.104913961
TC292513	BOP1_HUMAN (Q14137) Ribosome biogenesis protein BOP1 (Block of proliferatio	6.104777566

itm1	Danio rerio integral membrane protein 1 (itm1), mRNA [NM_201458]	6.104281376
TC293668	Q9VLP7 (Q9VLP7) CG7818-PA (LD06016p), partial (67%) [TC293668]	6.103653325
arha	Danio rerio ras homolog gene family, member A (arha), mRNA [NM_212749]	6.103519222
ENSDART00(	BC014051 small inducible cytokine subfamily E, member 1 {Homo sapiens;} , partia	6.103164732
cct6a	Danio rerio chaperonin containing TCP1, subunit 6A (zeta 1) (cct6a), mRNA [NM_2	6.102377113
pane1	proliferation associated nuclear element [Source:ZFIN;Acc:ZDB-GENE-040611-4] [	6.101739844
zgc:55970	Danio rerio zgc:55970 (zgc:55970), mRNA [NM_201176]	6.101585512
zgc:56055	Danio rerio zgc:56055 (zgc:56055), mRNA [NM_213049]	6.101082739
CN316175	AGENCOURT_21849026 NIH_ZGC_8 Danio rerio cDNA clone IMAGE:7261507 5'	6.100572453
hrmt1l2	Danio rerio HMT1 hnRNP methyltransferase-like 2 (S. cerevisiae) (hrmt1l2), mRNA	6.100443516
BC076043	Danio rerio cDNA clone IMAGE:7047554, partial cds. [BC076043]	6.099577673
TC290257	Q8JHI0 (Q8JHI0) Solute carrier family 25 member 5 protein (Solute carrier family 2	6.099481088
rtn4rl2a	Danio rerio reticulon 4 receptor-like 2 a (rtn4rl2a), mRNA [NM_203479]	6.099306384
hrmt1l2	Danio rerio HMT1 hnRNP methyltransferase-like 2 (S. cerevisiae) (hrmt1l2), mRNA	6.098334001
nfkbiab	Danio rerio nuclear factor of kappa light polypeptide gene enhancer in B-cells inhibi	6.097631749
TC281242	Q9SXQ6 (Q9SXQ6) FEN-1, partial (33%) [TC281242]	6.09698156
rpl3	Danio rerio ribosomal protein L3 (rpl3), mRNA [NM_001001590]	6.096964998
TC290321	Q8JHI0 (Q8JHI0) Solute carrier family 25 member 5 protein (Solute carrier family 2	6.096941329
fads2	Danio rerio fatty acid desaturase 2 (fads2), mRNA [NM_131645]	6.096138383
spag7	Danio rerio sperm associated antigen 7 (spag7), mRNA [NM_201125]	6.095015654
CK027852	AGENCOURT_16620228 NIH_ZGC_7 Danio rerio cDNA clone IMAGE:7053221 5'	6.094457943
zgc:101877	Danio rerio zgc:101877 (zgc:101877), mRNA [NM_001007376]	6.094419517
zgc:55553	Danio rerio zgc:55553 (zgc:55553), mRNA [NM_200163]	6.094357144
CO353882	DR_ATE_FL20_H10 adult testis full-length (TLL) Danio rerio cDNA, mRNA sequen	6.09398282
wu:fb13h08	AGENCOURT_17177074 NIH_ZGC_4 Danio rerio cDNA clone IMAGE:7086257 5'	6.092251116
zgc:55712	Danio rerio zgc:55712 (zgc:55712), mRNA [NM_199575]	6.092179852
zgc:73198	Danio rerio zgc:73198 (zgc:73198), mRNA [NM_200747]	6.091227335
CN022050	AGENCOURT_20754268 NIH_ZGC_14 Danio rerio cDNA clone IMAGE:7229320 5	6.090722418
wu:fc59f06	AGENCOURT_16619446 NIH_ZGC_7 Danio rerio cDNA clone IMAGE:7053017 5'	6.09001876
TC283416	Q86YQ9 (Q86YQ9) Morn protein, partial (49%) [TC283416]	6.089696744
zgc:92576	Danio rerio zgc:92576 (zgc:92576), mRNA [NM_001002729]	6.089014563
wu:fb60g09	AGENCOURT_21057238 NIH_ZGC_8 Danio rerio cDNA clone IMAGE:7245278 5'	6.088741907
ENSDART00(	Q8JHU8 (Q8JHU8) Calpain regulatory subunit, partial (90%) [TC289971]	6.088239486
zgc:101811	Danio rerio zgc:101811 (zgc:101811), mRNA [NM_001006049]	6.087873551
wdr1	Danio rerio WD repeat domain 1 (wdr1), mRNA [NM_201039]	6.087376021
zgc:100925	Danio rerio zgc:100925 (zgc:100925), mRNA [NM_001002746]	6.087182032
hnrpu	Danio rerio heterogeneous nuclear ribonucleoprotein U (hnrpu), mRNA [NM_0010(	6.08717603
nfkb2	Danio rerio nuclear factor of kappa light polypeptide gene enhancer in B-cells 2, p4	6.086829927
nek2	Danio rerio NIMA (never in mitosis gene a)-related kinase 2 (nek2), mRNA [NM_20	6.086507489
acta1	Danio rerio actin, alpha 1, skeletal muscle (acta1), mRNA [NM_131591]	6.086239603
TC285326	O81126 (O81126) 9G8-like SR protein (RSZp22 splicing factor), partial (8%) [TC28	6.085995645
ENSDART00(	BC017532 abhydrolase domain containing 4 {Mus musculus;} , partial (34%) [TC2	6.084823448
zgc:55569	Danio rerio zgc:55569 (zgc:55569), mRNA [NM_200935]	6.08471152
zgc:63555	Danio rerio zgc:63555 (zgc:63555), mRNA [NM_214766]	6.08418077
TC294112	Q9HB90 (Q9HB90) Rag C (Ras-related GTP binding C), partial (84%) [TC294112]	6.08313999
tcerg1	Danio rerio transcription elongation regulator 1 (CA150) (tcerg1), mRNA [NM_1983	6.083109053
malt1	Danio rerio mucosa associated lymphoid tissue lymphoma translocation gene 1 (ma	6.081301385
hnrpu	Danio rerio heterogeneous nuclear ribonucleoprotein U (hnrpu), mRNA [NM_0010(	6.081074529
caspa	caspase a [Source:ZFIN;Acc:ZDB-GENE-000616-3] [ENSDART00000034544]	6.079165294
AI626481	fc06g06.x1 Zebrafish WashU MPIMG EST Danio rerio cDNA clone IMAGE:372063	6.079018699
CN322300	AGENCOURT_21611959 NIH_ZGC_19 Danio rerio cDNA clone IMAGE:7256627 5	6.07784421
vasa	Danio rerio vasa homolog (vasa), mRNA [NM_131057]	6.077682637
zgc:91863	Danio rerio zgc:91863 (zgc:91863), mRNA [NM_001003468]	6.077251279
sb:cb124	STR00147 gastrula stage cDNA library Danio rerio cDNA clone CB124 5', mRNA s	6.076669626
mapkapk2	Danio rerio mitogen-activated protein kinase-activated protein kinase 2 (mapkapk2)	6.076540459
CO350434	DR_AOV_FL10_G04 adult ovary full-length (TLL) Danio rerio cDNA, mRNA sequer	6.076519076
BM034698	fu34f03.y3 zebrafish adult brain Danio rerio cDNA clone IMAGE:5331580 5', mRNA	6.076366595
nras	Danio rerio N-ras oncogene p21 (nras), mRNA [NM_131145]	6.075073811
CV488868	AGENCOURT_33241172 NIH_ZGC_15 Danio rerio cDNA clone IMAGE:7449084 3	6.073947084
zgc:101723	Danio rerio zgc:101723 (zgc:101723), mRNA [NM_001005600]	6.073665347
zgc:92851	Danio rerio zgc:92851 (zgc:92851), mRNA [NM_001002493]	6.073036963
TC269500	Q7ZY90 (Q7ZY90) Plod-prov protein, partial (65%) [TC269500]	6.072699594
hnrpr	Danio rerio heterogeneous nuclear ribonucleoprotein R (hnrpr), mRNA [NM_21342(	6.072635138
TC282628	AVEN_MOUSE (Q9D9K3) Cell death regulator Aven, partial (22%) [TC282628]	6.072535027
ucp4	Danio rerio uncoupling protein 4 (ucp4), mRNA [NM_199523]	6.072442976
rbm4l	Danio rerio RNA binding motif protein 4, like (rbm4l), mRNA [NM_199677]	6.07159113
zgc:92687	Danio rerio zgc:92687 (zgc:92687), mRNA [NM_001004571]	6.071085361
siat6	Danio rerio sialyltransferase 6 (N-acetyllacosaminide alpha 2,3-sialyltransferase) (s	6.070896547
zgc:92191	AGENCOURT_30540912 NIH_ZGC_19 Danio rerio cDNA clone IMAGE:7428255 5	6.07059438
zgc:66438	Danio rerio zgc:66438 (zgc:66438), mRNA [NM_199788]	6.070349628
CN015256	AGENCOURT_21022563 NIH_ZGC_14 Danio rerio cDNA clone IMAGE:7227340 5	6.069678723
wu:fb48d02	fi04g02.x1 Sugano Kawakami zebrafish DRA Danio rerio cDNA clone IMAGE:2600	6.069164194
zgc:92131	Danio rerio zgc:92131 (zgc:92131), mRNA [NM_001004594]	6.068983874
zgc:63526	Danio rerio zgc:63526 (zgc:63526), mRNA [NM_200433]	6.068813879
zgc:92471	Danio rerio zgc:92471 (zgc:92471), mRNA [NM_001002220]	6.06868319
sap18	Danio rerio sin3-associated polypeptide (sap18), mRNA [NM_200720]	6.068637895
zgc:101686	Danio rerio zgc:101686 (zgc:101686), mRNA [NM_001007432]	6.067701358
psmb1	AGENCOURT_20754132 NIH_ZGC_14 Danio rerio cDNA clone IMAGE:7229120 5	6.06752433
dhrs1	Danio rerio dehydrogenase/reductase (SDR family) member 1 (dhrs1), mRNA [NM_	6.067367298
BC090798	Danio rerio cDNA clone MGC:113102 IMAGE:7152841, complete cds. [BC090798]	6.067276596
zgc:100934	Danio rerio zgc:100934 (zgc:100934), mRNA [NM_205618]	6.065852675

zgc:91862	Danio rerio zgc:91862 (zgc:91862), mRNA [NM_001003469]	6.065768418
vps28	Danio rerio vacuolar protein sorting 28 (yeast) (vps28), mRNA [NM_200590]	6.06534452
si:zfos-47c12.	fc29d04.x1 Zebrafish WashU MPIMG EST Danio rerio cDNA clone IMAGE:372279	6.065102835
CN321581	AGENCOURT_21609287 NIH_ZGC_19 Danio rerio cDNA clone IMAGE:7256244 5	6.062658663
TC296080	BC067543 zgc:85610 protein {Danio rerio;} , partial (51%) [TC296080]	6.062146222
wu:fj10g10	fj10g10.x1 Zebrafish adult olfactory Danio rerio cDNA 3', mRNA sequence [AW203	6.061767274
TC286539	Q7SYC9 (Q7SYC9) Sb:cb39, partial (27%) [TC286539]	6.061380739
CK353164	AGENCOURT_17061379 NIH_ZGC_9 Danio rerio cDNA clone IMAGE:7071660 5'	6.060569415
irx6a	AGENCOURT_22402086 NIH_ZGC_9 Danio rerio cDNA clone IMAGE:7274722 5'	6.058856732
zgc:65847	Danio rerio zgc:65847 (zgc:65847), mRNA [NM_213124]	6.05798433
TC285489	MUSCAMC calmodulin {Mus musculus;} , partial (76%) [TC285489]	6.057927645
cops3	Danio rerio COP9 constitutive photomorphogenic homolog subunit 3 (cops3), mRN	6.057418252
zgc:56156	Danio rerio zgc:56156 (zgc:56156), mRNA [NM_200200]	6.056576767
TC283657	CLC2_CAVPO (Q9WU45) Chloride channel protein 2 (ClC-2), partial (29%) [TC283	6.056426176
zgc:101653	Danio rerio zgc:101653 (zgc:101653), mRNA [NM_001007441]	6.055972933
TC291958	Q7ZTM3 (Q7ZTM3) Slc7a8-prov protein, partial (40%) [TC291958]	6.055467254
TC269020	Q6NUU2 (Q6NUU2) Zgc:85935, partial (25%) [TC269020]	6.053848398
zgc:77591	Danio rerio zgc:77591 (zgc:77591), mRNA [NM_214702]	6.052530099
zgc:56708	Danio rerio zgc:56708 (zgc:56708), mRNA [NM_200310]	6.051856841
ap2b1	Danio rerio adaptor-related protein complex 2, beta 1 subunit (ap2b1), mRNA [NM_	6.051741798
c20orf11	STR00853 gastrula stage cDNA library Danio rerio cDNA clone CB482 5' similar to	6.051683932
anxa5	Danio rerio annexin A5 (anxa5), mRNA [NM_181757]	6.050203025
zgc:73265	Danio rerio zgc:73265 (zgc:73265), mRNA [NM_200766]	6.049259515
zgc:56023	Danio rerio zgc:56023 (zgc:56023), mRNA [NM_213054]	6.048707982
rplp0	Danio rerio ribosomal protein, large, P0, mRNA (cDNA clone MGC:77791 IMAGE:7	6.047714412
wu:fj46h05	fj46h05.y1 zebrafish adult brain Danio rerio cDNA 5' similar to gb:X07292_cds1 FR	6.047567815
zgc:103670	Danio rerio zgc:103670 (zgc:103670), mRNA [NM_001004664]	6.047190114
wdr21	Danio rerio WD repeat domain 21 (wdr21), mRNA [NM_200701]	6.046718627
ENSDART00(	AE003479 CG11624-PC {Drosophila melanogaster;} , partial (29%) [TC268183]	6.046034773
CO354205	DR_ATE_FL24_E07 adult testis full-length (TLL) Danio rerio cDNA, mRNA sequen	6.045965873
ndrg3a	Danio rerio N-myc downstream regulated family member 3a (ndrg3a), mRNA [NM_	6.04575896
zgc:55407	Danio rerio zgc:55407 (zgc:55407), mRNA [NM_200236]	6.045282535
TC279982	Q8AVK1 (Q8AVK1) MGC53939 protein, partial (97%) [TC279982]	6.045082498
rpa2	Danio rerio replication protein A2 (rpa2), mRNA [NM_131711]	6.044868441
zgc:77816	Danio rerio zgc:77816 (zgc:77816), mRNA [NM_200869]	6.044692138
zgc:66325	Danio rerio zgc:66325 (zgc:66325), mRNA [NM_201041]	6.044359315
TC298250	Q8JZT2 (Q8JZT2) Solute carrier family 25 (Mitochondrial carrier; phosphate carrier	6.043342389
ak2	Danio rerio adenylate kinase 2 (ak2), mRNA [NM_212596]	6.043195011
zgc:92747	Danio rerio zgc:92747 (zgc:92747), mRNA [NM_001002571]	6.042722121
zgc:101038	Danio rerio zgc:101038 (zgc:101038), mRNA [NM_001003589]	6.042100459
zgc:92284	Danio rerio zgc:92284 (zgc:92284), mRNA [NM_001004583]	6.041197157
rpa2	Danio rerio replication protein A2 (rpa2), mRNA [NM_131711]	6.040747505
BI474280	fp56e05.x3 zebrafish gridded kidney Danio rerio cDNA clone IMAGE:4760553 3', m	6.040642115
tpma	Danio rerio alpha-tropomyosin (tpma), mRNA [NM_131105]	6.040603222
BQ449833	faa61a03.y1 Gong zebrafish testis Danio rerio cDNA clone IMAGE:5898125 5' simi	6.040377748
fgb	Danio rerio fibrinogen, B beta polypeptide (fgb), mRNA [NM_212774]	6.040279051
AI794623	fc46f10.y1 Zebrafish WashU MPIMG EST Danio rerio cDNA clone IMAGE:372445	6.03954934
wu:fc10g05	fc10g05.x1 Zebrafish WashU MPIMG EST Danio rerio cDNA clone IMAGE:372101	6.038340172
wu:fi33h01	AGENCOURT_20754544 NIH_ZGC_15 Danio rerio cDNA clone IMAGE:7224034 5	6.036287497
zgc:92608	Danio rerio zgc:92608 (zgc:92608), mRNA [NM_001002706]	6.035916205
ENSDART00(	AGENCOURT_21030952 NIH_ZGC_8 Danio rerio cDNA clone IMAGE:7248997 5'	6.034950868
wu:fc22a07	Danio rerio wu:fc22a07 (wu:fc22a07), mRNA [NM_212669]	6.034750738
zgc:73293	Danio rerio zgc:73293 (zgc:73293), mRNA [NM_213028]	6.034355596
tcp1	Danio rerio t-complex polypeptide 1 (tcp1), mRNA [NM_131230]	6.034193178
TC297900	Q9QZ66 (Q9QZ66) Amino acid transporter y+LAT1, partial (22%) [TC297900]	6.034081465
wu:fj54e12	AGENCOURT_17517280 NIH_ZGC_4 Danio rerio cDNA clone IMAGE:7120599 5'	6.033718356
ldb3l	Danio rerio LIM domain binding 3 like (ldb3l), mRNA [NM_199858]	6.033398941
TC270041	CE05_HUMAN (Q9NYF5) Protein C5orf5 (GAP-like protein N61), partial (34%) [TC	6.033011817
scamp2	Danio rerio secretory carrier membrane protein 2 (scamp2), mRNA [NM_213378]	6.032855781
TC292314	Unknown	6.031590041
TC278021	GPXC_DIRIM (P52033) Glutathione peroxidase precursor (Di29) , partial (52%) [T	6.030652385
mp:zf637-1-0(	ZF637-1-000125 Zebrafish shield stage whole embryo cDNA library MPMGp637 Di	6.030292957
cldnd	Danio rerio claudin d (cldnd), mRNA [NM_180964]	6.030130028
ENSDART00(	Q9BWT1 (Q9BWT1) C-Myc target JPO1 (Cell division cycle associated protein 7, is	6.029726367
zgc:92131	Danio rerio zgc:92131 (zgc:92131), mRNA [NM_001004594]	6.029493644
zgc:76953	Danio rerio zgc:76953 (zgc:76953), mRNA [NM_214759]	6.02925996
BC083442	Danio rerio cDNA clone IMAGE:7254682. [BC083442]	6.029224134
zgc:64123	Danio rerio zgc:64123 (zgc:64123), mRNA [NM_213135]	6.029172772
sfrs5	Danio rerio splicing factor, arginine/serine-rich 5 (sfrs5), mRNA [NM_200867]	6.028886694
terfa	Danio rerio telomeric repeat binding factor a (terfa), mRNA [NM_173243]	6.028734016
TC269859	2BCC_H Chain H, Stigmatellin-Bound Cytochrome Bc1 Complex From Chicken. {G	6.028373985
zgc:101865	Danio rerio zgc:101865 (zgc:101865), mRNA [NM_001007378]	6.028337972
exosc4	Danio rerio exosome component 4 (exosc4), mRNA [NM_200739]	6.028160818
ap2b1	Danio rerio adaptor-related protein complex 2, beta 1 subunit (ap2b1), mRNA [NM_	6.028153731
BG729087	fp04e02.x1 zebrafish gridded kidney Danio rerio cDNA clone IMAGE:4728651 3' sir	6.027402786
TC297639	NIMM_MOUSE (O35683) NADH-ubiquinone oxidoreductase MWFE subunit (Com	6.02738127
TC301431	O42444 (O42444) Chemokine receptor, partial (32%) [TC301431]	6.027124318
sfpq	Danio rerio splicing factor proline/glutamine rich (polypyrimidine tract binding protei	6.027076605
cth	Danio rerio cystathionase (cystathionine gamma-lyase) (cth), mRNA [NM_212604]	6.025860548
zgc:77377	Danio rerio zgc:77377 (zgc:77377), mRNA [NM_213272]	6.025635271
zgc:66321	Danio rerio zgc:66321 (zgc:66321), mRNA [NM_201118]	6.025567325

zgc:77542	Danio rerio zgc:77542 (zgc:77542), mRNA [NM_212636]	6.025472963
zgc:103472	Danio rerio zgc:103472 (zgc:103472), mRNA [NM_001008611]	6.025035205
ENSDART00(	Q9I932 (Q9I932) Complement C4-2, partial (29%) [TC295319]	6.02422265
CO356423	DR_ATE_NRM19_E08 adult testis normalized (TLL) Danio rerio cDNA, mRNA seq	6.023823256
CN500606	AGENCOURT_22440389 NIH_ZGC_9 Danio rerio cDNA clone IMAGE:7271251 5'	6.023821155
TC297755	Q812D6 (Q812D6) Lingerer protein-1, partial (23%) [TC297755]	6.023501507
scarb1	Danio rerio scavenger receptor class B, member 1 (scarb1), mRNA [NM_198921]	6.022737755
si:ch211-101l	fb67g03.y1 Zebrafish WashU MPIMG EST Danio rerio cDNA clone IMAGE:371698	6.022516276
CN322300	AGENCOURT_21611959 NIH_ZGC_19 Danio rerio cDNA clone IMAGE:7256627 5	6.022379586
cd9l	Danio rerio CD9 antigen, like (cd9l), mRNA [NM_213428]	6.022045602
zgc:56218	Danio rerio zgc:56218 (zgc:56218), mRNA [NM_199700]	6.021528907
TC284132	Q9UWD6 (Q9UWD6) Ac-type transposase homolog (Fragment), partial (39%) [TC2	6.020958813
TC275584	GB13_HUMAN (Q14344) Guanine nucleotide-binding protein, alpha-13 subunit (G	6.020086439
TC290051	Q8JHI0 (Q8JHI0) Solute carrier family 25 member 5 protein (Solute carrier family 2	6.019872932
BC076165	Danio rerio cDNA clone IMAGE:7073958, partial cds. [BC076165]	6.019153208
flj10613l	Danio rerio guanine nucleotide binding protein-like 3 (nucleolar)-like (gnl3l), mRNA	6.018627444
TC271513	BC054651 zgc:66137 {Danio rerio;} , complete [TC271513]	6.018197994
ENSDART00(	fb11a09.y1 zebrafish fin day0 regeneration Danio rerio cDNA 5' similar to gb:X611	6.017567784
BC085675	Danio rerio cDNA clone MGC:92577 IMAGE:5912857, complete cds. [BC085675]	6.017147264
wu:fk84g05	AGENCOURT_20186052 NIH_ZGC_15 Danio rerio cDNA clone IMAGE:7226726 5	6.01663277
zgc:55807	Danio rerio zgc:55807 (zgc:55807), mRNA [NM_212757]	6.016361797
wu:fi26g08	AGENCOURT_16392001 NIH_ZGC_7 Danio rerio cDNA clone IMAGE:7036272 5'	6.015767614
btg1	Danio rerio B-cell translocation gene 1 (btg1), mRNA [NM_200020]	6.015712471
zgc:85979	Danio rerio zgc:85979 (zgc:85979), mRNA [NM_213259]	6.014887256
gnai2l	Danio rerio guanine nucleotide binding protein (G protein), alpha inhibiting activity p	6.014795153
Gamt	Danio rerio guanidinoacetate N-methyltransferase (Gamt), mRNA [NM_205741]	6.014706845
zgc:66471	Danio rerio zgc:66471 (zgc:66471), mRNA [NM_212684]	6.013872411
BI865759	ft26f02.x1 Zebrafish neuronal Danio rerio cDNA clone IMAGE:5082747 3' similar to	6.013768792
stka	Danio rerio serine/threonine kinase a (stka), mRNA [NM_212566]	6.013538787
gstal	Danio rerio glutathione S-transferase, alpha-like (gstal), mRNA [NM_213394]	6.012452458
nola2	Danio rerio nucleolar protein family A, member 2 (H/ACA small nucleolar RNPs), m	6.012389194
dap1b	Danio rerio death associated protein 1b (dap1b), mRNA [NM_131573]	6.012314208
hic1l	Danio rerio hypermethylated in cancer zinc finger/POZ-domain 1 protein (hzp1) mR	6.01183075
zgc:66034	Danio rerio zgc:66034 (zgc:66034), mRNA [NM_199606]	6.011580347
zgc:56632	Danio rerio zgc:56632 (zgc:56632), mRNA [NM_213404]	6.011295542
zgc:56424	Danio rerio zgc:56424 (zgc:56424), mRNA [NM_200306]	6.011272432
zgc:56692	Danio rerio zgc:56692 (zgc:56692), mRNA [NM_213104]	6.011114054
zgc:85763	Danio rerio zgc:85763 (zgc:85763), mRNA [NM_212788]	6.010042402
zgc:77243	Danio rerio zgc:77243 (zgc:77243), mRNA [NM_205544]	6.009326688
CK401034	AGENCOURT_17518620 NIH_ZGC_4 Danio rerio cDNA clone IMAGE:7116651 5'	6.0091128
atad1b	AGENCOURT_10700583 NCI_CGAP_ZKid1 Danio rerio cDNA clone IMAGE:6796	6.008960277
BQ481013	faa73g09.x1 Gong zebrafish testis Danio rerio cDNA clone IMAGE:5899577 3', mR	6.00895105
TC293627	Q7L5N2 (Q7L5N2) LENG4 protein (Fragment), partial (41%) [TC293627]	6.008354308
BC076555	Danio rerio cDNA clone IMAGE:7044154, partial cds. [BC076555]	6.008225466
zgc:103522	Danio rerio zgc:103522 (zgc:103522), mRNA [NM_001005993]	6.007856317
titf1b	Danio rerio thyroid transcription factor 1b (titf1b), mRNA [NM_131776]	6.007807996
TC291286	BC055209 zgc:63694 {Danio rerio;} , partial (24%) [TC291286]	6.007788673
TC269295	Q80TY1 (Q80TY1) MKIAA0553 protein (Fragment), partial (35%) [TC269295]	6.007278399
zgc:55852	Danio rerio zgc:55852 (zgc:55852), mRNA [NM_199567]	6.006937956
zgc:85947	Danio rerio zgc:85947 (zgc:85947), mRNA [NM_214740]	6.006639545
wu:fc27f04	fc27f04.x1 Zebrafish WashU MPIMG EST Danio rerio cDNA clone IMAGE:372262	6.006456955
zgc:56252	Danio rerio zgc:56252 (zgc:56252), mRNA [NM_213387]	6.006063041
ENSDART00(	fl95c07.y1 Zebrafish adult retina cDNA Danio rerio cDNA clone IMAGE:4144501 5'	6.004828136
rplp0	Danio rerio ribosomal protein, large, P0, mRNA (cDNA clone MGC:77791 IMAGE:7	6.004451108
zgc:55345	Danio rerio zgc:55345 (zgc:55345), mRNA [NM_200128]	6.004237303
zgc:77739	Danio rerio zgc:77739 (zgc:77739), mRNA [NM_200896]	6.003723572
zgc:65964	Danio rerio zgc:65964 (zgc:65964), mRNA [NM_200584]	6.003406047
zgc:73343	Danio rerio zgc:73343 (zgc:73343), mRNA [NM_213021]	6.001634617
TC291062	BC066558 zgc:77429 protein {Danio rerio;} , complete [TC291062]	6.000476463
wu:fb99c01	fb99c01.y1 Zebrafish WashU MPIMG EST Danio rerio cDNA clone IMAGE:372000	5.999753007
zgc:66471	Danio rerio zgc:66471 (zgc:66471), mRNA [NM_212684]	5.999533804
seta	SET translocation (myeloid leukemia-associated) A [Source:ZFIN;Acc:ZDB-GENE-	5.999435782
CK028474	CK028474 AGENCOURT_16620115 NIH_ZGC_7 Danio rerio cDNA clone IMAGE:	5.999327194
wu:fb66g07	AGENCOURT_20753534 NIH_ZGC_15 Danio rerio cDNA clone IMAGE:7222818 5	5.999027044
ssb	Danio rerio Sjogren syndrome antigen B (autoantigen La) (ssb), mRNA [NM_19954	5.998145578
im:7140002	DR_ATE_ORE38_G11 adult testis ORESTES (TLL) Danio rerio cDNA, mRNA sequ	5.997570716
zgc:56380	Danio rerio zgc:56380 (zgc:56380), mRNA [NM_200951]	5.996359023
TC269516	Q7Q517 (Q7Q517) AgCP6688 (Fragment), partial (7%) [TC269516]	5.99604003
wu:fc16a12	fc16a12.x1 Zebrafish WashU MPIMG EST Danio rerio cDNA clone IMAGE:372153	5.995866037
ivd	Danio rerio isovaleryl Coenzyme A dehydrogenase (ivd), mRNA [NM_201491]	5.995419012
gnai2l	Danio rerio guanine nucleotide binding protein (G protein), alpha inhibiting activity p	5.995189615
arf2	Danio rerio ADP-ribosylation factor 2 (arf2), mRNA [NM_201504]	5.994439035
TC272147	Q99MB3 (Q99MB3) Beta-amyloid binding protein, partial (57%) [TC272147]	5.99411764
zgc:73223	Danio rerio zgc:73223 (zgc:73223), mRNA [NM_200832]	5.993904103
sb:cb1058	AGENCOURT_19414472 NIH_ZGC_16 Danio rerio cDNA clone IMAGE:7212276 5	5.993673664
TC286583	Q7TPA6 (Q7TPA6) Ab1-042, partial (33%) [TC286583]	5.992647983
zgc:63694	Danio rerio zgc:63694 (zgc:63694), mRNA [NM_213106]	5.991527667
hgd	Danio rerio homogentisate 1,2-dioxygenase (hgd), mRNA [NM_152966]	5.991356051
npc2	Danio rerio Niemann-Pick disease, type C2 (npc2), mRNA [NM_173224]	5.990875572
CN512008	AGENCOURT_22824380 NIH_ZGC_9 Danio rerio cDNA clone IMAGE:7277066 5'	5.990676595
zgc:65915	Danio rerio zgc:65915 (zgc:65915), mRNA [NM_200822]	5.990492912

zgc:55257	Danio rerio zgc:55257 (zgc:55257), mRNA [NM_200078]	5.990409955
zgc:77845	Danio rerio zgc:77845 (zgc:77845), mRNA [NM_213194]	5.990401004
zgc:55366	Danio rerio zgc:55366 (zgc:55366), mRNA [NM_199806]	5.990236997
psmd13	Danio rerio proteasome (prosome, macropain) 26S subunit, non-ATPase, 13 (psmc	5.989909845
rpl10a	Danio rerio ribosomal protein L10a (rpl10a), mRNA [NM_199636]	5.989827334
CN836645	AGENCOURT_25168842 NIH_ZGC_4 Danio rerio cDNA clone IMAGE:7295017 5'	5.989602798
hnrpk	Danio rerio heterogeneous nuclear ribonucleoprotein K (hnrpk), mRNA [NM_21299	5.989503573
ENSDART00(	HSU79457 WW domain binding protein-1 {Homo sapiens;} , partial (22%) [TC2984	5.989354837
zgc:101801	Danio rerio zgc:101801 (zgc:101801), mRNA [NM_001006052]	5.989285302
ack1	fj16g04.x1 Zebrafish adult olfactory Danio rerio cDNA 3' similar to TR:O54967 O54	5.989205383
snrp70	Danio rerio small nuclear ribonucleoprotein 70kDa (snrp70), mRNA [NM_00100387	5.988598453
zgc:92082	Danio rerio zgc:92082 (zgc:92082), mRNA [NM_001002374]	5.988327268
zgc:91794	Danio rerio zgc:91794 (zgc:91794), mRNA [NM_001002217]	5.988091078
atp6ap1	Danio rerio ATPase, H+ transporting, lysosomal accessory protein 1 (atp6ap1), mR	5.987893501
gas8	Danio rerio growth arrest-specific 8 (gas8), mRNA [NM_199634]	5.987434867
smc1l1	Danio rerio chromosome adhesion protein SMC1-like mRNA, complete cds. [AY64	5.987396777
lyricl	Danio rerio lyric-like (lyricl), mRNA [NM_001007135]	5.98710293
ENSDART00(	VP36_HUMAN (Q12907) Vesicular integral-membrane protein VIP36 precursor (GI	5.986903682
BC085675	Danio rerio cDNA clone MGC:92577 IMAGE:5912857, complete cds. [BC085675]	5.986683816
zgc:77591	Danio rerio zgc:77591 (zgc:77591), mRNA [NM_214702]	5.98658165
ENSDART00(	Q93W25 (Q93W25) Cyclophilin A-3 (Cyclophilin A-1) , partial (73%) [TC285677]	5.986379353
max	Danio rerio myc-associated factor X, mRNA (cDNA clone IMAGE:6795370), partial	5.986276156
ENSDART00(	Unknown	5.985036751
zgc:55877	Danio rerio zgc:55877 (zgc:55877), mRNA [NM_213070]	5.984891603
BC083472	Danio rerio cDNA clone IMAGE:7265391. [BC083472]	5.984656599
ttll1	Danio rerio tubulin tyrosine ligase-like family, member 1 (ttll1), mRNA [NM_201019	5.984318326
TC296240	Q8VI63 (Q8VI63) Ovary-specific MOB-like protein, partial (86%) [TC296240]	5.984300931
TC291536	Unknown	5.984273793
tpi1a	Danio rerio triosephosphate isomerase 1a, mRNA (cDNA clone MGC:56599 IMAGI	5.984024637
TC272179	Q6P424 (Q6P424) MGC68627 protein, partial (71%) [TC272179]	5.984016928
CK016848	AGENCOURT_16544339 NIH_ZGC_10 Danio rerio cDNA clone IMAGE:7043477 5	5.98393166
TC268141	Q6NYT6 (Q6NYT6) LOC407660 protein (Fragment), complete [TC268141]	5.983790783
zgc:56195	Danio rerio zgc:56195 (zgc:56195), mRNA [NM_212995]	5.983337282
wu:fk48d07	AGENCOURT_30432586 NIH_ZGC_14 Danio rerio cDNA clone IMAGE:7409038 5	5.983266638
flj10613l	Danio rerio guanine nucleotide binding protein-like 3 (nucleolar)-like (gnl3l), mRNA	5.982778586
zgc:101814	Danio rerio zgc:101814 (zgc:101814), mRNA [NM_001006048]	5.98274273
zgc:76917	Danio rerio zgc:76917 (zgc:76917), mRNA [NM_200182]	5.982480258
rarg	Danio rerio retinoic acid receptor gamma (rarg), mRNA [NM_131339]	5.981361507
zgc:73333	Danio rerio zgc:73333 (zgc:73333), mRNA [NM_199932]	5.981100583
BM102193	fv14c08.x1 zebrafish adult brain Danio rerio cDNA clone IMAGE:5386383 3', mRNA	5.980945343
CN023559	AGENCOURT_20191286 NIH_ZGC_15 Danio rerio cDNA clone IMAGE:7225601 5	5.980898772
zgc:55709	Danio rerio zgc:55709 (zgc:55709), mRNA [NM_212715]	5.980831131
zgc:55648	Danio rerio zgc:55648 (zgc:55648), mRNA [NM_200138]	5.98083084
zgc:65996	AGENCOURT_21848961 NIH_ZGC_8 Danio rerio cDNA clone IMAGE:7261455 5'	5.980550286
zp2.3	Danio rerio zona pellucida glycoprotein 2.3 (zp2.3), mRNA [NM_131828]	5.980127035
zgc:56095	Danio rerio zgc:56095 (zgc:56095), mRNA [NM_213013]	5.979179109
zgc:85738	Danio rerio zgc:85738 (zgc:85738), mRNA [NM_214820]	5.978700846
ENSDART00(	O57397 (O57397) Nuclear pore complex glycoprotein p62, partial (46%) [TC26914	5.978219848
TC281523	BC053221 zgc:64046 {Danio rerio;} , partial (98%) [TC281523]	5.977546889
zgc:92414	Danio rerio zgc:92414 (zgc:92414), mRNA [NM_001002332]	5.977541534
mfap1	Danio rerio microfibrillar-associated protein 1 (mfap1), mRNA [NM_201017]	5.977315813
zgc:77303	Danio rerio zgc:77303 (zgc:77303), mRNA [NM_205653]	5.977314125
sf3a1	Danio rerio splicing factor 3a, subunit 1 (sf3a1), mRNA [NM_200094]	5.976835104
zgc:65811	Danio rerio zgc:65811 (zgc:65811), mRNA [NM_200552]	5.975487456
gtf2b	Danio rerio general transcription factor IIB (gtf2b), mRNA [NM_199697]	5.975190553
AL726525	AL726525 Danio rerio embryonic inner ear subtracted cDNA Danio rerio cDNA clor	5.974892043
rab2	RAB2, member RAS oncogene family [Source:ZFIN;Acc:ZDB-GENE-011212-2] [E	5.973077882
TC283786	Q6UX76 (Q6UX76) PP1665, partial (21%) [TC283786]	5.972771699
etv5	Danio rerio ets variant gene 5 (ets-related molecule) (etv5), mRNA [NM_214720]	5.97155337
zgc:77634	Danio rerio zgc:77634 (zgc:77634), mRNA [NM_200865]	5.970964485
wu:fi19h12	fi19h12.x1 Sugano Kawakami zebrafish DRA Danio rerio cDNA clone IMAGE:2601	5.970514488
Gamt	Danio rerio guanidinoacetate N-methyltransferase (Gamt), mRNA [NM_205741]	5.970039453
BM572001	fx05g04.y1 Gong zebrafish ovary Danio rerio cDNA clone IMAGE:5619246 5', mRN	5.969393671
zgc:56315	Danio rerio zgc:56315 (zgc:56315), mRNA [NM_201177]	5.968987289
vps35	fa66e03.s1 zebrafish fin day3 regeneration Danio rerio cDNA clone zbr2453 3', mR	5.968697739
ENSDART00(	SI:bZ1M12.3 (Novel protein similar to vertebrate junctophilins) (Fragment). [Source	5.968396821
TC281872	Q8AVC0 (Q8AVC0) Shmt1-prov protein, partial (40%) [TC281872]	5.967659196
prps1a	Danio rerio phosphoribosyl pyrophosphate synthetase 1A (prps1a), mRNA [NM_21	5.967317209
zgc:77225	Danio rerio zgc:77225 (zgc:77225), mRNA [NM_212785]	5.967109845
zfp36l1	AGENCOURT_16619068 NIH_ZGC_7 Danio rerio cDNA clone IMAGE:7053011 5'	5.966463614
ENSDART00(	Q98SS2 (Q98SS2) Egg envelope protein ZP2 variant B, partial (78%) [TC267946]	5.965917024
TC269857	Q6PCE6 (Q6PCE6) MGC69179 protein, partial (74%) [TC269857]	5.964857755
TC274241	Q7PI42 (Q7PI42) ENSANGP00000024316 (Fragment), partial (7%) [TC274241]	5.96403496
CF594979	AGENCOURT_15713286 NIH_ZGC_8 Danio rerio cDNA clone IMAGE:7015218 5'	5.963977707
CN316528	AGENCOURT_21844520 NIH_ZGC_10 Danio rerio cDNA clone IMAGE:7259378 5	5.963840718
wu:fe14h10	fe14h10.y1 Zebrafish WashU MPIMG EST Danio rerio cDNA clone IMAGE:373888	5.963479178
zgc:100812	Danio rerio zgc:100812 (zgc:100812), mRNA [NM_001003548]	5.963312495
TC267954	RBM8_HUMAN (Q9Y5S9) RNA-binding protein 8A (RNA binding motif protein 8A)	5.963227048
gpd1l	Danio rerio glycerol-3-phosphate dehydrogenase 1 (soluble), like (gpd1l), mRNA [N	5.962791901
cct2	Danio rerio chaperonin containing TCP1, subunit 2 (beta) (cct2), mRNA [NM_2014	5.962468812
mmp14b	Danio rerio matrix metalloproteinase 14 (membrane-inserted) beta (mmp14b), mRN	5.962283559

zgc:92414	Danio rerio zgc:92414 (zgc:92414), mRNA [NM_001002332]	5.962008115
flj12949l	Danio rerio hypothetical protein FLJ12949-like (H. sapiens) (flj12949l), mRNA [NM_	5.961853094
TC291829	BC048055 NIMA (never in mitosis gene a)-related kinase 2 {Danio rerio;} , complet	5.961833456
atp5d	Danio rerio ATP synthase, H+ transporting, mitochondrial F1 complex, delta subuni	5.960488408
zgc:55280	Danio rerio zgc:55280 (zgc:55280), mRNA [NM_212621]	5.960390712
gnai1	Danio rerio guanine nucleotide binding protein (G protein), alpha inhibiting activity p	5.96013317
TC280087	GOP3_MOUSE (Q9CRA5) Golgi phosphoprotein 3 (Coat-protein GPP34), partial (9	5.960010478
TC290427	Q7ZZR0 (Q7ZZR0) Methyl-CpG binding protein 3b, complete [TC290427]	5.959747549
zgc:103772	Danio rerio zgc:103772 (zgc:103772), mRNA [NM_001006005]	5.959284529
CK027543	AGENCOURT_16623603 NIH_ZGC_7 Danio rerio cDNA clone IMAGE:7053792 5'	5.958847788
zgc:92801	Danio rerio zgc:92801 (zgc:92801), mRNA [NM_001002535]	5.958733827
TC272553	Q8BYY5 (Q8BYY5) Mus musculus 6 days neonate skin cDNA, RIKEN full-length en	5.957731095
yars	Danio rerio tyrosyl-tRNA synthetase (yars), mRNA [NM_201316]	5.957268845
hnrpr	Danio rerio heterogeneous nuclear ribonucleoprotein R (hnrpr), mRNA [NM_21342	5.957043058
wbp2	Danio rerio WW domain binding protein 2 (wbp2), mRNA [NM_199710]	5.956997914
psmc3	Danio rerio proteasome (prosome, macropain) 26S subunit, ATPase, 3 (psmc3), m	5.956468508
AL917199	AL917199 PJR-Z1+Z2 Danio rerio cDNA clone 028-E06-2, mRNA sequence [AL91	5.956297754
tardbp	Danio rerio TAR DNA binding protein (tardbp), mRNA [NM_201476]	5.956028613
zgc:65964	Danio rerio zgc:65964 (zgc:65964), mRNA [NM_200584]	5.955760312
hfe2	Danio rerio hemochromatosis type 2 (hfe2), mRNA [NM_213643]	5.955625936
ENSDART00(	AGENCOURT_21411257 NIH_ZGC_17 Danio rerio cDNA clone IMAGE:7236499 5	5.955595115
fth1	Danio rerio ferritin, heavy polypeptide 1 (fth1), mRNA [NM_131585]	5.954437773
ywhaz	Danio rerio tyrosine 3-monooxygenase/tryptophan 5-monooxygenase activation prc	5.954116986
met	Danio rerio met proto-oncogene (hepatocyte growth factor receptor) (met), mRNA [	5.954079803
Gamt	Danio rerio guanidinoacetate N-methyltransferase (Gamt), mRNA [NM_205741]	5.953788547
zgc:64201	Danio rerio zgc:64201 (zgc:64201), mRNA [NM_200642]	5.953527628
zgc:65891	Danio rerio zgc:65891 (zgc:65891), mRNA [NM_200594]	5.953365165
AI959529	fd10f06.x1 Zebrafish WashU MPIMG EST Danio rerio cDNA clone IMAGE:373049	5.952622102
mef2c	Danio rerio myocyte enhancer factor 2c (mef2c), mRNA [NM_131312]	5.952043925
CK395556	AGENCOURT_17389578 NIH_ZGC_4 Danio rerio cDNA clone IMAGE:7120218 5'	5.951539962
TC283346	Q9KFR6 (Q9KFR6) BH0411 protein, partial (5%) [TC283346]	5.951496104
wu:fb55g09	AGENCOURT_16624119 NIH_ZGC_10 Danio rerio cDNA clone IMAGE:7050545 5	5.951201989
wu:fb55a06	fb55a06.x1 Zebrafish WashU MPIMG EST Danio rerio cDNA clone IMAGE:371576	5.950734095
ENSDART00(	Q78JW9 (Q78JW9) D7Wsu128e protein, partial (74%) [TC292735]	5.950321974
TC290699	CLDZ_BRARE (Q9YH90) Claudin-like protein ZF-A9, complete [TC290699]	5.949800799
wu:fb98h03	fb54c06.x1 Zebrafish WashU MPIMG EST Danio rerio cDNA clone IMAGE:371569	5.949591045
zgc:64178	Danio rerio zgc:64178 (zgc:64178), mRNA [NM_199936]	5.949495119
zgc:77049	Danio rerio zgc:77049 (zgc:77049), mRNA [NM_212874]	5.949418546
zgc:101826	Danio rerio zgc:101826 (zgc:101826), mRNA [NM_001004677]	5.948764181
arpp19	Danio rerio cAMP-regulated phosphoprotein 19 (arpp19), mRNA [NM_200630]	5.948278954
zgc:56086	Danio rerio zgc:56086 (zgc:56086), mRNA [NM_200975]	5.947587355
TC279431	Q802U8 (Q802U8) H1 histone family, member X, complete [TC279431]	5.947412565
TC291559	Q6PBN6 (Q6PBN6) Inositol hexaphosphate kinase 2, complete [TC291559]	5.946907484
ENSDART00(	AE003479 CG11624-PC {Drosophila melanogaster;} , partial (29%) [TC268183]	5.946393091
TC292243	Q8AVK0 (Q8AVK0) Dars-prov protein, partial (61%) [TC292243]	5.94610707
zgc:92313	Danio rerio zgc:92313 (zgc:92313), mRNA [NM_001002596]	5.946055466
ift172	Danio rerio intraflagellar transport 172 (ift172), mRNA [NM_001002312]	5.945598965
TC288572	Q802C9 (Q802C9) Eukaryotic translation initiation factor 4A, isoform 1A, partial (40	5.94552598
TC273084	SYIM_YEAST (P48526) Isoleucyl-tRNA synthetase, mitochondrial (Isoleucine--tRN	5.945318466
cdk9	Danio rerio cyclin-dependent kinase 9 (CDC2-related kinase) (cdk9), mRNA [NM_2	5.94462955
CO350383	DR_AOV_FL10_B04 adult ovary full-length (TLL) Danio rerio cDNA, mRNA sequer	5.944594726
zgc:64178	Danio rerio zgc:64178 (zgc:64178), mRNA [NM_199936]	5.94443308
plp2	AL916381 PJR-Z1+Z2 Danio rerio cDNA clone 014-F05-2, mRNA sequence [AL91	5.943845602
reverbb2	Danio rerio rev erb beta 2 (reverbb2), mRNA [NM_131065]	5.943736593
zgc:100934	Danio rerio zgc:100934 (zgc:100934), mRNA [NM_205618]	5.943456358
zgc:85649	Danio rerio cDNA clone MGC:85649 IMAGE:6805750, complete cds. [BC067558]	5.94340226
TC290307	Q8JHI0 (Q8JHI0) Solute carrier family 25 member 5 protein (Solute carrier family 2	5.943202055
sepw1	Danio rerio selenoprotein W, 1 (sepw1), mRNA [NM_178287]	5.94316921
zgc:63637	Danio rerio zgc:63637 (zgc:63637), mRNA [NM_213365]	5.942879138
tkt	Danio rerio transketolase (tkt), mRNA [NM_198070]	5.942460614
zgc:55881	Danio rerio zgc:55881 (zgc:55881), mRNA [NM_199721]	5.942407238
ivd	Danio rerio isovaleryl Coenzyme A dehydrogenase (ivd), mRNA [NM_201491]	5.942386878
cyp1a	Danio rerio cytochrome P450, family 1, subfamily A (cyp1a), mRNA [NM_131879]	5.94233174
wu:fb40a10	AGENCOURT_16620780 NIH_ZGC_7 Danio rerio cDNA clone IMAGE:7055414 5'	5.942266072
wu:fb06e02	AGENCOURT_32341965 NIH_ZGC_15 Danio rerio cDNA clone IMAGE:7450065 5	5.94158148
zgc:63736	Danio rerio zgc:63736 (zgc:63736), mRNA [NM_200486]	5.941511984
TC293438	Unknown	5.941050021
dt1p1a10l	Danio rerio hypothetical protein DT1P1A10 (human) - like (dt1p1a10l), mRNA [NM_	5.940847704
calr	Danio rerio calreticulin (calr), mRNA [NM_131047]	5.940839487
zgc:55783	Danio rerio zgc:55783 (zgc:55783), mRNA [NM_201098]	5.940680974
cox4i1	Danio rerio cytochrome c oxidase subunit IV isoform 1 (cox4i1), mRNA [NM_21470	5.940100151
TC268266	Q7ZU62 (Q7ZU62) Ik:tdsubc_1f2 protein (Fragment), partial (45%) [TC268266]	5.939643628
zgc:55931	Danio rerio zgc:55931 (zgc:55931), mRNA [NM_213663]	5.938846483
zgc:77825	Danio rerio zgc:77825 (zgc:77825), mRNA [NM_205643]	5.938671572
wu:fk47a03	fk47a03.y1 Zebrafish 15-19hr embryonic cDNA Danio rerio cDNA 5', mRNA sequer	5.938189236
atp13a	Danio rerio ATPase type 13A (atp13a), mRNA [NM_001001403]	5.937524983
sf3a1	Danio rerio splicing factor 3a, subunit 1 (sf3a1), mRNA [NM_200094]	5.93648294
hdac1	Danio rerio histone deacetylase 1, mRNA (cDNA clone MGC:101582 IMAGE:7223	5.936349874
ENSDART00(	fv73b01.y1 zebrafish adult brain Danio rerio cDNA clone IMAGE:5413968 5' similar	5.936301887
wu:fc80b03	fc80b03.x1 Zebrafish WashU MPIMG EST Danio rerio cDNA clone IMAGE:372766	5.935650188
zgc:103591	Danio rerio zgc:103591 (zgc:103591), mRNA [NM_001004681]	5.935138301

zgc:91819	Danio rerio zgc:91819 (zgc:91819), mRNA [NM_205594]	5.934061933
ldb3	Danio rerio LIM-domain binding factor 3 (ldb3), mRNA [NM_201505]	5.933861727
TC280006	Q6NZZ2 (Q6NZZ2) Actin related protein 2/3 complex subunit 4, complete [TC2800	5.933305706
ENSDART00(	Q8AVT5 (Q8AVT5) Mg:db03h09-prov protein, partial (57%) [TC292842]	5.932330841
TC274542	Q8CED3 (Q8CED3) Mus musculus 0 day neonate skin cDNA, RIKEN full-length en	5.932045137
ENSDART00(	fc83c01.y1 Zebrafish WashU MPIMG EST Danio rerio cDNA clone IMAGE:372796	5.931979988
BG306386	fm58d10.x1 Zebrafish adult retina cDNA Danio rerio cDNA clone IMAGE:4199491 3	5.93174152
TC269058	Q90ZC9 (Q90ZC9) Granulin 2, complete [TC269058]	5.930922154
zgc:66022	Danio rerio zgc:66022 (zgc:66022), mRNA [NM_200536]	5.930865243
zgc:92115	Danio rerio zgc:92115 (zgc:92115), mRNA [NM_001004544]	5.930763629
CN171076	AGENCOURT_21022083 NIH_ZGC_8 Danio rerio cDNA clone IMAGE:7250782 5'	5.930394959
zgc:63476	Danio rerio zgc:63476 (zgc:63476), mRNA [NM_213528]	5.930069383
A_15_P10005	Unknown	5.930027825
zgc:66137	Danio rerio zgc:66137 (zgc:66137), mRNA [NM_213477]	5.929292415
rab1a	Danio rerio RAB1A, member RAS oncogene family (rab1a), mRNA [NM_00100716	5.929065844
zgc:77065	Danio rerio zgc:77065 (zgc:77065), mRNA [NM_212884]	5.928737177
wu:fb02e09	Danio rerio wu:fb02e09 (wu:fb02e09), mRNA [NM_213638]	5.928098797
BI473831	fp47d01.y3 zebrafish gridded kidney Danio rerio cDNA clone IMAGE:4759728 5', m	5.92806251
zgc:101832	Danio rerio zgc:101832 (zgc:101832), mRNA [NM_001007383]	5.927874595
BM026694	fq86e12.y3 Zebrafish neuronal Danio rerio cDNA clone IMAGE:4887262 5', mRNA	5.927737607
zgc:66485	Danio rerio zgc:66485 (zgc:66485), mRNA [NM_200051]	5.927493841
TC292344	Q9I903 (Q9I903) Beta-catenin-interacting protein, complete [TC292344]	5.927422668
zgc:63790	Danio rerio zgc:63790 (zgc:63790), mRNA [NM_199896]	5.927171386
ing3	Danio rerio inhibitor of growth family, member 3 (ing3), mRNA [NM_200937]	5.926770185
zgc:56109	Danio rerio zgc:56109 (zgc:56109), mRNA [NM_199911]	5.926562946
wu:fb75d06	AGENCOURT_10697964 NCI_CGAP_ZKid1 Danio rerio cDNA clone IMAGE:6791	5.92599957
zgc:92231	Danio rerio zgc:92231 (zgc:92231), mRNA [NM_001004584]	5.92590264
ENSDART00(	GEM2_RAT (Q9QZP1) Survival of motor neuron protein-interacting protein 1 (SMN	5.924825821
BC090786	Danio rerio cDNA clone IMAGE:7152284. [BC090786]	5.924725918
BI980240	ft73h01.x1 Gong zebrafish ovary Danio rerio cDNA clone IMAGE:5159256 3', mRN	5.924214526
nitr5	Danio rerio novel immune-type receptor 5 (nitr5), mRNA [NM_001005768]	5.921377105
LOC493626	Danio rerio ras-dva small GTPase (LOC493626), mRNA [NM_001007781]	5.921349515
wu:fc35f01	fc35f01.x1 Zebrafish WashU MPIMG EST Danio rerio cDNA clone IMAGE:372338	5.920018109
psmc3	Danio rerio proteasome (prosome, macropain) 26S subunit, ATPase, 3 (psmc3), m	5.919192577
wu:fb18d11	fb18d11.y1 Zebrafish WashU MPIMG EST Danio rerio cDNA clone IMAGE:371224	5.919018326
sps2	Danio rerio selenophosphate synthetase 2 (sps2), mRNA [NM_001004295]	5.91897895
ing3	Danio rerio inhibitor of growth family, member 3 (ing3), mRNA [NM_200937]	5.918750178
zgc:56419	Danio rerio zgc:56419 (zgc:56419), mRNA [NM_200034]	5.918101052
ik:tdsubc_2f7	TDsubC_2F7_T7 Zebrafish shield stage whole embryo Danio rerio cDNA clone TD	5.917782573
zgc:76906	Danio rerio zgc:76906 (zgc:76906), mRNA [NM_200921]	5.917699282
cdkal1	Danio rerio CDK5 regulatory subunit associated protein 1-like 1 (cdkal1), mRNA [N	5.917691762
sb:cb793	STR00995 gastrula stage cDNA library Danio rerio cDNA clone CB793 5', mRNA s	5.917540201
isl3	Danio rerio islet3 (isl3), mRNA [NM_130964]	5.917080902
TC271674	Q8MIB3 (Q8MIB3) Brain multidrug resistance protein, partial (76%) [TC271674]	5.916716318
zgc:91951	Danio rerio zgc:91951 (zgc:91951), mRNA [NM_001007764]	5.91584295
TC281007	BC011391 Ureb1 protein {Mus musculus;} , partial (44%) [TC281007]	5.915814249
zgc:56526	Danio rerio zgc:56526 (zgc:56526), mRNA [NM_200267]	5.915753978
wu:fk26g04	AL714785 Danio rerio embryonic inner ear subtracted cDNA Danio rerio cDNA clor	5.915725134
zgc:77044	Danio rerio zgc:77044 (zgc:77044), mRNA [NM_212682]	5.914895918
zp2.3	Danio rerio zona pellucida glycoprotein 2.3 (zp2.3), mRNA [NM_131828]	5.914343574
zgc:85914	Danio rerio zgc:85914 (zgc:85914), mRNA [NM_213190]	5.91426155
gclc	Danio rerio glutamate-cysteine ligase, catalytic subunit (gclc), mRNA [NM_199277]	5.914196889
wu:fn06a08	fn06a08.y1 Zebrafish Research Genetics C32 fin Danio rerio cDNA clone IMAGE:4	5.914160131
arl6ip	Danio rerio ADP-ribosylation factor-like 6 interacting protein (arl6ip), mRNA [NM_20	5.913827484
cth	Danio rerio cystathionase (cystathionine gamma-lyase) (cth), mRNA [NM_212604]	5.913492916
ENSDART00(	AGENCOURT_27272445 NIH_ZGC_4 Danio rerio cDNA clone IMAGE:7288050 5'	5.913272574
ahcyl2	Danio rerio S-adenosylhomocysteine hydrolase-like 2 (ahcyl2), mRNA [NM_20134(	5.912786807
fem1c	Danio rerio fem-1 homolog c (C.elegans) (fem1c), mRNA [NM_198145]	5.912697144
arpc5b	Danio rerio actin related protein 2/3 complex, subunit 5B (arpc5b), mRNA [NM_201	5.912154765
ivns1abpb	Danio rerio influenza virus NS1A binding protein b (ivns1abpb), mRNA [NM_20148	5.911874778
BC067613	Danio rerio cDNA clone IMAGE:6960592, partial cds. [BC067613]	5.911066174
pvalb	Danio rerio parvalbumin (pvalb), mRNA [NM_205574]	5.910996271
zgc:55815	Danio rerio zgc:55815 (zgc:55815), mRNA [NM_200176]	5.910905854
ldb4	Danio rerio LIM-domain binding factor 4 (ldb4), mRNA [NM_131316]	5.910807559
zgc:86727	Danio rerio zgc:86727 (zgc:86727), mRNA [NM_001002072]	5.910743929
zgc:85609	Danio rerio zgc:85609 (zgc:85609), mRNA [NM_213101]	5.910447833
cct4	Danio rerio chaperonin containing TCP1, subunit 4 (delta) (cct4), mRNA [NM_2005	5.910030809
CN329188	AGENCOURT_21834957 NIH_ZGC_10 Danio rerio cDNA clone IMAGE:7258288 5	5.909888371
zgc:85724	Danio rerio zgc:85724 (zgc:85724), mRNA [NM_214743]	5.909486019
CD589947	RK055A1E12.T3 Zebrafish Kidney Marrow cDNA library Danio rerio cDNA clone RI	5.909313244
LOC407695	Danio rerio hypothetical protein LOC407695, mRNA (cDNA clone IMAGE:6965421	5.908462984
sgk	Danio rerio serum/glucocorticoid regulated kinase (sgk), mRNA [NM_199212]	5.908387811
zgc:92086	Danio rerio zgc:92086 (zgc:92086), mRNA [NM_001002370]	5.907747854
fts	Danio rerio fused toes homolog (fts), mRNA [NM_200105]	5.90765599
tpi1a	Danio rerio triosephosphate isomerase 1a, mRNA (cDNA clone MGC:56599 IMAGI	5.907638092
zgc:77634	Danio rerio zgc:77634 (zgc:77634), mRNA [NM_200865]	5.907578345
wsb1	Danio rerio SOCS box-containing WD protein SWiP-1 (wsb1), mRNA [NM_199633	5.90756596
zgc:91989	Danio rerio zgc:91989 (zgc:91989), mRNA [NM_001002227]	5.907167226
arf1l	Danio rerio ADP-ribosylation factor 1 like (arf1l), mRNA [NM_201480]	5.906412837
psmb6	Danio rerio proteasome (prosome, macropain) subunit, beta type, 6 (psmb6), mRN	5.906367211
zgc:77828	Danio rerio zgc:77828 (zgc:77828), mRNA [NM_212896]	5.906043312

BC091537	AGENCOURT_21612346 NIH_ZGC_19 Danio rerio cDNA clone IMAGE:7252475 5	5.905801868
ihpk2	Danio rerio inositol hexaphosphate kinase 2 (ihpk2), mRNA [NM_201470]	5.905472012
zfr	Danio rerio zinc finger RNA binding protein, mRNA (cDNA clone IMAGE:5915209),	5.905428223
TC293855	Q6P416 (Q6P416) MGC68514 protein, partial (39%) [TC293855]	5.905292039
TC281879	Q9PTK4 (Q9PTK4) Ribonucleoprotein, partial (56%) [TC281879]	5.905045969
zgc:92567	Danio rerio zgc:92567 (zgc:92567), mRNA [NM_001002731]	5.904768351
wu:fi28c07	AGENCOURT_14627825 NCI_CGAP_ZKid1 Danio rerio cDNA clone IMAGE:6961	5.904587586
zgc:63840	Danio rerio zgc:63840 (zgc:63840), mRNA [NM_200626]	5.904242248
CO958967	AGENCOURT_30802700 NIH_ZGC_19 Danio rerio cDNA clone IMAGE:7427013 5	5.903904724
hmbs	Danio rerio hydroxymethylbilane synthase (hmbs), mRNA [NM_201154]	5.90370354
zgc:85971	Danio rerio zgc:85971 (zgc:85971), mRNA [NM_213271]	5.90334478
CO351725	DR_AOV_NRM05_E08 adult ovary normalized (TLL) Danio rerio cDNA, mRNA sec	5.902418986
TC270570	Q63925 (Q63925) ICER, partial (80%) [TC270570]	5.902406098
zgc:77033	Danio rerio zgc:77033 (zgc:77033), mRNA [NM_213306]	5.902211723
wu:fc04g05	Danio rerio wu:fc04g05, mRNA (cDNA clone IMAGE:6791382), partial cds. [BC056	5.902069949
zgc:77429	Danio rerio zgc:77429 (zgc:77429), mRNA [NM_213262]	5.901791357
zgc:56165	Danio rerio zgc:56165 (zgc:56165), mRNA [NM_200961]	5.901706668
yrk	Danio rerio Yes-relayed kinase (yrk), mRNA [NM_212781]	5.901587535
BI879974	fm68b05.x1 Zebrafish adult retina cDNA Danio rerio cDNA clone IMAGE:4200513 3	5.901333904
zgc:55886	Danio rerio zgc:55886 (zgc:55886), mRNA [NM_200959]	5.901096483
ENSDART00(	Q921V3 (Q921V3) Nitrogen fixation, partial (88%) [TC269256]	5.900927777
zgc:85738	Danio rerio zgc:85738 (zgc:85738), mRNA [NM_214820]	5.900868445
kiaa0007l	Danio rerio KIAA0007 protein (human), like (kiaa0007l), mRNA [NM_173282]	5.900683878
zgc:92235	Danio rerio zgc:92235 (zgc:92235), mRNA [NM_001004563]	5.900411074
TC280895	Q7ZV95 (Q7ZV95) General transcription factor IIF, polypeptide 1, 74kDa, complete	5.900046449
wu:fb72g02	fb72g02.y1 Zebrafish WashU MPIMG EST Danio rerio cDNA clone IMAGE:371745	5.899933191
zgc:56020	Danio rerio zgc:56020 (zgc:56020), mRNA [NM_200188]	5.899620383
wu:fi11e03	fi11e03.y1 Sugano Kawakami zebrafish DRA Danio rerio cDNA clone IMAGE:2600	5.899140175
BC050157	Danio rerio, clone IMAGE:5604458, mRNA. [BC050157]	5.899091971
ENSDART00(	BC009439 THAP4 protein {Homo sapiens;} , partial (61%) [TC282971]	5.898892905
npl4	Danio rerio nuclear protein localization 4 (npl4), mRNA [NM_199807]	5.898373391
BI868116	ft68c04.y1 Gong zebrafish ovary Danio rerio cDNA clone IMAGE:5158279 5', mRN	5.897741011
zgc:65787	Danio rerio zgc:65787 (zgc:65787), mRNA [NM_213157]	5.897451963
zgc:66396	Danio rerio zgc:66396 (zgc:66396), mRNA [NM_200057]	5.897053507
zgc:65882	Danio rerio zgc:65882 (zgc:65882), mRNA [NM_200821]	5.896966246
TC268784	Q6NSR8 (Q6NSR8) Npepl1 protein, partial (89%) [TC268784]	5.896494959
zgc:55819	Danio rerio zgc:55819 (zgc:55819), mRNA [NM_199432]	5.895719017
TC268831	BC054684 zgc:66329 {Danio rerio;} , complete [TC268831]	5.895362538
TC285431	Q8WWH5 (Q8WWH5) TruB pseudouridine synthase-like protein 1 (TruB pseudouri	5.895077996
zgc:56257	Danio rerio zgc:56257 (zgc:56257), mRNA [NM_200218]	5.894881875
TC276048	Q8N108 (Q8N108) Mesoderm induction early response 1 N1-beta (Mesoderm indu	5.894788495
zgc:65781	Danio rerio zgc:65781 (zgc:65781), mRNA [NM_199632]	5.8946331
desm	Danio rerio desmin (desm), mRNA [NM_130963]	5.894011026
zgc:77398	Danio rerio zgc:77398 (zgc:77398), mRNA [NM_205664]	5.893908615
alcam	Danio rerio activated leukocyte cell adhesion molecule (alcam), mRNA [NM_13100	5.893905882
BC090281	Danio rerio cDNA clone MGC:113121 IMAGE:6905212, complete cds. [BC090281]	5.89383819
LOC402845	Danio rerio hypothetical protein LOC402845, mRNA (cDNA clone IMAGE:6793503	5.893548327
mylip	Danio rerio myosin regulatory light chain interacting protein (mylip), mRNA [NM_19	5.892596533
zgc:63609	Danio rerio zgc:63609 (zgc:63609), mRNA [NM_200441]	5.892564618
gtf2b	Danio rerio general transcription factor IIB (gtf2b), mRNA [NM_199697]	5.892317118
zgc:85781	Danio rerio zgc:85781 (zgc:85781), mRNA [NM_199588]	5.892225625
BC074047	Danio rerio cDNA clone IMAGE:7040135, partial cds. [BC074047]	5.892141542
BM342488	fw44e12.y1 Zebrafish SJD day 3 embryo Danio rerio cDNA clone IMAGE:5567710	5.892002164
slc9a3r2	Danio rerio solute carrier family 9 (sodium/hydrogen exchanger), isoform 3 regulatc	5.891953002
zgc:55635	Danio rerio zgc:55635 (zgc:55635), mRNA [NM_200170]	5.891672998
BF938883	fl96c04.y1 Zebrafish adult retina cDNA Danio rerio cDNA clone IMAGE:4144518 5'	5.891046129
TC292818	Q7SXN3 (Q7SXN3) Ahsa1l protein, complete [TC292818]	5.890829539
TC268566	Q7ZU14 (Q7ZU14) Catenin (Cadherin-associated protein), beta, complete [TC268	5.888338897
zgc:77760	Danio rerio zgc:77760 (zgc:77760), mRNA [NM_200859]	5.886831
max	Danio rerio myc-associated factor X, mRNA (cDNA clone IMAGE:6795370), partial	5.886340703
TC294273	KINH_HUMAN (P33176) Kinesin heavy chain (Ubiquitous kinesin heavy chain) (UK	5.886192505
BC090507	MIME_HUMAN (P20774) Mimecan precursor (Osteoglycin) (Osteoinductive factor)	5.886070824
zgc:101858	Danio rerio zgc:101858 (zgc:101858), mRNA [NM_001005597]	5.885501761
nsep1	Danio rerio nuclease sensitive element binding protein 1 (nsep1), mRNA [NM_1316	5.885486773
zgc:63914	Danio rerio zgc:63914 (zgc:63914), mRNA [NM_001002165]	5.885360146
faf1	Danio rerio Fas associated factor 1 (faf1), mRNA [NM_212973]	5.884093209
TC270221	Q7ZYX1 (Q7ZYX1) Fts protein, complete [TC270221]	5.882582037
wu:fa02f12	fa02f12.s1 Zebrafish ICRFzfls Danio rerio cDNA clone 2G16 3', mRNA sequence [A	5.882092249
TC269368	Q6QWF9 (Q6QWF9) CaMKII inhibitor protein alpha, partial (29%) [TC269368]	5.881820746
sertad2	Danio rerio SERTA domain containing 2 (sertad2), mRNA [NM_212794]	5.881673575
bcap37	Danio rerio B-cell receptor-associated protein 37 (bcap37), mRNA [NM_199681]	5.880745367
mkrn1	Danio rerio Makorin RING zinc-finger protein 1 (mkrn1) mRNA, partial cds. [AF277	5.880286308
zgc:65806	Danio rerio zgc:65806 (zgc:65806), mRNA [NM_201127]	5.880198051
zgc:101017	Danio rerio zgc:101017 (zgc:101017), mRNA [NM_001003597]	5.878661818
ENSDART00(	Q92074 (Q92074) Beta-1,4-galactosyltransferase , partial (67%) [TC293471]	5.877826808
gsk3a	Danio rerio glycogen synthase kinase 3 alpha (gsk3a), mRNA [NM_131390]	5.877821224
BM958205	fy70f10.y1 Sugano SJD adult male Danio rerio cDNA clone IMAGE:5605386 5' sim	5.877808768
lsm7	Danio rerio LSM7 homolog, U6 small nuclear RNA associated (S. cerevisiae) (lsm7	5.877720316
zgc:92250	Danio rerio zgc:92250 (zgc:92250), mRNA [NM_001004560]	5.87770532
siat6	Danio rerio sialyltransferase 6 (N-acetyllacosaminide alpha 2,3-sialyltransferase) (s	5.876978797
ptpru	Danio rerio protein tyrosine phosphatase, receptor type, U (ptpru), mRNA [NM_001	5.876949192

rarg	Danio rerio retinoic acid receptor gamma (rarg), mRNA [NM_131339]	5.87683092
zgc:77665	Danio rerio zgc:77665 (zgc:77665), mRNA [NM_199993]	5.876039089
zgc:63557	Danio rerio zgc:63557 (zgc:63557), mRNA [NM_201003]	5.875394203
TC293142	CHRD_BRARE (O57472) Chordin precursor (Chordino protein), complete [TC2931	5.875373099
slc26a11	Danio rerio solute carrier family 26, member 11 (slc26a11), mRNA [NM_199767]	5.874895121
CO958967	AGENCOURT_30802700 NIH_ZGC_19 Danio rerio cDNA clone IMAGE:7427013 5	5.874675228
ENSDART00(	AB049214 facilitative glucose transporter GLUT11-s {Homo sapiens;} , partial (31%	5.873081535
sgk	Danio rerio serum/glucocorticoid regulated kinase (sgk), mRNA [NM_199212]	5.872787647
im:7139999	AGENCOURT_10726497 NCI_CGAP_ZEmb3 Danio rerio cDNA clone IMAGE:679	5.872519203
CN316371	AGENCOURT_21834875 NIH_ZGC_10 Danio rerio cDNA clone IMAGE:7258259 5	5.872181783
zgc:92816	Danio rerio zgc:92816 (zgc:92816), mRNA [NM_001002514]	5.872113924
sepw1	Danio rerio selenoprotein W, 1 (sepw1), mRNA [NM_178287]	5.87204333
TC268559	Q6PC12 (Q6PC12) Wu:fi32b03 protein, complete [TC268559]	5.870786357
TC275938	Q6FHV7 (Q6FHV7) SGKL protein, partial (40%) [TC275938]	5.870530887
CF347101	AGENCOURT_15223819 NIH_ZGC_10 Danio rerio cDNA clone IMAGE:7002585 5	5.870383533
tef	Danio rerio thyrotroph embryonic factor (tef), mRNA [NM_131400]	5.870357244
zgc:103629	Danio rerio zgc:103629 (zgc:103629), mRNA [NM_001007771]	5.869809031
CN022011	AGENCOURT_20195787 NIH_ZGC_14 Danio rerio cDNA clone IMAGE:7228792 5	5.869713406
wu:fk54d01	AGENCOURT_30421498 NIH_ZGC_14 Danio rerio cDNA clone IMAGE:7409413 5	5.869677933
TC272214	BC004045 lactamase, beta 2 {Mus musculus;} , partial (67%) [TC272214]	5.869619334
BC083404	Danio rerio cDNA clone IMAGE:7238334, partial cds. [BC083404]	5.869428212
AI942590	fc73c10.y1 Zebrafish WashU MPIMG EST Danio rerio cDNA clone IMAGE:372702(	5.869356695
pxn	Danio rerio paxillin (pxn), mRNA [NM_201588]	5.869232513
zgc:100907	Danio rerio zgc:100907 (zgc:100907), mRNA [NM_205724]	5.86858355
slc9a3r2	Danio rerio solute carrier family 9 (sodium/hydrogen exchanger), isoform 3 regulatc	5.868571199
BM185499	fv72b07.y1 zebrafish adult brain Danio rerio cDNA clone IMAGE:5413957 5', mRNA	5.868553818
popdc3	Danio rerio popeye domain containing 3 (popdc3), mRNA [NM_001001848]	5.868303616
TC298357	Q6L967 (Q6L967) Solute carrier family 26 member 6 c, partial (31%) [TC298357]	5.866857257
zgc:73143	Danio rerio zgc:73143 (zgc:73143), mRNA [NM_200728]	5.866767599
ube2v2	Danio rerio ubiquitin-conjugating enzyme E2 variant 2 (ube2v2), mRNA [NM_21351	5.865732939
TC297039	Q06054 (Q06054) Zinc finger protein, partial (22%) [TC297039]	5.865047532
zgc:92633	Danio rerio zgc:92633 (zgc:92633), mRNA [NM_001002442]	5.8642802
BQ618300	faa59f04.x1 Gong zebrafish testis Danio rerio cDNA clone IMAGE:5898007 3', mRI	5.863351582
zgc:64113	Danio rerio zgc:64113 (zgc:64113), mRNA [NM_198810]	5.863042812
TC272114	Q9V832 (Q9V832) CG4866-PA (RE57564p), partial (75%) [TC272114]	5.862786634
TC292674	Unknown	5.862786214
TC292508	BC049316 zgc:56444 {Danio rerio;} , complete [TC292508]	5.862378056
TC293467	Q91941 (Q91941) ERCC2/XPD protein, partial (43%) [TC293467]	5.861957285
CK400431	AGENCOURT_17518817 NIH_ZGC_4 Danio rerio cDNA clone IMAGE:7118344 5'	5.861922637
im:7145273	fl62g06.y1 Sugano Kawakami zebrafish DRA Danio rerio cDNA clone IMAGE:3818	5.861506565
zgc:91819	Danio rerio zgc:91819 (zgc:91819), mRNA [NM_205594]	5.861135455
AW165036	fd99c03.x1 Zebrafish WashU MPIMG EST Danio rerio cDNA clone IMAGE:373747	5.860438985
casp3	Danio rerio caspase 3, apoptosis-related cysteine protease (casp3), mRNA [NM_13	5.860430073
TC272167	Q76IQ7 (Q76IQ7) Granulosa cell HMG-box protein-1, partial (41%) [TC272167]	5.860222001
zgc:92698	Danio rerio zgc:92698 (zgc:92698), mRNA [NM_001002404]	5.859995579
TC278257	GUB_RHOMR (P45798) Beta-glucanase precursor (Endo-beta-1,3-1,4 glucanase)	5.859574095
rpl7	Danio rerio ribosomal protein L7 (rpl7), mRNA [NM_213644]	5.859277767
zgc:86900	Danio rerio zgc:86900 (zgc:86900), mRNA [NM_001002678]	5.859207421
snrpfl	Danio rerio small nuclear ribonucleoprotein polypeptide F-like (snrpfl), mRNA [NM_	5.859198173
dtnb	Danio rerio dystrobrevin, beta (dtnb), mRNA [NM_199709]	5.858899782
bscv	Danio rerio bscv (C20orf3) homolog (bscv), mRNA [NM_212608]	5.858797782
zgc:76972	Danio rerio zgc:76972 (zgc:76972), mRNA [NM_213320]	5.858642872
zgc:86935	Danio rerio zgc:86935 (zgc:86935), mRNA [NM_001002083]	5.856174805
zgc:56150	Danio rerio zgc:56150 (zgc:56150), mRNA [NM_200942]	5.856006214
prkri	Danio rerio protein-kinase, interferon-inducible double stranded RNA dependent inl	5.855290766
arpc5b	Danio rerio actin related protein 2/3 complex, subunit 5B (arpc5b), mRNA [NM_201	5.855008438
bactin1	Danio rerio bactin1, mRNA (cDNA clone MGC:77623 IMAGE:6996683), complete c	5.85482668
TC287044	Q8QGB0 (Q8QGB0) VHSV-induced protein-10, partial (45%) [TC287044]	5.85454201
zgc:100860	Danio rerio zgc:100860 (zgc:100860), mRNA [NM_001003532]	5.854131543
zgc:63759	Danio rerio zgc:63759 (zgc:63759), mRNA [NM_200488]	5.852743664
TC282810	NPH1_CANFA (Q9TU19) Nephrocystin 1 (Fragment), partial (48%) [TC282810]	5.851816235
jak2b	Danio rerio mRNA for protein tyrosine kinase (jak2b), partial. [AJ005691]	5.851538783
CN839230	AGENCOURT_25053294 NIH_ZGC_4 Danio rerio cDNA clone IMAGE:7287032 5'	5.851414114
ldha	Danio rerio lactate dehydrogenase A4 (ldha), mRNA [NM_131246]	5.851251933
krt8	Danio rerio keratin 8 (krt8), mRNA [NM_200080]	5.850097154
pitpnb	Danio rerio phosphotidylinositol transfer protein, beta (pitpnb), mRNA [NM_200920	5.849286268
AW019648	fd55b04.x1 Zebrafish WashU MPIMG EST Danio rerio cDNA clone IMAGE:373361	5.849173399
kiaa0007l	Danio rerio KIAA0007 protein (human), like (kiaa0007l), mRNA [NM_173282]	5.848959814
zgc:64067	Danio rerio zgc:64067 (zgc:64067), mRNA [NM_212611]	5.848953288
TC287604	1VID Catechol O-Methyltransferase. {Rattus norvegicus;} , partial (41%) [TC28760	5.848810091
zgc:101085	Danio rerio zgc:101085 (zgc:101085), mRNA [NM_001003763]	5.848358203
TC274602	SMA6_HUMAN (O43541) Mothers against decapentaplegic homolog 6 (SMAD 6) (	5.848099742
zgc:76972	Danio rerio zgc:76972 (zgc:76972), mRNA [NM_213320]	5.847550955
TC280463	Unknown	5.847048363
zgc:73257	Danio rerio zgc:73257 (zgc:73257), mRNA [NM_213397]	5.845547181
zgc:77247	Danio rerio zgc:77247 (zgc:77247), mRNA [NM_213240]	5.845465696
ENSDART00(	Unknown	5.845171313
zgc:101722	Danio rerio zgc:101722 (zgc:101722), mRNA [NM_001008630]	5.844948243
etfa	Danio rerio electron-transfer-flavoprotein, alpha polypeptide (etfa), mRNA [NM_198	5.842224321
zgc:86607	Danio rerio zgc:86607 (zgc:86607), mRNA [NM_001002050]	5.840014839
wu:fb81c12	fc13h01.y1 Zebrafish WashU MPIMG EST Danio rerio cDNA clone IMAGE:372129	5.838298378

BQ132634	fz61f11.y1 zebrafish fin day1 regeneration Danio rerio cDNA clone IMAGE:590762(	5.838165934
ENSDART00(	fb99d04.y1 Zebrafish WashU MPIMG EST Danio rerio cDNA clone IMAGE:372000	5.837945511
TC284674	Q8UWM1 (Q8UWM1) Beta-3-galactosyltransferase, partial (42%) [TC284674]	5.837851601
zgc:64089	Danio rerio zgc:64089 (zgc:64089), mRNA [NM_200410]	5.837618277
zgc:55807	Q7ZU41 (Q7ZU41) Wu:fb14h09 protein, partial (97%) [TC291168]	5.8375189
pgd	Danio rerio phosphogluconate hydrogenase (pgd), mRNA [NM_213453]	5.836391292
zgc:77380	Danio rerio zgc:77380 (zgc:77380), mRNA [NM_213270]	5.83501223
wu:fb52f06	fb52f06.x1 Zebrafish WashU MPIMG EST Danio rerio cDNA clone IMAGE:371552:	5.834464304
ENSDART00(	AF297050 prostacyclin synthase {Homo sapiens;} , partial (20%) [TC274387]	5.833879508
TC296477	Q96BN8 (Q96BN8) LOC90268 protein, partial (9%) [TC296477]	5.833674458
TC281501	UBF1_HUMAN (P17480) Nucleolar transcription factor 1 (Upstream binding factor	5.832629535
BI983424	ft71e08.x1 Gong zebrafish ovary Danio rerio cDNA clone IMAGE:5158766 3', mRN	5.831930818
zgc:64135	Danio rerio zgc:64135 (zgc:64135), mRNA [NM_213130]	5.831488473
aldh9a1	Danio rerio aldehyde dehydrogenase 9 family, member A1 (aldh9a1), mRNA [NM_:	5.830943946
slc1a3	Danio rerio solute carrier family 1 (glial high affinity glutamate transporter), member	5.830736568
wu:fi75a02	fi75a02.y1 Sugano Kawakami zebrafish DRA Danio rerio cDNA clone IMAGE:2643	5.829975649
TC273111	BC008281 guanosine monophosphate reductase {Homo sapiens;} , partial (98%) [T	5.829699547
TC273438	SYN_MOUSE (Q8BP47) Asparaginyl-tRNA synthetase, cytoplasmic (Asparagine--	5.829146078
zgc:66371	Danio rerio zgc:66371 (zgc:66371), mRNA [NM_200689]	5.828395375
CO936527	AGENCOURT_30539272 NIH_ZGC_19 Danio rerio cDNA clone IMAGE:7429593 5	5.825713846
zgc:85729	Danio rerio zgc:85729 (zgc:85729), mRNA [NM_214811]	5.825434984
pgd	Danio rerio phosphogluconate hydrogenase (pgd), mRNA [NM_213552]	5.823691826
ENSDART00(	AF182424 MDS011 {Homo sapiens;} , partial (69%) [TC272682]	5.823557625
zgc:63719	Danio rerio zgc:63719 (zgc:63719), mRNA [NM_213499]	5.821505285
TC294304	YAF2_HUMAN (Q8IY57) YY1-associated factor 2, partial (98%) [TC294304]	5.821375052
degs	Danio rerio degenerative spermatocyte homolog, lipid desaturase (Drosophila) (deg	5.82122775
TC270369	Q9NS37 (Q9NS37) HCF-binding transcription factor Zhangfei, partial (38%) [TC27(	5.820751974
BQ109731	imageqc_7_2001 [BQ109731]	5.820528581
LOC407660	Danio rerio hypothetical protein LOC407660, mRNA (cDNA clone IMAGE:6971411	5.820195369
ube2h	Danio rerio ubiquitin-conjugating enzyme E2H (UBC8 homolog, yeast) (ube2h), mR	5.819807407
BI879676	fm64b01.x1 Zebrafish adult retina cDNA Danio rerio cDNA clone IMAGE:4200121 3	5.818445494
TC290770	AE003479 CG11624-PC {Drosophila melanogaster;} , partial (22%) [TC290770]	5.817173411
TC281115	Q9CWM6 (Q9CWM6) Mus musculus ES cells cDNA, RIKEN full-length enriched lib	5.816192877
BQ077770	fy69f05.x1 Sugano SJD adult male Danio rerio cDNA clone IMAGE:5605017 3', mR	5.815708336
TC279379	Q8AV10 (Q8AV10) Sdf1a (Chemokine ligand 12), complete [TC279379]	5.813960388
ndpkz4	Danio rerio nucleoside diphosphate kinase-Z4 (ndpkz4), mRNA [NM_130929]	5.811520304
zgc:73356	Danio rerio zgc:73356 (zgc:73356), mRNA [NM_200804]	5.810474108
TC295052	Unknown	5.807052045
sox17	Danio rerio SRY-box containing gene 17 (sox17), mRNA [NM_131287]	5.806426802
CN328293	CN328293 AGENCOURT_21843070 NIH_ZGC_10 Danio rerio cDNA clone IMAGE	5.806067223
appa	Danio rerio amyloid beta (A4) precursor protein a (appa), mRNA [NM_131564]	5.804233103
AL914296	AL914296 PJR-Z1+Z2 Danio rerio cDNA clone 149-F06-2, mRNA sequence [AL91	5.803564303
TC279012	SYU_TORCA (P37379) Synuclein, partial (66%) [TC279012]	5.800505974
TC301592	Q6WNU3 (Q6WNU3) Transcription factor Sox1a, partial (39%) [TC301592]	5.797375289
flj11749l	Danio rerio hypothetical protein FLJ11749-like (H. sapiens) (flj11749l), mRNA [NM_	5.7926995
fn1	Danio rerio fibronectin 1 (fn1), mRNA [NM_131520]	5.792526783
BC081644	Danio rerio cDNA clone IMAGE:7054369. [BC081644]	5.789767927
zgc:56454	Danio rerio zgc:56454 (zgc:56454), mRNA [NM_200289]	5.780766846

Supplemental Table 17. Intersection between chromatin marks associated genes and transcripts from mature sperm. All marks are scored in proximal TSS region, -2 ~ +1 kb. Sperm transcripts retrieved showed at least 5.8 fold enrichment.

	sperm transcripts, 1731 genes	
	enrichment over random	P-value
H3K4me3 >2.0, 849 genes	1.5243 (98/64.2920)	<1/1000
H3K4me3 >1.8, 1824 genes	1.6768 (232/138.3600)	<1/1000
H3K4me2 >2.0, 1589 genes	1.4970 (179/119.5760)	<1/1000
H3K4me2 >1.8, 3094 genes	1.4786 (346/234.0120)	<1/1000
H3K14Ac >0.81, 784 genes	1.4707 (87/59.1570)	<1/1000
H3K14Ac >0.63, 1558 genes	1.5588 (184/118.0390)	<1/1000
Sperm UnMe <-1.2, 2288 genes	1.1742 (203/172.8840)	0.009
Sperm UnMe <-1.4, 949 genes	1.2744 (92/72.1900)	0.013
Sperm Me >1.2, 633 genes	1.1060 (53/47.9220)	0.243
H3K4me3 >1.8 & DNAUnMe <-1.2, 866 genes	1.6331 (107/65.5210)	<1/1000
H3K27me3 >0.43, 1534 genes	0.7993 (93/116.3560)	0.995
H2AFV >0. 34, 771 genes	1.0126 (59/58.2650)	0.481

Supplemental Table 18. Genes that begin their expression at specified stages.

2 hpf	4 hpf	6 hpf
aars	admp	anxa1a
abcf1	adrm1b	anxa4
adka	ak3l1	apoa1
aldoaa	anxa1c	aqp3
arf1l	bmp2b	arl6ip5
bc2	ccnd1	arpc5a
carm1	cdv3	arpp19
casc3	cldne	atf4
cct6a	ctsl1b	atp1b1a
cct7	cxcr4b	atp1b3a
cdk9	dynll2	bin2l
chchd3	erm	bmp7
copb1	fgfr4	cahz
cops7a	flh	capns1
copz1	foxa3	ccnf
cpeb4	foxd5	ccr6a
cpsf2	fzd7a	cd99l2
cul3	g12	cdh2
dctn3	gata2	cdx4
ddx18	h2afx	cebpa
dpp3	id1	cirbp
eif1b	irx7	ckmt1
eya1	ivns1abpa	cldnf
glud1a	klf2b	cldng
gnl2	klf4	cldnj
gspt1	marcksl1	clica
hsf2	mcm3	clint1
isl2b	msxd	cnn2
kpnb3	net1	cpn1
lyricl	nola1	crygm4
ncl	paics	cth
nola1	psmc2	ctps
pigp	psmc5	ctsl1b
pknox1.1	rbmx	ctsll
plrg1	rpl7l1	dhx16
polb	si:dkey-252h13.6	dlc
ppig	si:dkey-261j4.9	dld
prim1	si:rp71-45k5.4	eif3s4
prps1a	si:xx-bac7cse.2	eif3s6ip
psat1	slc25a22	eif3s7
psmc1a	sox11a	eif3s8
psmc4	sox19a	eif4e1a
psmd2	stm	elavl1
psmd7	tbx16	elovl5
ptges3	tfap2a	fgf8
rbb4l	usp14	fzd7b
scarb1	vent	fzd8a
seph	vox	fzd9
sfxn2	vtn	gata5
shmt1	yy1	gata6
sox11b	zgc:111843	gnl3
tcerg1	zgc:123178	gpr137bb
tmem50a	zgc:56335	gsnl1
tomm22	zgc:64105	gtpbp4

tra2a
tuba8l
uap1
ube2n
usp5
vta1
xbp1
yars
zfr
zgc:101755
zgc:103619
zgc:103692
zgc:110682
zgc:136473
zgc:55687
zgc:55690
zgc:55697
zgc:55818
zgc:56682
zgc:63491
zgc:64042
zgc:64105
zgc:73124
zgc:76917
zgc:77069
zgc:77262
zgc:85615
zgc:86762
zgc:92345
zgc:92639
zgc:64138
zgc:77455
zgc:85717
zgc:92784
zic2b
znfl1
her7
her9
hif1al
hnrpu
hnrpul1
hoxa3a
hs6st2
hsp47
icat
id3
iglc2
im:6893299
kny
krt4
krt5
krt8
lcp1
lhx1a
lhx5
lig3
lmnb2
lmo1
maf
magi1
mcm6
mki67ipl
msgn1
msxc
nlcam
nlz1
notch3
nqo1
nrarpa
otop1
otx2
papss2
pcdh8
ppp1r14b
ranbp1
rheb
rhoaa
rpl37
rpl5a
rpl8
rtk6
sall1
sb:cb742
sc:d0144
sfpq
six3b
six4.3
slc38a4
slc46a1
smo
smox
sox2
sox32

sp5
sp5l
sp8l
spag1
spon2a
stard3nl
stau1
szl
tardbp
tbx6
tcf2
tfa
th
tpbgl
utp15
vtg1
wdr3
wu:fc04c01
yy1
zgc:100864
zgc:100900
zgc:101594
zgc:103627
zgc:109868
zgc:110689
zgc:136656
zgc:158360
zgc:55764
zgc:55852
zgc:55876
zgc:56585
zgc:63783
zgc:64214
zgc:66282
zgc:66286
zgc:73292
zgc:73324
zgc:77259
zgc:77262
zgc:77541
zgc:86889
zgc:91802
zgc:91861
zgc:91960
zgc:92116
zgc:92278
zgc:92451
zgc:92467
zgc:92888
zic2a

Supplemental Table 19. List of primers. Sequences start from 5' to 3'.

Primer name	Primer set
Primers for bisulphite sequencing	
Eve1	5-TTA TGT TTT TTT GAT TTT AAT GGT AGG TTT-3 5-ATT TAA ATA ACA TTT TAA TCT CCA AAC ATA-3
Eve1 nested	5-ATA TAA GAG TTT GTT ATA GTG ATG ATG ATG-3 5-TAA ATA AAC TCC AAA TTT AAC TTC AAT ACT-3
hoxb3a	5- AAA ATG AGA TTA GAT AAT ATA ATT TGG GGT -3 5- CAT ACC TCA AAT CTT TCA TAC TAA ACC -3
hoxb3a nested	5- GAT AAT ATA ATT TGG GGT GTA TTT ATT TAG -3 5- TAT AAA CTT TAA ACT TTC TTA TTA ATT ACA AC -3
tbx2b	5- GAT TAA GTA AAA AGG TGA TGA GTA GAT AAT -3 5- AAT CAA ATA AAC AAA AAA AAC CTT AAA TCA -3
tbx2b nested	5- TGT ATA AAT ATT AAA TGG TTA TGT TAT GTA TG -3 5- CTA CAA TAA ATA AAT TTA CAA ATA ACA ACA TT -3
Sox2	5- GTT TAG ATT GAT ATT TGG AGT AGA TTG ATA -3 5- ACT ACA ACA AAA AAA AAA CAA TAA TAA CTT -3
Sox2 nested	5- GGA GTA GAT TGA TAT TTG GAT TTA AAG TAA -3 5- ATA ATA ACT TCA ATC AAA ATA CTA CCC TAA -3
dre-mir-15a-2	5- TTT GGA GAA ATT TTT GGA TAT TTG GAG AA -3 5- TTT CTC CAT CAC AAC TTC ACT AAC C -3
dre-mir-15a-2 nested	5- GGG TTA AAA GTA TTT AGG ATA ATT TTG AG -3 5- TTC ACT AAC CAC CTC TAA AAT ATC AA -3
pou5f1	5- TAATTTGGGATAGTTTAGGTTAGAAATTAG -3 5- CTTTCTTATTTAAAATCTCAACAACCTT -3
pou5f1 nested	5-GTTTTGATTTTAGATGGTATTTTAATTTGT-3 5- ATCTAATTTTTAACAAAACCCATTTCA -3
Sox3	5- GTATTGTTGTGGAGATTTTTGAAAGA-3 5- TCAATCAAAAATTTCCAATCAACAC-3
Sox3 nested	5- GTTTGAGTTTTTTGAATTTTTGATTGA-3 5- TATACATTTTAAAATTCTCCTAAACCATC-3
Hoxb5a	5- TTGGAAATGTATAAAAGGATTAGTAGGT-3 5- ATTAACAACTTAATTCCAAAATACTTCC-3
Hoxb5a nested	5- ATTTTATAAGTTATGTTTGATTTTGGTTTG-3 5- ACTTTCATACATTTTTATCAAAAAAACTAACT-3
Hoxb8a	5- TTAAAAAGTTGTTAGGTTTTTATGAGG-3 5- CCAACAATAACAACAACTCTTTATCC-3
Hoxb8a nested	5- ATTTTAAATTTTATTTATGTAAGGATTGTAAG-3 5- AAACATTAACACTATACATAATCAACAATACT-3
Random region from Chr7	5- GATAGTTAGAGTTTTGAGTTTGTGAATG-3 5- CAATATCCCTCATTCTTAAAACTAACA-3
Random region from Chr7 nested	5- TATTTTAGGTTATTGTTGTTGGAAAGA-3 5- TATAACACCACTCTCTCATCTCTTC-3
foxi3b	5- GGTTGAGTTGTAAATTTTTATTATTGAAG-3 5- ACTACATTCTTATCATTCAACCATTCTA-3
foxi3b nested	5- GTTTATAAATAAAGTAGATTATTTTGATAGTGA-3 5- ACAAATTCAAATAATTTACTTCTTTACTTAC-3
Primers for qPCR	

Hoxb5a	5- CCT CAC CCG AAG AAG GAG GAT A -3 5- TAC CTG CGG TAG CCA GAC T -3
Tbx4	5- GAA TGG CAG CAG CCA GAA TAG -3 5- CAA CAG AAA ACC GCC TTT CCA TA -3
Sox3	5- GTG CGC TAA GCT CAG CTG TTA -3 5- GAG GAG TGT GAG GTG CTG T -3
Hoxc9	5- TAC CAC AGG CAT TTC AGG ATT TG -3 5- GTT CGG CCT ACA ACG ACA AT -3
Fgf24	5- AAA TGC AAA ACC CAG ACG TGT TT -3 5- CAC CCC AGA GGC TGT GAA ATT A -3
Zic2b	5- ATG TAC ACA TTT CGT ACG TTT TCA AA -3 5- CAA CTG AGT GGC TGT TAC TTG -3
flh	5- CTT ATG GAC AAT CAG CAC GTC CTT -3 5- AGC GCA GAG CTG GAG ACA G -3
Gsc 5'	5- GAC AAA AAC CGC GAA TTC TGT TTG-3 5- AAA GCA GAG CAG GAG GTT CA-3
Gsc 3'	5- TGTGCAACAGCAAGACAACA -3 5- AAA GCG ACG TGG ATT CTG AC -3
Bactin2 5'	5- CGT GTG GAG GAG CTC AAA GT -3 5- AGA GCA CAG AGC TCC GAA AG -3
Bactin2 3'	5- TCT CAG CTG TGG TGG TGA AG -3 5- GTG CCC ATC TAC GAG GGT TA -3
Klf4 5'	5- ATC CCA AGC GTC ATG AGA ACG -3 5- GAG GCA GAC AAT GCG TCT CT -3
Klf4 3'	5- GTG AGA AGC CCT ACC ACT GC -3 5- GTG TCC GGT GTG TTT CCT GTA G -3
Eve1 5'	5- AGC CAA CTC TTT GCT TTC AGC -3 5- TAG ACC CCA ATG ACA GTG CA -3
Eve1 3'	5- AGG TGG TCT TCC ACA ACC AG -3 5- TAG ATG AAT GGG TAA GCG GGG -3
Foxh1 5'	5- CTC CTC AAC CCC TCA GAC TG -3 5- TCA CCT TGA CTG CAG AAT CGG -3
Foxh1 3'	5- ATG ACG TGC ACC AGA CAG AC -3 5- CAC TTC CAC CCT CTA GCA GG -3
Ddx5 5'	5- TGA CTG AGG TAA TGC CGC TA -3 5- TCC AGT GTC GGT AGT GAC C -3
Ddx5 3'	5- GAT GCT TGA CAT GGG ATT TGA ACC -3 5- TCC AGG TGT GGC AAT ACA AAT CTC -3

Supplemental Methods

Computational analytical methods

TIMAT2, the open source application, was used in this analysis and obtained from the project website, http://sourceforge.net/projects/timat2. Zebrafish annotation and genomic sequence (Zv7 assembly, April 2007) were retrieved from the Ensembl website.

Low-level ChIP-chip analysis

Details about low- and high-level ChIP-chip analysis have been described in Hammoud et al. (2009). Microarray data from two biological replicas or inputs were first quantile normalized and median scaled to 100 (data not shown; Bolstad et al., 2003). Oligos with a calculated enrichment ratio (mean treatment replicas/mean control replicas in the log2 ratio) were then mapped to Zv7 assembly. Summary scores were assigned to the center position of 400 bp windows (the majority size of fragments after whole genome amplification) covering at least two oligo start positions. High-scoring windows located within 250 bp distance were merged as intervals. The replica-averaged R^2 values for microarray were as follows: 0.98 for the two sperm MeDIP replicas; 0.98 for the two muscle MeDIP replicas; 0.93 for the two H3K4me3 replicas; 0.93 for the two H3K4me2 replicas; 0.91 for the two H3K14Ac replicas; 0.90 for the two H3K27me3 replicas; 0.80 for the two H2AFV replicas; 0.88 for the two H3K36me3 replicas; and 0.97 for the two H3K9me3 replicas.

High-level ChIP-chip analysis

Genes associated with histone modifications were first identified through the "find neighboring genes (FNG)" application in TIMAT2 package. The top 800 genes located within 12kb of enriched loci were uploaded to GoMiner (http://discover.nci.nih.gov/gominer/index.jsp) for GO term analysis. To calculate the percentage of developmental genes associated with multiple histone modifications, the highest enrichment fold of modifications for each gene was scored in proximal promoter regions (-2 ~ +1 kb of TSS). Correlation significance between chromatin modifications-enriched regions was determined by using "intersect regions" application. This application generates 1000 random data sets which are comparable to the original regions in chromosome, size, and GC contents. Correlation P-value and fold enrichment over random (fraction real intersection/fraction average random data set intersection) can then be assessed. The "Intersect lists" application applies random permutation to estimate correlation significance between two enriched gene lists or an enriched gene list and expression profile.

Bisulphite sequencing

Bisulphite sequencing was performed as described (Clark et al., 1994). In brief, 2 ug of genomic DNA from sperm or muscle were treated with 0.2 M NaOH at 70^{o}C for 10 minutes, and 2.5 M sodium bisulfite and 5 uM hydroquinone at 50^{o}C overnight. After de-sulphonation with 0.3 M NaOH and 0.4 M NaOAc, the DNA sample was then purified with a Qiagen PCR clean-up kit. Nested PCR was applied to amplify loci of interest (primers listed in Supplemental Table 19). Amplicons were then subcloned and sequenced.

Supplemental Figure Legends

Supplemental Figure 1. Comparison of histone bulk level between sperm (Sp) and the fibroblast cell line ZF4 (Fib). (A) Immunoblotting against H1 shows that H1 in ZF4 is ~25% of the level observed in sperm. (B) Immunoblotting against H3 shows normalization of H3 level to cell number and verifies ZF4 as an octaploid cell line. (C) Immunoblotting against tetra-acetylation on H4 Lys 5, 8, 12, and 16 shows no signal in sperm cells but a robust signal in fibroblast cells. (D) Immunoblotting against H4R3me2 demonstrates the vast majority of the H4 tail is intact in sperm chromatin.

Supplemental Figure 2. Quality control of input for ChIP with sperm cells. (A) Different doses of MNase were applied to release nucleosomes. (B) Input DNA was shown before (lane 1) and after (lane 2) whole genome amplification. M1 and M2, DNA markers starts from 1 kb with a 1-kb increment and from 100 bp with a 100-bp increment, respectively.

Supplemental Figure 3. Developmental loci with multivalent and regional chromatin features. ChIP- and MeDIP- chip profiles, with fold enrichment over input in $\log_2$ scale (y-axis). (A) *hoxb* cluster. (B) *hoxc* cluster. Lines above the tracks indicate nontiled regions on the array. (C) A random region in the genome showed a superimposable DNA methylation profile between sperm and muscle.

Supplemental Figure 4. Confirmation of DNA hypomethylation at the developmental loci in sperm by bisulphite sequencing. Each circle represents a CG dinucleotide, with open circles for unmethylated CG and closed circles for methylated CG. All loci tested match MeDIP data.

Supplemental Figure 5. Intersection analyses between H3K36me3 and other marks (or H2AFV) associated genes. Genes here were retrieved from proximal promoter regions (-2 ~ +1 kb of TSS). Enrichment of H3K36me3 in gene promoters shows significant correlation with H3K27me3, H3K4me3, and H2AFV, but not H3K14ac.

Supplemental Figure 6. Coincidence of H3K27me3 and H3K36me3 at developmental loci confirmed by sequential ChIP. qPCR result from sequential ChIP H3K27me3/H3K36me3 showed at least 3.5 fold enrichment over background (H3K27me3/beads) at the promoter regions of developmental genes.

Supplemental Figure 7. Examination of H3K36me3 enrichment in embryos and H3K36me2 in sperm by ChIP-qPCR. (A) H3K36me3 is enriched in the coding region of genes in zebrafish embryos. As opposed to sperm, we observed enrichment of H3K36me3 at 3' ends of transcribed genes at shield stage (6 hpf). (B) H3K36me2 is enriched at 3' ends of expressed genes (*bactin2*, *ddx5*) but not enriched at developmental genes (*gsc*, *klf4*). Amplicon for qPCR analysis locates at either 5' or 3' end of a gene as specified. Intergenic, 1 kb upstream of *ctsl1b*, is not enriched with any marks in the sperm ChIP-chip data and serves as a negative control.

Supplemental Figure 8. Chromatin profiles of repeat regions and noncoding RNAs. (A) Type 1 (LINE) and (B) Type 2 (SINE) transposons are DNA methylated and deficient in activating marks tested. Bars indicate designed probes for the repeat elements. (C) *5S* rDNA and (D) *5.8S* rDNA show enrichment of DNA methylation, as well as H3K36me3 and H3K9me3. (E) tRNA clusters (tRNA-Leu and tRNA-Ser) were enriched with DNA methylation and particular repressive marks (H3K9me3 and H3K36me3). (F) Stand-alone tRNA-Ala located in the region of active chromatin.

CHAPTER 3

DNA METHYLATION PROFILING IN ZEBRAFISH

Wu, et al., 2011. Originally published in Methods in Cell Biology. VOL. 104: 327-339

CHAPTER 18

DNA Methylation Profiling in Zebrafish

Shan-Fu Wu[*,†], Haiying Zhang[*,†], Saher Sue Hammoud[*,†], Magdalena Potok[*,†], David A. Nix[†], David A. Jones[†] and Bradley R. Cairns[*,†]

[*]Howard Hughes Medical Institute, Chevy Chase, Maryland, USA

[†]Department of Oncological Sciences, Huntsman Cancer Institute, University of Utah School of Medicine, Salt Lake City, Utah, USA

Abstract

DNA methylation on cytosine in vertebrates such as zebrafish serves to silence gene expression by interfering with the binding of certain transcription factors and through the recruitment of repressive chromatin machinery. Cytosine DNA methylation is chemically stable and heritable through the germline – but also reversible through many modes, making it a useful and dynamic epigenetic modification. Virtually all of the enzymes and factors involved in the deposition, binding, and removal of cytosine methylation are conserved in zebrafish, and therefore the organism an excellent model for understanding the use of DNA methylation in the control of gene regulation and other processes. Here, we discuss the main approaches to quantifying DNA methylation levels genome-wide in zebrafish: one

METHODS IN CELL BIOLOGY, VOL 104

0091-679X/10 $35.00
DOI 10.1016/B978-0-12-374814-0.00018-5

is an established method for revealing regional methylation (methylated DNA immunoprecipitation (MeDIP)), and the other is an emerging method that reveals DNA methylation at base-pair resolution (shotgun bisulphite sequencing). We also introduce some of the analytical methods that are useful for identifying regions of hypo- or hyper-methylation, and ways to identify differentially methylated regions.

I. Introduction

Cytosine DNA methylation is a major negative regulator of gene activity and an important epigenetic modification. Prominent examples of DNA methylation in normal biology include monoallelic X chromosome inactivation and genomic imprinting in plants and animals, each of which results in stable and heritable epigenetic states and gene repression (Heard, 2005; Martienssen *et al.*, 2004). DNA methylation in eukaryotic cells occurs primarily at cytosine residues in a CpG dinucleotide context (Bird, 1996). This dinucleotide pair is under-represented in vertebrate genomes and occurs at only 20–25% of the expected frequency (Antequera and Bird, 1993a, 1993b). This under-representation is thought to result from the high rate of spontaneous (or catalyzed) deamination of methylated cytosines into thymidine (Bird *et al.*, 1995). If left unrepaired prior to DNA replication, a C to T transition occurs, which becomes an inherited mutation.

The human genome contains ~35,000 regions of high-density CpGs known as CpG islands (Antequera and Bird, 1993b, 1994) that have a low steady-state level of cytosine methylation. These islands often reside in the promoter regions of housekeeping genes and also at genes with tissue-restricted expression patterns. The methylation state of promoter-proximal CpG islands often correlates inversely with gene expression. Gene silencing occurs by two modes: first, many (but not all) transcription factors will not bind their cognate recognition site if it is methylated. Second, cytosine methylation is detected by a family of methylated DNA binding (MBD) proteins (Ballestar and Wolffe, 2001; Hendrich and Tweedie, 2003; Jorgensen and Bird, 2002; Wade, 2001), typified by MeCP2, which bind to methylated CpG stretches *in vitro* and *in vivo* and recruit histone deacetylases to repress transcription (Ballestar and Wolffe, 2001; Hendrich and Tweedie, 2003; Jorgensen and Bird, 2002; Wade, 2001). Indeed, this mechanism is likely the reason why the majority of CpG methylation within the human genome targets transposons, which constitute up to 45% of the human genome (Smit and Riggs, 1996) – with the associated transcriptional repression acting to limit transposon expression and maintaining genome integrity (Bestor and Bourc'his, 2004).

A. DNA Methylation in Mammalian Development and Cancer

Beyond transposon silencing, roles for DNA methylation in regulating genes important for both cancer and development have been established. In cancer cells,

although there is a general trend of genomic *hypo*methylation (Feinberg and Vogelstein, 1983, 1987; Feinberg *et al.*, 1988; Gama-Sosa *et al.*, 1983; Goelz *et al.*, 1985), the promoters of a number of genes are *hyper*methylated (Feinberg and Tycko, 2004; Jones, 2003, 2005). Although this suggests mis-targeting of DNA methylation in cancer, a clear model reconciling these two observations has not been presented. In fact, the primary focus of studies investigating the relationship between DNA methylation and cancer in recent years has been on defining hypermethylation of individual genes and the biological consequences of DNA methylation-dependent gene silencing. These findings have shown that a number of tumor suppressors (p16, p15, Rb, estrogen receptor, hMLH1, and E-cadherin) are hypermethylated in cancer cells (Feinberg and Tycko, 2004; Jones, 2003, 2005), but the mechanism underlying their methylation is not entirely clear.

Although DNA methylation-directed gene silencing has been proposed to play an important role in establishing tissue-specific expression patterns during development, this notion has been controversial. Indeed, CpG islands are rarely methylated in normal tissues, even at genes that are transcriptionally silent. Until recently, there were very few examples of dynamic changes in the methylation state of a CpG island itself during development. However, several studies now support roles for alterations in DNA methylation at promoters and CpG islands during development and for silencing germline genes in the soma (Back *et al.*, 1999; Beri *et al.*, 2007; Borgel *et al*., 2010; De Smet *et al.*, 1999; Douet *et al.*, 2007; Hammoud *et al.*, 2009; Hsu *et al.*, 2007; van der Ploeg and Flavell, 1980).

B. DNA Methylation in Zebrafish

Zebrafish is a major model system for the study of development, and has been emerging as a major model system for the study of cancer. In mammals, the enzymes that conduct cytosine DNA methylation fall into three families: DNMT1, DNMT2, and the DNMT3 family which includes DNMT3a, DNMT3b, and the catalytically inactive DNMT3L. Representatives of all three DNMT families are present in zebrafish (Fig. 1). Here, the zebrafish ortholog of DNMT1 (which conducts the majority of maintenance methylation in vertebrates) is highly conserved with its mammalian counterpart. Likewise, zebrafish *dnmt2* is also highly conserved with mammalian DNMT2, though DNMT2 enzymes are likely focused on the methylation of RNAs in all organisms (Goll *et al.*, 2006; Rai *et al.*, 2007). Interestingly, zebrafish harbors five *dnmt* genes in the DNMT3 family (which conduct the majority of *de novo* methylation); however, they do not clearly partition into sets that are more DNMT3a- or DNMT3b-like (Fig. 1). Finally, we have not found a zebrafish ortholog of mammalian DNMT3L, which conducts (in partnership with DNMT3a) imprinting in mammals. This fact, combined with other analyses (unpublished) suggests that zebrafish lacks the same imprinting modes observed in mammals, though parent-of-origin specific methylation remains possible. Beyond the DNMTs themselves, virtually all of the additional enzymes involved in the control of

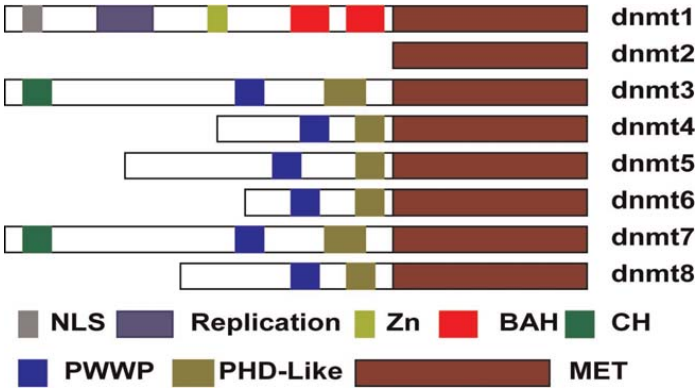

Fig. 1 DNA methyltransferases in zebrafish. Zebrafish harbors members of each vertebrate DNA methyltransferase family, including Dnmt1, Dnmt2, and Dnmt3. The families all share a highly conserved catalytic DNA methyltransferase domain (MET). However, N-terminal sequences of vertebrate DNMTs vary and may confer specific functions to each family. Zebrafish Dnmt enzymes Dnmt3–Dnmt7 are all related to the mammalian DNMT3 family, which is greatly expanded in zebrafish (Rai *et al.*, 2010a). NLS, nuclear-localization sequence; Replication, domain targeting to replication foci; Zn, zinc finger domain; BAH, bromo-adjacent homology domain; CH, calponin homology domain; PWWP domain, binds H3K36me and DNA; PHD-like, binds histone modifications; and MET, the conserved catalytic methyltransferase domain. (See color plate.)

chromatin structure, including those known to interact with DNA methylation machinery, are conserved (unpublished observations). Therefore, zebrafish has excellent potential as a model for understanding the use of DNA methylation dynamics in the control of gene regulation and its mis-regulation in cancer. We believe that these studies will be greatly enabled by methods that allow genome-wide assessments of DNA methylation.

We note that early studies questioned whether DNA methylation dynamics occurred during early zebrafish development (Macleod *et al.*, 1999), as relatively high levels of DNA methylation were observed at the blastula stage, where DNA methylation levels are low in mammals (Monk *et al.*, 1987). However, as zebrafish lacks a hypomethylated trophectoderm lineage, they display relatively high levels of DNA methylation at the blastula stage. Later studies revealed that the zebrafish sperm genome is initially hypermethylated, and then rapidly demethylated following fertilization, with zygotic methylation reaching a low point at the 1–2-cell stage – reaching levels lower than the levels observed in the oocyte itself (Mhanni and McGowan, 2004) (Fig. 2). DNA methylation levels begin to rise in the early blastula and by the mid-blastula stage reach levels observed in differentiated tissues (i.e., adult muscle). We have confirmed this result using highly sensitive mass spectrometric analysis (Rai *et al.*, 2008) (Fig. 2). Thus, zebrafish shares with mammals the process of gametic DNA demethylation occurring in the one-cell embryo, followed by gradual

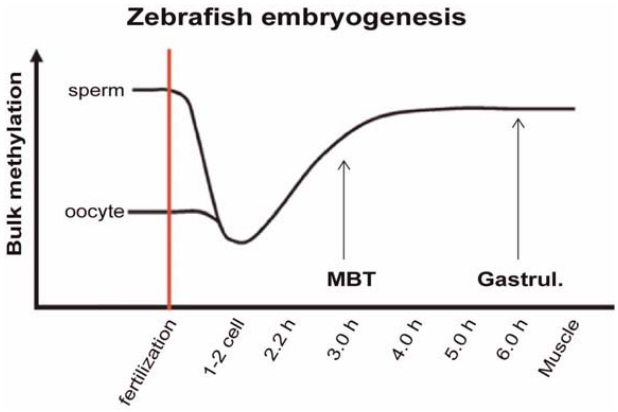

Fig. 2 Dynamic changes in DNA methylation during early zebrafish development. Genome-wide demethylation at fertilization and early blastula is followed by re-establishment of methylation through unknown mechanisms. The figure depicts data from Mhanni and McGowan (2004), as well as recent data from our lab (Rai *et al.*, 2008) and from Phillipe Collas' lab (Lindeman *et al.*, 2010b). We speculate that individual zebrafish Dnmts target specific genes required for tissue-specific terminal differentiation events (see (Rai *et al.*, 2010a)). (See color plate.)

de novo methylation. This process may help prepare the embryo for zygotic transcription and somatic development. Thus, a central question for all vertebrates is to define the methylation patterns of the gamete genomes, early embryos, and during the process of development both in the embryo and in particular tissues.

In zebrafish, very recent data from our lab has begun to reveal the sites of methylation genome-wide (Wu *et al*., in press). We have shown that the promoters of particular transcription factors (i.e., *hox* genes) are unmethylated in sperm but highly methylated in a differentiated somatic tissue (muscle) (see Fig. 3), which raises the possibility that critical developmental transcription factors are regulated by methylation (Wu *et al*., in press). Our work on sperm–soma comparisons complements and extends (to a genome-wide scale) recent and earlier studies on the methylated states of selected transcription factor promoters in the embryo (Lindeman *et al.*, 2010b; Yamakoshi and Shimoda, 2003). Furthermore, we find that many germline genes are unmethylated in the sperm but methylated in the soma in zebrafish, in keeping with studies in mammals (Wu *et al*., in press). Prior functional work, which involved the knock down of Dnmt1 or Dnmt3b (*via* morpholino oligonucleotides) in zebrafish embryos or discovery of *dnmt1* genetic mutations, has revealed tissue-specific terminal differentiation defects (Anderson *et al.*, 2009; Rai *et al.*, 2010a, 2006) that provide clear evidence for the importance of zebrafish Dnmt enzymes in development. Here, *dnmt1* morphant embryos harbored intestinal and exocrine pancreas differentiation defects. In contrast, the liver and endocrine pancreas

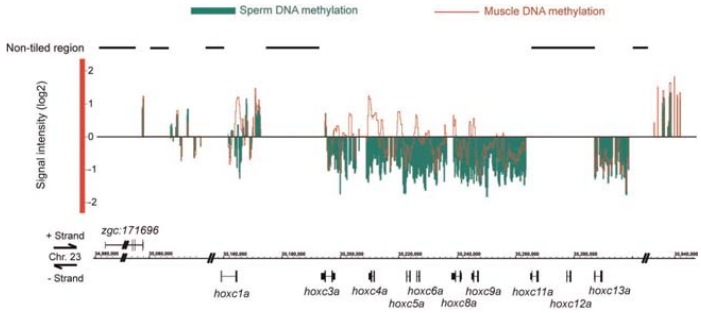

Fig. 3 Differentially methylated regions between zebrafish sperm and muscle. We show here the methylation status of a cluster of *hoxc* genes and its neighboring genes as an example of MeDIP-chip. Fold enrichment over input in log2 scale is shown on the *y*-axis. Almost the entire *hoxc* cluster is hypomethylated in sperm (compared to the genome average, 0 in signal intensity), and most of the *hoxc* genes are hypermethylated in muscle. This reveals dynamic methylation of a suite of genes that regulate development. (See color plate.)

of *dnmt1* morphants appeared normal. Taken together, these studies strongly suggest the selective use of Dnmt enzymes in tissue-specific differentiation in zebrafish.

II. Rationale

The two current approaches to study cytosine DNA methylation on a genome-wide scale are: (1) methylated DNA immunoprecipitation (MeDIP) (Weber *et al.*, 2007), and (2) genome-wide shotgun bisulphite sequencing (Cokus *et al.*, 2008; Lister *et al.*, 2009). The methods below are designed to allow researchers to conduct their choice of the two for DNA methylation profiling. The MeDIP is technically simpler, has available analysis pipelines, and provides regional information (∼250 bp resolution) with moderate dynamic range. In contrast, the shotgun bisulphite method provides base-pair resolution of cytosine DNA methylation, but requires very deep sequencing and considerable computational expertise for data analysis, though analysis programs are now emerging. Both involve the initial extraction of DNA from cells/tissues of interest but diverge in the subsequent steps.

III. Methods

A. Extraction of Zebrafish Genomic DNA

To extract genomic DNA from zebrafish adult tissue, embryos, or cell lines, we utilize the Gentra Puregene Tissue Kit (Qiagen Inc., Valencia, CA) with the following modifications. Instead of using a mortar and pestle to grind frozen tissues, fresh chunks of tissues (e.g., muscle or liver) are minced quickly on ice (*Note*: this is

omitted for embryos and cells). All source materials are incubated with the "Cell Lysis Solution" and Proteinase K (1 mg/mL) at 65 °C overnight, and then incubated with RNaseA (4 mg/mL) at 37 °C for 2 h. In the final step, we use 10 mM Tris (pH 8.0) to rehydrate DNA. The expected yield from 5–10 mg of tissues is 2–15 μg of DNA.

B. The MeDIP Procedure, Coupled to Genome-Scale Tiling Arrays

The MeDIP procedure begins by the shearing of genomic DNA by sonication to the desired size (typically 200–600 bp, median 400 bp), followed by purification with a PCR purification kit (Qiagen Inc.) or equivalent approach; in the final step DNA is eluted with 10 mM Tris (pH 8.0). Four micrograms of sheared genomic DNA (50 μL in a microcentrifuge tube) is then denatured at 93 °C for 10 min, and then transferred to and kept on ice. Ice-cold IP buffer (20 mM Tris (pH 7.5), 140 mM NaCl, 0.05% Triton X-100) and 10 μg of antibody raised against 5-methylcytidine (Eurogentec BI-MECY-0100) are added to the sheared genomic DNA (final volume 500 μL) and incubated with rotation at 4 °C for 2 h. About 12×10^6 Pan Mouse IgG magnetic Dynabeads (Invitrogen 110.41) are washed with PBS (pH 7.4) plus 5 mg/mL BSA and then added to the DNA–antibody mixture for incubation at 4 °C for 2 h. Non-specific proteins and DNA are removed with IP buffer (3 × 1 mL, washes), and the DNA–antibody–bead complexes are treated with Proteinase K (2 μg/μL in 200 μL IP buffer) at 50 °C for 3 h to release the DNA from the antibody–bead complex. Methylated DNA was then purified from the supernatant with a Qiagen PCR purification kit; elute DNA from the column with 10 mM Tris (pH 8.0).

To detect regional methylation levels, methylated DNA is applied to a "tiling" microarray containing oligonucleotide probes that tile the whole genome or all promoters (termed "MeDIP-chip") (Weber *et al*., 2007). The purified DNA fragments derived from the antibody pull-down above, and (separately) the DNA input for MeDIP (representing the whole genome), are amplified by a whole-genome amplification kit (Sigma WGA2) and labeled (separately) with either Cy3 or Cy5 dyes. Samples are then hybridized to the desired microarray. The precise protocols for labeling and hybridization can be found on the Agilent website, and examples involving our data can be accessed at the GEO public database, GSM655008.

We have developed one of the zebrafish genome-scale tiling microarrays, which utilizes the platform from Agilent Technologies, and we have made this publicly available (Agilent G4495A). Our customized zebrafish microarray was adapted from an existing zebrafish promoter array (Wardle *et al.*, 2006) by adding hundreds of additional genes and genetic elements. This array design is printed on two slides, each bearing 244,000 60-mer oligonucleotides, tiled at an average spacing of 250 bp and covering the "extended promoter" region (−9 to +3 kb from transcription start site) of ∼13,000 mRNA genes. Good representation of most of the known (in 2007) miRNAs, tRNAs, rRNAs, repeat elements, CpG islands, and two centromeric heterochromatin regions (GEO platforms GPL6600 and GPL6601) are also included. Probe design was based on genome versions Zv4, Zv5, and Zv6. Additional effective

options for whole genome tiling microarrays are available from Agilent and Nimblegen, including the GEO platforms GPL9970 (Vastenhouw *et al.*, 2010) and GPL10835 (Lindeman *et al.*, 2010a).

C. Shotgun Bisulphite Sequencing, Coupled to High-throughput Sequencing

Bisulphite treatment of genomic DNA coupled with DNA sequencing is the standard approach to detect individual methylated cytosine residues. Here, unmethylated cytosine is converted to uracil, whereas methylated cytosine remains unchanged (Clark *et al.*, 1994). Specific loci can then be examined by PCR, subcloning, and sequencing. However, to reveal DNA methylation at base-pair resolution at a genome-wide scale, bisulphite conversion is coupled to whole-genome shotgun high-throughput sequencing (termed "shotgun bisulphite sequencing") (Cokus *et al.*, 2008; Lister *et al.*, 2009). Complete genome-wide maps of cytosine DNA methylation at base pair resolution *via* shotgun sequencing in zebrafish have not been published, but have been successfully produced by our lab (unpublished). Here we provide our latest protocol.

We begin with 3 μg of genomic DNA derived *via* non-organic purification, which we find improves the "behavior" of the nucleic acid in subsequent steps. Next, we spike the genomic DNA with unmethylated lambda DNA (30 ng, to 1% of total DNA) to provide an internal control for bisulphite conversion efficiency. (*Note*: lambda reads are parsed from the dataset and examined for C > T conversion rates, and our procedure consistently provides >99% conversion.) The genomic DNA (with lambda) is sheared with a sonicator (Covaris Inc., Woburn, MA) to an average size of ~400 bp. Then, we follow the instructions for the "TruSeq DNA Sample Prep Kit" (Illumina Inc., San Diego, CA) to repair sheared DNA ends and to add an adenine to one strand. We then ligate adaptors (bearing methylated cytosine bases) provided by Illumina, Inc., to the DNA fragments according to manufacturer instructions. The methylated cytosines in the adaptors resist conversion in the subsequent bisulphite step. A PCR purification kit or MiniElute PCR purification kit (Qiagen Inc.) is used to purify the DNA after each treatment. For bisulphite conversion, we use and follow the "EpiTect Bisulphite Kit" (Qiagen Inc.). However, we modify the thermal cycler conditions for all DNA denaturation steps to 98 °C for 10 min and add an additional 2 h of incubation at 60 °C at the end of the procedure to ensure complete conversion. We have tested this modification to ensure that minimal degradation/fragmentation of DNA occurs and that >99% of unmethylated cytosines are converted thymidine. Subsequently, high-fidelity Phusion DNA polymerase is applied for strand replication of all bisulphite-converted DNA per instructions in the Illumina TruSeq kit. After purification with a PCR purification kit (Qiagen Inc.), DNA fragments are then separated on a 1% agarose gel, and those in the 300–400 bp size range are excised. The resulting library of bisulphite-converted DNA fragments is then sequenced on an Illumina system. We currently prefer sequencing with an Illumina HiSeq2000 machine using the 101-base paired end format for ease of mapping because it yields optimal read lengths and read numbers.

D. Analysis of Genome-wide Methylation Data

We are using two effective methods to analyze MeDIP-chip data: TIMAT2 (T2) and SLAM. We have used T2 extensively for the analysis of DNA methylation patterns (Wu *et al*., in press) and here provide a figure of the *hoxc* locus that displays both the extent of hypomethylation of developmental transcription factors in zebrafish sperm and the acquisition of methylation at several *hoxc* gene promoters in differentiated muscle (Fig. 3). T2 is an open source application developed by the Bioinformatics Shared Resource at the University of Utah, and the program and tutorials are available at http://bioserver.hci.utah.edu/BioInfo/index.php/Software: T2. Zebrafish annotation and genomic sequence can be retrieved from the Ensembl or UCSC Genome Bioinformatics website. Microarray data from biological replicates or inputs are first quantile normalized and median scaled to 100 (Bolstad *et al.*, 2003). Oligos with calculated enrichment ratio (mean treatment replicas/mean control replicas in the log2 ratio) are then mapped to the zebrafish genome assembly. Summary scores are assigned to the center position of 400-bp windows (the majority size of fragments after whole genome amplification) covering at least two oligo start positions. High-scoring windows located within 250-bp distance are merged as intervals. Intervals are then ranked by their best window scores and these intervals represent hypermethylated regions. Additionally, T2 can be set up to make intervals with reduced window scores by setting "true" for both "quantileNormalizeAll" and "makeReducedWindows" in the parameter file. These intervals with reduced scores represent hypomethylated regions and possibly regions with contiguous poor probes and hybridization. When comparing methylation level between two different materials, one is set as "treatment" and the other is set as "control" for T2 analysis. This will generate differentially methylated regions. To view the datasets, DAS/2 compliant genome browsers such as IGB (http://www.bioviz.org/igb/) can be used. Genes near hypo- or hyper-methylated regions can be identified by the application called "find neighboring genes (FNG)" in the T2 package. To have an overview of a group of genes, we retrieve the top 800 or 1600 genes located within 12 kb of loci of interest and submit to GoMiner (http://discover.nci.nih.gov/gominer/index.jsp) for GO term analysis.

A second, effective program is SLAM: gauSsian dynamic Linear Analysis of Methylated chip data. SLAM is a new method developed by W. Evan Johnson and colleagues (Yumei Li, Timothy M. Bahr, Spencer Clark) that quantifies the probe-wise methylation levels for two-color MeDIP-chip arrays using four steps: normalization, smoothing, mixture modeling, and transformation. We find SLAM exceptionally useful for the identification of differentially methylated regions of biological relevance; regions that convert from mostly methylated to mostly unmethylated (or *vice versa*), rather than regions that convert from entirely methylated to mostly methylated (for example). SLAM is available for downloading at http://jlab.byu.edu/SLAM/Home.html. SLAM is packaged for Windows users with a user-friendly graphical user interface. It also exists in a command-line Python script built for MacOS, UNIX, and Linux users. SLAM is created for use with Agilent and

Nimblegen tiling arrays as well as for Illumina's GoldenGate and Infinium platforms. SLAM has been utilized in the analysis of zebrafish and human datasets (Rai *et al.*, 2010b) and will be used by our laboratory in future publications.

Currently, there is not a single established pipeline for the analysis of shotgun bisulphite sequencing, because the technique is relatively new and the analysis interests of users are diverse. However, applications to analyze shotgun bisulphite sequencing are under development in many labs, including those that first applied the technique (Cokus *et al.*, 2008; Lister *et al.*, 2009), and our laboratory (in collaboration with the Bioinformatics Shared Resource (University of Utah), and with W. Evan Johnson (Brigham Young University). To facilitate progress in this area, our laboratory will be providing protocols and data analysis methods for chromatin and epigenetics analysis in zebrafish prior to publication. Our progress can be observed at links present at http://bioserver.hci.utah.edu/BioInfo/index.php/Software, and we intend to have a website focused on chromatin and DNA methylation analysis in zebrafish publicly available during Fall, 2011.

IV. Discussion

Zebrafish harbors all the enzymes and factors presently known in mammals to be involved in the deposition and binding of cytosine DNA methylation. Zebrafish also possesses orthologous pathways of DNA demethylation, including AID, MBD4, TDG, and the recently discovered TET1/2/3 family of enzymes, which are involved in the hydroxylation of methyl-cytosine (Rai *et al.*, 2008; Tahiliani *et al.*, 2009). Also, many functional studies strongly suggest that most of the modes of regulation of DNA methylation and demethylation (imprinting likely being an exception) are conserved in zebrafish. Furthermore, zebrafish harbor the systems for the generation of piRNAs, which may help direct DNA methylation and other modifications to repeat regions and other loci in the genome. Given the many advantages of zebrafish for the analysis, isolation, and manipulation of tissues in early development (and the germline), zebrafish should prove an important model organism for future studies in this area. Here, the ability to examine DNA methylation profiles on a genome-wide scale is transforming our understanding of the dynamics of DNA methylation and its use in developmental processes. We hope that the methods described here, and by other colleagues in the field, will help stimulate the study of chromatin and DNA modifications in the zebrafish and that studies on this important developmental model will help break new conceptual ground in the chromatin field.

Acknowledgments

The authors thank Brian Dalley for expert genomics work and advice, and W. Evan Johnson and colleagues at BYU for the use of SLAM and for many useful discussions. This work was supported by grants from the National Institute of Child Health and Development (HD 058506 to B.R.C and D.A.J), HHMI (support of B.R.C), the Huntsman Cancer Institute (support of D.A.N), and the Cancer Center Support Grant (CA042014) for core facilities.

References

Anderson, R. M., Bosch, J. A., Goll, M. G., Hesselson, D., Dong, P. D., Shin, D., Chi, N. C., Shin, C. H., Schlegel, A., Halpern, M., and Stainier, D. Y. (2009). Loss of Dnmt1 catalytic activity reveals multiple roles for DNA methylation during pancreas development and regeneration. *Dev. Biol.* **334**, 213–223.

Antequera, F., and Bird, A. (1993 a). CpG islands. *EXS* **64**, 169–185.

Antequera, F., and Bird, A. (1993 b). Number of CpG islands and genes in human and mouse. *Proc. Natl Acad. Sci. U. S. A.* **90**, 11995–11999.

Antequera, F., and Bird, A. (1994). Predicting the total number of human genes. *Nat. Genet.* **8**, 114.

Back, W., Loff, S., Jenne, D., and Bleyl, U. (1999). Immunolocalization of beta catenin in intestinal polyps of Peutz-Jeghers and juvenile polyposis syndromes. *J. Clin. Pathol.* **52**, 345–349.

Ballestar, E., and Wolffe, A. P. (2001). Methyl-CpG-binding proteins. Targeting specific gene repression. *Eur. J. Biochem.* **268**, 1–6.

Beri, S., Tonna, N., Menozzi, G., Bonaglia, M. C., Sala, C., and Giorda, R. (2007). DNA methylation regulates tissue-specific expression of Shank3. *J. Neurochem.* **101**, 1380–1391.

Bestor, T. H., and Bourc'his, D. (2004). Transposon silencing and imprint establishment in mammalian germ cells. *Cold Spring Harb. Symp. Quant. Biol.* **69**, 381–387.

Bird, A., Tate, P., Nan, X., Campoy, J., Meehan, R., Cross, S., Tweedie, S., Charlton, J., and Macleod, D. (1995). Studies of DNA methylation in animals. *J. Cell Sci. Suppl.* **19**, 37–39.

Bird, A. P. (1996). The relationship of DNA methylation to cancer. *Cancer Surv.* **28**, 87–101.

Bolstad, B. M., Irizarry, R. A., Astrand, M., and Speed, T. P. (2003). A comparison of normalization methods for high density oligonucleotide array data based on variance and bias. *Bioinformatics* **19**, 185–193.

Borgel, J., Guibert, S., Li, Y., Chiba, H., Schubeler, D., Sasaki, H., Forne, T., and Weber, M. (2010). Targets and dynamics of promoter DNA methylation during early mouse development. *Nat. Genet.* **42**, 1093–1100.

Clark, S. J., Harrison, J., Paul, C. L., and Frommer, M. (1994). High sensitivity mapping of methylated cytosines. *Nucleic Acids Res.* **22**, 2990–2997.

Cokus, S. J., Feng, S., Zhang, X., Chen, Z., Merriman, B., Haudenschild, C. D., Pradhan, S., Nelson, S. F., Pellegrini, M., and Jacobsen, S. E. (2008). Shotgun bisulphite sequencing of the Arabidopsis genome reveals DNA methylation patterning. *Nature* **452**, 215–219.

De Smet, C., Lurquin, C., Lethe, B., Martelange, V., and Boon, T. (1999). DNA methylation is the primary silencing mechanism for a set of germ line- and tumor-specific genes with a CpG-rich promoter. *Mol. Cell Biol.* **19**, 7327–7335.

Douet, V., Heller, M. B., and Le Saux, O. (2007). DNA methylation and Sp1 binding determine the tissue-specific transcriptional activity of the mouse Abcc6 promoter. *Biochem. Biophys. Res. Commun.* **354**, 66–71.

Feinberg, A. P., Gehrke, C. W., Kuo, K. C., and Ehrlich, M. (1988). Reduced genomic 5-methylcytosine content in human colonic neoplasia. *Cancer Res.* **48**, 1159–1161.

Feinberg, A. P., and Tycko, B. (2004). The history of cancer epigenetics. *Nat. Rev. Cancer* **4**, 143–153.

Feinberg, A. P., and Vogelstein, B. (1983). Hypomethylation distinguishes genes of some human cancers from their normal counterparts. *Nature* **301**, 89–92.

Feinberg, A. P., and Vogelstein, B. (1987). Alterations in DNA methylation in human colon neoplasia. *Semin. Surg. Oncol.* **3**, 149–151.

Gama-Sosa, M. A., Slagel, V. A., Trewyn, R. W., Oxenhandler, R., Kuo, K. C., Gehrke, C. W., and Ehrlich, M. (1983). The 5-methylcytosine content of DNA from human tumors. *Nucleic Acids Res.* **11**, 6883–6894.

Goelz, S. E., Vogelstein, B., Hamilton, S. R., and Feinberg, A. P. (1985). Hypomethylation of DNA from benign and malignant human colon neoplasms. *Science* **228**, 187–190.

Goll, M. G., Kirpekar, F., Maggert, K. A., Yoder, J. A., Hsieh, C. L., Zhang, X., Golic, K. G., Jacobsen, S. E., and Bestor, T. H. (2006). Methylation of tRNAAsp by the DNA methyltransferase homolog Dnmt2. *Science* **311**, 395–398.

Hammoud, S. S., Nix, D. A., Zhang, H., Purwar, J., Carrell, D. T., and Cairns, B. R. (2009). Distinctive chromatin in human sperm packages genes for embryo development. *Nature* **460**, 473–478.

Heard, E. (2005). Delving into the diversity of facultative heterochromatin: the epigenetics of the inactive X chromosome. *Curr. Opin. Genet. Dev.* **15**, 482–489.

Hendrich, B., and Tweedie, S. (2003). The methyl-CpG binding domain and the evolving role of DNA methylation in animals. *Trends Genet.* **19**, 269–277.

Hsu, M., Mabaera, R., Lowrey, C. H., Martin, D. I., and Fiering, S. (2007). CpG hypomethylation in a large domain encompassing the embryonic β-like globin genes in primitive erythrocytes. *Mol. Cell Biol.* **27**, 5047–5054.

Jones, P. A. (2003). Epigenetics in carcinogenesis and cancer prevention. *Ann. N. Y. Acad. Sci.* **983**, 213–219.

Jones, P. A. (2005). Overview of cancer epigenetics. *Semin. Hematol.* **42**, S3–S8.

Jorgensen, H. F., and Bird, A. (2002). MeCP2 and other methyl-CpG binding proteins. *Ment. Retard. Dev. Disabil. Res. Rev.* **8**, 87–93.

Lindeman, L. C., Reiner, A. H., Mathavan, S., Alestrom, P., and Collas, P. (2010a). Tiling histone H3 lysine 4 and 27 methylation in zebrafish using high-density microarrays. *PLoS ONE* **5**, e15651.

Lindeman, L. C., Winata, C. L., Aanes, H., Mathavan, S., Alestrom, P., and Collas, P. (2010b). Chromatin states of developmentally-regulated genes revealed by DNA and histone methylation patterns in zebrafish embryos. *Int. J. Dev. Biol.* **54**, 803–813.

Lister, R., Pelizzola, M., Dowen, R. H., Hawkins, R. D., Hon, G., Tonti-Filippini, J., Nery, J. R., Lee, L., Ye, Z., Ngo, Q. M., Edsall, L., Antosiewicz-Bourget, J., Stewart, R., Ruotti, V., Millar, A. H., Thomson, J. A., Ren, B., and Ecker, J. R. (2009). Human DNA methylomes at base resolution show widespread epigenomic differences. *Nature* **462**, 315–322.

Macleod, D., Clark, V. H., and Bird, A. (1999). Absence of genome-wide changes in DNA methylation during development of the zebrafish. *Nat. Genet.* **23**, 139–140.

Martienssen, R., Lippman, Z., May, B., Ronemus, M., and Vaughn, M. (2004). Transposons, tandem repeats, and the silencing of imprinted genes. *Cold Spring Harb. Symp. Quant. Biol.* **69**, 371–379.

Mhanni, A. A., and McGowan, R. A. (2004). Global changes in genomic methylation levels during early development of the zebrafish embryo. *Dev. Genes Evol.* **214**, 412–417.

Monk, M., Boubelik, M., and Lehnert, S. (1987). Temporal and regional changes in DNA methylation in the embryonic, extraembryonic and germ cell lineages during mouse embryo development. *Development* **99**, 371–382.

Rai, K., Chidester, S., Zavala, C. V., Manos, E. J., James, S. R., Karpf, A. R., Jones, D. A., and Cairns, B. R. (2007). Dnmt2 functions in the cytoplasm to promote liver, brain, and retina development in zebrafish. *Genes Dev.* **21**, 261–266.

Rai, K., Huggins, I. J., James, S. R., Karpf, A. R., Jones, D. A., and Cairns, B. R. (2008). DNA demethylation in zebrafish involves the coupling of a deaminase, a glycosylase, and gadd45. *Cell* **135**, 1201–1212.

Rai, K., Jafri, I. F., Chidester, S., James, S. R., Karpf, A. R., Cairns, B. R., and Jones, D. A. (2010a). Dnmt3 and G9a cooperate for tissue-specific development in zebrafish. *J. Biol. Chem.* **285**, 4110–4121.

Rai, K., Nadauld, L. D., Chidester, S., Manos, E. J., James, S. R., Karpf, A. R., Cairns, B. R., and Jones, D. A. (2006). Zebra fish Dnmt1 and Suv39h1 regulate organ-specific terminal differentiation during development. *Mol. Cell Biol.* **26**, 7077–7085.

Rai, K., Sarkar, S., Broadbent, T. J., Voas, M., Grossmann, K. F., Nadauld, L. D., Dehghanizadeh, S., Hagos, F. T., Li, Y., Toth, R. K., Chidester, S., Bahr, T. M., Johnson, W. E., Sklow, B., Burt, R., Cairns, B. R., and Jones, D. A. (2010b). DNA demethylase activity maintains intestinal cells in an undifferentiated state following loss of APC. *Cell* **142**, 930–942.

Smit, A. F., and Riggs, A. D. (1996). Tiggers and DNA transposon fossils in the human genome. *Proc. Natl Acad. Sci. U. S. A.* **93**, 1443–1448.

Tahiliani, M., Koh, K. P., Shen, Y., Pastor, W. A., Bandukwala, H., Brudno, Y., Agarwal, S., Iyer, L. M., Liu, D. R., Aravind, L., and Rao, A. (2009). Conversion of 5-methylcytosine to 5-hydroxymethylcytosine in mammalian DNA by MLL partner TET1. *Science* **324**, 930–935.

van der Ploeg, L. H., and Flavell, R. A. (1980). DNA methylation in the human gamma delta beta-globin locus in erythroid and nonerythroid tissues. *Cell* **19**, 947–958.

Vastenhouw, N. L., Zhang, Y., Woods, I. G., Imam, F., Regev, A., Liu, X. S., Rinn, J., and Schier, A. F. (2010). Chromatin signature of embryonic pluripotency is established during genome activation. *Nature* **464**, 922–926.

Wade, P. A. (2001). Methyl CpG-binding proteins and transcriptional repression. *Bioessays* **23**, 1131–1137.

Wardle, F. C., Odom, D. T., Bell, G. W., Yuan, B., Danford, T. W., Wiellette, E. L., Herbolsheimer, E., Sive, H. L., Young, R. A., and Smith, J. C. (2006). Zebrafish promoter microarrays identify actively transcribed embryonic genes. *Genome Biol.* **7**, R71.

Weber, M., Hellmann, I., Stadler, M. B., Ramos, L., Paabo, S., Rebhan, M., and Schubeler, D. (2007). Distribution, silencing potential and evolutionary impact of promoter DNA methylation in the human genome. *Nat. Genet.* **39**, 457–466.

Wu, S. F., Zhang, H., and Cairns, B. R. (2011). Genes for embryo development are packaged in blocks of multivalent chromatin in zebrafish sperm. *Genome Res.* **21**, 578–589.

Yamakoshi, K., and Shimoda, N. (2003). *De novo* DNA methylation at the CpG island of the zebrafish no tail gene. *Genesis* **37**, 195–202.

CHAPTER 4

H2AFVA POTENTIALLY SETS UP DNA METHYLATION PROFILE OF PLURIPOTENCY/TOTIPOTENCY IN ZEBRAFISH EMBRYOS

Abstract

One central question in development is how totipotency and pluripotency are established. Bivalent marks, as the chromatin signature of pluripotency, are not persistent and diluted during early synchronous cell division, making them arguable to be heritable epigenetic marks. Studies in early embryos indicate DNA methylation status is fundamental to confer totipotency and pluripotency. The anticorrelation between DNA methylation profiles and H2A.Z occupancy is conserved from plants to vertebrates. Here, we examined H2afva occupancy in early embryos in zebrafish by ChIP-seq. We found both H2afva level and enrichment remain consistent from sperm to embryos. H2afva is enriched in the proximal promoter region in the first nucleosome. Consistent with previous studies, H2afva occupancy is anticorrelated to DNA methylation both in the promoters and outside of promoters. These data suggest H2afva is potentially a heritable epigenetic mark and sets up DNA methylation profiles of totipotency and pluripotency.

Introduction

Replacement of canonical histones by histone variants is critical to regulate gene activity and DNA-related cellular processes (Zlatanova and Thakar 2008; Marques et al. 2010). Canonical histones are synthesized in a replication-dependent manner in S phase, whereas histone variants are synthesized and incorporated into chromatin throughout the cell cycle (Ahmad and Henikoff 2002; Krogan et al. 2003; Kobor et al. 2004). H2A.Z, an H2A variant, is evolutionarily conserved from protozoan (*Plasmodium falciparum*) and budding yeast (*Saccharomyces cerevisiae*) to humans with 90% sequence conservation (Iouzalen et al. 1996). Exchange of H2A-H2B dimers to H2A.Z-H2B dimers depends on

the ATP-dependent Swr1 complex in yeast, named after the SWR1 catalytic subunit (Krogan et al. 2003; Kobor et al. 2004; Mizuguchi et al. 2004). Orthologs of Swr1 complex in vertebrates are SRCAP and P400 complexes, and there is no functional overlap between these two for incorporation of H2A.Z (Wu et al. 2005; Cai et al. 2006). Budding yeast has a single copy of the H2A.Z gene (HTZ1), whereas mammals have two H2A.Z genes (H2afv and H2afz), whose protein products differ by three residues, and they are possibly not redundant (Faast et al. 2001; Eirin-Lopez et al. 2009). Here, H2A.Z will be referred as the general name of the variant in different species. Zebrafish have two H2A.Z genes, *h2afva* and *h2afvb*. The H2afva protein sequence is 100% identical to vertebrate H2A.Z and H2afvb has an extra 21 residues in the N-terminus and 2 different residues in the rest of 128 residues; little is known about H2afvb. H2A.Z shares 60% of sequence identity to H2A, suggesting the uniqueness and importance of H2A.Z (Jackson and Gorovsky 2000). Deletion of H2A.Z leads to lethality in many organisms, such as *Tetrahymena thermophile*, *Drosophila melanogaster*, *Xenopus leavis*, and *Mus musculus* (van Daal and Elgin 1992; Iouzalen et al. 1996; Liu et al. 1996; Clarkson et al. 1999; Faast et al. 2001; Ridgway et al. 2004). In budding yeast, H2A.Z is not essential but is involved in many biological processes including transcriptional activation and repression, chromosome stability, and DNA repair (Santisteban et al. 2000; Meneghini et al. 2003; Krogan et al. 2004; Mizuguchi et al. 2004; Zhang et al. 2005). In mammalian cells, H2A.Z is important for transcriptional regulation, chromosome segregation, centromeric functions, and cancer metastasis (Rangasamy et al. 2003; Rangasamy et al. 2004; Gevry et al. 2007; Gevry et al. 2009).

The role of H2A.Z in transcription remains unclear. In human cells and *Drosophila*, the level of H2A.Z in promoter regions is positively correlated with gene activity, whereas in yeast cells, it is inversely correlated (Guillemette et al. 2005; Li et al. 2005; Zhang et al. 2005; Barski et al. 2007; Mavrich et al. 2008). Interestingly, in response to changes in growth conditions, H2A.Z in yeast cells is required to promote full gene activation and shows redistribution from activated promoters to repressed/basal promoters (Li et al. 2005; Zhang et al. 2005). Biochemical studies further show H2A.Z-associated nucleosomes are more susceptible to loss, suggesting H2A.Z poises repressed/basal promoters for activation through loss of histones—see below for the poising role of H2A.Z in ES cells (Placek et al. 2005; Zhang et al. 2005). Posttranslational modifications of H2A.Z could partially explain the conflicting role of H2A.Z in transcription. Acetylation in the N-terminus of H2A.Z is associated with active transcription in yeast and mammalian cells, whereas monoubiquitylation in the C-terminus of H2A.Z is found on the inactive X chromosome of female mammals (Millar et al. 2006; Sarcinella et al. 2007; Talbert and Henikoff 2010; Ku et al. 2012; Valdes-Mora et al. 2012).

Loss of H2A.Z in mice leads to embryonic lethality by the gastrulation stage (Faast et al. 2001). The mutant embryo develops normal ICM and trophectoderm but fails to further differentiate beyond the blastocyst stage, suggesting H2A.Z is indispensable for efficient differentiation of stem cells (Banaszynski et al. 2010). Genomic localization of H2A.Z in ES cells coincides with Suz12, a core subunit of the PRC2 complex, in the promoters of developmental regulators, and the co-occupancy is interdependent

(Creyghton et al. 2008). Consistent with mouse models, H2A.Z-depleted ES cells fail to differentiate upon induction.

Analyses of nucleosome dynamics during ES cell differentiation show both nucleosome depletion and *de novo* incorporation occur, typically in the promoters and exons of genes (Li et al. 2012b). Interestingly, H2A.Z is localized to nucleosome depletion regions in undifferentiated ES cells (Li et al. 2012b; Hu et al. 2013). H2A.Z-associated nucleosomes are enriched with H3K4me3 in promoters and enhancers. Furthermore, H2A.Z-associated nucleosomes encompass binding sites for the endoderm "pioneer" transcription factor FoxA2. Both H2A.Z and FoxA2 are required for nucleosome depletion and efficient ES cell differentiation. Knockdown of H2A.Z impairs Oct4, MLL, and PRC2 complexes for efficient binding to target genes. Taken together, these data suggest H2A.Z maintains chromatin accessibility in ES cells and poises genes for activation during differentiation.

DNA methylation is often observed on cytosine in the context of CpG dinucleotide and involved in gene silencing. CpG-rich regions, CGIs, mostly occur in the promoter regions but lack methylation irrespective of the transcription status. DNA methylation and H2A.Z incorporation are reported as antagonistic in both animals and plants (Zilberman et al. 2008; Conerly et al. 2010; Zemach et al. 2010). H2A.Z in *Arabidopsis* is found specifically at the 5' promoter regions of genes where CGIs reside, and DNA are unmethylated (Zilberman et al. 2008). Another profound example is the pericentromere regions, which contain many transposons and heavily methylated DNA, but a very low level of H2A.Z. Loss of MET1 DNA methyltransferase in *Arabidopsis* causes both losses and gains of DNA methylation and leads to opposite changes in

H2A.Z deposition. Conversely, loss of PIE1, homolog of SWR1, leads to a loss of H2A.Z deposition, especially at intragenic regions, and to a corresponding gain of DNA methylation. During B-cell lymphomagenesis, H2A.Z is progressively lost and this is generally correlated to a gain of DNA methylation (Conerly et al. 2010). Differential comparison on H2A.Z occupancy and DNA methylation between cell states shows that gain of H2A.Z occupancy at the gene body corresponds to loss of DNA methylation in the transition from transformed cells to tumors. When 5-azacytidine, a cytosine analogue that inhibits DNMTs, is applied to mammalian culture cells, regional loss of DNA methylation corresponds to a gain of H2A.Z despite CG density (Yang et al. 2012). Moreover, mutual exclusion between H2A.Z and DNA methylation is observed in the entire gene in puffer fish (Zemach et al. 2010). These data suggest the conserved anticorrelation relationship between H2A.Z occupancy and DNA methylation and a potential mechanism for targeting of DNA methylation.

Dynamic DNA methylation accompanies and potentially guides developmental processes. To confer pluripotency in the embryo, methylation on paternal genomes is erased globally by active demthylation before first cell division in the zygote, whereas the maternal genome is demethylated by passive dilution over cleavage divisions (Mayer et al. 2000; Oswald et al. 2000; Howell et al. 2001). Studies in zebrafish examine DNA methylation from gametes to early embryos, suggesting DNA methylation profiles underlie embryo totipotency and pluripotency, and zebrafish appear to achieve a totipotent chromatin state when zygotic genome activates (Jiang et al. 2013; Potok et al. 2013).

In ES cells, the combination of active and silent modifications termed “bivalent domain” (H3K4me3 and H3K27me3) is enriched in the highly conserved noncoding regions, which encompass many developmentally important regulators (Bernstein et al. 2006). Studies have proposed the role of bivalent domain in guiding developmental genes for activation or repression during lineage specification (Mikkelsen et al. 2007; Li et al. 2012a). Therefore, the bivalent domain is considered as the chromatin signature of pluripotency in ES cells. Vastenhouw et al. (2010) suggest chromatin attributes including bivalent marks cannot be detected by immunoblotting until ZGA and chromatin signature is reestablished when zygotic genome activates in zebrafish (Vastenhouw et al. 2010). After ZGA, the majority of genes are enriched with H3K4me3 and developmental regulators are highly enriched with bivalent domain. These data suggest a model where chromatin signature is not inherited from gametes but is reestablished in early embryos. In contrast, studies from Wu et al. (2011) and Lindeman et al. (2011) show a similar chromatin profile between sperm and pre-MBT embryos and suggest an inheritance model (Lindeman et al. 2011; Wu et al. 2011). They are able to detect H3K4me3 by immunoblotting and immunostaining before ZGA and further show bivalent domains are enriched in the promoters of developmental genes before ZGA—though at lower level compared to post-ZGA. It is still unclear if the diluted level of bivalent marks is instructive for embryogenesis and if there is any heritable epigenetic mark from gametes to embryos.

Examination of dynamic DNA methylation in early embryos suggests totipotency and pluripotency are conferred through DNA methylation profiles. However, how DNA methylation is targeted in early embryos remains unknown. Here, we determine the

genomic localization of H2afva in zebrafish early embryos, before, during, and after ZGA by ChIP-seq (chromatin immunoprecipitation and sequencing). H2afva is enriched in the promoters of genes, including both early and late expressed genes in early embryos. This promoter-enriched pattern in zebrafish is consistent with other vertebrates. H2afva profile in early embryos is very similar to that in sperm and potentially inherited from sperm. Notably, the strong anticorrelation relationship between DNA methylation and H2afva is observed in early embryos, especially before zygotic genome is activated. This anticorrelation has been reported previously in zebrafish mature sperm by ChIP-chip from our lab (Wu et al. 2011), and is consistent with other vertebrates and plants (Zilberman et al. 2008; Conerly et al. 2010; Zemach et al. 2010). Taken together, these data suggest H2afva could be inherited from gametes to embryos and potentially sets up DNA methylation profiles of totipotency and pluripotency in sperm and early embryos.

Results

Enrichment of H2afva at Promoter Regions in Sperm and Early embryos

Global zygotic transcription is not launched until the 1k-cell stage in zebrafish. Before ZGA, the occupancy of bivalent chromatin marks is diluted due to multiple rounds of synchronous cell division cycles. To investigate the epigenetic role of H2afva in very early embryos, we determined the bulk level and genomic localization of H2afva before, during, and after ZGA. Immunoblotting was performed against H2afva in sperm, 256-cell, high (one stage after 1k-cell), and dome embryos (Figure 4.1A). Notably, H2afva is relatively abundant at the 256-cell stage compared to sperm and other stages,

suggesting H2afva is potentially inherited from gametes and not diluted after multiple rounds of cell division in very early embryos. In contrast to diluted bivalent marks before ZGA (Vastenhouw and Schier 2012), H2afva is persistent and could play an important role during very early embryogenesis.

Next, we determined H2afva genomic localization by performing ChIP-seq. From 50 bp single-end sequencing, we retrieved more than 20 million aligned reads from each stage and normalized IP to input to calculate enrichment fold and FDR (false discovery rate). To show its genomic enrichment, H2afva is plotted around TSS (transcription start site) and TTS (transcription termination site) (Figure 4.1B–C). H2afva is roughly enriched at the first nucleosome, which represents a conserved feature of eukaryotic genes, as reported in yeast, plants, and humans (Guillemette et al. 2005; Li et al. 2005; Raisner et al. 2005; Zhang et al. 2005; Millar et al. 2006; Barski et al. 2007). In contrast, H2afva is less abundant and even depleted in gene bodies and intergenic regions. H2afva has overall better enrichment at high stage (Figure 4.1B), but shows the same pattern at all stages after normalizing internally (Figure 4.1C). The similar pattern between sperm and early embryos suggests the H2afva pattern is already established in sperm and potentially passed to early embryos. Interestingly, H2afva enrichment after ZGA (at dome and high stages) mirrors that before ZGA (at sperm and 256-cell stages), suggesting H2afva as bivalent marks is prepatterned prior to ZGA (Lindeman et al. 2011). Gene Ontology (GO) analysis showed H2afva in sperm and early embryos is enriched in a variety of genes including transcription factors, housekeeping genes, and terminal differentiated markers (Table 4.1, and exemplified in Figure 4.2).

Anticorrelation between H2afva and DNA Methylation in Sperm and Early Embryos

DNA methylation profiles underlie embryo totipotency and pluripotency (Jiang et al. 2013; Potok et al. 2013). However, how DNA methylation is set up in early embryos remains unknown. H2A.Z has been reported to antagonize DNA methylation in several organisms (Zilberman et al. 2008; Conerly et al. 2010; Zemach et al. 2010; Wu et al. 2011). To examine if H2afva is involved in setting up DNA methylation profile in early embryos, H2afva enrichment and DNA methylation profiles are plotted around TSS and TTS in a genome-wide scale (Figure 4.2A–C). Consistent with previous promoter-based microarray results in zebrafish sperm, H2afva and DNA methylation from deep sequencing show anticorrelation in promoter regions as well (Figure 4.2A; Wu et al. 2011). Moreover, not only in the promoters in sperm, anticorrelation between H2afva and DNA methylation is also observed outside of promoter regions in sperm, as well as in early embryos (Figure 4.2A–C and 4.3). In the examples of genomic snapshots, one can easily identify the coincidence of H2afva enrichment and DNA hypomethylation (Figure 4.3). We then compare the overall H2afva-enriched regions and DNA methylation status. DNA hypo- and intermediate methylated regions are correlated to H2afva-enriched regions (FDR < 5%) with a significant P-value (< 0.001) in sperm and early embryos (Table 4.2). Notably, regions lack of DNA methylation are predominantly occupied by H2afva in early embryos, 62% before ZGA, and 70% after ZGA. In contrast, DNA methylated regions tend to be depleted of H2afva with P-values less than 0.001 for anticorrelation.

Studies in ES cells show H2A.Z is highly enriched at both promoters and enhancers (Hu et al. 2013). Enhancer regions defined by H3K4me1 in zebrafish embryos are poorly overlapped with H2afva in early embryos (3.8% before ZGA, 6% after ZGA) (Bogdanovic et al. 2012). Interestingly, H2afva shows anticorrelation to DNA methylation in enhancer regions in early embryos (Figure 4.2 D–E). The majority of enhancer regions in early embryos are DNA methylated and lack of H2afva. Despite the low occupancy of H2afva in enhancers, H2afva-enriched regions show DNA demethylation (similar data observed in sperm and dome embryos and not shown). Taken together, H2afva is anticorrelated to DNA methylation at both promoters and enhancers in sperm and very early embryos. The consistent patterns of H2afva and anticorrelation to DNA methylation from sperm to very early embryos suggest H2afva is heritable and potentially sets up DNA methylation profiles of totipotency and pluripotency.

Discussion

We attempt to address how epigenetic signatures of totipotency and pluripotency are established. DNA methylation status is fundamental to confer totipotency and pluripotency in embryos. Totipotency in embryos is achieved at ZGA with paternal DNA methylome compatibility and maternal methylome reprogramming (Jiang et al. 2013; Potok et al. 2013). It remains unknown how the DNA methylation profile is set up in early embryos. Genome-wide anticorrelation between H2A.Z and DNA methylation in plant, mouse tumor cells, and puffer fish indicates a possibility to set up DNA methylation profiles by H2A.Z (Zilberman et al. 2008; Conerly et al. 2010; Zemach et al. 2010). Our previous work in zebrafish sperm also suggests H2afva enrichment is

anticorrelated to DNA methylation in promoter regions (Wu et al. 2011). Here, we utilized the ChIP-seq approach to examine genomic localization of H2afva in sperm and early embryos and then compared them to corresponding DNA methylation profiles. Consistent with previous studies, H2afva is enriched at DNA hypomethylated regions in both promoters and enhancers from sperm to early embryos, whereas DNA methylated regions are deprived of H2afva (Figure 4.4). These data suggest H2afva is a potential factor to set up DNA methylation profiles of totipotency and pluripotency in embryos.

Bivalent chromatin as the chromatin signature of pluripotency is identified in sperm and ES cells (Bernstein et al. 2006; Mikkelsen et al. 2007; Li et al. 2012a). Genome-wide profiling of epigenetic features has proposed two potential models, re-establishment and inheritance models, to establish chromatin signature of pluripotency in early embryos. The Schier group detected bivalent chromatin in developmental regulators after ZGA but not before ZGA, suggesting the chromatin signature is erased and reestablished in early embryos (Vastenhouw et al. 2010). Our previous studies in zebrafish sperm, however, suggest chromatin signature (bivalency or multivalency) is already established in male gamete and potentially inherited to embryos (Wu et al. 2011). The Collas group was able to detect bivalent chromatin in developmental regulators before ZGA (256-cell stage), though at a relatively low level compared to that after ZGA (Lindeman et al. 2011). Notably, a significant portion of bivalent genes is shared between sperm cells and pre-MBT embryos, suggesting a certain degree of inheritance of chromatin signature from gametes to embryos. One might argue if the low level of bivalent marks is indeed inherited and, importantly, instructive for gene poising during embryogenesis and/or antagonizing DNA methylation. We reason bivalency is not the

only option to establish pluripotency/totipotency in embryos, and other factors could possibly contribute to competency as well. This is exemplified by the programming of dynamic DNA methylation (Jiang et al. 2013; Potok et al. 2013), and incorporation of H2afva nucleosomes. Other possibilities include histone marks rather than H3K4me3 and H3K27me3, histone variants, transcription and transcription factors, and noncoding RNA.

Before ZGA, embryos undergo synchronous cell divisions and the genome is inactive. The levels of bivalent chromatin marks are diluted during cleavage cycles prior to ZGA, making them debatable as heritable epigenetic marks, even though the pattern is maintained from sperm to post-ZGA (Figure 4.4; Lindeman et al. 2011; Vastenhouw and Schier 2012). Studies of DNA methylation dynamics indicate the maternal genome undergoes reprogramming in very early embryos but not for the paternal genome (Jiang et al. 2013; Potok et al. 2013). It remains unclear if chromatin marks are reprogrammed, somewhat similar to DNA methylation reprogramming, in early embryos. Nonetheless, examination of H2afva in zebrafish sperm and early embryos shows both the level and occupancy likely remain consistent, even during cleavage cycles (63% of H2afva protein remained after 8 cleavage cycles, at 256-cell stage, compared to sperm cells, Figure 4.1A–B). The identification of the high level of the H2afva nucleosomes before ZGA is very important as this suggests H2afva is not diluted by cell division and is potentially inherited as the epigenetic memory from gametes to early embryos. The enrichment of H2afva before ZGA favors the inheritance model of epigenetic marks. The next question is whether H2afva is instructive to embryogenesis, that is, whether H2afva drives gene expression underlying embryogenesis.

Several possible mechanisms have been proposed to set up DNA methylation profiles (Iouzalen et al. 1996; Heintzman et al. 2007; Thomson et al. 2010). For example, H3K4me3, the permissive chromatin mark, is correlated with DNA hypomethylation (Weber et al. 2007). Cfp1, a subunit of H3K4 methyltransferase, binds unmethylated CG dinucleotides and thus connects methylation on H3K4 to DNA hypomethylation (Iouzalen et al. 1996; Heintzman et al. 2007; Thomson et al. 2010). Our study focused on the antagonism between H2A.Z and DNA methylation, which has been reported in many organisms and is evolutionally conserved. Overlapping between H2afva-enriched regions and DNA methylation status suggests the majority of DNA hypomethylated regions are occupied with H2afva in very early embryos—over 62% at 256-cell and dome stages, but only 28% in sperm. Although H2afva is the dominant factor to set up DNA methylation profiles in very early embryos (before ZGA, Table 4.2), there could be other factors involved in the setup. Since H3K4me3 level and enrichment are low and zygotic transcription is inactive at a very early stage, we reason that CG density and/or other histone variants could play a role in the targeting of DNA methylation. Regions with low CG density tend to be methylated whereas dense CGIs resist methylation. We will incorporate CG density into our analysis. Another histone variant, marcoH2A, is enriched at developmental genes in pluripotent cells and regulates expression of these genes during cellular differentiation and embryo development (Buschbeck et al. 2009). The localization and function of macroH2A during embryo development suggests its potential to be an important epigenetic mark. It will be interesting to examine how macroH2A relates to DNA methylation profiles.

H2A.Z protein sequence is 100% identical among vertebrates, and the anticorrelation to DNA methylation is reported from fish, plants, and to humans, suggesting H2A.Z is an evolutionally conserved protein with some fundamental functions. Indeed, deletion of H2A.Z leads to embryonic lethality in many organisms (van Daal and Elgin 1992; Iouzalen et al. 1996; Liu et al. 1996; Clarkson et al. 1999; Faast et al. 2001; Ridgway et al. 2004). The zygotic genome is activated at 1000-cell stage (midblastula transition, MBT) in zebrafish, but between 2- to 8- cell stages in mammals. The timing difference might be attributed to the need of transcription profiles to specify extraembryonic tissue and inner cell mass lineages in mammals. Our studies in zebrafish suggest H2afva could be a heritable epigenetic mark from gametes to embryos, and the anticorrelation between H2afva occupancy and DNA methylation in both sperm and embryos—providing a potential mechanism to set up DNA methylation profiles. In *C. elegans*, HTZ-1 is essential for normal development and highly expressed when the zygotic genome activates (Whittle et al. 2008). Since there is no DNA methylation in *C. elegans*, we suspect there is no need of HTZ-1 before ZGA. In contrast, H2A.Z has been detected before ZGA in *Xenopus* and at least at blastula in mice (Faast et al. 2001; Ridgway et al. 2004). Despite the timing difference of ZGA between zebrafish and mammals, we speculate a conserved role of H2A.Z in vertebrates as a heritable epigenetic mark with the potential to set up DNA methylation profiles of totipotency and pluripotency.

Methods

Zebrafish Stocks

A wild-type zebrafish line (Tübingen) is maintained as described previously (Wu et al. 2011). Embryos were collected from sexually mature zebrafish by standard procedures (Westerfield 2000).

Western Blotting and Antibody

Sperm cells were counted using a hemacytometer, washed with PBS, and then lysed in 2X sample buffer. Western blotting was done according to standard procedures with H2AFV antibody (Abcam ab4174).

ChIP-seq

The procedures of ChIP on sperm cells or embryos were described previously (Lee et al. 2006; Wu et al. 2011). Briefly for the lysis step, 10^7 of sperm cells were treated with 0.05% lysophosphatidylcholine (Sigma L1381) in PBS on ice for 10 minutes. 15 units of micrococcal nuclease (MNase, USB 70196Y) was then applied to release oligonucleosomes at 37^{o}C for 5 minutes. Embryos (need >2000 256-cell embryos) were fixed in 1.85% formaldehyde for 15 minutes at room temperature, and lysed in low-salt cell lysis buffer [10 mM Tris (pH 8.1), 10 mM NaCl, 0.5% NP-40, and protease inhibitors]. Genomic DNA was then sheared by sonication to 200–500 bp. 2 μg of specific antibody conjugated to Dynabeads were incubated with the nucleosome lysate. The pulled-down DNA fragments and input DNA were subjected to an Illumina TruSeq ChIP sample preparation kit (Illumina IP-202-1012) for end repairing, adaptor ligation,

and library construction according to Illumina's protocol. Deep sequencing was performed on Illumina HiSeq 2000 for a 50 bp single-end run.

Bioinformatics Analyses

Illumina Fastq files were aligned using Novoalign (Novocraft) to Zv9 genome version (danRer7 at UCSC). All DNA methylation data were extracted from Potok et al. (2013). Enhancer regions defined by H3K4me1 in zebrafish embryos were obtained from Bogdanovic et al. (2012). ChIP-seq enrichment and further bioinformatics analyses were performed with the USeq package (http://sourceforge.net/projects/useq/) and BioToolBox package (http://code.google.com/p/biotoolbox/). Aggregate Plotter (http://useq. sourceforge.net/cmdLnMenus.html#AggregatePlotter) was used to plot a class average map and BisSeq Aggregate Plotter (http://useq.sourceforge.net/cmdLnMenus. html#BisSeqAggregatePlotter) for DNA methylation data. Intersect Regions (http://useq.sourceforge.net/cmdLnMenus.html#IntersectRegions) was used to compare two sets of regions and compared to a set of random regions to calculate a P-value. The closest enriched genes within 10kb were retrieved with Find Neighboring Genes (http://useq.sourceforge.net/cmdLnMenus.html#FindNeighboringGenes) and submitted to GoMiner (http://discover.nci.nih.gov/gominer/ GoCommandWebInterface.jsp) for GO analysis. IGB (http://bioviz.org/igb/) was used to browse genomic datasets.

References

Ahmad K, Henikoff S. 2002. Histone H3 variants specify modes of chromatin assembly. *Proc Natl Acad Sci* **99 Suppl 4**: 16477–16484.

Banaszynski LA, Allis CD, Lewis PW. 2010. Histone variants in metazoan development. *Dev Cell* **19**(5): 662–674.

Barski A, Cuddapah S, Cui K, Roh TY, Schones DE, Wang Z, Wei G, Chepelev I, Zhao K. 2007. High-resolution profiling of histone methylations in the human genome. *Cell* **129**(4): 823–837.

Bernstein BE, Mikkelsen TS, Xie X, Kamal M, Huebert DJ, Cuff J, Fry B, Meissner A, Wernig M, Plath K et al. 2006. A bivalent chromatin structure marks key developmental genes in embryonic stem cells. *Cell* **125**(2): 315–326.

Bogdanovic O, Fernandez-Minan A, Tena JJ, de la Calle-Mustienes E, Hidalgo C, van Kruysbergen I, van Heeringen SJ, Veenstra GJ, Gomez-Skarmeta JL. 2012. Dynamics of enhancer chromatin signatures mark the transition from pluripotency to cell specification during embryogenesis. *Genome Res* **22**(10): 2043–2053.

Buschbeck M, Uribesalgo I, Wibowo I, Rue P, Martin D, Gutierrez A, Morey L, Guigo R, Lopez-Schier H, Di Croce L. 2009. The histone variant macroH2A is an epigenetic regulator of key developmental genes. *Nat Struct Mol Biol* **16**(10): 1074–1079.

Cai Y, Jin J, Gottschalk AJ, Yao T, Conaway JW, Conaway RC. 2006. Purification and assay of the human INO80 and SRCAP chromatin remodeling complexes. *Methods* **40**(4): 312–317.

Clarkson MJ, Wells JR, Gibson F, Saint R, Tremethick DJ. 1999. Regions of variant histone His2AvD required for Drosophila development. *Nature* **399**(6737): 694–697.

Conerly ML, Teves SS, Diolaiti D, Ulrich M, Eisenman RN, Henikoff S. 2010. Changes in H2A.Z occupancy and DNA methylation during B-cell lymphomagenesis. *Genome Res* **20**(10): 1383–1390.

Creyghton MP, Markoulaki S, Levine SS, Hanna J, Lodato MA, Sha K, Young RA, Jaenisch R, Boyer LA. 2008. H2AZ is enriched at Polycomb complex target genes in ES cells and is necessary for lineage commitment. *Cell* **135**(4): 649–661.

Eirin-Lopez JM, Gonzalez-Romero R, Dryhurst D, Ishibashi T, Ausio J. 2009. The evolutionary differentiation of two histone H2A.Z variants in chordates (H2A.Z-1 and H2A.Z-2) is mediated by a stepwise mutation process that affects three amino acid residues. *BMC Evol Biol* **9**: 31.

Faast R, Thonglairoam V, Schulz TC, Beall J, Wells JR, Taylor H, Matthaei K, Rathjen PD, Tremethick DJ, Lyons I. 2001. Histone variant H2A.Z is required for early mammalian development. *Curr Biol* **11**(15): 1183–1187.

Gevry N, Chan HM, Laflamme L, Livingston DM, Gaudreau L. 2007. p21 transcription is regulated by differential localization of histone H2A.Z. *Genes Dev* **21**(15): 1869–1881.

Gevry N, Hardy S, Jacques PE, Laflamme L, Svotelis A, Robert F, Gaudreau L. 2009. Histone H2A.Z is essential for estrogen receptor signaling. *Genes Dev* **23**(13): 1522–1533.

Guillemette B, Bataille AR, Gevry N, Adam M, Blanchette M, Robert F, Gaudreau L. 2005. Variant histone H2A.Z is globally localized to the promoters of inactive yeast genes and regulates nucleosome positioning. *PLoS Biol* **3**(12): e384.

Heintzman ND, Stuart RK, Hon G, Fu Y, Ching CW, Hawkins RD, Barrera LO, Van Calcar S, Qu C, Ching KA et al. 2007. Distinct and predictive chromatin signatures of transcriptional promoters and enhancers in the human genome. *Nat Genet* **39**(3): 311–318.

Howell CY, Bestor TH, Ding F, Latham KE, Mertineit C, Trasler JM, Chaillet JR. 2001. Genomic imprinting disrupted by a maternal effect mutation in the Dnmt1 gene. *Cell* **104**(6): 829–838.

Hu G, Cui K, Northrup D, Liu C, Wang C, Tang Q, Ge K, Levens D, Crane-Robinson C, Zhao K. 2013. H2A.Z facilitates access of active and repressive complexes to chromatin in embryonic stem cell self-renewal and differentiation. *Cell Stem Cell* **12**(2): 180–192.

Iouzalen N, Moreau J, Mechali M. 1996. H2A.ZI, a new variant histone expressed during Xenopus early development exhibits several distinct features from the core histone H2A. *Nucleic Acids Res* **24**(20): 3947–3952.

Jackson JD, Gorovsky MA. 2000. Histone H2A.Z has a conserved function that is distinct from that of the major H2A sequence variants. *Nucleic Acids Res* **28**(19): 3811–3816.

Jiang L, Zhang J, Wang JJ, Wang L, Zhang L, Li G, Yang X, Ma X, Sun X, Cai J et al. 2013. Sperm, but not oocyte, DNA methylome is inherited by zebrafish early embryos. *Cell* **153**(4): 773–784.

Kobor MS, Venkatasubrahmanyam S, Meneghini MD, Gin JW, Jennings JL, Link AJ, Madhani HD, Rine J. 2004. A protein complex containing the conserved Swi2/Snf2-Related ATPase Swr1p deposits histone variant H2A.Z into euchromatin. *PLoS Biol* **2**(5): E131.

Krogan NJ, Baetz K, Keogh MC, Datta N, Sawa C, Kwok TC, Thompson NJ, Davey MG, Pootoolal J, Hughes TR et al. 2004. Regulation of chromosome stability by the histone H2A variant Htz1, the Swr1 chromatin remodeling complex, and the histone acetyltransferase NuA4. *Proc Natl Acad Sci* **101**(37): 13513–13518.

Krogan NJ, Keogh MC, Datta N, Sawa C, Ryan OW, Ding H, Haw RA, Pootoolal J, Tong A, Canadien V et al. 2003. A Snf2 family ATPase complex required for recruitment of the histone H2A variant Htz1. *Mol Cell* **12**(6): 1565–1576.

Ku M, Jaffe JD, Koche RP, Rheinbay E, Endoh M, Koseki H, Carr SA, Bernstein BE. 2012. H2A.Z landscapes and dual modifications in pluripotent and multipotent stem cells underlie complex genome regulatory functions. *Genome Biol* **13**(10): R85.

Lee JE, Wu SF, Goering LM, Dorsky RI. 2006. Canonical Wnt signaling through Lef1 is required for hypothalamic neurogenesis. *Development* **133**(22): 4451–4461.

Li B, Pattenden SG, Lee D, Gutierrez J, Chen J, Seidel C, Gerton J, Workman JL. 2005. Preferential occupancy of histone variant H2AZ at inactive promoters influences local histone modifications and chromatin remodeling. *Proc Natl Acad Sci* **102**(51): 18385–18390.

Li M, Liu GH, Izpisua Belmonte JC. 2012a. Navigating the epigenetic landscape of pluripotent stem cells. *Nat Rev Mol Cell Biol* **13**(8): 524–535.

Li Z, Gadue P, Chen K, Jiao Y, Tuteja G, Schug J, Li W, Kaestner KH. 2012b. Foxa2 and H2A.Z mediate nucleosome depletion during embryonic stem cell differentiation. *Cell* **151**(7): 1608–1616.

Lindeman LC, Andersen IS, Reiner AH, Li N, Aanes H, Ostrup O, Winata C, Mathavan S, Muller F, Alestrom P et al. 2011. Prepatterning of developmental gene expression by modified histones before zygotic genome activation. *Dev Cell* **21**(6): 993–1004.

Liu X, Li B, Gorovsky MA. 1996. Essential and nonessential histone H2A variants in Tetrahymena thermophila. *Mol Cell Biol* **16**(8): 4305–4311.

Marques M, Laflamme L, Gervais AL, Gaudreau L. 2010. Reconciling the positive and negative roles of histone H2A.Z in gene transcription. *Epigenetics* **5**(4): 267–272.

Mavrich TN, Jiang C, Ioshikhes IP, Li X, Venters BJ, Zanton SJ, Tomsho LP, Qi J, Glaser RL, Schuster SC et al. 2008. Nucleosome organization in the Drosophila genome. *Nature* **453**(7193): 358–362.

Mayer W, Niveleau A, Walter J, Fundele R, Haaf T. 2000. Demethylation of the zygotic paternal genome. *Nature* **403**(6769): 501–502.

Meneghini MD, Wu M, Madhani HD. 2003. Conserved histone variant H2A.Z protects euchromatin from the ectopic spread of silent heterochromatin. *Cell* **112**(5): 725–736.

Mikkelsen TS, Ku M, Jaffe DB, Issac B, Lieberman E, Giannoukos G, Alvarez P, Brockman W, Kim TK, Koche RP et al. 2007. Genome-wide maps of chromatin state in pluripotent and lineage-committed cells. *Nature* **448**(7153): 553–560.

Millar CB, Xu F, Zhang K, Grunstein M. 2006. Acetylation of H2AZ Lys 14 is associated with genome-wide gene activity in yeast. *Genes Dev* **20**(6): 711–722.

Mizuguchi G, Shen X, Landry J, Wu WH, Sen S, Wu C. 2004. ATP-driven exchange of histone H2AZ variant catalyzed by SWR1 chromatin remodeling complex. *Science* **303**(5656): 343–348.

Oswald J, Engemann S, Lane N, Mayer W, Olek A, Fundele R, Dean W, Reik W, Walter J. 2000. Active demethylation of the paternal genome in the mouse zygote. *Curr Biol* **10**(8): 475–478.

Placek BJ, Harrison LN, Villers BM, Gloss LM. 2005. The H2A.Z/H2B dimer is unstable compared to the dimer containing the major H2A isoform. *Protein Sci* **14**(2): 514–522.

Potok ME, Nix DA, Parnell TJ, Cairns BR. 2013. Reprogramming the maternal zebrafish genome after fertilization to match the paternal methylation pattern. *Cell* **153**(4): 759–772.

Raisner RM, Hartley PD, Meneghini MD, Bao MZ, Liu CL, Schreiber SL, Rando OJ, Madhani HD. 2005. Histone variant H2A.Z marks the 5' ends of both active and inactive genes in euchromatin. *Cell* **123**(2): 233–248.

Rangasamy D, Berven L, Ridgway P, Tremethick DJ. 2003. Pericentric heterochromatin becomes enriched with H2A.Z during early mammalian development. *Embo J* **22**(7): 1599–1607.

Rangasamy D, Greaves I, Tremethick DJ. 2004. RNA interference demonstrates a novel role for H2A.Z in chromosome segregation. *Nat Struct Mol Biol* **11**(7): 650–655.

Ridgway P, Brown KD, Rangasamy D, Svensson U, Tremethick DJ. 2004. Unique residues on the H2A.Z containing nucleosome surface are important for Xenopus laevis development. *J Biol Chem* **279**(42): 43815–43820.

Santisteban MS, Kalashnikova T, Smith MM. 2000. Histone H2A.Z regulats transcription and is partially redundant with nucleosome remodeling complexes. *Cell* **103**(3): 411–422.

Sarcinella E, Zuzarte PC, Lau PN, Draker R, Cheung P. 2007. Monoubiquitylation of H2A.Z distinguishes its association with euchromatin or facultative heterochromatin. *Mol Cell Biol* **27**(18): 6457–6468.

Talbert PB, Henikoff S. 2010. Histone variants—ancient wrap artists of the epigenome. *Nat Rev Mol Cell Biol* **11**(4): 264–275.

Thomson JP, Skene PJ, Selfridge J, Clouaire T, Guy J, Webb S, Kerr AR, Deaton A, Andrews R, James KD et al. 2010. CpG islands influence chromatin structure via the CpG-binding protein Cfp1. *Nature* **464**(7291): 1082–1086.

Valdes-Mora F, Song JZ, Statham AL, Strbenac D, Robinson MD, Nair SS, Patterson KI, Tremethick DJ, Stirzaker C, Clark SJ. 2012. Acetylation of H2A.Z is a key

epigenetic modification associated with gene deregulation and epigenetic remodeling in cancer. *Genome Res* **22**(2): 307–321.

van Daal A, Elgin SC. 1992. A histone variant, H2AvD, is essential in Drosophila melanogaster. *Mol Biol Cell* **3**(6): 593–602.

Vastenhouw NL, Schier AF. 2012. Bivalent histone modifications in early embryogenesis. *Curr Opin Cell Biol* **24**(3): 374–386.

Vastenhouw NL, Zhang Y, Woods IG, Imam F, Regev A, Liu XS, Rinn J, Schier AF. 2010. Chromatin signature of embryonic pluripotency is established during genome activation. *Nature* **464**(7290): 922–926.

Weber M, Hellmann I, Stadler MB, Ramos L, Paabo S, Rebhan M, Schubeler D. 2007. Distribution, silencing potential and evolutionary impact of promoter DNA methylation in the human genome. *Nat Genet* **39**(4): 457–466.

Westerfield M. 2000. *The zebrafish book. A guide for the laboratory use of zebrafish (Danio rerio)*. Univ. of Oregon Press, Eugene, Oregon.

Whittle CM, McClinic KN, Ercan S, Zhang X, Green RD, Kelly WG, Lieb JD. 2008. The genomic distribution and function of histone variant HTZ-1 during C. elegans embryogenesis. *PLoS Genet* **4**(9): e1000187.

Wu SF, Zhang H, Cairns BR. 2011. Genes for embryo development are packaged in blocks of multivalent chromatin in zebrafish sperm. *Genome Res* **21**(4): 578–589.

Wu WH, Alami S, Luk E, Wu CH, Sen S, Mizuguchi G, Wei D, Wu C. 2005. Swc2 is a widely conserved H2AZ-binding module essential for ATP-dependent histone exchange. *Nat Struct Mol Biol*: 1064–1071.

Yang X, Noushmehr H, Han H, Andreu-Vieyra C, Liang G, Jones PA. 2012. Gene reactivation by 5-aza-2'-deoxycytidine-induced demethylation requires SRCAP-mediated H2A.Z insertion to establish nucleosome depleted regions. *PLoS Genet* **8**(3): e1002604.

Zemach A, McDaniel IE, Silva P, Zilberman D. 2010. Genome-wide evolutionary analysis of eukaryotic DNA methylation. *Science* **328**(5980): 916–919.

Zhang H, Roberts DN, Cairns BR. 2005. Genome-wide dynamics of Htz1, a histone H2A variant that poises repressed/basal promoters for activation through histone loss. *Cell* **123**(2): 219–231.

Zilberman D, Coleman-Derr D, Ballinger T, Henikoff S. 2008. Histone H2A.Z and DNA methylation are mutually antagonistic chromatin marks. *Nature* **456**(7218): 125–129.

Zlatanova J, Thakar A. 2008. H2A.Z: view from the top. *Structure* **16**(2): 166–179.

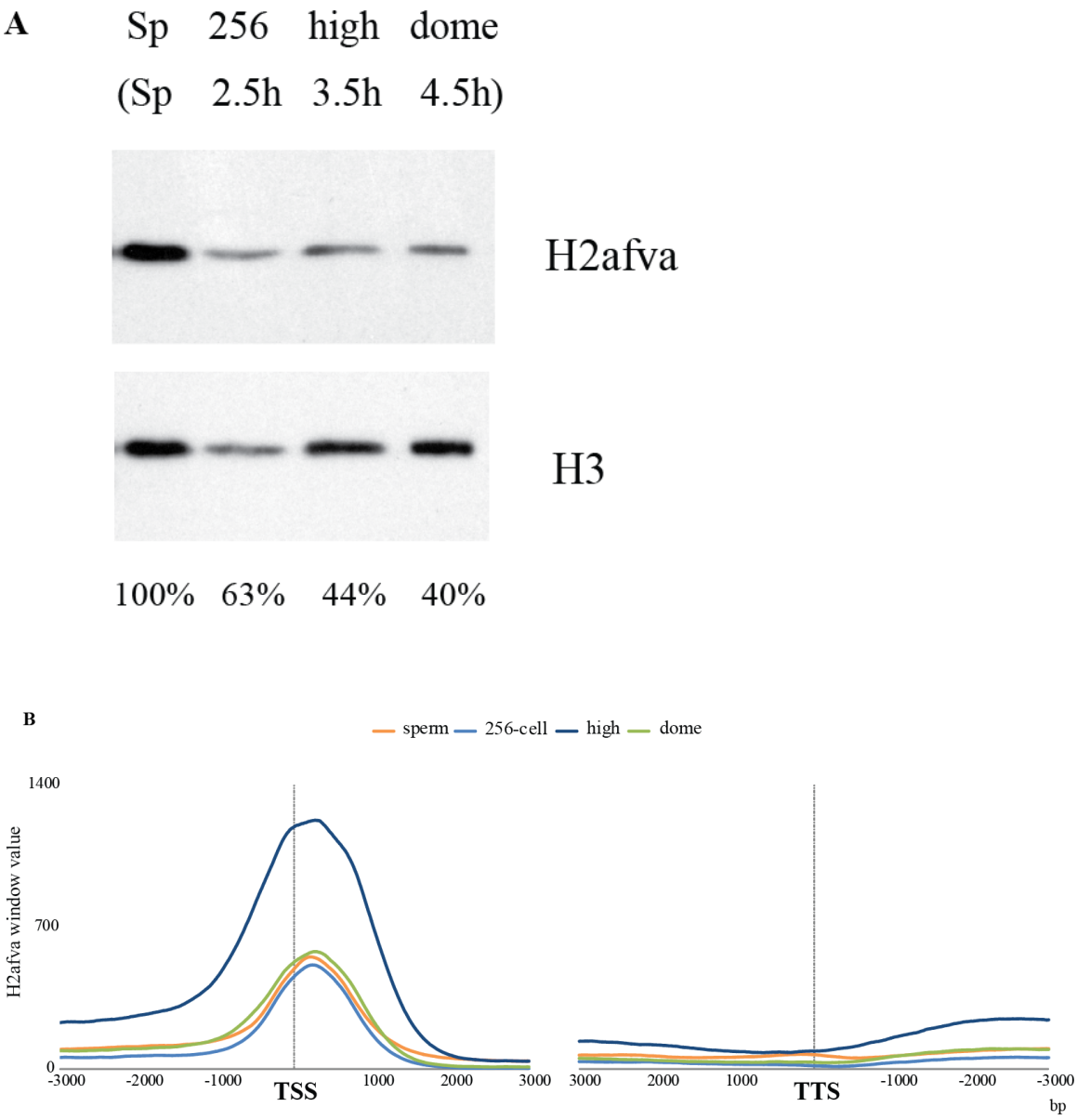

Figure 4.1 H2afva is enriched at promoter regions in early embryos and potentially inherited from sperm. (A) Bulk level of H2afva is determined by immunoblotting against H2afva and normalized by H3 level. H2afva is abundant in early embryos, even before zygotic genome activation (256-cell stage). Sp, sperm. h, hours post fertilization. (B) H2afva is enriched in +1 nucleosome and shows similar pattern in sperm and early embryos. H2afva enrichment is plotted in window values around TSS or TTS. (C) As in (B), but H2afva window values are scaled within each stage.

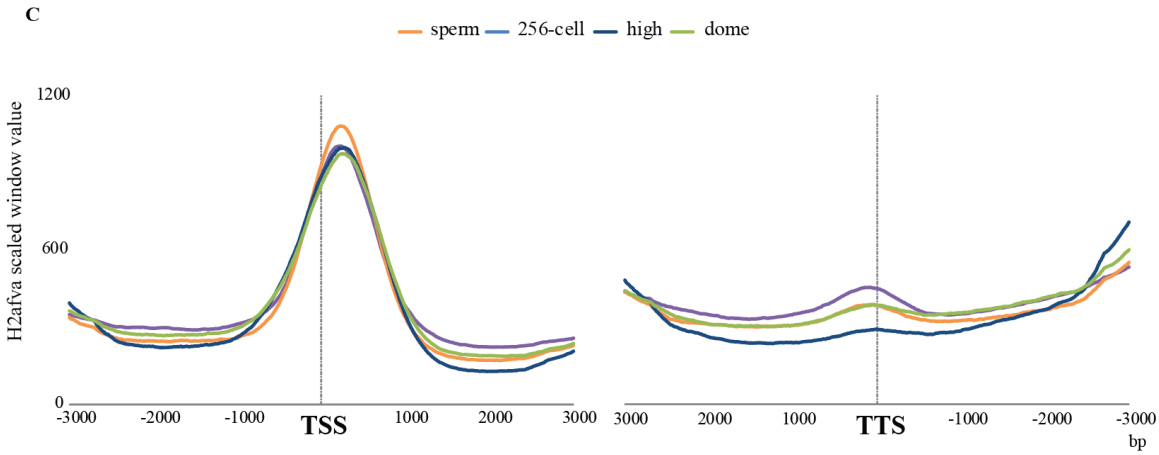

Figure 4.1 Continued

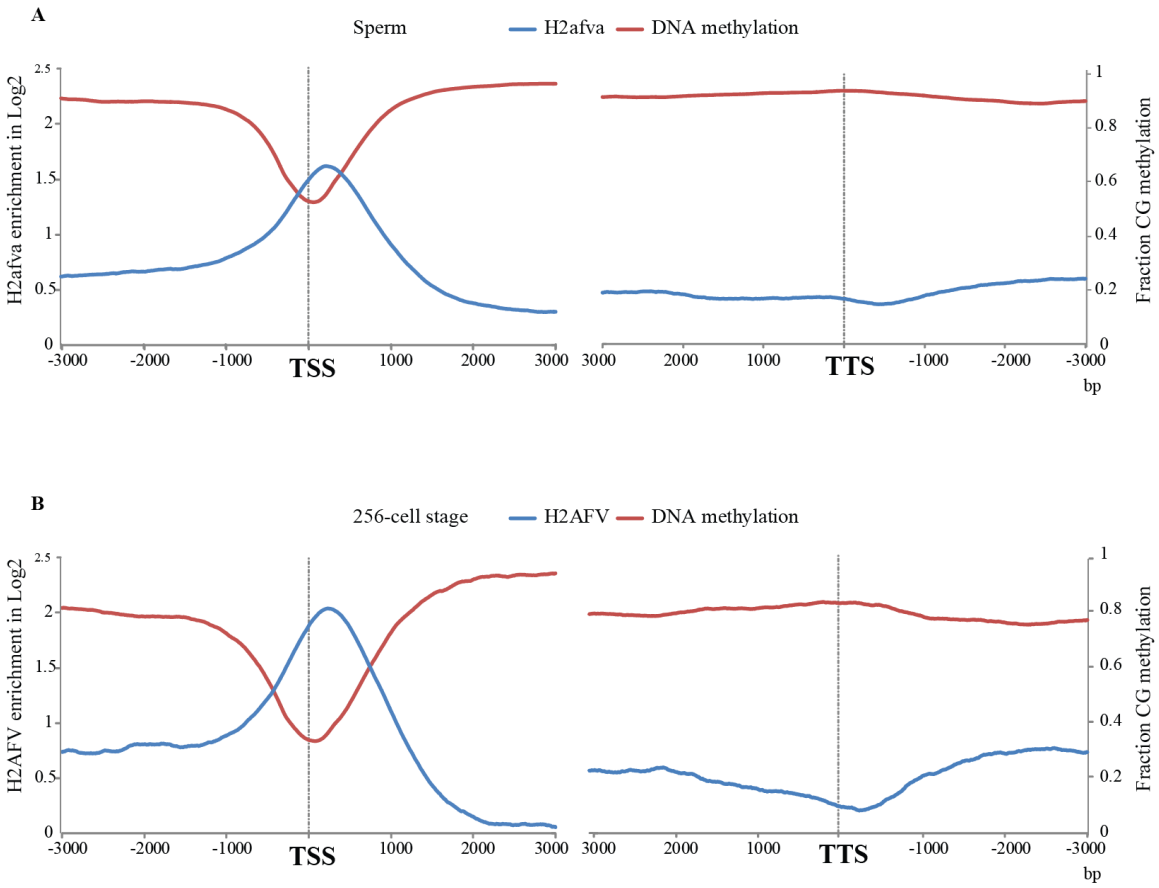

Figure 4.2 H2afva is anticorrelated to DNA methylation in sperm and early embryos. (A–C) H2afva enrichment is normalized to input and plotted with fraction CG methylation around TSS or TTS in sperm cells (A), 256 cells (B), and dome embryos (C). (D) H2afva enrichment is normalized to input and plotted with fraction CG methylation upstream or downstream 3000 bp of enhancer. H2afva is anticorrelated to DNA methylation at enhancer regions in early embryos. 833 enhancer regions (out of 22093 regions, 3.8%) overlapped with H2afva (5% FDR and log2 above 1). (E) H2afva enrichment is normalized to input and plotted with fraction CG methylation upstream or downstream 3000 bp of enhancer. Enhancer regions are defined by H3K4me1 enrichment in zebrafish embryos (Bogdanovic et al., 2012). 47166 enhancer regions (out of 47970 regions, 98.3%) not overlapped with H2afva (5% FDR and log2 above 1). DNA methylation data are from Potok et al., 2013.

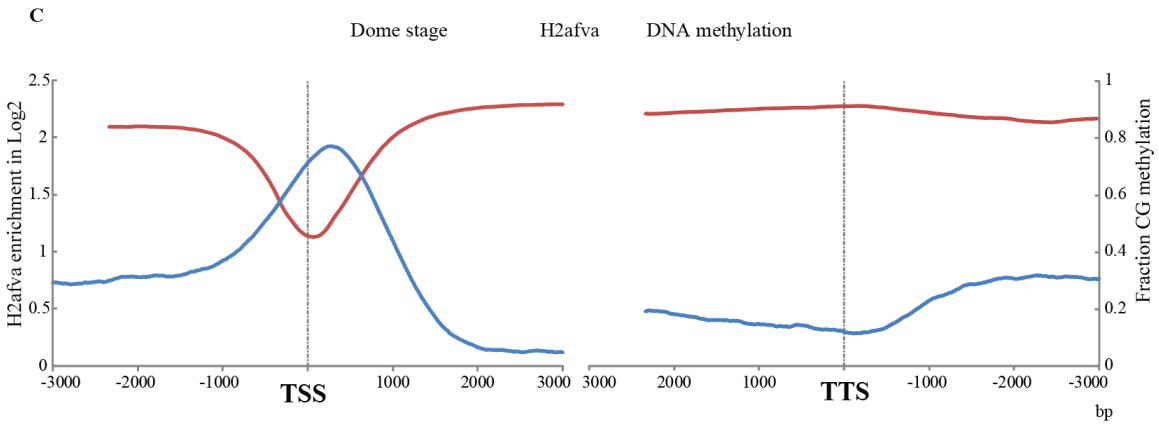

Figure 4.2 Continued

D

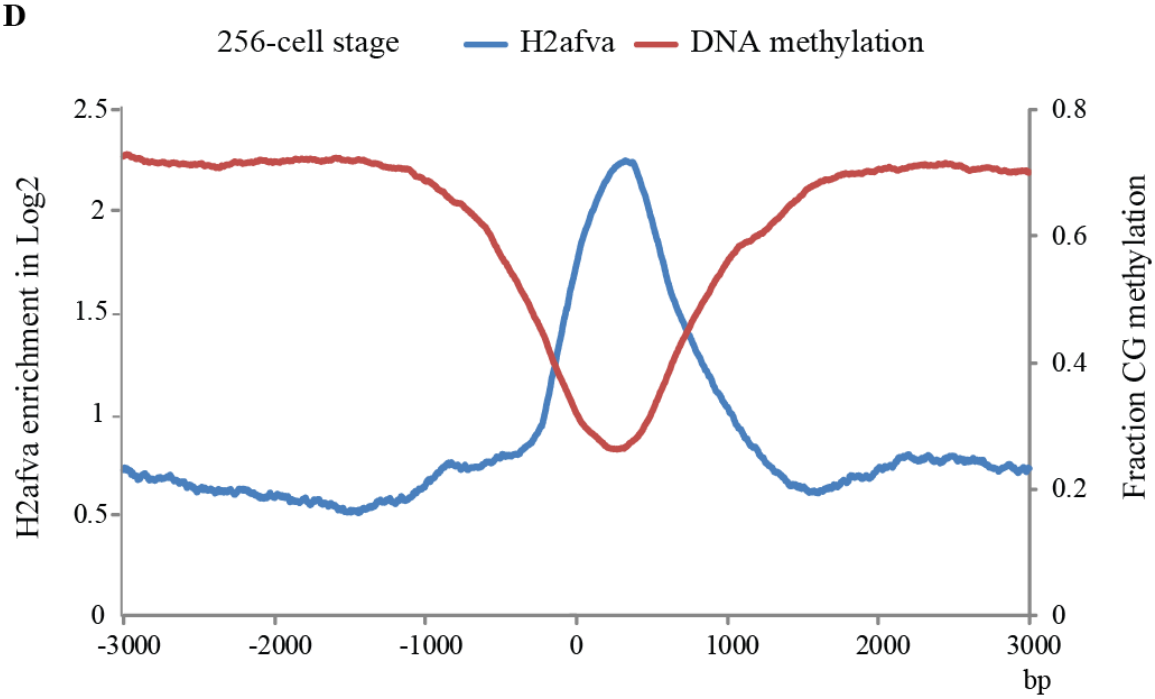

Figure 4.2 Continued

E

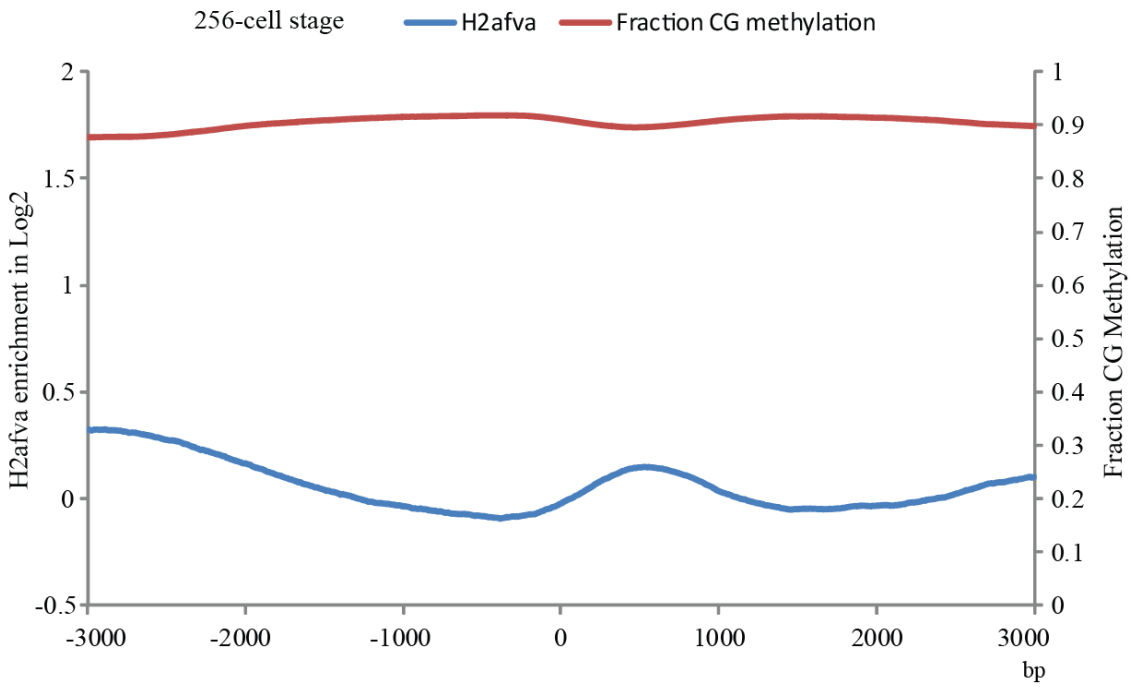

Figure 4.2 Continued

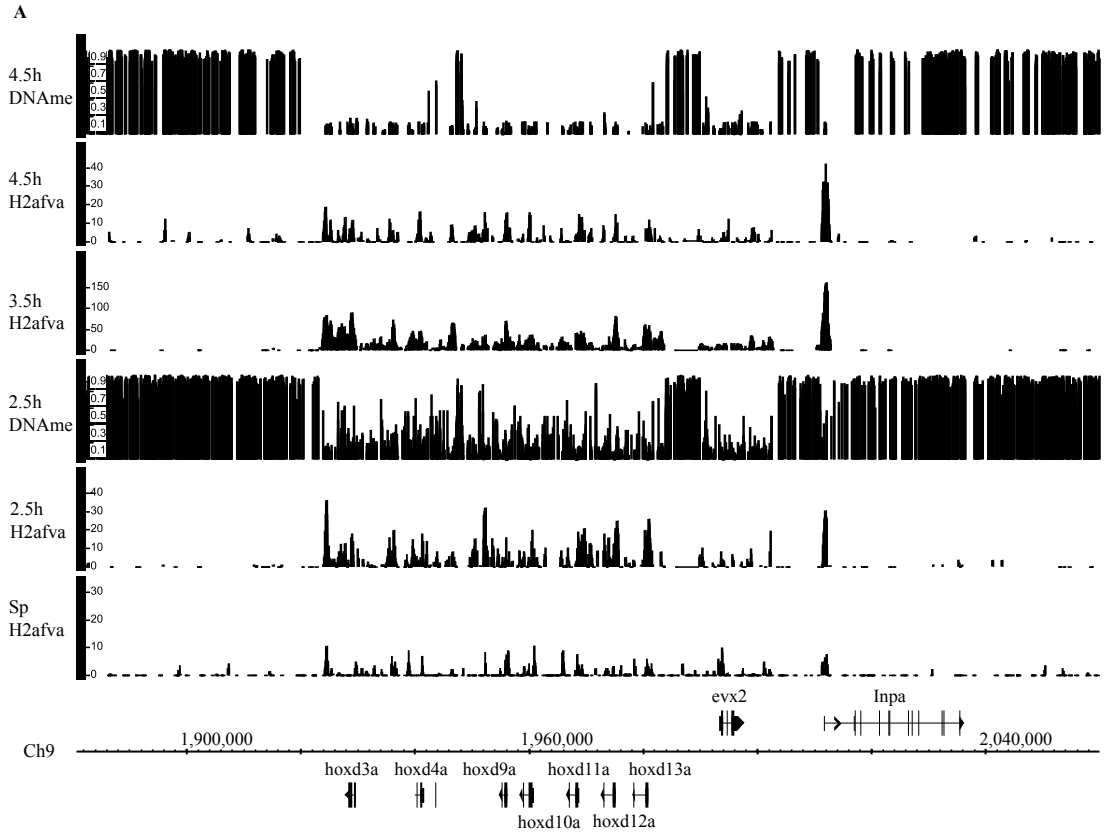

Figure 4.3 Enrichment of H2afva in promoter regions and anticorrelation between H2afva and DNA methylation in early embryos. QFDR of H2afva is shown is in y-axis (QFDR 30 = 0.1%, QFDR 20 = 1%, QFDR 13 = 5%). DNA methylation is shown as fraction of CG methylation. (A) A broad region includes hoxd cluster. (B) A broad region includes ntla. (C) ntla and its promoter region. (D) A broad region includes late-expressed genes such as hibadha.

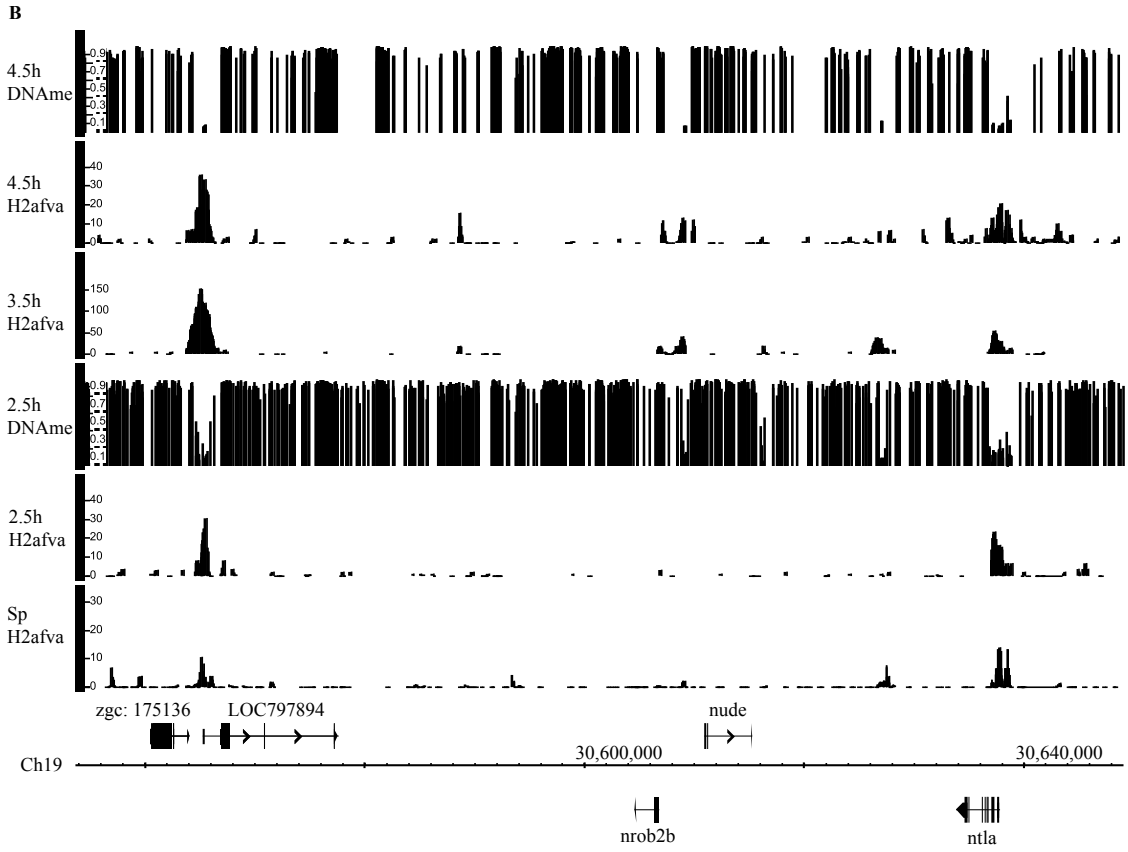

Figure 4.3 Continued

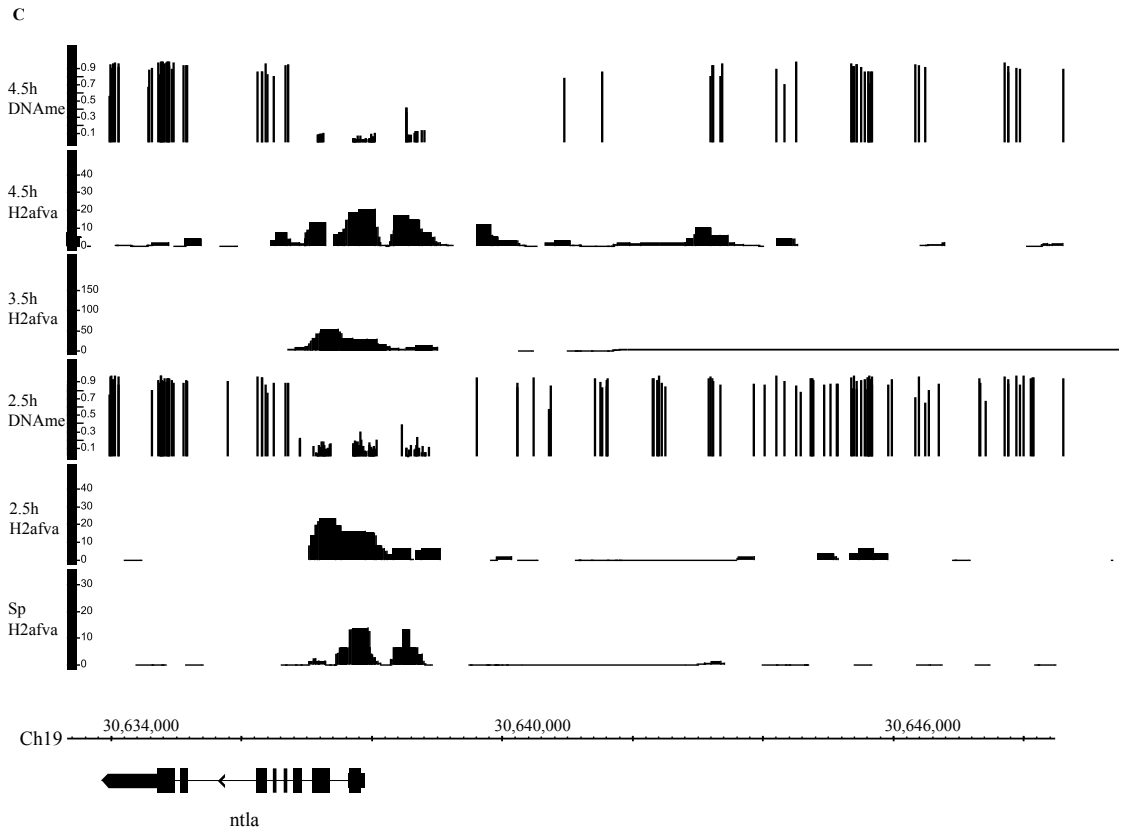

Figure 4.3 Continued

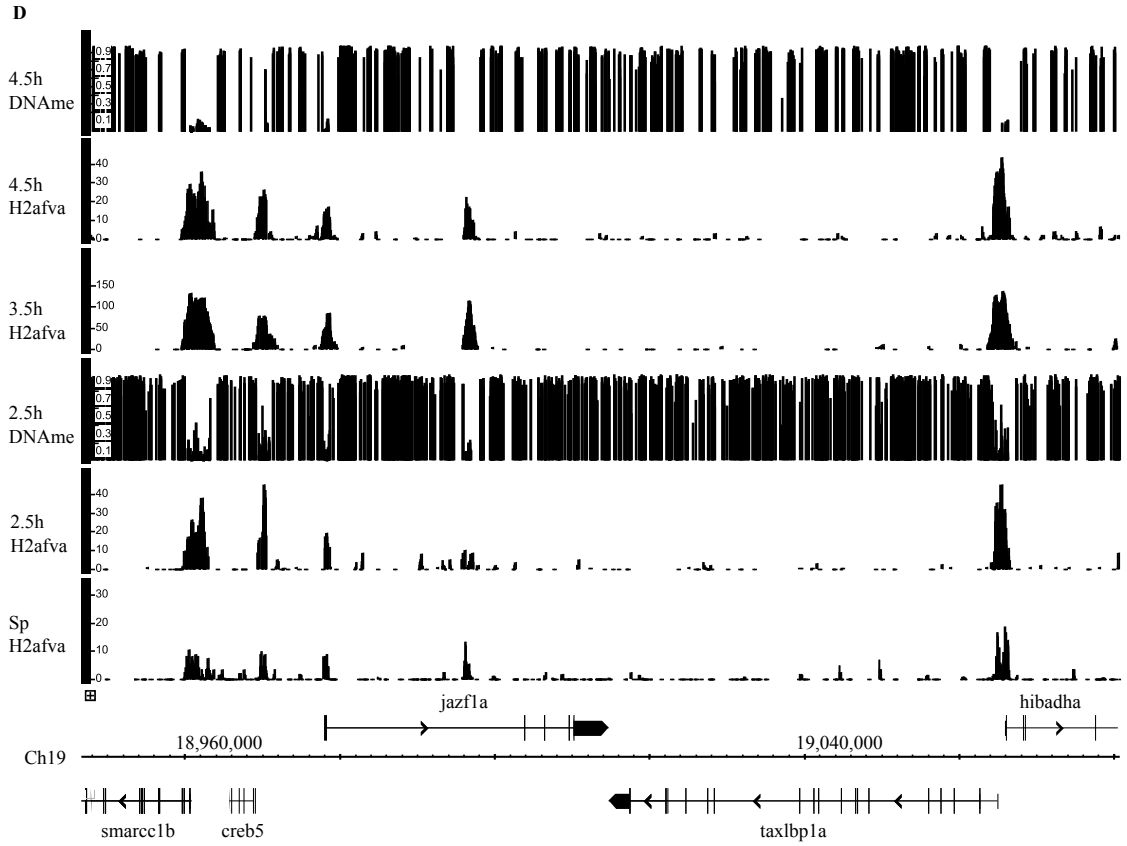

Figure 4.3 Continued

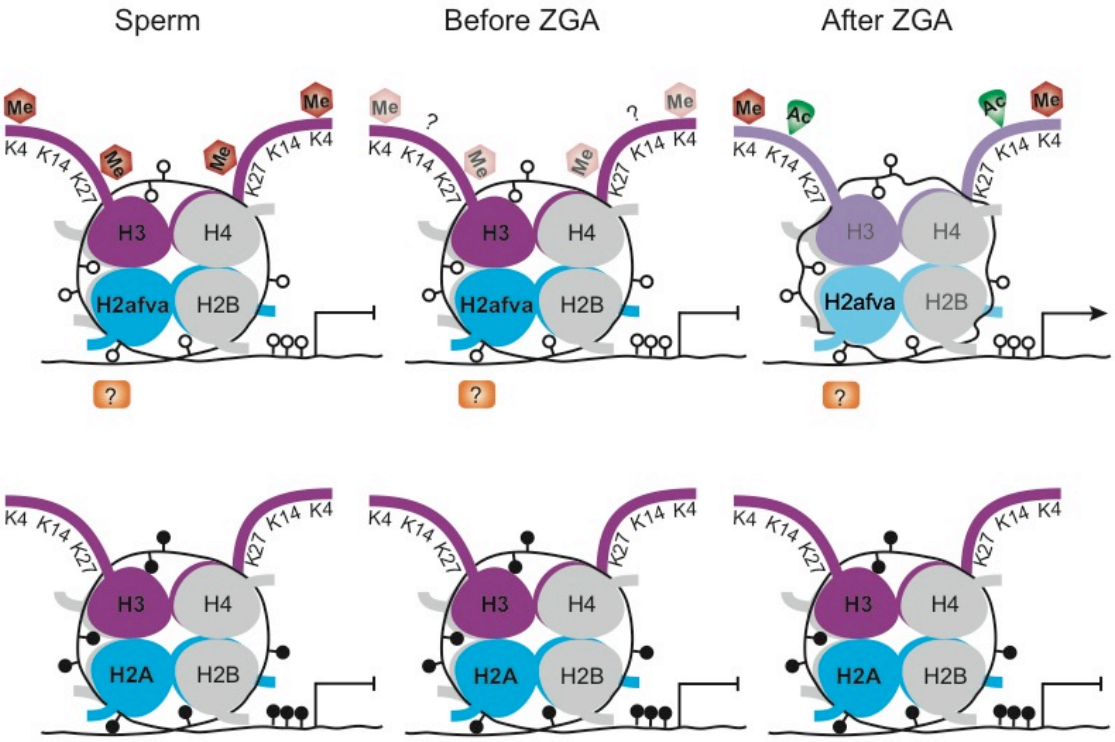

Figure 4.4 H2afva is potentially a heritable epigenetic mark and antagonizes DNA methylation from sperm to embryos. Both H2afva level and occupancy remain consistent from sperm to early embryos, whereas bivalent marks are diluted by cell division before ZGA (lighter color for H3K4 and H3K27 Me). DNA methylation profiles are set up by H2afva nucleosomes and possibly other factors (denoted by ?), especially before ZGA when important chromatin marks are low. After ZGA, chromatin marks, as well as transcription factors, could play a role in setting up DNA methylation profiles.

Table 4.1 Summary of H2afva enriched gene categories.

H2afva in sperm*
(1) Metabolic process; (2) translation; (3) regulation of cell cycle; (4) cell development; (5) regulation of cell death.
H2afva at 256-cell
(1) Chromatin organization; (2) translation; (3) metabolic process; (4) transcription; (5) cell cycle.
H2afva at high stage
(1) Translation; (2) metabolic process; (3) development; (4) transcription; (5) cell division.
H2afva at dome stage*
(1) Vesicle mediated transport; (2) phosphorylation; (3) metabolic process; (4) catabolic process; (5) erythrocyte maturation.

Top 5 nonredundant gene categories were retrieved from Gene Ontology analyses with FDR < 0.01 unless otherwise specified. * FDR < 0.05.

Table 4.2 Statistics for DNA methylation and H2afva.

First	Second	% overlapped	–	Correlation P-Value	Anticorrelation P-Value
Sp DNA HypoMe	**Sp_h2afva**	**28.5%**	**(5703/19984)**	**<1/1000**	
Sp DNA InterMe	Sp_h2afva	6.25%	(389/6226)	<1/1000	
Sp DNA HyperMe	Sp_h2afva	0.06%	(231/402381)		<1/1000
2.5h DNA HypoMe	**2.5h_h2afva**	**62.0%**	**(16829/27136)**	**<1/1000**	
2.5h DNA InterMe	2.5h_h2afva	15.2%	(3202/21024)	<1/1000	
2.5h DNA HyperMe	2.5h_h2afva	0.5%	(2284/454266)		<1/1000
4.5h DNA HypoMe	**4.5h_h2afva**	**68.0%**	**(13960/20544)**	**<1/1000**	
4.5h DNA InterMe	4.5h_h2afva	19.7%	(1276/6475)	<1/1000	
4.5h DNA HyperMe	4.5h_h2afva	0.73%	(2835/389042)		<1/1000

H2afva is anticorrelated to DNA methylation in sperm and early embryos with P-value less than 0.001. DNA hypomethylation has fraction of CG methylation less than 0.19; DNA intermediate 0.2 to 0.79; DNA hypermethylation above 0.8. All H2afva enriched regions here have FDR below 5%. P-value was calculated based on comparison to a set of random regions.

CHAPTER 5

SUMMARY AND PERSPECTIVES

Zebrafish Utilize Nucleosomes and Linker Histones to Package Sperm Genome

Our goals are to understand how epigenetic features are programmed and their contributions to totipotency and pluripotency in germ cells and early embryos. By studying zebrafish as a model system, we found that the zebrafish sperm genome is packaged completely with nucleosomes and abundant linker histones to reach a moderate-high level of condensation. In mammals and some fishes, the sperm genome is packaged with protamines into a highly condensed and compact structure. It is not clear why some teleost fish use protamine or protamine-like proteins to package the sperm genome and some do not (Shimizu et al. 2000). However, our analysis of histone modification states and packaging composition suggests an alternative strategy to condense the sperm genome involving the coordinated use of nucleosomes lacking H4K16ac, various linker histones, and possibly ISWI-type remodelers. Despite the difference, as discussed below, zebrafish appear very similar to humans in their packaging of genes important for embryonic development, suggesting that zebrafish may serve as an important animal model for developmental gene packaging and marking.

Features of Gene Packaging in Germ Cells and ES Cells

Genome-wide mapping of epigenetic features in zebrafish sperm revealed a programmed packaging strategy (Figure 5.1). Active marks including H3K4me3, H3K4me2, and H3K14ac are enriched in genes involved in spermatogenesis and early cellular processes before MBT such as the cell cycle, suggesting that epigenetic status in sperm represents a memory from a previous program and potentially a preparation for a

future program (early embryogenesis). Interestingly, genes highly enriched with active marks in sperm tend to be expressed in very early embryo (before ZGA, Chapter 2). Important developmental regulators in zebrafish sperm are marked with bivalent chromatin (H3K4me3 and H3K27me3), along with additional features including atypical placement of H3K36me3, H2AFV nucleosomes, and lack of DNA methylation. Despite the different strategy to condense sperm genomes, both mammals and zebrafish package developmental regulators in bivalent chromatins with depleted DNA methylation, suggesting the conserved mode of gene packaging in vertebrate germ cells (Hammoud et al. 2009; Brykczynska et al. 2010). Interestingly, germ cells share similar aspects of packaging developmental regulators with bivalent marks, DNA hypomethylation around TSS, and the presence of H2A.Z nucleosomes (Bernstein et al. 2006; Creyghton et al. 2008; Fouse et al. 2008). These similarities suggest a potential contribution of epigenetic mechanisms to pluripotency in ES cells and totipotency in germ cells.

The bivalent chromatin signature of pluripotency is observed in ES cells and sperm cells. The following questions are when and how the signature is established during the life cycle. Based on the similarity of epigenetic features between ES cells and mature sperm, one possibility is that the bivalent signature is established initially in the germline and maintained or reestablished by pluripotency factors in ES cells (see below for more discussion). In contrast to a narrow range of bivalency around TSS in ES cells, both standalone and cluster of developmental genes in zebrafish sperm typically display a contiguous block of multivalent modifications (Bernstein et al. 2006; Mikkelsen et al. 2007; Hammoud et al. 2009; Brykczynska et al. 2010). This raises a strong possibility that the epigenetic signature is mechanistically established in the germline. Interestingly,

studies have proposed PGCs undergo global chromatin programming to establish epigenetic features of totipotency after genome-wide erasure of DNA methylation at E11.5 (Hajkova et al. 2002; Surani et al. 2007; Hajkova et al. 2008). Mechanisms such as DNA repair and 5hmC-related pathways involved in active DNA methylation are likely linked to the process of epigenetic programming (Hajkova et al. 2010; Cantone and Fisher 2013). To better understand the establishment of epigenetic features, it is critical to overcome the technical challenge of handling a small number of PGCs and germ cells from gametogenesis.

In zebrafish sperm, we observed additional epigenetic features along with bivalent marks including atypical placement of H3K36me3 and incorporation of H2AFV nucleosomes. We termed this complex multivalent chromatin, which includes multiple positive and negative marks. To insure the robustness of the poising potential of developmental regulators, several studies indicated that multivalent chromatin possibly resides in ES cells as well. This includes H3K4me2 as an additional positive mark and H3K9me3 as an additional repressive mark along with H3K4me3 and H3K27me3 (Meissner et al. 2008; Bilodeau et al. 2009). Furthermore, H2A.Z nucleosomes largely coincide with PRC2 complex and H3K27me3 in developmental regulators in ES cells (Creyghton et al. 2008). The underlying DNA is GC-rich and depleted of methylation (Meissner et al. 2008). In ES cells, paused RNA Pol II is associated with developmental regulators and bivalent chromatin, but it is not clear if this happens in sperm since the level of RNA Pol II is very low and transcription is inert (Kierszenbaum and Tres 1975; Guenther et al. 2007; Marks et al. 2012).

Though DNA is highly condensed in mature sperm, it is still considered interesting to identify DNA regulatory elements in sperm cells. These regions with open chromatin are typically bound by transcription factors or other regulatory proteins, and could be identified by nuclease hypersensitivity or FAIRE (formaldehyde-assisted isolation of regulatory elements) approach (Song et al. 2011; Simon et al. 2012). Our studies were primarily focused on epigenetic features in sperm promoter regions. It is still unknown if epigenetic features are associated with other DNA regulatory elements in sperm cells. Chromatin signatures of enhancers have been characterized based on genome-wide profiling of histone modifications. H3K4me1 is enriched in the majority of active and poised enhancers, whereas H3K4me3 is in the promoters (Heintzman et al. 2007). Modifications on H3K27 enable differentiation between active and poised enhancers. In ES cells, acetylation on H3K27 is enriched in active enhancers, whereas H3K27me3 is enriched in poised enhancers (Creyghton et al. 2010; Rada-Iglesias et al. 2011).

To understand how totipotency is established in germ cells, it is critical to understand how epigenomic status is set up in oocytes and during gametogenesis. Due to the size and number of oocytes, studying egg epigenomics will be a real challenge. However, DNA methylomes in oocytes and during oogenesis are relatively feasible. Since bivalent chromatins (or multivalent chromatins) are identified in sperm and ES cells to establish totipotency and pluripotency, respectively, we speculate oocytes take a similar or the same packaging strategy. To investigate epigenomics during spermatogenesis, one alternative approach is to use cells from in vitro production. In vitro spermatogenesis has been successfully performed in both mouse and zebrafish (Sakai

2002; Sato et al. 2011). Comparison between in vivo and in vitro mature sperm cells would give an insight if there is any difference between these two.

Potential Inheritance of Epigenetic Features from Germ Cells to Embryos

Bivalent chromatin as the chromatin signature of pluripotency is identified in sperm and ES cells (Bernstein et al. 2006; Mikkelsen et al. 2007; Li et al. 2012). The following question is how the signature is established in early embryos. Genome-wide profiling of epigenetic features has proposed two potential models, reestablishment and inheritance models, to establish the chromatin signature of pluripotency in early embryos. The Schier group detected bivalent chromatin in developmental regulators after ZGA but not before ZGA, suggesting chromatin signature is erased and reestablished in early embryos (Vastenhouw et al. 2010). Our studies in zebrafish sperm, however, suggest the chromatin signature (bivalency or multivalency) is already established in the male gamete, and potentially inherited to embryos. The Collas group was able to detect bivalent chromatin in developmental regulators before ZGA (256-cell stage), though at a relatively low level compared to that after ZGA (Lindeman et al. 2011). Notably, a significant portion of bivalent genes is shared between sperm cells and pre-MBT embryos, suggesting a certain degree of inheritance of chromatin signature from gametes to embryos. One might argue if the low level of bivalent marks is indeed inherited and, importantly, instructive for gene poising and/or antagonizing DNA methylation. We reason bivalency is not the only option to establish pluripotency in embryos, and other factors could possibly contribute to competency as well. This is exemplified by the

programming of dynamic DNA methylation (Potok et al. 2013) and incorporation of H2afva nucleosomes (Chapter 4, and discussed below). Other possibilities include histone marks rather than H3K4me3 and H3K27me3, histone variants, transcription and transcription factors, and noncoding RNA.

Profiling of differential DNA methylomes in two gametes and early embryos suggests the DNA methylation pattern of the paternal genome is set up in mature sperm and this pattern mirrors blastomeres which undergo ZGA to achieve totipotency (Potok et al. 2013). In contrast, the DNA methylation pattern of the maternal genome is reprogrammed to a state corresponding to the paternal genome by ZGA. Despite the difference between the paternal and maternal methylome setup, the majority of DNA methylation patterns are very similar. The data from paternal and maternal DNA methylation patterns suggest a coordination model of both inheritance and reprogramming in early embryos. It will be important to examine if there are other factors involved in the establishment of totipotency in early embryos.

Paternal contribution to embryogenesis has long been underestimated. Studies showed a subset of RNA including known and unknown protein-coding RNAs, and noncoding RNAs were identified in mature sperm cells (Krawetz 2005). These RNAs were proposed to be involved in various processes such as spermatogenesis, fertilization, and early embryogenesis. Moreover, retention of nucleosomes, bivalent chromatin, and competency of paternal DNA methylome in vertebrate sperm suggest the potential of epigenetic inheritance to influence embryogenesis (Hammoud et al. 2009; Brykczynska et al. 2010; Wu et al. 2011; Rando 2012; Potok et al. 2013).

The Potential Role of H2afva as the Epigenetic Memory

The identification of a high level of H2afva nucleosomes before ZGA is very important as this suggests H2afva is not diluted by cell division and is potentially heritable as the epigenetic memory. Before ZGA, the levels of bivalent chromatin marks are diluted during cleavage cycles, making them debatable as heritable epigenetic marks, even though the pattern is maintained from sperm to post-ZGA (Vastenhouw et al. 2010; Lindeman et al. 2011). Nonetheless, examination of H2afva in zebrafish sperm and early embryos shows both the level and occupancy likely remain consistent, even during cleavage cycles. These data suggest the histone variant H2afva could potentially be a heritable epigenetic mark from gametes to early embryos—which favors the inheritance model of epigenetic marks (Figure 4.4). To further prove H2afva is inherited from gametes, it is critical but challenging to examine very early time points after fertilization. Another critical question is whether H2afva is instructive to embryogenesis, that is, whether H2afva drives gene expression underlying embryogenesis.

Transcriptional memory of *INO1* and *GAL1* genes in yeast depends on H2A.Z-mediated localization to nuclear periphery (Brickner et al. 2007). H2A.Z is involved in recruitment of SWI/SNF, a nucleosome remodeler, for transcriptional memory, suggesting H2A.Z plays a role in mediating epigenetic transcriptional memory (Kundu et al. 2007; Lemieux et al. 2008). Interestingly, studies in zebrafish indicate H2afva, but not bivalent marks, is inherited from sperm to embryos, making H2afva a potential candidate for the study of transgenerational epigenetic inheritance.

The next important question will be how H2afva is established in early embryos. H2A.Z nucleosomes are exchanged with H2A nucleosomes by Srcap. How Srcap is

targeted to particular regions is not fully understood, but studies suggest acetylation on histones correlates with H2A.Z occupancy (Kurdistani et al. 2004; Zhang et al. 2005). A member in SWR1 complex, named Bdf1, contains two bromodomains which binds acetylated histones (Matangkasombut et al. 2000; Krogan et al. 2003; Kobor et al. 2004). Moreover, loss of Bdf1 or histone acetyltransferase (such as Gcn5) in yeast leads to a decrease of Htz1 occupancy, suggesting that acetylated histones could potentially target SWR1 and Htz1 deposition (Zhang et al. 2005). It will be important to examine if acetylated histones coincide with H2fava in early embryos. Another potential approach is a reinforcement model—H2afva is deposited in embryos based on the pattern in gametes. *De novo* deposition of H2afva could depend on trans- and/or cis-elements. H2A.Z is often enriched at -1 nucleosome where the nucleosome-depleted region (NDR) is. Studies have shown sequence preference for NDR (Segal et al. 2006; Kaplan et al. 2009), so it is possible that H2A.Z is preferentially deposited based on DNA sequence.

Setting up DNA Methylation Profiles of Totipotency/Pluripotency

Several possible mechanisms have been proposed to set up DNA methylation profiles (Lee and Skalnik 2005; Thomson et al. 2010; Schuettengruber et al. 2011). For example, H3K4me3, the permissive chromatin mark, is correlated with DNA hypomethylation (Weber et al. 2007). Cfp1, a subunit of H3K4 methyltransferase, binds unmethylated CG dinucleotides and thus connects methylation on H3K4 to DNA hypomethylation (Lee and Skalnik 2005; Thomson et al. 2010; Schuettengruber et al. 2011). Our study focused on the antagonism between H2A.Z and DNA methylation,

which has been reported in many organisms and is evolutionally conserved. Overlapping between H2afva-enriched regions and DNA methylation status suggests the majority of DNA hypomethylated regions are occupied with H2afva very early. Although H2afva is the dominant factor to set up DNA methylation profiles in very early embryos (before ZGA), there could be other factors involved in the setup. Since the H3K4me3 level and enrichment are low and zygotic transcription is inactive at a very early stage, we reason that CG density and/or other histone variants could play a role in the targeting of DNA methylation. Regions with low CG density tend to be methylated whereas dense CGIs resist methylation. Another histone variant, marcoH2A, is enriched at developmental genes in pluripotent cells and regulates expression of these genes during cellular differentiation and embryo development (Buschbeck et al. 2009). The localization and function of macroH2A during embryo development suggests its potential to be an important epigenetic mark. It will be interesting to examine how macroH2A relates to DNA methylation profiles.

DNA methyltransferase, DNMT, has been shown to associate with PRC2 in cancer cell lines (Vire et al. 2006). Knock down of EZH2, the catalytic subunit of PRC2, leads to a decrease of H3K27me3 and DNA methylation in several EZH2 target genes, suggesting a correlation between EZH2/H3K27me3 and DNA methylation in cancer cells. Other studies, however, indicate EZH2 is not required to maintain DNA methylation in cancer cell lines (McGarvey et al. 2007; Kodach et al. 2010). To further understand the relationship between H3K27me3 and DNA methylation, it is crucial to conduct a genomic approach in multiple cell lines. It will also be important to examine the interplay in normal cells and during development.

H2A.Z protein sequence is 100% identical among vertebrates, and the anticorrelation to DNA methylation is reported from fish, to plants, to humans, suggesting H2A.Z is an evolutionally conserved protein with some fundamental functions. Indeed, deletion of H2A.Z leads to embryonic lethality in many organisms (van Daal and Elgin 1992; Iouzalen et al. 1996; Liu et al. 1996; Clarkson et al. 1999; Faast et al. 2001; Ridgway et al. 2004). The zygotic genome is activated at 1000-cell stage (midblastula transition, MBT) in zebrafish, but between 2- to 8- cell stages in mammals. The timing difference might be attributed to the need of transcription profiles to specify extraembryonic tissue and inner cell mass lineages in mammals. Our studies in zebrafish suggest H2afva could be a heritable epigenetic mark from gametes to embryos, and the anticorrelation between H2afva occupancy and DNA methylation in both sperm and embryos—providing a potential mechanism to set up DNA methylation profiles (Figure 4.4). In *C. elegans*, HTZ-1 is essential for normal development and highly expressed when the zygotic genome activates (Faast et al. 2001; Ridgway et al. 2004; Whittle et al. 2008). Since there is no DNA methylation in *C. elegans*, we suspect there is no need of HTZ-1 before ZGA. In contrast, H2A.Z has been detected before ZGA in *Xenopus*, and at least at blastula in mice (Faast et al., 2001; Ridgway et al., 2004). Despite the timing difference of ZGA between zebrafish and mammals, we speculate a conserved role of H2A.Z in vertebrates as a heritable epigenetic mark with the potential to set up DNA methylation profiles of totipotency and pluripotency.

In conclusion, this dissertation unveils how epigenomes are set up in male gametes and early embryos in zebrafish, which potentially helps to establish pluripotency/totipotency. In zebrafish sperm, active chromatin modifications including

H3K4me3, H3K4me2, and H3K14ac, are highly enriched at genes involved in spermatogenesis and housekeeping (such as cell cycle, metabolic, and catabolic processes). This epigenomic pattern in mature sperm represents a memory from previous process (spermatogenesis) and a preparation for the near future (embryogenesis). Importantly, developmental genes in zebrafish sperm are associated with bivalent chromatin marks, along with H3K36me3 and the histone variant, H2afva. Despite lack of protamine in zebrafish, both zebrafish and mammals use bivalent chromatin to package developmental genes in sperm. This suggests the bivalent chromatin feature at important loci in sperm is conserved among vertebrates. Moreover, in ES cells, bivalent chromatin has been reported at developmental loci and maintains pluripotency. These studies suggest the bivalent feature is potentially set up in gametes already, and potentially confers totipotency in the zygote.

In addition to chromatin marks, our studies indicate a potential role of H2afva in establishing pluripotency/totipotency by targeting DNA methylation. DNA methylome in zebrafish suggest DNA methylation confers pluripotency/totipotency in gametes and early embryos. Profiling of H2afva and DNA methylation reveals a conserved and strong anticorrelation in zebrafish sperm and early embryos. Unlike the low level of bivalent chromatin in early embryos, both the level and enrichment of H2afva nucleosomes are persistent from sperm to early embryos. Taken together, our studies suggest H2afva is potentially a heritable epigenetic mark from gametes to embryos and plays an important role in targeting DNA methylation profile of pluripotency/totipotency.

References

Bernstein BE, Mikkelsen TS, Xie X, Kamal M, Huebert DJ, Cuff J, Fry B, Meissner A, Wernig M, Plath K et al. 2006. A bivalent chromatin structure marks key developmental genes in embryonic stem cells. *Cell* **125**(2): 315–326.

Bilodeau S, Kagey MH, Frampton GM, Rahl PB, Young RA. 2009. SetDB1 contributes to repression of genes encoding developmental regulators and maintenance of ES cell state. *Genes Dev* **23**(21): 2484–2489.

Brickner DG, Cajigas I, Fondufe-Mittendorf Y, Ahmed S, Lee PC, Widom J, Brickner JH. 2007. H2A.Z-mediated localization of genes at the nuclear periphery confers epigenetic memory of previous transcriptional state. *PLoS Biol* **5**(4): e81.

Brykczynska U, Hisano M, Erkek S, Ramos L, Oakeley EJ, Roloff TC, Beisel C, Schubeler D, Stadler MB, Peters AH. 2010. Repressive and active histone methylation mark distinct promoters in human and mouse spermatozoa. *Nat Struct Mol Biol* **17**(6): 679–687.

Buschbeck M, Uribesalgo I, Wibowo I, Rue P, Martin D, Gutierrez A, Morey L, Guigo R, Lopez-Schier H, Di Croce L. 2009. The histone variant macroH2A is an epigenetic regulator of key developmental genes. *Nat Struct Mol Biol* **16**(10): 1074–1079.

Cantone I, Fisher AG. 2013. Epigenetic programming and reprogramming during development. *Nat Struct Mol Biol* **20**(3): 282–289.

Clarkson MJ, Wells JR, Gibson F, Saint R, Tremethick DJ. 1999. Regions of variant histone His2AvD required for Drosophila development. *Nature* **399**(6737): 694–697.

Creyghton MP, Cheng AW, Welstead GG, Kooistra T, Carey BW, Steine EJ, Hanna J, Lodato MA, Frampton GM, Sharp PA et al. 2010. Histone H3K27ac separates active from poised enhancers and predicts developmental state. *Proc Natl Acad Sci* **107**(50): 21931–21936.

Creyghton MP, Markoulaki S, Levine SS, Hanna J, Lodato MA, Sha K, Young RA, Jaenisch R, Boyer LA. 2008. H2AZ is enriched at Polycomb complex target genes in ES cells and is necessary for lineage commitment. *Cell* **135**(4): 649–661.

Faast R, Thonglairoam V, Schulz TC, Beall J, Wells JR, Taylor H, Matthaei K, Rathjen PD, Tremethick DJ, Lyons I. 2001. Histone variant H2A.Z is required for early mammalian development. *Curr Biol* **11**(15): 1183–1187.

Fouse SD, Shen Y, Pellegrini M, Cole S, Meissner A, Van Neste L, Jaenisch R, Fan G. 2008. Promoter CpG methylation contributes to ES cell gene regulation in parallel with Oct4/Nanog, PcG complex, and histone H3 K4/K27 trimethylation. *Cell Stem Cell* **2**(2): 160–169.

Guenther MG, Levine SS, Boyer LA, Jaenisch R, Young RA. 2007. A chromatin landmark and transcription initiation at most promoters in human cells. *Cell* **130**(1): 77–88.

Hajkova P, Ancelin K, Waldmann T, Lacoste N, Lange UC, Cesari F, Lee C, Almouzni G, Schneider R, Surani MA. 2008. Chromatin dynamics during epigenetic reprogramming in the mouse germ line. *Nature* **452**(7189): 877–881.

Hajkova P, Erhardt S, Lane N, Haaf T, El-Maarri O, Reik W, Walter J, Surani MA. 2002. Epigenetic reprogramming in mouse primordial germ cells. *Mech Dev* **117**(1–2): 15–23.

Hajkova P, Jeffries SJ, Lee C, Miller N, Jackson SP, Surani MA. 2010. Genome-wide reprogramming in the mouse germ line entails the base excision repair pathway. *Science* **329**(5987): 78–82.

Hammoud SS, Nix DA, Zhang H, Purwar J, Carrell DT, Cairns BR. 2009. Distinctive chromatin in human sperm packages genes for embryo development. *Nature* **460**(7254): 473–478.

Heintzman ND, Stuart RK, Hon G, Fu Y, Ching CW, Hawkins RD, Barrera LO, Van Calcar S, Qu C, Ching KA et al. 2007. Distinct and predictive chromatin signatures of transcriptional promoters and enhancers in the human genome. *Nat Genet* **39**(3): 311–318.

Iouzalen N, Moreau J, Mechali M. 1996. H2A.ZI, a new variant histone expressed during Xenopus early development exhibits several distinct features from the core histone H2A. *Nucleic Acids Res* **24**(20): 3947–3952.

Kaplan N, Moore IK, Fondufe-Mittendorf Y, Gossett AJ, Tillo D, Field Y, LeProust EM, Hughes TR, Lieb JD, Widom J et al. 2009. The DNA-encoded nucleosome organization of a eukaryotic genome. *Nature* **458**(7236): 362–366.

Kierszenbaum AL, Tres LL. 1975. Structural and transcriptional features of the mouse spermatid genome. *J Cell Biol* **65**(2): 258–270.

Kobor MS, Venkatasubrahmanyam S, Meneghini MD, Gin JW, Jennings JL, Link AJ, Madhani HD, Rine J. 2004. A protein complex containing the conserved Swi2/Snf2-Related ATPase Swr1p deposits histone variant H2A.Z into euchromatin. *PLoS Biol* **2**(5): E131.

Kodach LL, Jacobs RJ, Heijmans J, van Noesel CJ, Langers AM, Verspaget HW, Hommes DW, Offerhaus GJ, van den Brink GR, Hardwick JC. 2010. The role of EZH2 and DNA methylation in the silencing of the tumour suppressor RUNX3 in colorectal cancer. *Carcinogenesis* **31**(9): 1567–1575.

Krawetz SA. 2005. Paternal contribution: new insights and future challenges. *Nat Rev Genet* **6**(8): 633–642.

Krogan NJ, Keogh MC, Datta N, Sawa C, Ryan OW, Ding H, Haw RA, Pootoolal J, Tong A, Canadien V et al. 2003. A Snf2 family ATPase complex required for recruitment of the histone H2A variant Htz1. *Mol Cell* **12**(6): 1565–1576.

Kundu S, Horn PJ, Peterson CL. 2007. SWI/SNF is required for transcriptional memory at the yeast GAL gene cluster. *Genes Dev* **21**(8): 997–1004.

Kurdistani SK, Tavazoie S, Grunstein M. 2004. Mapping global histone acetylation patterns to gene expression. *Cell* **117**(6): 721–733.

Lee JH, Skalnik DG. 2005. CpG-binding protein (CXXC finger protein 1) is a component of the mammalian Set1 histone H3-Lys4 methyltransferase complex, the analogue of the yeast Set1/COMPASS complex. *J Biol Chem* **280**(50): 41725–41731.

Lemieux K, Larochelle M, Gaudreau L. 2008. Variant histone H2A.Z, but not the HMG proteins Nhp6a/b, is essential for the recruitment of Swi/Snf, Mediator, and SAGA to the yeast GAL1 UAS(G). *Biochem Biophys Res Commun* **369**(4): 1103–1107.

Li M, Liu GH, Izpisua Belmonte JC. 2012. Navigating the epigenetic landscape of pluripotent stem cells. *Nat Rev Mol Cell Biol* **13**(8): 524–535.

Lindeman LC, Andersen IS, Reiner AH, Li N, Aanes H, Ostrup O, Winata C, Mathavan S, Muller F, Alestrom P et al. 2011. Prepatterning of developmental gene expression by modified histones before zygotic genome activation. *Dev Cell* **21**(6): 993–1004.

Liu X, Li B, Gorovsky MA. 1996. Essential and nonessential histone H2A variants in Tetrahymena thermophila. *Mol Cell Biol* **16**(8): 4305–4311.

Marks H, Kalkan T, Menafra R, Denissov S, Jones K, Hofemeister H, Nichols J, Kranz A, Stewart AF, Smith A et al. 2012. The transcriptional and epigenomic foundations of ground state pluripotency. *Cell* **149**(3): 590–604.

Matangkasombut O, Buratowski RM, Swilling NW, Buratowski S. 2000. Bromodomain factor 1 corresponds to a missing piece of yeast TFIID. *Genes Dev* **14**(8): 951–962.

McGarvey KM, Greene E, Fahrner JA, Jenuwein T, Baylin SB. 2007. DNA methylation and complete transcriptional silencing of cancer genes persist after depletion of EZH2. *Cancer Res* **67**(11): 5097–5102.

Meissner A, Mikkelsen TS, Gu H, Wernig M, Hanna J, Sivachenko A, Zhang X, Bernstein BE, Nusbaum C, Jaffe DB et al. 2008. Genome-scale DNA methylation maps of pluripotent and differentiated cells. *Nature* **454**(7205): 766–770.

Mikkelsen TS, Ku M, Jaffe DB, Issac B, Lieberman E, Giannoukos G, Alvarez P, Brockman W, Kim TK, Koche RP et al. 2007. Genome-wide maps of chromatin state in pluripotent and lineage-committed cells. *Nature* **448**(7153): 553–560.

Potok ME, Nix DA, Parnell TJ, Cairns BR. 2013. Reprogramming the maternal zebrafish genome after fertilization to match the paternal methylation pattern. *Cell* **153**(4): 759–772.

Rada-Iglesias A, Bajpai R, Swigut T, Brugmann SA, Flynn RA, Wysocka J. 2011. A unique chromatin signature uncovers early developmental enhancers in humans. *Nature* **470**(7333): 279–283.

Rando OJ. 2012. Daddy issues: paternal effects on phenotype. *Cell* **151**(4): 702–708.

Ridgway P, Brown KD, Rangasamy D, Svensson U, Tremethick DJ. 2004. Unique residues on the H2A.Z containing nucleosome surface are important for Xenopus laevis development. *J Biol Chem* **279**(42): 43815–43820.

Sakai N. 2002. Transmeiotic differentiation of zebrafish germ cells into functional sperm in culture. *Development* **129**(14): 3359–3365.

Sato T, Katagiri K, Gohbara A, Inoue K, Ogonuki N, Ogura A, Kubota Y, Ogawa T. 2011. In vitro production of functional sperm in cultured neonatal mouse testes. *Nature* **471**(7339): 504–507.

Schuettengruber B, Martinez AM, Iovino N, Cavalli G. 2011. Trithorax group proteins: switching genes on and keeping them active. *Nat Rev Mol Cell Biol* **12**(12): 799–814.

Segal E, Fondufe-Mittendorf Y, Chen L, Thastrom A, Field Y, Moore IK, Wang JP, Widom J. 2006. A genomic code for nucleosome positioning. *Nature* **442**(7104): 772–778.

Shimizu Y, Mita K, Tamura M, Onitake K, Yamashita M. 2000. Requirement of protamine for maintaining nuclear condensation of medaka (Oryzias latipes) spermatozoa shed into water but not for promoting nuclear condensation during spermatogenesis. *Int J Dev Biol* **44**(2): 195–199.

Simon JM, Giresi PG, Davis IJ, Lieb JD. 2012. Using formaldehyde-assisted isolation of regulatory elements (FAIRE) to isolate active regulatory DNA. *Nat Protoc* **7**(2): 256–267.

Song L, Zhang Z, Grasfeder LL, Boyle AP, Giresi PG, Lee BK, Sheffield NC, Graf S, Huss M, Keefe D et al. 2011. Open chromatin defined by DNaseI and FAIRE identifies regulatory elements that shape cell-type identity. *Genome Res* **21**(10): 1757–1767.

Surani MA, Hayashi K, Hajkova P. 2007. Genetic and epigenetic regulators of pluripotency. *Cell* **128**(4): 747–762.

Thomson JP, Skene PJ, Selfridge J, Clouaire T, Guy J, Webb S, Kerr AR, Deaton A, Andrews R, James KD et al. 2010. CpG islands influence chromatin structure via the CpG-binding protein Cfp1. *Nature* **464**(7291): 1082–1086.

van Daal A, Elgin SC. 1992. A histone variant, H2AvD, is essential in Drosophila melanogaster. *Mol Biol Cell* **3**(6): 593–602.

Vastenhouw NL, Zhang Y, Woods IG, Imam F, Regev A, Liu XS, Rinn J, Schier AF. 2010. Chromatin signature of embryonic pluripotency is established during genome activation. *Nature* **464**(7290): 922–926.

Vire E, Brenner C, Deplus R, Blanchon L, Fraga M, Didelot C, Morey L, Van Eynde A, Bernard D, Vanderwinden JM et al. 2006. The Polycomb group protein EZH2 directly controls DNA methylation. *Nature* **439**(7078): 871–874.

Weber M, Hellmann I, Stadler MB, Ramos L, Paabo S, Rebhan M, Schubeler D. 2007. Distribution, silencing potential and evolutionary impact of promoter DNA methylation in the human genome. *Nat Genet* **39**(4): 457–466.

Whittle CM, McClinic KN, Ercan S, Zhang X, Green RD, Kelly WG, Lieb JD. 2008. The genomic distribution and function of histone variant HTZ-1 during C. elegans embryogenesis. *PLoS Genet* **4**(9): e1000187.

Wu SF, Zhang H, Cairns BR. 2011. Genes for embryo development are packaged in blocks of multivalent chromatin in zebrafish sperm. *Genome Res* **21**(4): 578–589.

Zhang H, Roberts DN, Cairns BR. 2005. Genome-wide dynamics of Htz1, a histone H2A variant that poises repressed/basal promoters for activation through histone loss. *Cell* **123**(2): 219–231.

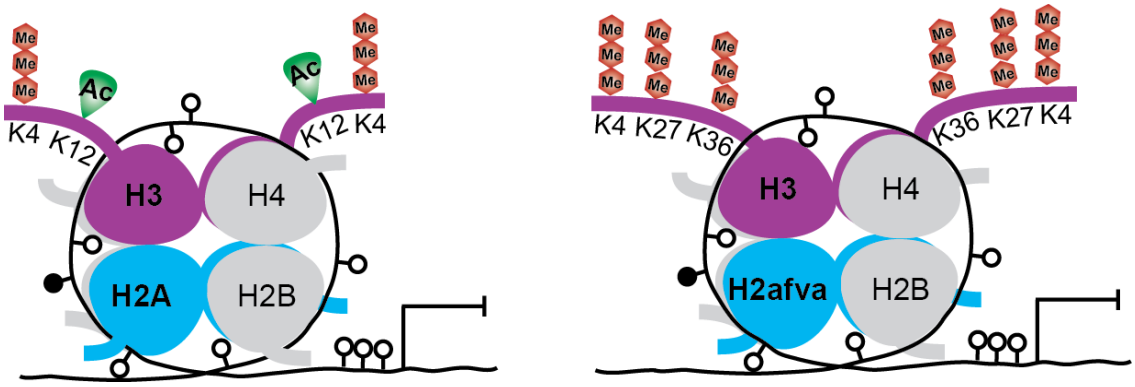

Figure 5.1 Programmed epigenome in zebrafish sperm. Two prominent groups of genes are observed in zebrafish sperm. One group of genes is highly enriched with active marks (left side), including tri- and di-methylation on H3K4 and H3K12Ac. These are genes involved in spermatogenesis and housekeeping processes (early cellular processes), suggesting epigenetic status in mature sperm represents a memory from previous process and also a preparation for future program. The other group of genes is enriched with bivalent marks (H3K4me3 and H3K27me3), H2afva, and H3K36me3. The majority of this group of genes is transcription factors involved in various developmental processes. Both groups of genes are lack of DNA methylation.